The first Iberian UV-Visible instruments intercomparison. Final report

MINISTERIO
DE MEDIO AMBIENTE

DIRECCIÓN GENERAL
DEL INSTITUTO NACIONAL
DE METEOROLOGÍA

The first Iberian UV-Visible instruments intercomparison. Final report

Edited by **Instituto Nacional de Meteorología (INM, Spain)**

Scientific editors:
Antonio Labajo and Emilio Cuevas (INM); Benito de la Morena (INTA).

With the contribution from:
V. Cachorro, V. Carreño, E. Cuevas, A. M. Díaz, J. P. Díaz, F. Expósito, A. M. de Frutos, J. Gröbner, K. Lamb, J. A. Martínez-Lozano, B. A. de la Morena, L. S. Muniosguren, R. Pedrós, A. Redondas, C. Torres, M. P. Utrillas, R. Vergaz, J. M. Vilaplana.

* * * * *

Madrid, January 2004

MINISTERIO DE MEDIO AMBIENTE
SECRETARÍA GENERAL PARA LA PREVENCIÓN DE LA CONTAMINACIÓN Y DEL CAMBIO CLIMÁTICO
DIRECCIÓN GENERAL DEL INSTITUTO NACIONAL DE METEOROLOGÍA

2004

Table of contents

PROLOGUE

The interest of the scientific community in the content, spatial distribution and temporal development of ozone in the atmosphere has grown steadily in the last decades, as the progressive depletion of this atmospheric component as a result of Man's actions has been verified, and determined through measurements taken both by networks of surface spectrophotometers and by satellites equipped with instruments to measure this particular component. The rest of society has taken note of this interest and it is causing a certain degree of concern about the direct and indirect effects the drop in the total content of ozone in the atmosphere may have on living beings, and, in particular, on human health.

The measures taken by the international community to prevent the continual depletion of the stratospheric ozone layer came about with the enforcement of The Vienna Convention for the Protection of the Ozone Layer and the subsequent Montreal Protocol on Substances That Deplete the Ozone Layer. These international agreements not only cover the scientific aspects, but also others, such as the observation and monitoring of the development of ozone and other trace gases, aerosols, and so on, and the publishing of periodic evaluation reports, with the most recent in 2002. Nowadays ozone monitoring systems, which are basically maintained by various national meteorological services and other specialised state agencies, consist of observation networks of spectrophotometers which send information daily to the World Data Centres, in the same way as is done with conventional meteorological variables.

The Instituto Nacional de Meteorología (INM) started, between the end of the 1980's and the beginning of the 1990's, systematically measuring the total content of ozone and vertical distribution in the atmosphere at two observatories, with the idea of increasing the number of observation points and setting up a national network to measure the total content of ozone and which would provide quantitative accurate information on the ozone in the atmosphere above national territory and its effects on other climatic elements such as ultraviolet B radiation.

This goal was met with the setting up of the Brewer spectrophotometer network to measure the total content of atmospheric ozone and ultraviolet B radiation reaching the earth's surface.

The present Brewer spectrophotometer network is the result of the firm decision of the INM to install an operative monitoring system for total ozone in columns and ultraviolet radiation within the framework of the Programa de la Vigilancia Atmosférica Global de la Organización Meteorológica Mundial (OMM), (World Meteorological Organisation's Global Atmospheric Watch Program). The setting up of this network would not have been possible without the active support of the Comisión Interministerial de Ciencia y Tecnología (CICYT), (Joint Ministry of Science and Technology Commission), which partially financed the project through aid for scientific infrastructure projects.

Within the co-ordinated project CLI97-0345-C05, financed by the CICYT and with the participation of research groups from the INM, the Instituto de Técnica Aeroespacial (INTA), the universities of Barcelona, Valencia, Valladolid and La Laguna, a fundamental facet in a scientific measurements network like this was undertaken - quality control. To check the accuracy and inter-comparability of the measurements taken by different instruments at different places we have to carry out inter-comparison campaigns of the instruments like that carried out at the Centro de Experimentación de El Arenosillo

PRÓLOGO

El interés por parte de la comunidad científica por el conocimiento del contenido de ozono en la atmósfera, su distribución espacial y su evolución temporal ha ido aumentando progresivamente en las últimas décadas, conforme se ha ido verificando la disminución progresiva de este componente atmosférico provocada por las actividades humanas, y determinada mediante las medidas directas llevadas a cabo tanto en las redes de espectrofotómetros de superficie, como por los satélites con instrumentos específicos para la medida de este componente. Este interés se ha trasladado al resto de la sociedad provocando un cierto nivel de preocupación, debido a los efectos directos e indirectos que la disminución del contenido total de ozono en la atmósfera puede tener sobre los seres vivos y en particular sobre la salud humana.

Las medidas llevadas a cabo por la comunidad internacional para evitar el continuo deterioro de la capa de ozono estratosférico se materializaron con la entrada en vigor de la Convención de Viena para la Protección de la Capa de Ozono y del posterior Protocolo de Montreal sobre sustancias que reducen la capa de Ozono. Estos acuerdos internacionales contemplan no solo los aspectos científicos sino también otros tales como la observación y vigilancia de la evolución tanto del ozono como de otros gases traza, aerosoles, etc., publicando periódicamente informes de evaluación, el último de ellos en 2002. Hoy día los sistemas de vigilancia del ozono, mantenidos básicamente por diferentes servicios meteorológicos nacionales y otras agencias estatales especializadas, están constituidos por redes de observación de espectrofotómetros que envían información diariamente a los Centros Mundiales de Datos, de forma similar a como se hace con las variables meteorológicas convencionales.

El Instituto Nacional de Meteorología (INM) inició a finales de los ochenta y principios de los noventa la medida sistemática del contenido total de ozono y su distribución vertical en la atmósfera en dos observatorios, con la idea de ir ampliando el número de puntos de observación y llegar a establecer una red de medida de contenido total de ozono de cobertura nacional que permitiera disponer de una información cuantitativa y precisa sobre el ozono existente en la atmósfera situada sobre el territorio nacional y su incidencia sobre otros elementos climáticos como la radiación ultravioleta B.

Este objetivo quedó cubierto con el establecimiento de la red de espectrofotómetros Brewer para la medida del contenido total de ozono atmosférico y de la radiación ultravioleta B que alcanza la superficie terrestre.

La actual red de espectrofotómetros Brewer es el resultado de la apuesta decidida del INM de implantar un sistema operativo de vigilancia del ozono total en columna y la radiación ultravioleta en el marco del Programa de la Vigilancia Atmosférica Global de la Organización Meteorológica Mundial (OMM). El establecimiento de esta red no hubiera sido posible sin el concurso activo de la Comisión Interministerial de Ciencia y Tecnología (CICYT) que la ha financiado parcialmente mediante ayudas a proyectos de infraestructura científica.

En el marco del proyecto coordinado CLI97-0345-C05, financiado por la CICYT, y en el que participaron grupos de investigación del INM, del Instituto de Técnica Aeroespacial (INTA) y de las universidades de Barcelona, Valencia, Valladolid y La Laguna se acometió una faceta fundamental en una red de medidas científicas como ésta, que es la del control de calidad. Para conocer la exactitud e intercomparabilidad de

(INTA) between August 31st and September 10th, 1999. Not only all the Brewer spectrophotometers in the national network participated in this first inter-comparison, but also almost all the spectroradiometers and wide band radiometers used by Spanish groups studying the atmosphere. This inter-comparison was a first at national level, as it not only made it possible to compare different kinds of instruments, different methodology and measuring techniques, but was also a national meeting point for technicians and atmosphere researchers, where they exchanged experiences and ideas, and where, above all, the union and close collaboration of research groups who had until then worked individually and independently was consolidated.

This report presents the development and results of this inter-comparison, as well as the conclusions taken from the analysis and study of the data obtained. All the groups in Spain working on experimental research of total ozone, ultraviolet radiation and atmospheric aerosols from an optic point of view have taken part. This report is, furthermore, a reference document for those students and researchers who, in coming years, may wish to follow this fascinating line of investigation.

Milagros Couchoud Gregori
General Director of INM

las medidas realizadas por diferentes instrumentos en distintos emplazamientos es necesario llevar a cabo campañas de intercomparación de los instrumentos como la que se llevó a cabo en el Centro de Experimentación de El Arenosillo (INTA) entre el 31 de agosto y el 10 de septiembre de 1999. En esta primera intercomparación no solo participaron todos los espectrofotómetros Brewer de la red nacional sino también la práctica totalidad de los espectrorradiómetros y radiómetros de banda ancha utilizados por los grupos españoles que se dedican a la investigación atmosférica. Esta intercomparación constituye un hito a nivel nacional, porque no solo permitió la comparación de diferentes tipos de instrumentos y de distintas metodologías y técnicas de medida, sino porque además constituyó un punto de encuentro nacional de técnicos e investigadores de la atmósfera donde se intercambiaron experiencias e ideas, y sobre todo donde se consolidó la unión y la estrecha colaboración de grupos de investigación que hasta entonces trabajaban de forma dispersa e independiente.

Esta publicación presenta el desarrollo y los resultados de esta intercomparación así como las conclusiones deducidas del análisis y estudio de los datos obtenidos. En ella han intervenido todos los grupos que se dedican en España a la investigación experimental del ozono total, la radiación ultravioleta y los aerosoles atmosféricos desde un punto de vista óptico. Esta publicación constituye, además, un documento de referencia para aquellos estudiantes e investigadores que en los próximos años quieran adentrarse en esta apasionante línea de investigación.

Milagros Couchoud Gregori
Directora General del INM

IN MEMORY OF CARLOS GONZÁLEZ-FRÍAS MARTÍNEZ

To once again remember Carlos González-Frías, on a drab blank sheet, produces a bittersweet taste in the mouth. Distance, as we know, is never so great as to cause the memory of a friend to fade, whilst reality, many-faced and cold, hits us hard with the thought of him.

And today Carlos González-Frías is once again here with us, with his dossier of great deeds under his arm, as it is well known that Man should be remembered for all he achieved in life and never for his human failings. And so, Carlos was a fierce defender of those tasks imposed upon him or set by himself, an appreciated collaborator and a tireless scientific researcher.

He is here, in these pages on his own merits, as a great driving force behind the Brewer Spectrometer Network and for his continuous and justified concern about atmospheric ozone throughout his long career. It is thanks to that dedication, to his indefatigable drive, it is right to dedicate this work published by the Instituto Nacional de Meteorología as part of the Monographic Series under the title of «The First Iberian UV-Visible Instruments Intercomparison».

Within the varied field in which our friend and colleague worked, studies on solar radiation, climatology, environmental applications and so on, ozone was the main issue that kept him busy until the end of his days – when no one could have imagined such an unexpected and devastating end – and to which he dedicated the very best of his time as was witnessed by those who worked with him on such achievements.

For you, Carlos, our friend forever in our memory.

EN RECUERDO DE CARLOS GONZÁLEZ-FRÍAS MARTÍNEZ

Volver a recordar a Carlos González-Frías, sobre la insulsa cuartilla blanca proporciona un sabor agridulce. La distancia, es sabido, nunca es tan grande que disipe el recuerdo de un amigo, al tiempo que la realidad, poliédrica y fría, nos asalta dura para echar de menos su presencia.

Y vuelve hoy aquí Carlos González-Frías con su legajo de grandezas bajo el brazo, que también es sabido que al ser humano hay que tenerle presente por cuanto pudo conseguir en vida y nunca por sus humanos olvidos. Fue pues Carlos defensor entusiasta de cuantos trabajos le impusieron o se impuso, un apreciado colaborador y un incansable investigador científico.

Está aquí, en estas páginas por méritos propios, como gran impulsor de la Red de Espectrómetro Brewer y por su permanente y justificada preocupación por el ozono atmosférico a lo largo de su dilatada trayectoria profesional. Merced a esta dedicación, a su denodado impulso es de justicia dedicarle esta obra que publica el Instituto Nacional de Meteorología dentro de sus Series Monográficas bajo el título «The First Iberian UV-Visible instruments intercomparison».

Dentro del variado campo donde nuestro amigo y compañero se movió, estudios sobre radiación solar, climatología, aplicaciones medioambientales etc., fue éste, el ozono, el tema fundamental que le ocupó hasta el final de sus días –cuando nadie podíamos esperar un desenlace tan fulminante e imprevisto– al que le dedicó todo su mejor tiempo y así lo han sabido reconocer cuantos con él en tales logros participaron.

Para ti Carlos amigo, el mejor de nuestros recuerdos.

CHAPTER 1
INTRODUCTION

L. S. Muniosguren
Instituto Nacional de Meteorología

SUMMARY

In this chapter, the main objectives of the Intercomparison are summarized. A general description of the major activities is presented. Information about the participants and instruments are given.

RESUMEN

En este capítulo se presentan los principales objetivos de la Intercomparación y se resume el programa de actividades generales desarrollado. Finalmente se da la lista de las personas participantes y de los instrumentos que intervinieron en la Intercomparación.

1.1. THE INTERCOMPARISON

The accurate knowing of the incident ultraviolet (UV) solar radiation and its possible variation is important to evaluate its effects on public health and ecosystems. Different Institutions and Universities measure solar radiation on a routine basis, and recently spectral and broad-band UV measurement networks have been implemented. Therefore, the inter-comparability of measurements performed at different stations, and an accurate knowledge of the status and characteristics of the involved instruments are important activities.

One of the activities planned in the working program of the coordinated research program CLI97-0345-C05, supported by CICYT (Comisión Interministerial de Ciencia y Tecnología), was to perform a UV spectral radiometer Intercomparison. Initially, the instruments scheduled in the Intercomparison were those of the participants in the research program, that is: the INM (Instituto Nacional de Meteorología), INTA (Instituto Nacional de Técnica Aeroespacial) and the Universities of Barcelona, Valencia and Valladolid. Due to the interest of other research groups in participating, the Intercomparison was open to other Institutions of Spain and Portugal. The Intercomparison was also extended to UV broad band radiometers and to visible (VIS) range instruments.

1.2. OBJECTIVES

The main objective of the Intercomparison was to know the state of most instruments used to measure the spectral atmospheric UV solar radiation in networks of Spain and Portugal, and to calibrate the against standard references.

Simultaneous UV and VIS outdoor measurements were performed under different atmospheric conditions. Sun measurements were "blind". That means that none of the participants exchanged data among them. Ancillary atmospheric measurements were also performed.

Outdoor measurements were complemented by irradiance calibration and spectral characterization of spectrophotometers in laboratory using reference lamps traceable to NIST (National Institute of Standards and Technology, USA).

Another objective of the Intercomparison was to calibrate the total ozone measurements with Brewer spectrophotometers towards the traveling reference instrument Brewer#017.

Finally, an important goal was training of Brewer operators. Intercomparison procedures, operation programs and data evaluation and analysis were discussed among participants.

1.3. DATE AND SITE

The Intercomparison was held from August 31 to September 10, 1999 in the Centro de Experimentación de El Arenosillo (CEDEA) of INTA. The CEDEA is located in km 33.3 of the road Huelva-Matalascañas, in Huelva province (Spain).

1.4. GENERAL ACTIVITIES

The activities schedule and logistic arrangements were established in two Circulars distributed by mail in May and August 1999. Technical coordination was prepared by INM and local facilities and soundings were provided by CEDEA. The INM contracted two international experts and the traveling reference Brewer#017 through *AFC Ingenieros* company.

The activities were develop according to the following time schedule:

- **August 31 and September 1**: Arrival and instruments set up.
- **September 2**: Ending of equipment installation. Coordination meeting and information about outdoor measurement schedule (Brewer, Bentham and Optronic instruments), and dark-room calibrations. Brewer lamp tests. Measurement program with Licor spectroradiometers and other VIS instruments.
- **September 3 and 4**: Outdoor measurements. Meeting to review the working program. On September 3 an atmospheric sounding is performed at 12.05 local time.
- **September 5**: Outdoor measurements. Preparation of the calibration laboratory.
- **September 6**: Spectrophotometer calibration in dark room. Outdoor measurement of the rest of radiometers. Meeting about spectrophotometer network. Meeting about final report. Meeting to review the working program.
- **September 7**: Spectrophotometer calibration in dark room. Outdoor measurement of the rest of radiometers. Direct sun observations by the Universities of Valencia and Valladolid. Water vapor and aerosol optical depth measurements with Microtops sun-photometer by INM. Atmospheric sounding at 16.02 local time.
- **September 8**: Spectrophotometer calibration in dark room. Outdoor measurement of the rest of radiometers. Change of Brewer data acquisition software to correct the "Year 2000 effect". Preparation of Brewer and Dobson to perform Umkehr measurements the following day.
- **September 9**: Umkehr measurements at sunrise and sunset. Ozone soundings at 13.32 and 16.36 local time. Equipment packing.
- **September 10**: Finishing of packing and departure.

During the intercomparison campaign, INM reported weather forecast on a daily basis.

1.5. PARTICIPANTS AND INSTRUMENTS

The list of participants is shown in Annex 1 with their respective filiations.

Participating instruments are shown in the Annex 2.

ANNEX 1
LIST OF PARTICIPANTS IN THE INTERCOMPARISON

Organization	Participant	Organization	Participant
IMP (Portugal)	Diamantino Henriques	*INTA (Torrejón)*	Rosa de la Torre
INM (Izaña)	Emilio Cuevas Alberto Redondas Carlos J. Torres Virgilio Carreño	*University of Barcelona*	Jerónimo Lorente Xavier de Cabo Miguel Martín
INM (A Coruña)	Víctor Joaquín López M.ª Lina Vázquez	*University Complutense*	María Cascón
INM (Madrid)	Luis V. Sánchez-Muniosguren Carlos González-Frías Juan M.ª Cisneros Juan Manzano	*University of Girona*	Josep-Abel González Joseph Calbó
INM (Murcia)	Plácido García	*University of La Laguna*	Juan Pedro Díaz Fco. Javier Expósito
INM (Zaragoza)	Ángel Clemente José M.ª Ruiz	*University of Valencia*	José A. Martínez M.ª Pilar Utrillas Roberto Pedrós
INTA (CEDEA)	Benito A. de la Morena José Manuel Vilaplana Gloria Miró Pilar Sanz Manuel Vázquez Federico Soubrier Jesús de Dios	*University of Valladolid*	Victoria Cachorro Ángel de Frutos Ricardo Vergaz
		AFC Ingenieros - IOS	José Manuel Fernández Julian Gröbner Ken C. Lamb

ANNEX 2
INSTRUMENTS

1. SPECTRAL INSTRUMENTS				
REFERENCE		(CAB)	Brewer MK-II	no. 17
IMP		(POB)	Brewer MK-II	no. 47
INM	(Izaña)	(IZ1)	Brewer MK-III	no. 98-157
		(IZ2)	Bentham 150	
	(A Coruña)	(COB)	Brewer MK-IV	no. 98-151
	(Madrid)	(MAB)	Brewer MK-IV	no. 91-070
	(Murcia)	(MUB)	Brewer MK-IV	no. 95-117
	(Zaragoza)	(ZAB)	Brewer MK-II	no. 87-033
INTA		(ARB)	Brewer MK-III	no. 97-150
			Dobson	no. 120
UNIVERSITY OF BARCELONA			LI-1800	no. PRS-312
UNIVERSITY OF GIRONA		(GIO)	ORIEL MS257	
UNIVERSITY OF LA LAGUNA		(ULL)	Bentham 150	
UNIVERSITY OF VALENCIA		(UVL)	Optronic-OL 754	
			LI-1800	no. PRS-413
UNIVERSITY OF VALLADOLID			LI-1800	no. PRS-487
2. BROADBAND INSTRUMENTS				
INM	(Izaña)		Yankee UVB (reference)	no. 970825
			Yankee UVB	no. 970845
	(Madrid)		Yankee UVB (reference)	no. 970839
			Yankee UVA	no. 930302
INTA			Yankee UVB	no. 941208
3. OTHER INSTRUMENTS				
INM			NILU-UV	no. 10
			MICROTOPS II	
INTA			OZONE SOUNDER	
			RADIOSONDE	
UNIVERSITY OF BARCELONA			TUVR	
			SUV	
UNIVERSITY OF VALENCIA			MICROTOPS II	
UNIVERSITY OF VALLADOLID			Cimel Electronique	no. 114 (AERONET)

CHAPTER 2
CHARACTERISTICS AND DESCRIPTION OF THE ATMOSPHERIC SOUNDING STATION "EL ARENOSILLO"

Benito A. de la Morena
INTA-CEDEA / Atmospheric Sounding Station "El Arenosillo", Huelva, Spain, *morenacb@inta.es*

2.1. INTRODUCTION

The Atmospheric Sounding Station "El Arenosillo" (hereinafter called ESAt) at present dependent on the Atmospheric Reserch and Instrumentation Area of the Earth Observation, Remote Sensing and Aeronomy Department (Space Science Division at the intercomparison date) of the National Institute for Aerospacial Technique (INTA), is situated at CEDEA (Centro de Experimentación El Arenosillo) in Mazagón - Moguer, Huelva, Spain.

The ESAt is an Observatory dedicated to the atmospheric research since 1969, located in Southwest Europe (37.1N-6.7W). Due to the almost 300 clear sky days a year and uniform albedo (~0.1 in the visible region and ~0.05 in the UV region). El Arenosillo is considered to be a good platform for optical observations. Numerous Institutions and Institutes, national and international, take advantage of its optimal conditions for campaigns or permanent observation of the most varied atmospheric parameters: aerosols, UV.B., UV.A, PAR, NO_2, BrO, total ozone, ozone in surface, ozone profiles, erithemal dose in the human beings by biofilm techniques and its effect in other biological systems.

Since 1969, the ESAt is collaborating with numerous national and international institutes and universities in the measures and research of the neutral and ionised atmosphere. It is integrated in the Ionosphere International Network, code EA-036, in the World Ozone Ultraviolet Data Centre with the number 213 and in the Aeronet aerosol network.

The Arenosillo has databases of ionosphere (since 1975), stratospheric Ozone (since 1980), Solar Ultraviolet B radiation (since 1996), aerosol (since 1996) and ozone in surface (since 1997). All registered data are analysed and sent systematically to the World Data Centres, Universities and Institutions that request them.

Fig. 1. Panoramic view of the CEDA environment.

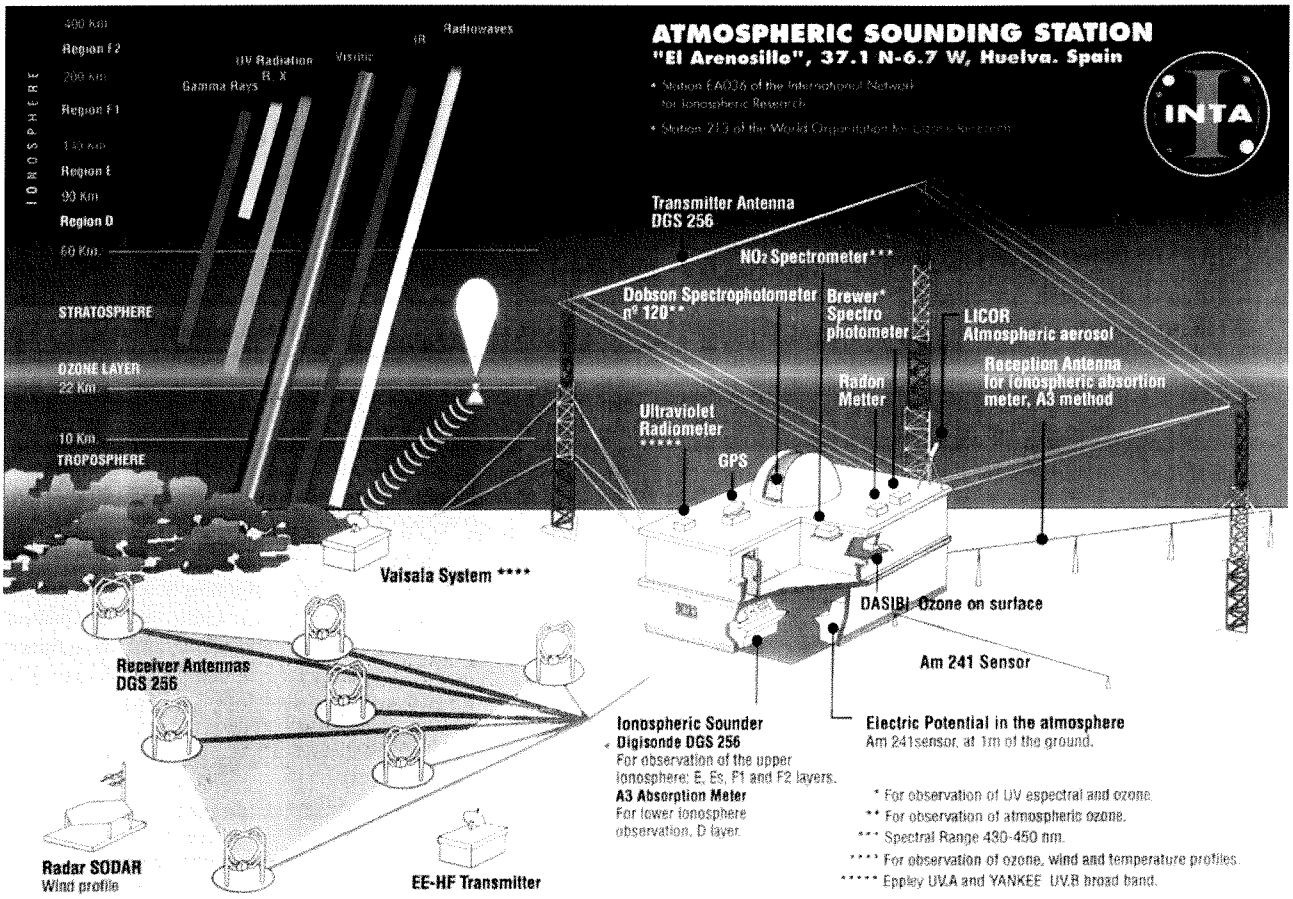

Fig. 2. Scheme of the instruments at the ESAt.

2.2. MAIN RESEARCH LINES OF THE ESAt

- Continuous monitoring of: total Ozone, tropospheric ozone, aerosols, ultraviolet spectral irradiance, irradiance integrated in the regions UV.B, UV.A and PAR (in collaboration with the environmental area of the regional government of Andalucia).
- Calibration, characterization and development of instrumentation for solar radiation and ozone measurement.
- Development of radiative transference models and ultraviolet index and ozone prediction (collaboration with Valladolid University).
- Study of the superficial ozone behaviour and its precursors in the Province of Huelva. (Huelva University collaboration).
- Characterization of the atmospheric aerosol at the Gulf of Cadiz region. Design of instrumentation (collaboration with Valladolid University).
- Ionospheric parameters measurements. Characterization and prediction of the ionospheric channel in HF communications.
- Effect of the ionosphere on satellites-satellites and satellites-Earth links. Total Electron Content measurements validation (TEC).
- Ionospheric variability associated to irregular eventualities/ events in the Sun-Earth system (geomagnetic storms, solar fulgurations, ...) (collaboration with the Ebro Observatory).
- Quality control of data bases and data distribution to international data centres and research groups.
- Making of Doctoral Thesis, Master Thesis, and contributions to workshops.

2.3. FACILITIES AND INSTRUMENTS AT THE ESAt

2.3.1 Facilities

The ESAt was under reconstruction to increase the building and facilities at the intercomparison date and the inauguration will take place in March 2000. For this reason, it was used as the platform of the intercomparison an other building of the CEDEA near from the ESAt.

The ESAt is equipped with facilities for continuous monitoring of the atmosphere, instrument calibration, data analysis and training of scientific staff (Doctoral Thesis, Master thesis, etc.).

- It has several computer connections in the local network with Internet access.
- Technical library about neutral and ionized atmosphere.
- Two meeting rooms.
- The acquisition room is bellow the roof. There are some other rooms that could be used if necessary for acquisition and equipment control.
- A big roof in two different levels with clear horizon and uniform albedo. With RS-232 connections and power connectors available for intercomparisons.
- A meteorological tower (5 m), totally equipped (meteo, temperature, humidity, etc.).
- UPS (Uninterrupted Power Supply) in all buildings, to guaranty the stability of the power.
- An automatic generator, to guaranty the power in case of long power fail.
- Fire detection systems all over the building.
- Security systems for inner and outer vigilance.

2.3.2 Other facilities

The ESAt is integrated in the "El Arenosillo" Experimental Centre (CEDEA). One of its main activities is rocket and balloons testing. It has the corresponding assembly and launch areas, drones, radar and optronic trayectography, and telemetry. It has also a laboratory available for studying renewable energies (solar, hydrogen power plants, ...).

Other CEDEA facilities that could be available are: three meeting rooms (60, 30 and 12 people), meteorological tower with 5 measurement levels up to 100 meters, Meteosat Observation System, global and diffuse radiation, two heliport areas, computers department, UPS and auxiliary power generators, administrative and communications area, general services facilities (electricity, mechanics, drivers, buses, fire brigade, cleaners, bar, etc) and possibility of accommodation inside the institute with 20 beds.

2.3.3 Instruments

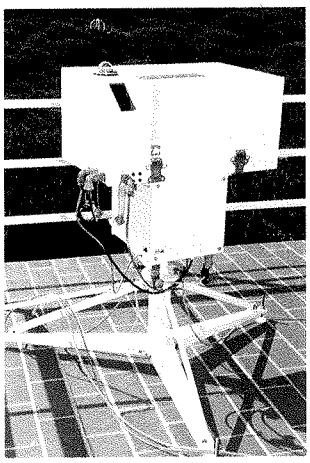

Brewer MK-III number 150 of the WODC network (total ozone and spectral UV).

Fig. 3. Brewer MK-III.

Dobson Spectrophotometer number 120 of the WODC network (total ozone).

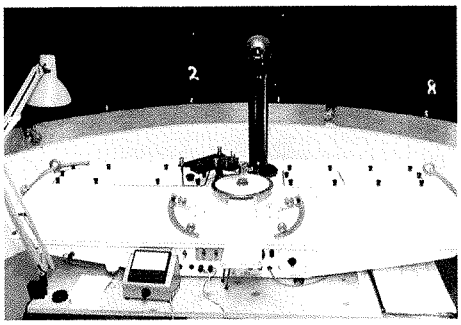

Fig. 4. Dobson Spectrophotometer.

- YES UVB-1 Pyranometer (erithemal irradiance).
- Microtops II Sunphotometer (total ozone, water vapour and AOD).
- Licor 1800 Spectroradiometer (spectral irradiance 300-1100 nm).
- YES MFR-7 multifilter rotating shadow band (global, direct and difuse irradiance in 7 wavelength in the visible region and a broadband channel. H_2O, aerosol and ozone).
- Vaisala ozone soundings facility (ozone and meteorological profile).
- SODAR DOPPLER for meteorological profiles to 1500 m (wind direction and speed).
- Ozone and NOx air analyser (Dasibi 1008RS and 8001 respectively).
- Ionospheric Absorption meter A3 method (low ionospheric radiowave absorption in D region).

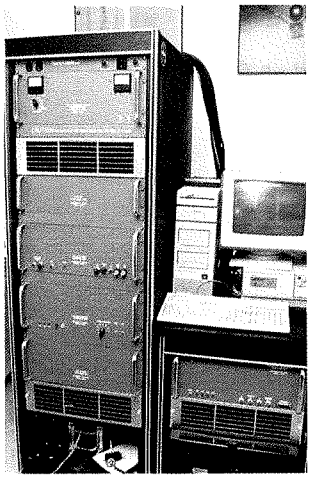

Ionospheric Digisonde 256 (upper ionospheric parameters E, F1, F2 layers) number EA0036 of ionospheric network.

Fig. 5. Digisonde 256.

2.3.4 New facilities

In the near future it will be available the following instruments and facilities:

- Cimel number114 of Aeronet network (aerosol optical depth and water vapour).
- Some broadband ELDONET instruments in the UV, visible, and NIR region.
- Differential Mobility Analyzer-Optical Particle Counter SMPS DMA-OPC (submicrometer), TSI company. (Concentration and size distribution of submicrometer particles *in situ*.
- Calibration facilities: Irradiance calibration with 1000 W halogen lamps, one of them certificated by NIST, a discharge lamps set, Hg, Cd, Zn and In for wavelength calibration, and cosine error calibration. This facilities are being improved in collaboration with the andalisian government and the Valladolid University.

2.4. FIRST IBERIAN INTERCOMPARISON CAMPAIGN OF SUN RADIOMETERS

Due to the facilities, general services and instruments available at the ESAt for ionosphere, ozone, solar radiation, aerosol, meteorological parameters, the excellent climate, and uniform albedo, the ESAt was chosen by the group that develops the CICYT Project (CLI 97/0345-C05) for the "Measure and Modelling of the space-time distribution in Spain of the UV radiation" to organise the 1st Iberian Intercomparison of radiometers in the solar ultraviolet and visible radiation.

This intercomparison took place from the 1st to the 10th of September 1999, with the attendance of representatives of 14 Iberian organisms and institutions and International Ozone Services Inc. with the travelling standards for ozone Brewer #017. Mr. Ken Lamb and Mr. Julian Gröbner performed the calibrations and checked all Brewers VS the travelling standard reference.

Fig. 6. *Picture of the first Iberian intercomparison of sun radiometers.*

2.5. HUELVA. SUN AND BEACH

Huelva, a city of Tartessus origin, surrounded by white, beautiful villages, is internationally known by its gastronomy (wines, ham, seafood, fish...), the high quality of its 120 km of beaches and tourist towns perfectly communicated by its local and national road network and railway. It is situated 50 min from San Pablo's Airport at Seville by the Madrid-Huelva motorway A-49, and 1h from Faro's Airport in Portugal (motorway). In this beautiful region with 40% natural parks, intensive agriculture (orange, strawberry...) and a high quality tourism, INTA has available for you the scientific means for the observation of the atmosphere at the Atmospheric Sounding Station El Arenosillo.

CHAPTER 3
METEOROLOGICAL CONDITIONS DURING THE INTERCOMPARISON

E. Cuevas, C. Torres, V. Carreño and A. Redondas
Observatorio Atmosférico de Izaña, Instituto Nacional de Meteorología. C/ La Marina, 20, 38071 Santa Cruz de Tenerife, Spain. *ecuevas@inm.es*

SUMMARY

Meteorological and cloudiness conditions during the First National Spectroradiometer Intercomparison Campaign held in the "El Arenosillo" station (Huelva) in September 1999 are shown in this chapter. Hourly values of pressure, temperature, relative humidity and wind from an automatic weather station (EMA) managed by the Regional Meteorological Center of Western Andalusia (INM) at the El Arenosillo station are provided and discussed. Photosynthetical Active Radiation (PAR: 400 nm-700 nm integrated radiation) andCloud Transmission (CLT) are calculated, as parameters representative of cloudiness, from the measurements performed with a multi-channel moderated bandwidth filter radiometer NILU-UV from the INM-Izaña group. A daily value of precipitable water computed from measurements performed with a filter sunphotometer from the INM-Izaña group is provided. The precipitable water is validated against that integrated from the meteorological sounding launched on September 3.

RESUMEN

En este capítulo se muestran las condiciones meteorológicas y de nubosidad durante la Primera Campaña de Intercomparación de Espectrorradiómetros que tuvieron lugar en la estación de "El Arenosillo"(Huelva) en septiembre de 1999. Se muestran valores horarios de presión, temperatura, humedad relativa y viento de la estación meteorológica automática (EMA) que el Centro Meteorológico Territorial en Andalucía Occidental (INM) posee en la estación de El Arenosillo. Se ha calculado la radiación fotosintética activa (PAR: radiación integrada en el rango 400 nm-700 nm) y el factor de transmisión de nubes (CLT) como parámetros indicativos de la presencia de nubosidad, a partir de las medidas efectuadas con el radiómetro multicanal de ancho de banda moderada NILU-UV de INM-Izaña. Por último se proporciona un valor diario del contenido de agua precipitable a lo largo de la campaña, obtenido con el fotómetro solar de filtros Microtops-II de INM-Izaña, validándolo con un sondeo realizado el 3 de septiembre de 1999 en El Arenosillo.

3.1. WEATHER DURING THE CAMPAIGN

Surface pressure, geopotential height at 500 hPa, and Relative Humidity at 700 hPa analysis at 12 GMT from the INM-HIRLAM (Instituto Nacional de Meteorología-HIgh Resolution Limited Area Model), as well as NOAA-14 AVHRR images are shown in Figure 1. Surface pressure fields indicate a stable meteorological situation, in general, with high pressures over the El Arenosillo station, for the whole campaign period. The Azores high was present every day. However, a low over Western Portugal was located at 700 hPa and 500 hPa on September 1, 4 and 5, resulting in some cloudiness over its south-eastern flank, just over the El Arenosillo. On days 2 and 3 this low moved northward, to the West of Galicia, lessening its influence over south-western Spain. More stable conditions at all levels and clear skies were recorded at the end of the campaign, on September 6, 7 and 8 as is indicated by relative humidity analysis at 700 hPa and by satellite information.

3.2. IN-SITU METEOROLOGICAL INFORMATION

Meteorological information at the El Arenosillo has been obtained from the automatic weather station (EMA #08384), managed by the Regional Meteorological Center in Western Andalusia (INM). Hourly data of pressure, temperature and relative humidity (RH) from Day 244 to Day 251 (September 1-8 1999) are plotted in Figures 2, 3 and 4, respectively. Pressure ranged from 1 005 hPa to 1 011 hPa during the whole campaign (Figure 2). Two daily pressure peaks were observed at around 9 GMT and 21 GMT, respectively, while minima pressure values are observed at around 03 GMT and 16 GMT. The lowest pressure was recorded on September 1, 4 and 5, days when the low is observed at western Portugal.

The diurnal temperature variation ranged from 15°C to 25°C (Figure 3), except during the last day of the intercomparison when temperatures significantly increased, reaching a maximum of 28°C at noon. At 06 GMT, at sunrise, a sharp temperature increase is observed every day, peaking at around 13 GMT. The coldest days were September 1 and 4. The RH (Figure 4) is close to saturation during night time. As the temperature increases, the RH decreases showing a minimum of 60%-70% at noon. On September 8 the RH was significantly lower than that recorded during the rest of the campaign.

Ground heating and cooling drives the sea-to-land and land-to-sea breeze regimes, respectively. As can be seen in Figure 5, everyday a light breeze (2 m s^{-1} - 4 m s^{-1}) from the W-SW sector (from the sea) blows during daytime. During the night, calms or very light land breezes (from N-NE sector) is the normal regime.

3.3. RADIATION AND CLOUD TRANSMISSION

Sunrise and sunset times, as well as solar noon time corresponding to the first and last days of the campaign are shown in Table 1.

Table I. *Sunrise and sunset times on September 1and 8 1999 at El Arenosillo.*

El Arenosillo (37.1°N-6.7°W)	Apparent sunrise (GMT)	Solar noon (GMT)	Apparent sunset (GMT)
Day 244 (September 1st)	5.57	12:26:55	18:56
Day 251 (September 8th)	6.03	12:24:37	18:46

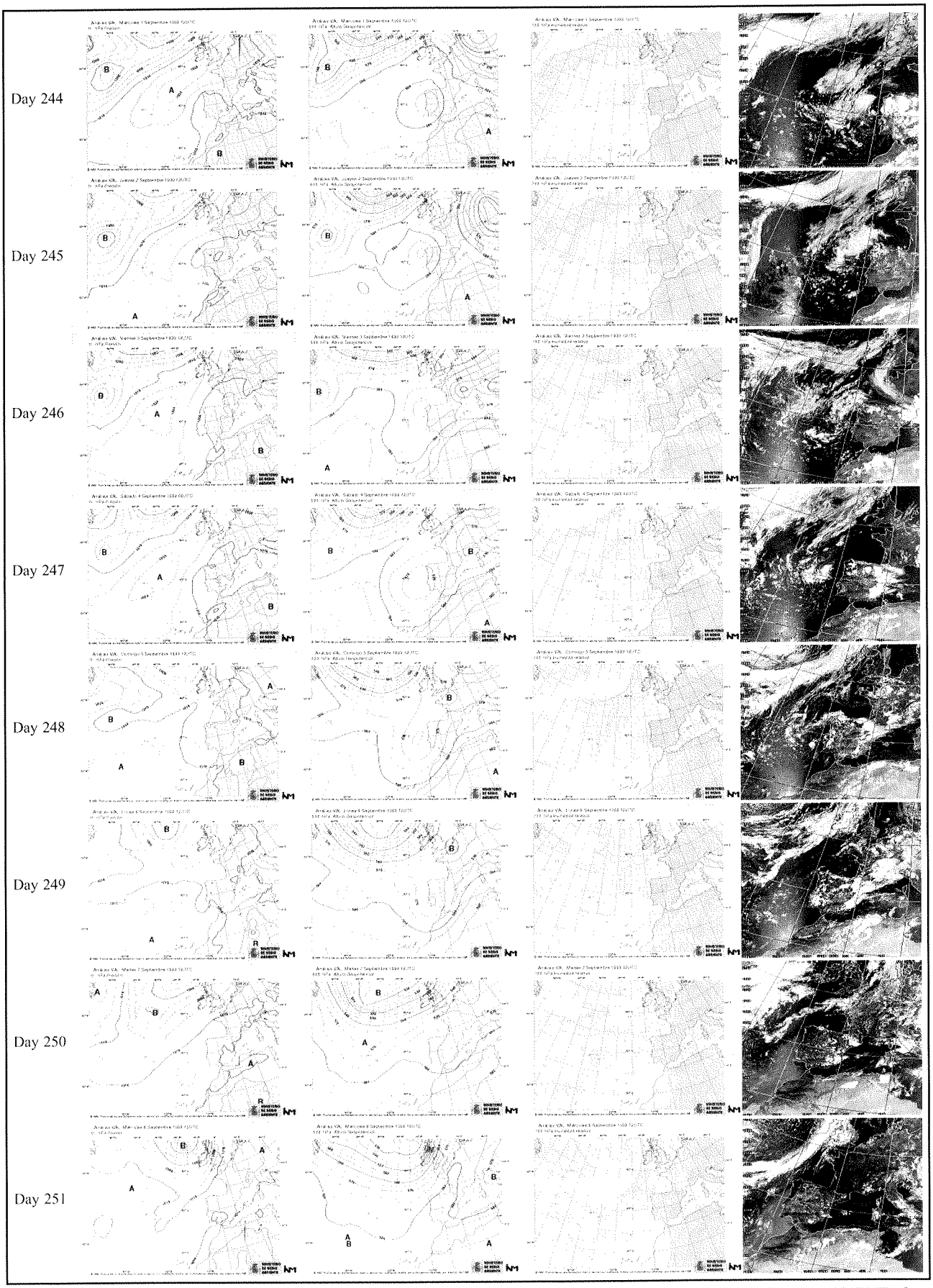

Figure 1. *Surface pressure (first column), 500 hPa geopotential height and 700 hPa relative humidity analysis (at 12 GMT) from the INM-HIRLAM model during the El Arenosillo campaign (September 1st-8th, 199; Days 244-251). NOAA-14 AVHRR visible channel images around 15:00 GMT are shown in the last column.*

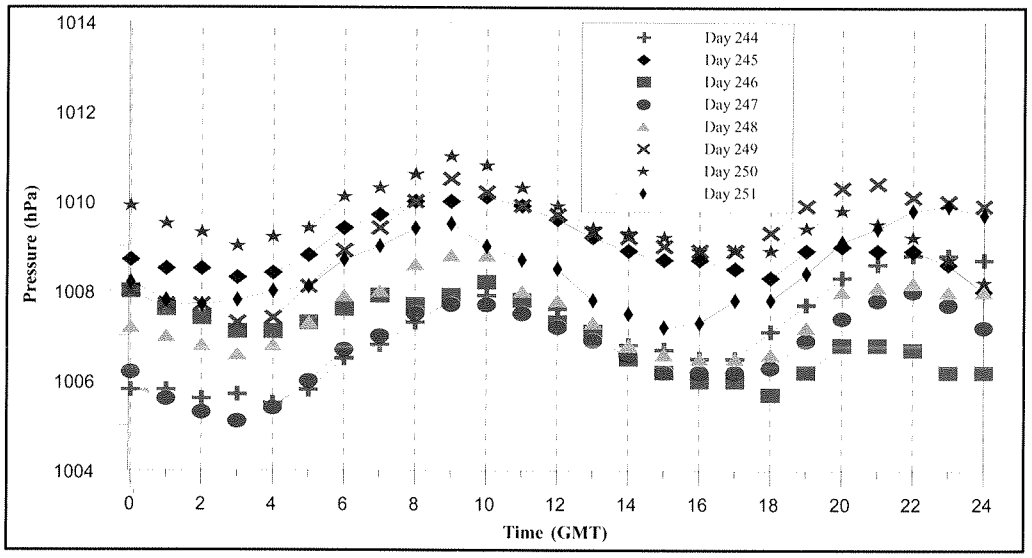

Figure 2. *Hourly pressure (hPa) at The Arenosillo station in the period September 1st-8th (Days 244-251) from the automatic weather station (EMA #08384), managed by the Regional Meteorological Center in the Western Andalusia (INM).*

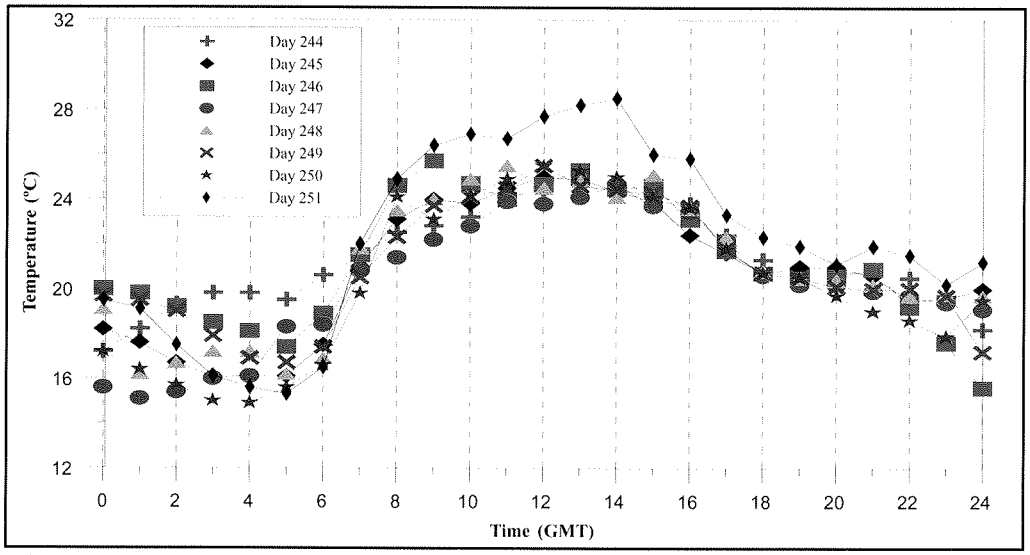

Figure 3. *Hourly temperature (ºC) at The Arenosillo station in the period September 1st-8th (Days 244-251) from the automatic weather station (EMA #08384), managed by the Regional Meteorological Center in the Western Andalusia (INM).*

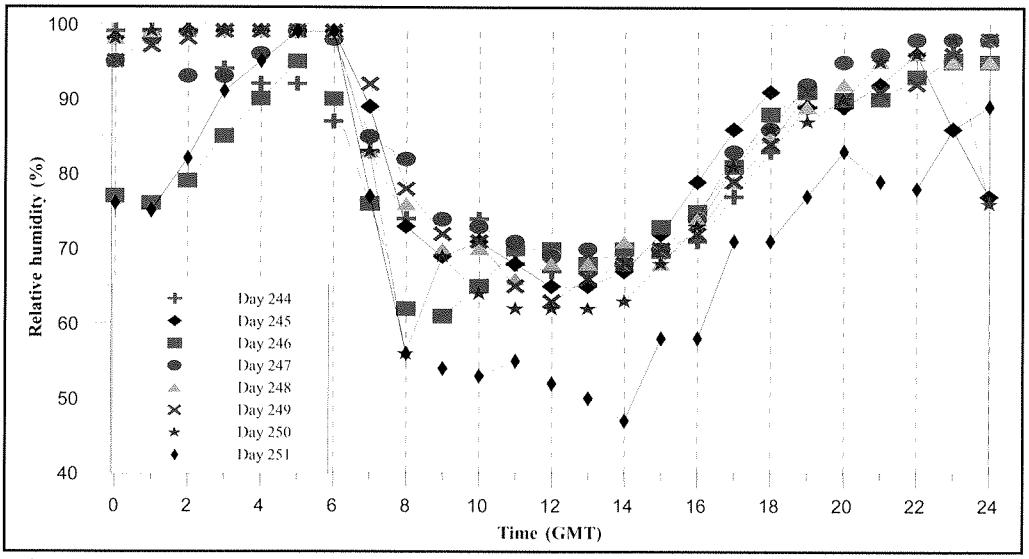

Figure 4. *Hourly relative humidity (%) at The Arenosillo station in the period September 1st-8th (Days 244-251) from the automatic weather station (EMA #08384), managed by the Regional Meteorological Center in the Western Andalusia (INM).*

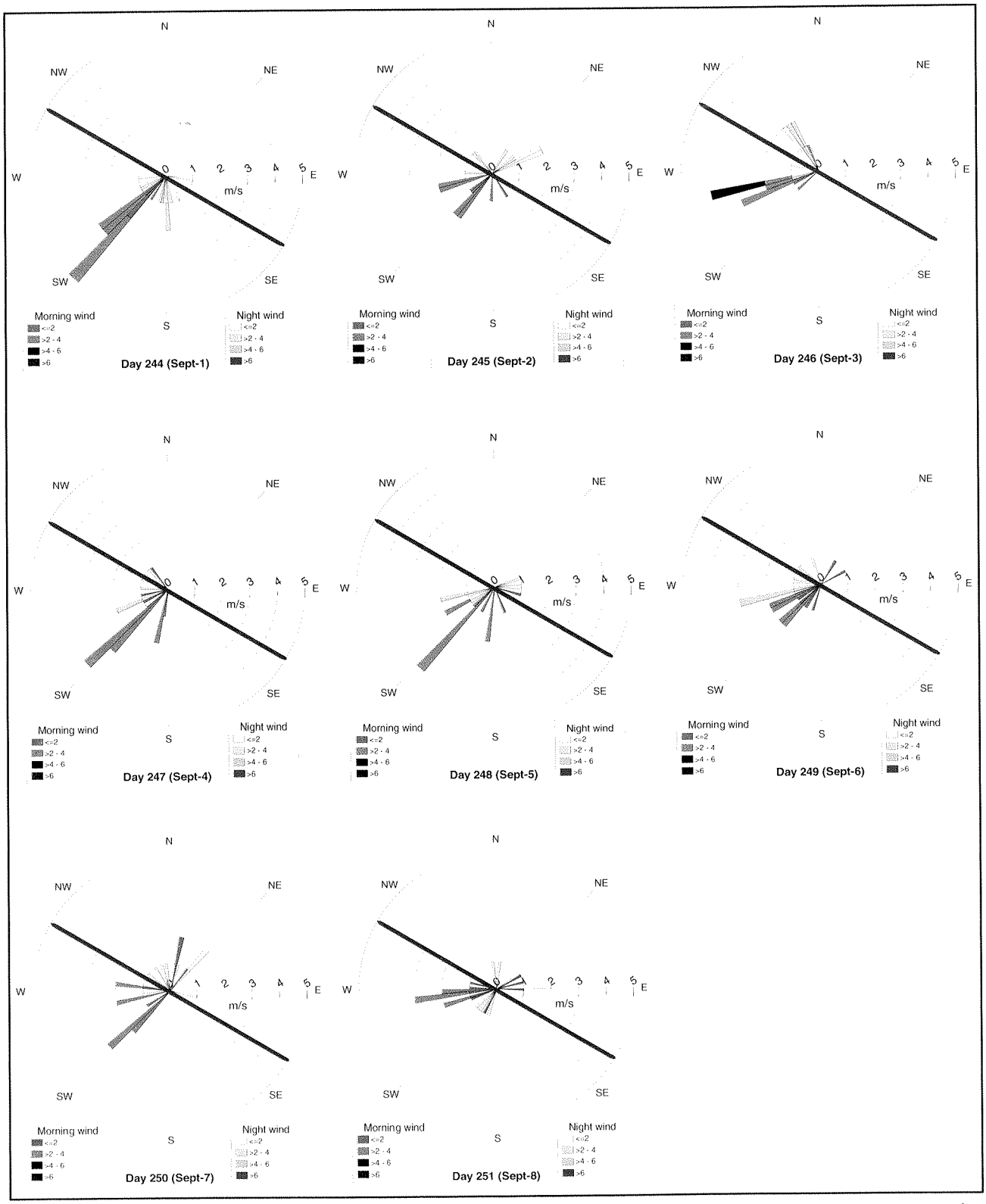

Figure 5. *Wind data at The Arenosillo station (EMA 08384) for the period September 1st-8th 1999 (Days 244-251). Brown bar indicates the coast line direction. In blue, wind in the morning. In yellow-red, wind during the night.*

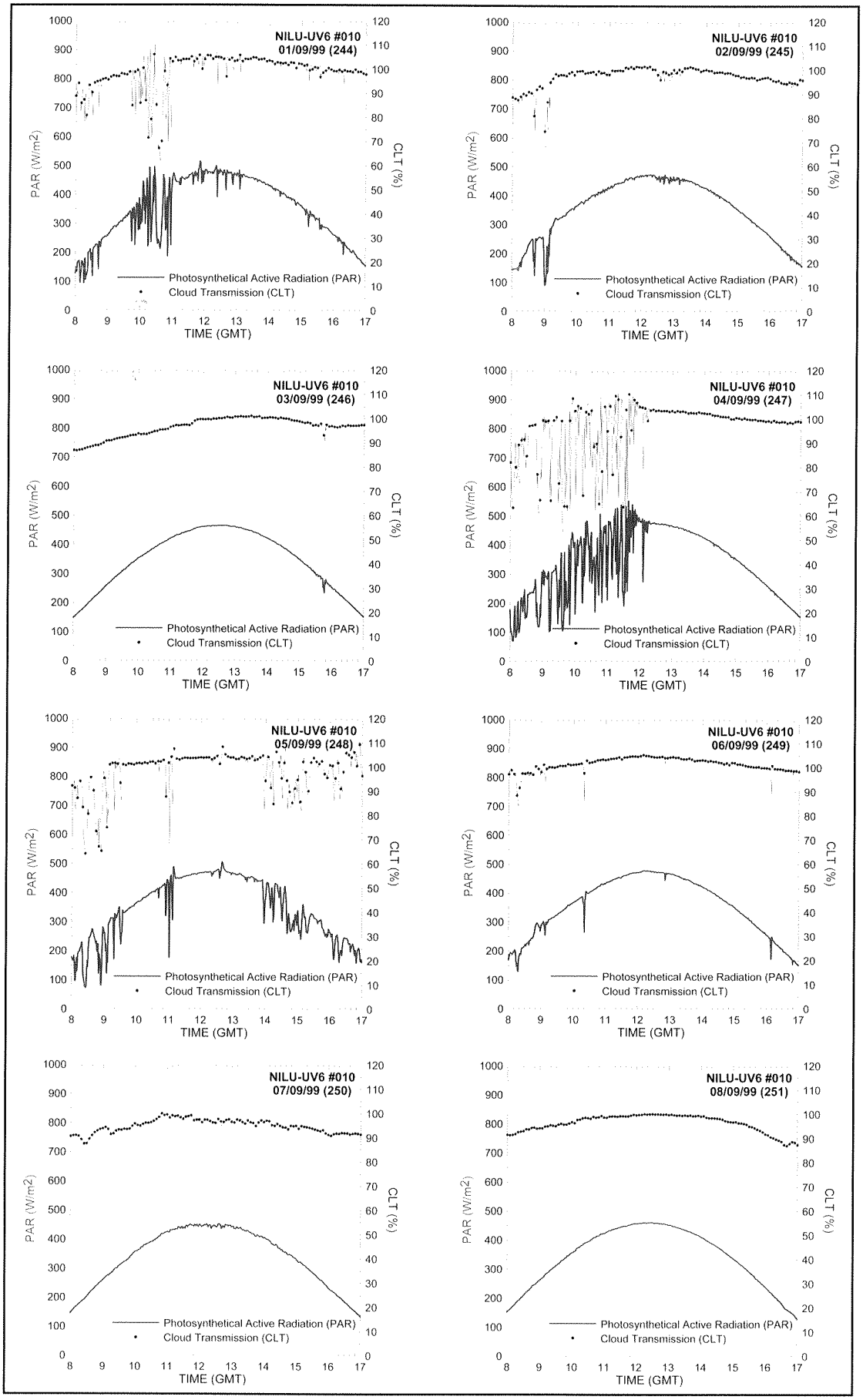

Figure 6. *One-minute Photosynthetical Active Radiation (PAR) and Cloud Transmission (CLT) at The Arenosillo station for the period September 1st-8th 1999 (Days 244-251).*

Photosynthetical Active Radiation (PAR), the integrated irradiance in the 400 nm-700 nm range is provided by the sixth channel of the multi-channel moderated bandwidth filter radiometer NILU-UV from INM-Izaña. PAR provides helpful information concerning cloudiness. In Figure 6 PAR is shown for the period September 1-8 (natural days 244-251).

The NILU-UV-6 measures the irradiance at 5 bands in the ultraviolet part of the spectrum: 305 nm, 312 nm, 320 nm, 340 nm and 380 nm, all with a bandwidth of approximately 10 nm. Irradiance at 340 and 380 nm is not affected by ozone absorption but are strongly affected by clouds (Mie scattering). The effect of clouds on UV penetration will, in general, depend on cloud type, height, and morphology. The influence of clouds on the irradiance reaching the ground may be quantified by comparing the measured irradiance to the anticipated clear sky value at a wavelength where the ozone absorption is minimum, i.e. 340 nm (Stamnes et al., 1991; Dahlback, 1996). Alternatively the cloud effect can be characterised by a ratio, the Cloud Transmission Factor (CLT), defined as the irradiance actually received by the instrument divided by the irradiance that would have existed under clear skies. If we use the 340 nm channel, the CLT is defined as follows:

$$CTL = I340(measured, SZA)/I340(clear\ sky, SZA) * 100$$

Where the measured and clear-sky values of the irradiance in the 340 nm channel is taken at the actual zenith angle (SZA). In addition to clouds, the CLT is strongly affected by surface albedo. However the albedo at El Arenosillo is quite low (0.2) because the station is in the middle of dense pine(-tree) forest by the sea. CLT is plotted together with PAR in Figure 6.

From PAR and CLT plots we can see that days 245, 246, 249, 250 and 251 are almost clear days. Day 247 in the afternoon also shows good sky conditions. On days 244, 247 in the morning,and days 248 and 249 variable cloud cover was present. The observed CLT higher than 100% occurs in situations of broken cloud cover when clouds appear to be the sun but this is not blocked by the clouds. In such a situation the direct radiation equals the clear sky scenario, but the diffuse radiation is enhanced compared with the clear sky situation, due to increased scattering by clouds close to the sun. Under these circumstances the instruments performing direct sun measurements should not be affected, whereas the instruments measuring global radiation might be influenced.

3.4. COLUMN WATER VAPOR CONTENT

The precipitable water, or column water vapor content (CWV) (in cm) gives us an idea of the marine aerosols contained in the marine mixing layer, since all the days of the intercomparison campaign were quite stable under the meteorological point of view. So, it can be assumed that most of the CWV is concentrated in this layer. The CWV measurement is based on a pair of radiometric measurements in the infrared band. The 936 nm filter is located in the water absorption peak, while the 1 020 nm filter is only affected by aerosol scattering. A detailed discussion of the CWV retrieval with the Microtops-II and other radiometers is performed by Cachorro et al. (2003) (Chapter 9 of this Report). However, in this chapter we are only interested in relative variations of this parameter through the campaign period. In Figure 7 the daily CWV obtained with the Microtops-II sunphotometer from INM-Izaña is shown and compared with those computed from the meteorological radiosounding launched on September 3 at noon at El Arenosillo (Figure 8), and the radiosoundings performed at theby station of Gibraltar. The agreement is fairly good although a systematic offset is observed between both records.

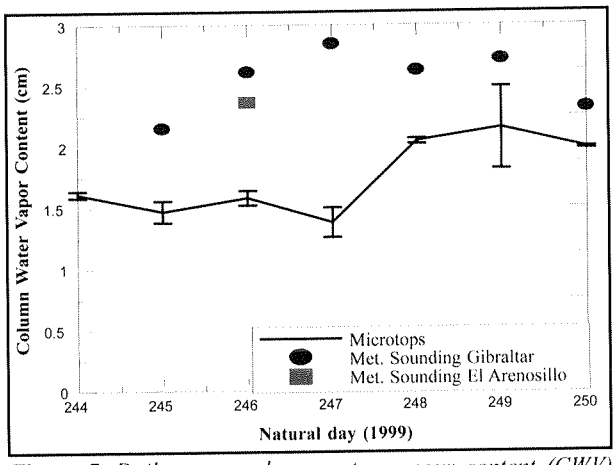

Figure 7. *Daily mean column water vapour content (CWV) obtained with the Microtops-II sunphotometer from INM-Izaña (line), with the corresponding standard deviation. CWV integrated from the meteorological radiosounding launched on September 3rd at noon at El Arenosillo (full square), and from the radiosoundings performed at the near station of Gibraltar (full circles).*

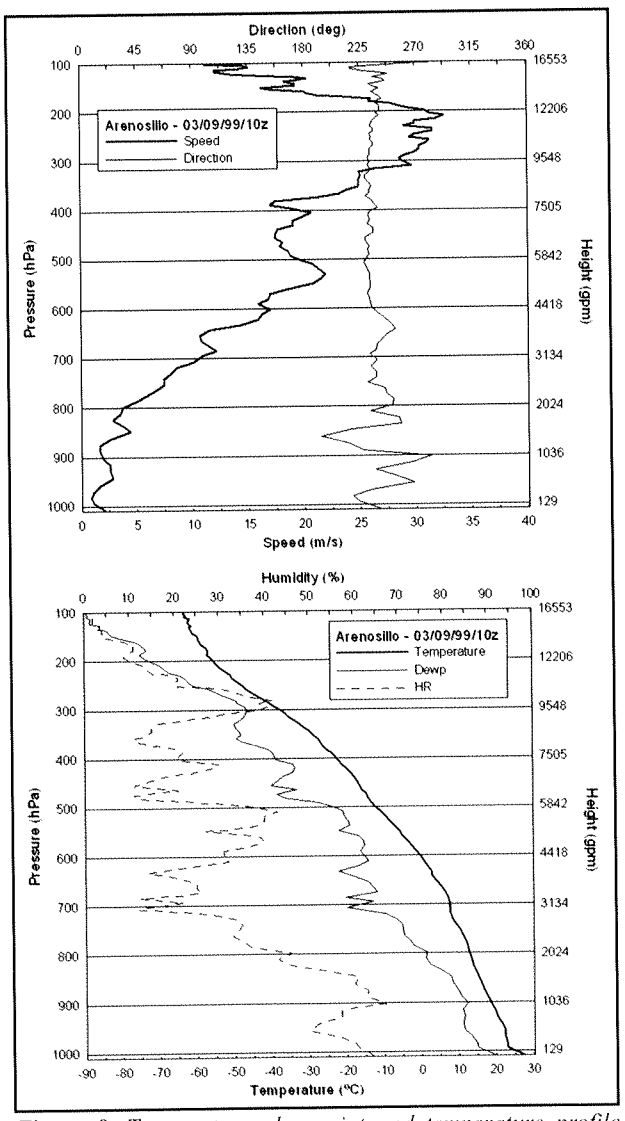

Figure 8. *Temperature, dew-point and temperature profile (down), and wind speed and direction profile (up) from the radiosounding launched on September 3rd at 10 GMT at The Arenosillo station. A jet stream is found at about 250 hPa.*

From the meteorological vertical profile (Figure 8) it can be deduced that the marine mixing layer is to the first 1 000 m a.s.l. A jet stream is found at about 250 hPa with associated wind speed higher than 30 m s^{-1} from SW.

3.5. CONCLUSIONS

Clear skies dominated during the El Arenosillo campaign, and a number of days were quite suitable for performing radiation and total column ozone calibrations. September 2, 3, 6, 7 and 8 showed specially clear and clean skies. The weather was, in general, quite stable and the in-situ meteorological conditions were quite similar throughout the campaign. The only outstanding meteorological feature at the site was the extremely high relative humidity recorded during the night (saturation) which meant a major effort to keep the instruments dry.

ACKNOWLEDGEMENTS

This work was funded by CICYT under Project CLI97-0345-CO5. We wish to thank the Director of the Regional Meteorological Center in Western Andalusia (INM), Mr. José Ramón Marín, for providing meteorological information at the El Arenosillo station, as well as Dr. Benito de la Morena, from the El Arenosillo station (INTA) for launching the meteorological sounding on September 3.

Satellite images courtesy of the University of Dundee: (http://www.sat.dundee.ac.uk/).

REFERENCES

CACHORRO, V., R. VERGAZ and A. M. DE FRUTOS, 2003: Determination, monitoring and comparison of atmospheric components: aerosol parameters (aerosol optical depth and radiative properties) and water vapour. Chapter 9 in this Report.

DAHLBACK, A., 1996: Measurements of biologically effective UV doses, total ozone abundances, and cloud effects with multichannel, moderate bandwidth filter instruments. *Appl. Opt.*, Vol. 35., No. **33**, 6514-6521.

STAMNES, K., J. SLUSSER and M. BOWEN: 1991: Derivation of total ozone abundance and cloud effects from spectral irradiance measurements. *Appl. Opt.*, **30**, 4418-4426.

CHAPTER 4
INSTRUMENTS: MAIN CHARACTERISTICS

J. M. Vilaplana
INTA / Atmospheric Sounding Station "El Arenosillo", Huelva, Spain, *vilaplanagjm@inta.es*

4.1. DOBSON SPECTROPHOTOMETER

4.1.1. Description of the Instrument

The principle of operation of the Dobson spectrophotometer is based on an optic system of double monocromator that we will explain briefly with reference to the Figure 2.

The solar light enters in the instrument through a window located in the upper part of the instrument, after being directed by a mirror mounted in a periscope, and after being reflected in a total reflection prism, it goes through the slit S1 to the spectroscope. This spectroscope is formed by a quartz lens that completes a double mission: to colimate the radiation coming from the slit (to create a parallel beam) and to collect the light later, once broken up into its spectral colours by the first monocromator; a prism (first monocromator) that breaks up the light in its spectrum; and a mirror that reflects the light through the prism and the lens to form a spectrum in the focal plane of the instrument. The required wavelengths are isolated by means of the slits S2, S3 and S4 located in the focal plane of the instrument that acts therefore as a polychromatic.

Two shutter bars are mounted in the base of the spectrophotometer. The S4 is only used in the tests of the spectrophotometer and it should remain pushed all in the instrument to carry out ozone observations. The wavelengths selector rod, blocks the exit of the light that passes through the slits S2 or S4. With this rod in the short, alone position are open the slits S2 and S3 and the observation can be made with the pairs of wavelengths TO, B, C or D. With the wavelengths selector rod in the long, alone position the slits S3 and S4 are open and observations can only be carried out with wavelengths C'.

Selecting the wavelengths A, C, C' or D, the measures of ozone will be made in a precise way rotating the wedges Q1 and Q2 in order to adjust the position of the wavelengths required in the focal plane of the instrument according to the position specified in the Q Settings Table provided with the instrument, in accordance with the pair that we want to select (Q2) and the changes in the index of refraction of the optic elements (glasses and quartz prism) due to the changes in the temperature of the instrument (Q1).

An optic wedge of variable transmittance, constituted by two similar glasses of chromed quartz, is mounted in front of the slit S3. The position of the wedge is controlled by a wheel with a graduate dial located above the instrument. With the dial located in 0 degrees, this optic wedge is located in front of the slit S3 so that the light passes practically through the wedge and the slit S3 without loss of intensity. With the dial in the position of 300 degrees, the light that passes through the slit S3 is totally absorbed by this chromed wedge. Therefore, it is necessary to rotate the dial from 0 up to 300 degrees until finding the position in which the intensity of the light that passes through the wedge and the slit S3 has been reduced to

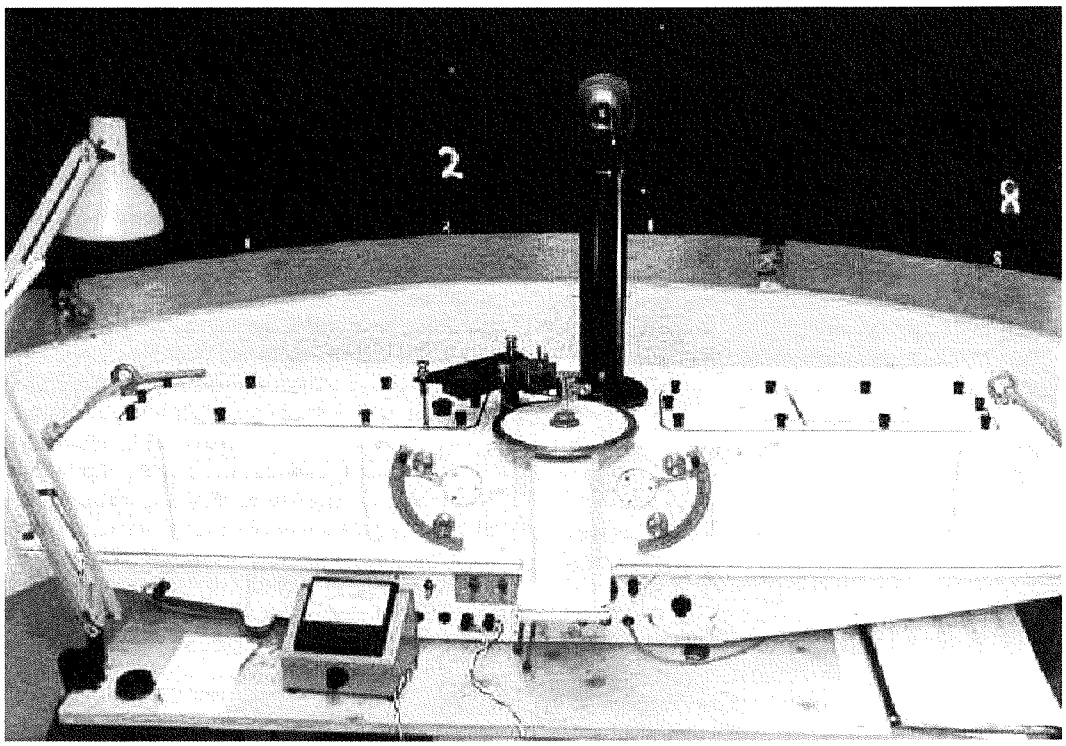

Fig. 1. View of the Dobson #120 operative at "El Arenosillo".

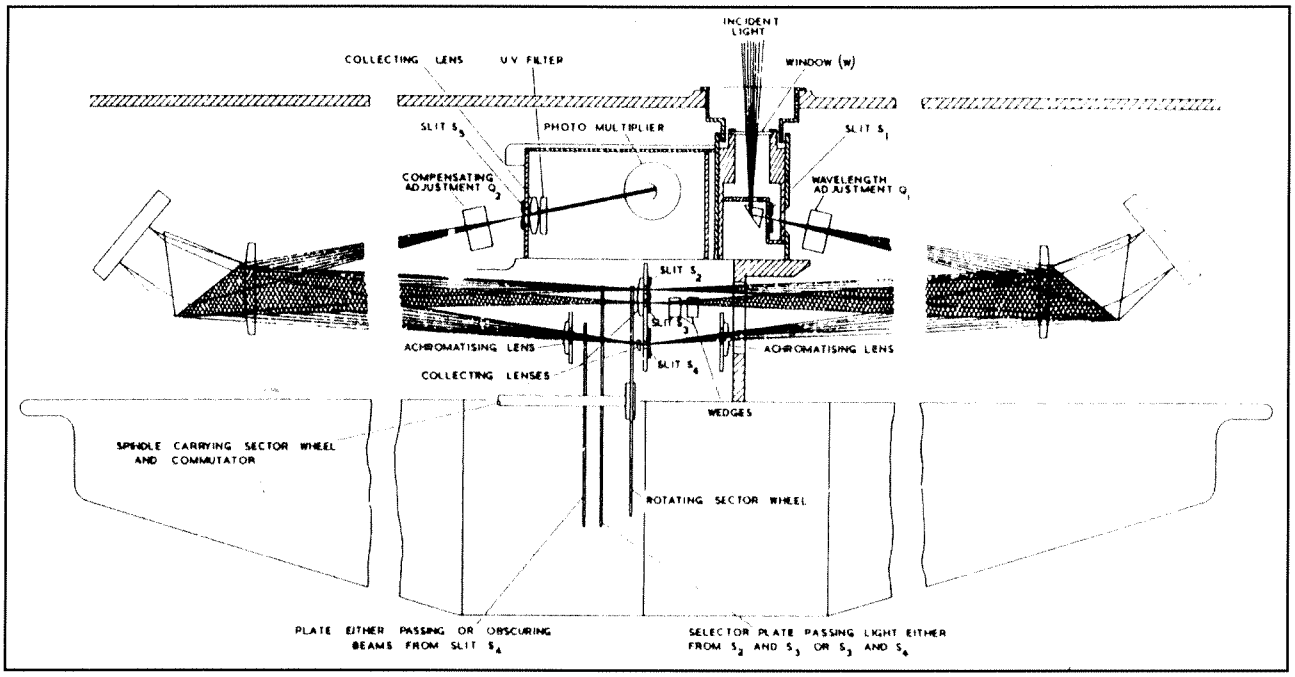

Fig. 2. *Optical system of the Dobson spectrophotometer (Komhyr, 1980).*

the level of the intensity of the light of wavelengths that go by the slit S2 (or the wavelengths of the slit S4 if we carry out the observations with C' pair). For the possible positions of the dial, the intensity of the light that passes through the chromed wedge is attenuated in a defined reason that was determined during the original calibration of the spectrophotometer. thus, to measure the order of the relative intensities of the two wavelengths of the observation, it will be necessary only to determine the position in the dial in with we have been able to equal the intensities of the two wavelengths.

The determination of this position in the dial is made in the following way: in the initial position of the dial, the two beams leaving the slits S3 and S2 (or S4) are of unequal intensities. The light beams then pass through a rotating selector wheel, driven by a motor, which selects the wavelength that allows the two beams to proceed alternately in the second monocromator and finally to reach the photomultiplier located after the slit S5. The purpose of the second monocromator is to eliminate the effect of the scattered light that we don't want to measure (other wavelengths) in its journey through the optic systems of the instrument (straylight). As the two beams that arrive alternately to the photomultiplier they have different intensity, the photomultiplier generates an electric current that is amplified by an alternating current amplifier to the exit of the photomultiplier, it is rectified by a switch, and it is registered by a microamperimeter. If we now rotate the dial attenuating the intensity of the beam without ozone absorption until equalling their intensity to that of the beam that presents a bigger ozone absorption, the two faces that impact alternately in the photomultiplier will make it with the same intensity, so that we will find the exit of the photomultiplier a continuous current, which won't be amplified by the amplifier of alternating current and consequently, the microamperimeter will read zero. The microamperimeter reading zero indicates us that the dial is in the balance position that as we have previously mentioned, it is calibrated according to some charts characteristic of the instrument.

4.1.2. Measure procedure: principle of operation and methodology

The measure of the total content of ozone with the Dobson spectrophotometer is based on measuring the relative difference of the intensity with which we receive the ultraviolet radiation emitted directly by the Sun or the Moon in different pairs of wavelengths, according to the law of Beer and, in an indirect way, for the brightness of the zenith.

These pairs of wavelengths are those previously mentioned as A, C, C' and D that expressed in nanometers correspond to:

A	C	C'	D
305.5 – 325.4	314.4 – 332.4	332.4 – 453.6	317.6 – 339.8

The pair A for example, consists of 305.5 nm which is strongly absorbed by the ozone, and of 325.4 nm which arrives to us with more intensity due to a poor absorption by the ozone. The extraterrestrial intensities registered in these two wavelengths are essentially the same. In the path of both beams through the atmosphere, both rays are attenuated by the scattering of the molecules of air (Rayleigh) and by the aerosols; additionally, $\lambda = 305.5$ nm is strongly attenuated when crossing the ozone layer, while the attenuation registered for this reason to $\lambda = 325.4$ nm is relatively poor. Therefore, an increment in the total ozone content present in the atmosphere is translated into a bigger absorption in $\lambda = 305.5$ nm with its rising loss of intensity, while $\lambda = 325.4$ nm remains practically unalterable.

The observations are carried out according to the recommendations from the OMM to some certain solar angles. In practice, all the observatories equipped with this system carry out five daily observations to some μ preset whenever the meteorological conditions allow it.

For an observation of the total ozone content with a pair of wavelengths like A, C, D or C', the equation can be expressed as:

$$X = \{N - (\beta - \beta')m - (\delta - \delta')\sec(z)\}/(\alpha - \alpha')\mu$$

Where:

X = The total amount of ozone in Dobson (D.U.) and N is the total atmospheric optical depth:

$$N = L - L' = \log \frac{I}{I_0} - \log \frac{I_0'}{I'} = \log \left[\frac{I}{I_0} \frac{I'}{I_0'} \right]$$

I_0 & I'_0 = intensities of radiation outside the atmosphere for the selected pair of wavelengths.

I & I' = intensities of the radiation in the instrument for the selected pair of wavelengths.

β & β' = scattering coefficients due to the air molecules in the atmosphere for the selected pair of wavelengths.

δ & δ' = scattering coefficients for particulate meter in the atmosphere for the selected pair of wavelengths.

α & α' = absorption coefficients for the ozone for the selected pair of wavelengths.

m = the equivalent path-length of sunlight through the atmosphere allowing the refraction and curvature of the earth.

p y p_0 = the atmospheric pressure at the observatory and at the sea level.

z = the solar zenith angle.

μ = the relative path-length of sunlight through the ozone layer (ozone supposed situated at 22 km).

$$m = \{\sec z - 0.0018167(\sec z - 1) - 0.002875(\sec z - 1)^2 - 0.0008083(\sec(z-4)^3\} p/p_0$$

$$\mu = \frac{(R + h)}{\sqrt{(R + h)^2 - (R + r)^2 \sin^2 z}}$$

Where: R = the radio of the earth (6371.23 km);
r = the observatory altitude above the sea level;
h = the ozone layer altitude above the sea level.

The difficulty in this expression is presented when evaluating the term $\delta - \delta'$ corresponding to the scattering coefficient for aerosol. Due to this, what is made in practice is to measure in two pairs of wavelengths.

In practice, all the measures are made and indexed to the pairs AD which are those recommended by the International Ozone Commission. Other pairs are selected in those stations where it is not possible to make measures to direct sun which is the requirement to use the pairs AD. Therefore the previous expression can be rewritten for the pair A and D to eliminate the scattering effect of the aerosol.

$$X_A = \frac{N_A}{1.748\mu} - 0.066 \frac{m}{\mu} - \frac{(\delta - \delta')_A}{1.748} \frac{\sec(z)}{\mu}$$

$$X_D = \frac{N_D}{0.360\mu} - 0.289 \frac{m}{\mu} - \frac{(\delta - \delta')_D}{0.360} \frac{\sec(z)}{\mu}$$

$$X_{AD} = \frac{N_A - N_D}{1.388\mu} - 0.066 \frac{m}{\mu} - \frac{(\delta - \delta')_A - (\delta - \delta')_D}{1.388} \frac{\sec(z)}{\mu}$$

As the scattering for aerosols in the pair A and D is similar, we can eliminate the last term and the expression will be:

$$X_{AD} = \frac{N_A - N_D}{1.388\mu} - 0.009 \frac{m}{\mu}$$

Where N_A and N_D have been determined by reading the dial of the spectrophotometer Dobson.

4.1.3. Maintenance and tests of routine of the spectrophotometer Dobson

To guarantee the good operation of the system and the reliability of the registered data, it is necessary clean certain components that accumulate dust, when necessary (trying to reduce to the minimum the occasions in which the optic components are manipulated), it is recommended to maintain the instrument at 23°±5°C (although it is made a correction in temperature with Q1, outside of this range the measure loses reliability progressively). Once a month there are carried out test of mercury lamp and test of standard lamp and case of being necessary the derived correction factors are applied from the test to the data registered from the last calibration.

The aim of the mercury lamp test is to detect possible mechanical deformations or movement of some optic component, what would modify the wavelengths that cross the slits S2, S3 and S4. As routine checking, it is enough to measure the value of Q1 when the peak of intensity of 312.9 nm goes through the centre of the slit S2. The test should be carried out at different temperatures with the purpose of determining possible dependences with them.

The object of the test of standard lamp is to verify that the calibration of the spectrophotometer is stable and if the gradient of the wedge in the region in which we work remains constant and it doesn't vary during the period of measures.

The spectrophotometer Dobson is a robust and stable system in spite of the years lapsed since its commercialisation. It has been chosen as the standard instrument for the measure of the total content of ozone in the world net and it is used for the validation and calibration of measures with satellite.

Nevertheless the system presents certain limitations as: the impossibility of discriminating against the absorption due to the ozone of the one taken by SO_2 and NO_2 and the fact that the system is totally manual, with the consequent dependence on an operator that can induce certain errors in the measures as well as the problem of the lack of measurements outside labour schedule and on holidays.

4.2. BREWER SPECTROPHOTOMETER

4.2.1. General description

The Brewer spectrophotometer is made for outdoor use. It is designed to measure spectral UV solar radiation, total ozone content, SO_2 (NO_2 optional) and to determine vertical

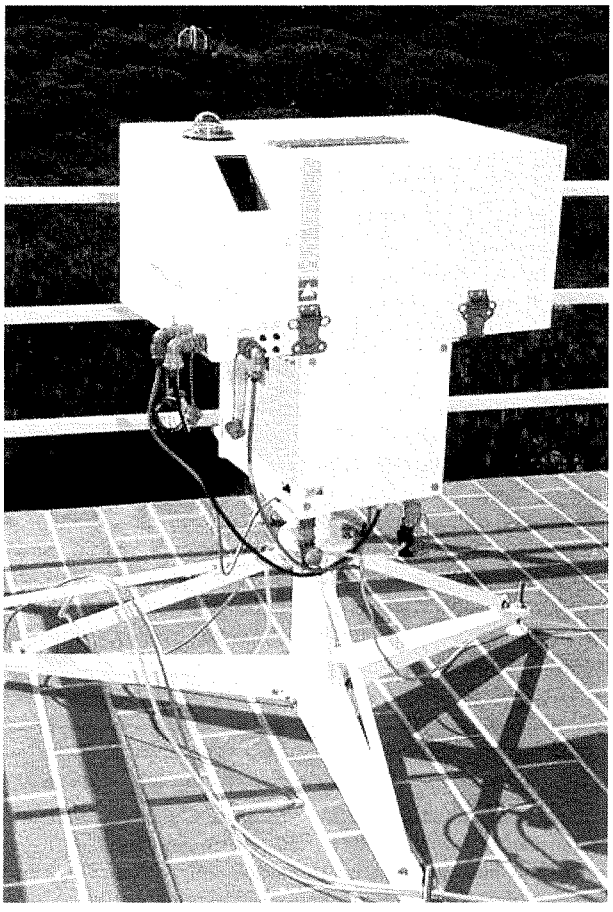

Fig. 3. View of the Brewer MK-III #150 operative at "El Arenosillo".

profiles of ozone in the atmosphere using the Umkehr method. This system works in a completely automatic way assisting to a series of commands preset in a schedule.

The complete system is constituted by a tripod, a tracker or system of pursuit azimuth on which the sealed box is mounted to harbour the spectrophotometer and a computer PC from which the system is controlled and it stores the registered information.

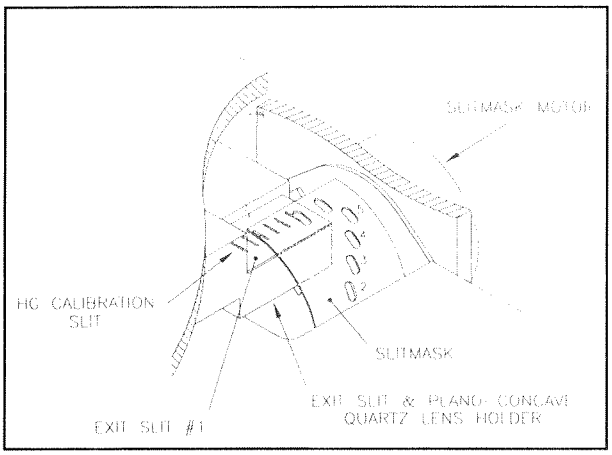

Fig. 4. *Slit mask assembly (Operator's manual).*

The spectrophotometer consists of an optic system of entrance, which has two possibilities, through a dome or through a prism that points directly to the sun. The election of the receiver will be made according to the observation type (direct sun, ultraviolet zenith, global irradiance or calibration lamps). The sitting of sun as well as the attenuation of the beam by means of two filter wheels to adapt the level of the signal to the operation range of the system to avoid that it is saturated is made in an automatic way.

The spectrophotometer is a modified Elbert that in the case of the Brewer MK-III, is constituted by a double monocromator that operates with a holographic grating of diffraction. The first monocromator disperses the light in the focal plane where six exit slits are positioned for the corresponding wavelengths (λ=302.2 nm used in the calibration with mercury lamp, λ_1=306.6 nm, λ_2=310.1 nm, λ_3=315.5 nm, λ_4=316.8 nm and λ_5=320.1 nm) with a resolution (FWHM) of 0.6 nm. The second monocromator has the function of filtering the stray light.

The instrument has two operation possibilities: a quick one, employed for the measure of the total content of ozone (3 min to direct sun, 4 min to the zenith) measuring the five wavelengths cyclically while the diffraction grating remains fixed, and other slow (8-9 min) in the ultraviolet measure, in which the diffraction grating moves carrying out two scans (up and down) between 286.5 nm and 363 nm.

The light coming from the second monocromator, is focused by means of a Fabry lens to the photomultiplier (low noise EMI 9789QA). The PC communicates with the spectrophotometer by means of a connection RS-232.

The calibration of the instrument stays as well in an automatic way by means of a halogen internal lamp of tungsten and the spectral lines of a mercury lamp.

The figures 4, 5 & 6 illustrate the internal configuration of the Brewer MK-III.

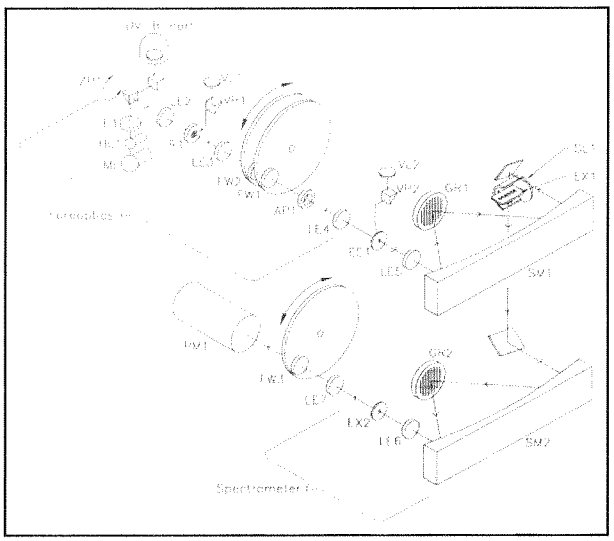

Fig. 5. *Diagrammatic view of the optical elements (Operator's manual).*

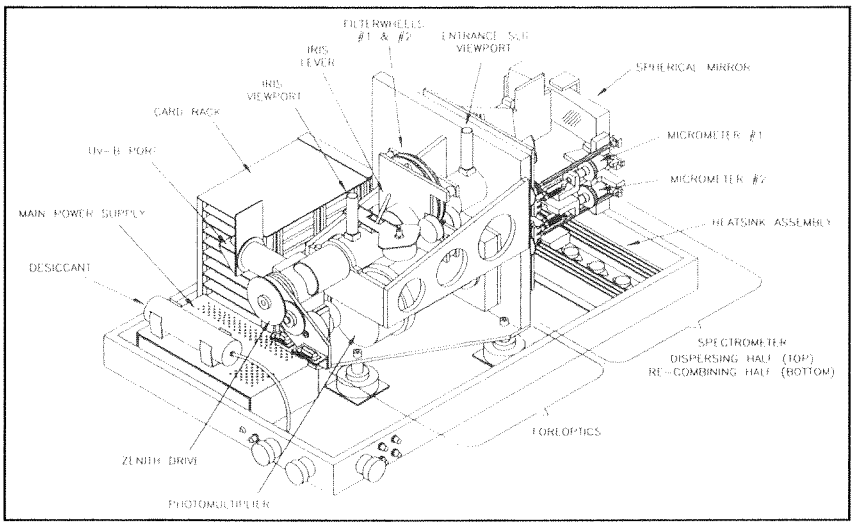

Fig. 6. *View of spectrophotometer with top cover removed (Operator's manual).*

4.2.2. Measurements of the Total Ozone Content with the Brewer Spectrophotometer

The principle of measure of the spectrophotometer Brewer is the same one as that of the Dobson. The total ozone content is calculated by relative measures from the intensity of light to certain wavelengths, which are five in the case of the Brewer instead of the pairs of wavelengths used by the Dobson.

The spectrophotometer Brewer measures the intensity of the light in the ultraviolet absorption spectrum of the ozone in five wavelengths with a resolution of 0.6 nm: $\lambda_1 = 306.3$ nm, $\lambda_2 = 310.1$ nm, $\lambda_3 = 313.5$ nm, $\lambda_4 = 316.8$ nm and $\lambda_5 = 320.1$ nm. The SO_2 present a strong absorption in this spectral region overlapped partly with the absorption by the ozone. The first one (λ_1) is located in a maximum of absorption of the SO_2, while λ_2 and λ_5 present considerably less absorption.

The measure of the intensity of the direct solar radiation at each of these five wavelengths can be expressed according to the law of Beer as:

$$\log I_\lambda = \log I_{0\lambda} - \beta_\lambda m - \delta_\lambda \sec\theta - \alpha_\lambda O_3 \mu - \alpha^1_\lambda SO_2 \mu^1 \quad (1)$$

Where:

I_λ = the measured light intensity at λ.
$I_{0\lambda}$ = the measured extra terrestrial light intensity at wavelength λ.
β_λ = the Rayleigh scattering coefficient at λ.
m = the number of atmospheres along the incident light path.
δ_λ = the aerosol scattering coefficient at λ.
$\sec\theta$ = the secant of the solar zenith angle.
α_λ = the ozone absorption coefficient at λ.
O_3 = the column amount of ozone.
μ = the effective geometric enhancement of the solar path through the ozone column.
α^1_λ = the SO_2 absorption coefficient at λ.
SO_2 = the column amount of SO_2.
μ^1 = the enhancement of the solar path through SO_2.

The light intensity measurements given in eq. 1 for the Brewer wavelengths 2 and 5 may be combined to give the following expression:

$$F = F_0 - \Delta\beta m - \Delta\delta \sec\theta - \Delta\alpha O_3 \mu - \Delta\alpha^1 SO_2 \mu^1 \quad (2)$$

Where:

$F = \log I_2 - 0.5 \log I_3 - 2.2 \log I_4 + 1.7 \log I_5$
$F_0 = \log I_{02} - 0.5 \log I_{03} - 2.2 \log I_{04} + 1.7 \log I_{05}$
$\Delta\beta = \beta_2 - 0.5\beta_3 - 2.2\beta_4 + 1.7\beta_5$
$\Delta\delta = \delta_2 - 0.5\delta_3 - 2.2\delta_4 + 1.7\delta_5 = 0$
$\Delta\alpha = \alpha_2 - 0.5\alpha_3 - 2.2\alpha_4 + 1.7\alpha_5 \neq 0$
$\Delta\alpha^1 = \alpha^1_2 - 0.5\alpha^1_3 - 2.2\alpha^1_4 + 1.7\alpha^1_5 = 0$

Ozone measurements made with the Brewer as well as the Dobson suggests that δ is a slowly varying monotonic function of wavelength. The weighting coefficients of 1, –0.5, –2.2, 1.7 have been selected to make such a function negligible. These weighting coefficients also give a negligible value for the effective SO_2 absorption coefficient $\Delta\alpha^1$. If the eq. 2 is rewritten ignoring the negligible terms the following expression results:

$$F + \Delta\beta m = F_0 - \Delta\alpha O_3 \mu \quad (3)$$

Once the values of F_0 and $\Delta\alpha$ are known, it is possible to determine the total content of ozone substituting the measure of F in the expression (3).

The measure of the total content of SO_2 is calculated by the combination of the measured intensities of light in the following way:

$$S + \Delta^*\beta m = S_0 - \Delta^*\alpha O_3 \mu - \Delta^*\alpha^1 SO_2 \mu^1 \quad (4)$$

Where:

$S = \log I_1 - 4.2 \log I_4 + 3.2 \log I_5$
$S_0 = \log I_{01} - 4.2 \log I_{04} + 3.2 \log I_{05}$
$\Delta^*\beta = \beta_1 - 4.2\beta_4 + 3.2\beta_5$
$\Delta^*\alpha = \alpha_1 - 4.2\alpha_4 + 3.2\alpha_5$
$\Delta^*\alpha^1 = \alpha^1_1 - 4.2\alpha^1_4 + 3.2\alpha^1_5 \neq 0$

In the above expression, significant absorption appears for SO_2 content. Once are known S_0, $\Delta^*\alpha$ and $\Delta^*\alpha^1$, the total amount of SO_2 is determined substituting the total content of ozone calculated in (3) and the measures of the intensities of light measured in the equation (4).

4.2.3. Measurements of the ultraviolet global irradiance with the Brewer

As we have mentioned before, there are Brewer spectrophotometers which mount a single monocromator (MK-II and MK-IV) with a measure range from 290 to 325 nm and the Brewer MK-III that mounts two monocromators and have a measure range from 286.5 to 363 nm. To determine of the total ozone content, five wavelengths are measured cyclically by means of a slits mask that select each wavelengths alternately. However, in the case of the spectral solar ultraviolet irradiancie measurements, it is the grating the one that moves carrying out two scans (up and down) between 286.5 and 363 nm, this process takes about 8 or 9 minutes.

4.2.4. Quality guarantee and maintenance of Brewer Spectrophotometer

1) General considerations

The quality of the data obtained with the spectrophotometer depends on the quality of the instrument as well as on the maintenance and the its supervision. Same importance has the auxiliary information, used for the analysis of the registered data. Subsequently we will expose the main aspects that characterize the instrument and the quality of the registered data, for which, we will follow the approach and recommendations of G. Seckmeyer.

The specifications that should complete the spectrophotometer, are conditioned by the requirements of the investigation lines in the environment of the ultraviolet radiation and their effects. These general objectives can be summarized basically in:

- To create databases by long-term monitoring of UV measures with climatological purposes.
- To be able to detect trends in the global ultraviolet irradiance, especially spectrally resolved.
- To provide datasets for radiative transfer models validation and the irradiancie at the earth's surface determined by satellites.
- To determine the geographical differences in the global spectral ultraviolet irradiance.
- To determine the radiation levels effective UV and the ultraviolet index UVI.

These objectives force to guarantee a great precision of the measures and excellent stability in long periods, able to detect very subtle tendencies. On the other hand, the instrumental requirements to determine the dose effective UV and the ultraviolet index for information to the population are less strict.

2) Detection of changes in the UV irradiance

The main interest of the UV radiation measures, is its increment due to the decrease of the total column of ozone. Therefore, it would be desirable to be able to detect changes in the UV spectral irradiance due to a variation of 1% in the vertical column of ozone.

The experience shows that the minimum uncertainty that can be established in instruments of ultraviolet spectral irradiance measurement is of the order of +5%. The uncertainty of the instrument occurs especially in short wavelength which is the most critical region where small changes in the total content of ozone can cause relatively big changes in the irradiance.

Quantitatively, it is considered that for a change of 1% in the total content of ozone and for a solar zenith angle SZA = 70°, the variations more significant are in short wavelengths. For overhead sun, a radiation change of 5% occurs at approximately 295 nm, when the absolute change in irradiance is about 10^{-4} W m^{-2} nm^{-1}. At larger SZA, the condition of the 5% change in irradiance takes place in longer wavelengths. Nevertheless, the variation in absolute terms is smaller and consequently, more difficult to detect. An added problem is that the observatories located in high latitudes will not be able to make observations during the whole year with enough solar elevation. The final conclusion is that considering 5% of uncertainty in the calibration of the instrument, the increment of the UV irradiance due to a decrease of 1% in the total ozone content, will be able to be detected if the threshold of detection of the instrument is of the order of 10^{-6} W m^{-2} nm^{-1} or lower.

Besides the problem of the precision in the calibration and of the detection threshold, another error source in the measure of the spectral UV irradiance is the uncertainty in the alignment of the wavelength. For example, at 295 nm a wavelength error of 0.1 corresponds to an irradiance error of approximately 9% for SZA = 30°. Therefore, the detection of changes in UV irradiance due to a 1% total ozone content variation, demands a precision in the wavelength alignment of ±0.05 nm as minimum.

For the radiative transfer models validation, the precision of the instrument should be comparable to the one required for the tendency detection. For the determination of the current levels of radiation UV, interpretation of geographical differences and calculation of the ultraviolet index, the requirements of the instrument are less strict.

With the purpose of reaching the required precision, the instrument should be characterized in terms of the following parameters: cosine error, minimum spectral range, full width at half maximum (FWHM), wavelength accuracy and precision, sampling interval, dependence on the temperature, scan time, integration time and measurement frequency.

3) *Instrument characteristics*

Cosine error

They are usual instruments with cosine error of −10% for an incidence angle of 60° and around −15% for an incidence angle of 70°. These instruments are underestimating the global irradiance between 7% and 13% depending on the solar elevation. In long wavelengths, this effect is more accused. In the UV-B region, the derived uncertainty of the cosine response error is smaller because the ratio direct radiation/diffuse radiation is smaller in this spectral range; nevertheless, in this UV-B range the errors can exceed 10% due to the cosine error. Therefore, it becomes necessary a good characterization of the cosine error of the instrument and to adopt measurements appropriate correction procedures may lead to an improvement. The error associated to the cosine response should be smaller than 5% for angle of incidence of 60°. The uncertainty associated to this cosine error is comparable to the uncertainty associated to the calibration in irradiance and there are several methods to reduce this error associated to the solar incidence angle.

This directional response of the instrument is measured typically in the laboratory rotating a lamp in a spherical arch that is centred in the diffuser. A possible system consists of using the tracker of the Brewer. The irradiance of the lamp has to be previously stabilized so that the successive measures in different angles can be related to the measures to a normal incidence. The irradiance of the lamp also has to be high enough to allow irradiance measurements at high solar zenith angles with a good signal with regard to the level of noise.

Minimum spectral range

The changes in the spectral ultraviolet irradiance are especially significant in the UV-B range and are not detectable for wavelengths above 340 nm. These changes induced by the ozone must be detected superimposed to those taken place by other parameters like the aerosol and clouds, it is necessary to measure in the region where the effect of the ozone is dominant (UV-B). The necessary measure range is from 290 to 360 nm, although little absorption exists for the ozone in the region of 340-360 nm this region must also be included in the analysis of tendencies in UV. For the application to the human health, the World Health Organization (WHO), recommends to measure from 290 to 400 nm biological effects as the erythema action spectrum proposed by the CIE they include wavelengths up to 400 nm. On the other hand, the scattering coefficient varies significantly in this wider spectral interval, and we will have more detail for the investigation in radiative transfer models, allowing a better separation of the influence of ozone, atmospheric aerosol, clouds and Rayleigh scattering.

On the other hand, a wider wavelength range increases the necessary time to take a spectrum and consequently the conditions can change during the scan. Therefore, this increment of time, reduces the number of spectrum in a given time.

Wavelength accuracy and precision

Due to the steep increase in the UV-B irradiance with the wavelength, small uncertainties in the wavelength alignment will lead considerable error in the measured irradiance. For example, it is considered that for a solar elevation SZA = 60° and a total ozone content of 300 D.U., a displacement in the wavelength of 0.1 nm corresponds an error in the irradiance measured approximately from 9% to 295 nm and of 5% at 300 nm. Equally, to a displacement of 0.1 nm in wavelength corresponds an uncertainty of 2% in the erythemal irradiance. Therefore, the uncertainty in the wavelength alignment should be smaller than 0.1 nm and for the objectives enunciated at the beginning of this section, the uncertainty in wavelength should be smaller than +0.05 nm.

In the example that is illustrated in the section of "sampling interval" we have obtained a difference of 0.027 nm between the experimental measure of the Brewer and the nominal wavelength of a emission line of the internal mercury lamp.

Repeatability

The repeatability of an instrument is a measure of its capacity to reproduce a measurement of a stable source over a short time period. For example, we show in the following figures, the analysis that has been carried out with the Brewer#150 based on 4 scans taken with a 1 000 W stable lamp at 50 cm from the receiver.

The figure 7 shows superimposed the four irradiance spectrum taken from the lamp L955 under laboratory conditions.

The figure 8, shows the ratio between the standard deviation and the mean of these four scans vs wavelength. The reason for representing this ratio, is to give us an idea of the standard deviation compared to the registered values of

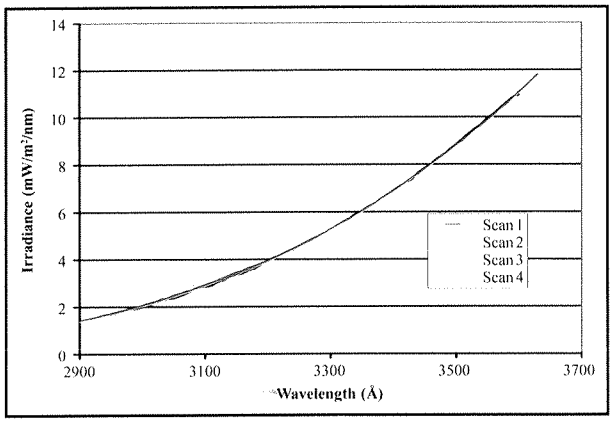

Fig. 7. 1 000 W lamp irradiance calculated from 4 different scans with a double Brewer.

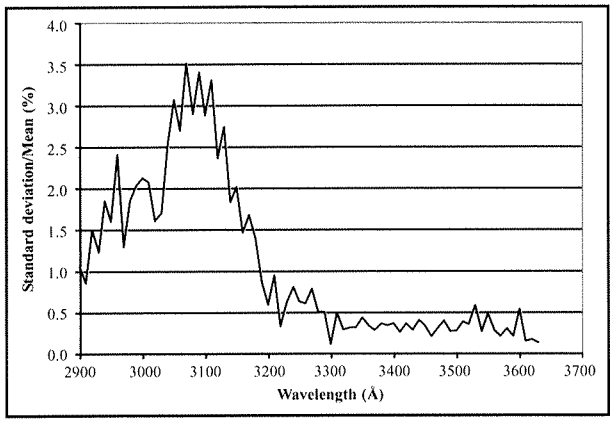

Fig. 8. Uncertainty 1 000 W lamp irradiance calculation from 4 different scans with a double Brewer.

irradiance. In this figure can be observed values above 1% for wavelengths under 219 nm. The reason for this increase in standard deviation vs the mean measured irradiance is due to the deviation observed in the fourth spectrum in this region (it appears represented in blue line in the figure 8). We cannot explain this deviation in the fourth spectrum, it could be due to a problem in the power stabilization of the lamp.

Sampling interval

In general, it is recommended that the sampling wavelength interval be is smaller than the bandwidth (FWHM). The advantages of this oversampling are that we obtain a bigger precision in wavelength and that decreases the interpolation noise. The disadvantages are on the other hand, the time to cover a scan and the technical limitations of the instrument.

The spectrophotometer Brewer MK-III in its habitual way of work for the measurement of ultraviolet spectral irradiance, makes a scan from 286.5 to 363 nm with a step of 0.5 nm and it needs for it about nine minutes. These nine minutes are the reason why the spectrum is taken with 0.5 nm step when it has capacity to make it with steps of 0.05 nm. The figure 9 shows the slit function for a certain emission line of the internal mercury lamp of the Brewer. The full width at half maximum (FWHM) for the Brewer#150 calculated from this spectral line of 296.728 nm (Joseph Reader et al., 1980) of a mercury lamp is 0.62 nm. As for the wavelength precision, the centre of our curve, once symmetriced, is 296.755 nm, with that the error made with the Brewer when determining the position of this line is 0.027 nm.

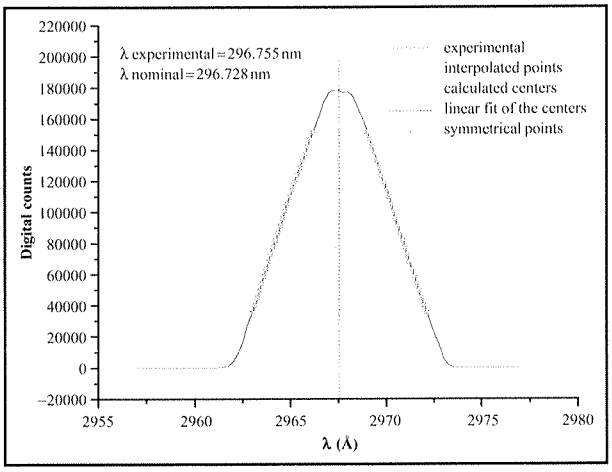

Fig. 9. Wavelength accuracy in a Hg line scan.

Temperature dependence

Generally, the spectrophotometers present a dependence on the temperature in some of their parameters like the wavelength alignment and the spectral response. The temperature of the instrument should fluctuate inside the thresholds specified for each instrument.

It is important to characterize the instrument, and to register the internal temperature of the instrument with a temperature sensor and if corrections are made, the method used should be well described.

The spectrophotometer Brewer has internal lamps, mercury (Hg) and halogen (Sl), with the purpose of correcting automaticaly the effects due to the variations of the interior temperature of the instrument.

Straylight

It constitutes a systematic error of the instrument and it acts increasing the irradiance registered by the instrument due to the light coming from secondary sources which are counted by the instrument.

This effect can produce an error that can even reach 100% in wavelengths below 295 nm. Therefore, instruments where this effect is not corrected can overestimate the spectral irradiance very significantly in short wavelengths that have a bigger weight erythemal effect. There are methods to attenuate this effect when processing the measured spectrum, but without a doubt, the best thing is to have an instrument of double monocromator in that the stray light decreases drastically.

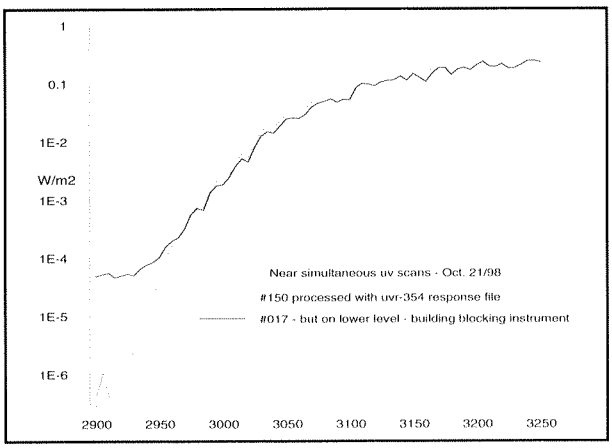

Fig. 10. Global irradiance spectra performed with a double and single Brewer.

The figure 10, two simultaneous spectrums are shown superimposed, taken respectively with the Brewer#150 (double monocromador) and the Brewer#017 (a single monocromador). As it can be appreciated, the stray light in the instrument of a single monocromador is very strong in the shortest wavelengths (290-295 nm) and the error in the determination of the irradiance in this spectral interval is near to 100%.

Scan time

Ideally, all the wavelengths of the spectrum should be measured simultaneously, otherwise, the analysis and interpretation of the spectrum becomes more complicated. The spectrophotometer Brewer makes scans from 286.5 nm to 363 nm with a 0.5 nm step and it takes about 9 minutes, which is then the interval of time that separates the measure of the shortest wavelengths in the longest. In general the limit allowed to take a spectrum is of 10 minutes, because it is the time requested by a great number of spectrophotometers to carry out a scan.

Measure frequency

It is advisable to take as many spectra as possible, the minimum to be able to study the day variation of the global spectral irradiance is one spectrum per hour. At the moment, the Brewers, in general, alternate measures of ozone with those of ultraviolet irradiance, and they need some checking and automatic adjustments, so the habitual is to take two spectrums per hour. Two spectrum per hour are enough for the evaluation of the ultraviolet irradiance along the day, evaluation and validation of models, detection of tendencies etc.; but it is insufficient for studies of quick variations of the associate irradiance for example to the clouds.

The basic characteristics of the spectrophotometers Brewer appears described in the following table:

Precision	1% (in ozone direct sun measurement)
Resolution	0.6 nm @ 303.2, 306.3, 310.1, 313.5, 316.8, 320.1 nm
Physical dimensions	70 × 46 × 21 cm models MK-II y MK-IV 70 × 46 × 34 cm model MK-III
Weigh	25 kg (90 kg whole system) models MK-II y MK-IV 34 kg (90 kg whole system) models MK-III
Power requirements	100 VAC @ 1st (2nd with heater), 50/60 Hz 240 VAC @ 1st (2nd with heater), 50/60 Hz
Operating temperature range	–20ºC a +40ºC
UV wavelengths	Precision: 0.005 nm Stability: 0.01 nm over full temperature range Range: 290-325 nm MK-II Range: 286.5-363 nm MK-III Range: 286.5-363 nm and 430-540 nm MK-IV
Microprocessor board	RCA COSMAC 18S601
Interface	RS232C, maximum distance PC/Brewer ≈ 15 m
Photomultiplier	Low noise EMI 9789QA or equivalent
Optic	• Spectrophotometer Elbert modified, focal distance 16cm, width 11cm and opening F/6, MK-II y MK-IV • Double spectrophotometer Elbert modified, focal distance 16cm, width 11cm, opening F/6, 3600 spectral lines MK-III
Standard lamp	Internal halogen Tungsten lamp, 20 W, 12 V
Calibration in λ	Internal Mercury lamp
UV calibration checking	Tungsten halogen lamp, 50 W, 12 V at 5cm from the diffuser
Cyclic Shutter	0.112 seconds for the slit 1, y 1.6 sec. the whole cycle with 6 slits
Azimuth tracking	Total height 91 cm, motor box 30 × 30 × 35 cm, power 100 VAC/240 VAC, 50/60 Hz, resolution 0.02º/step
Zenith Traking	Resolution: 0.13º/step
UV Scan	Quartz dome and Teflon diffuser with a good cosine response
Software	Main control program in GWBASIC

4.3. UVB-1 PYRANOMETER *YANKEE ENVIRONMENTAL SYSTEM*

The UVB-1 Pyranometer is a precision instrument that measures biologically-effective UV-B radiation. The instrument's measurement technique uses coloured glass filters and a sensitive fluorescent UV-B phosphor to cancel all visible light of the sun and to convert UV-B to visible light, which is then measured by a solid state photodetector. The rugged design of the instrument ensures stable operation during long-term, unattended use in the field.

The UVB-1 Pyranometer measures global solar UV-B irradiance, radiation received by a horizontal surface from the entire hemisphere of the sky. Global radiation includes both light transmitted directly through the atmosphere, and light scattered by atmospheric gases and particulate matter in the atmosphere. Unlike visible light, scattered UV-B is a main component and, under certain conditions, the dominant of global radiation. The design of the UVB-1 ensures proper measurement of both direct and diffuse components.

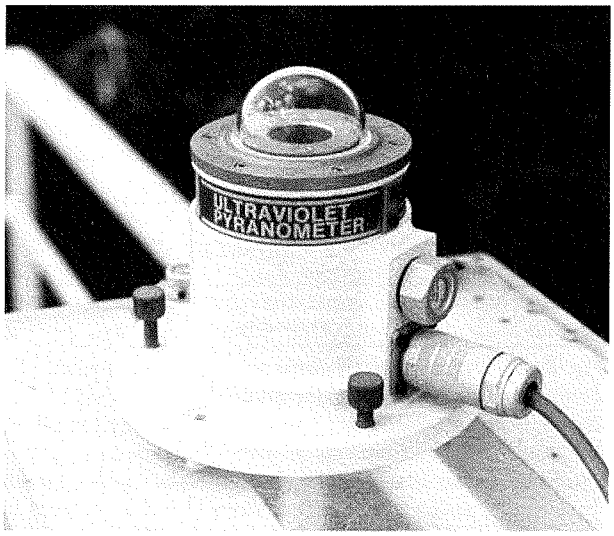

Fig. 11. *View of a YES UVB-1.*

4.3.1. Applications

The UV-B portion of the solar spectrum, 280 to 320 nm, is very strongly absorbed by stratospheric ozone, and any change in the total amount of ozone affect the levels of UV-B radiation reaching the ground. The measurement of solar UV-B radiation, using the UVB-1 Pyranometer, can be used to monitor the ozone level, as well as to verify the measurements of independent ozone. The spectral response of the instrument is similar to the erithemal (sunburns) and DNA damage spectra, making it ideal for climatological and biological impact studies.

Typical applications for the UVB-1 Pyranometer include:

- Esrithemal dose rate studies.
- Effects of UV-B on communities.
- Climatological data gathering.
- Layer depletion impact studies.

4.3.2. Principle of operation

The UVB-1 Piranometre uses a fluorescent phosphor to convert incoming UV-B radiation to visible light which is then measured by a solid state photodiode.

The direct and diffuse solar radiation, is transmitted through the quartz dome. The first filter, a UV-transmitting black glass, absorbs all the visible light except for a small fraction of the red light.

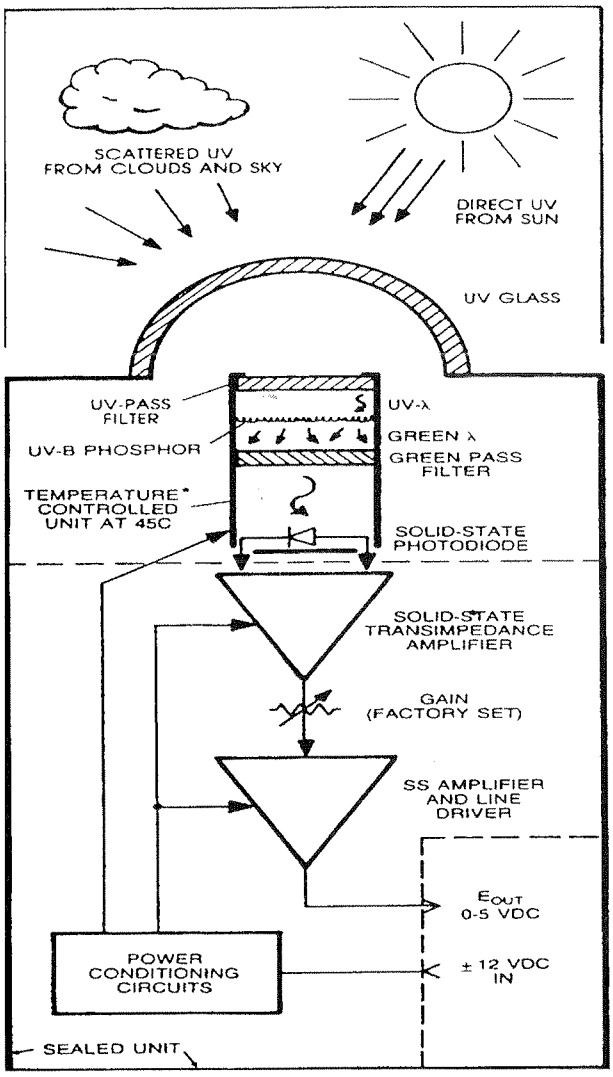

Fig. 12. Diagrammatic view of the YES UVB-1 (User Guide).

The light transmitted through this filter strikes a UV-B sensitive phosphor. This material absorbs the UV-B light and re-emites it as a visible light, mainly in the green lengthwaves. A second green glass filter passes the fluorescent light from the phosphor while blocking the red light transmitted by the black glass. The intensity of the fluorescent light is measured by a solid state (GaAsp) photodiode. A thermally-stable transimpedance amplifier drives a line amplifier to provide a low impedance 0-4 VDC output signal. The intensity of the fluorescent light is measured by a solid state photodiode of GaAsP. The glass filters, phosphor, and photodioide are kept at +45° C to ensure that the output is not sensitive to changes in ambient temperature.

4.3.3. Specifications

- *Spectral response:* 280 a 300 nm
- *Cosine response:* ±5% for 0°-60° solar zenith angle
- *Sensitivity:* 2.5 V ($W m^{-2}$) of total UV-B irradiance
- *Sensor's effective area:* 1″ diameter (2.54 cm)X
- *Power requirement:* –12 VDC @ 5 mA; +12 VDC load varies with ambient temperature: 120 mA at +20°C, 500 mA-40°C; the maximun allowable supply voltage range is 11 to 14 VDC
- *Output signal:* 0-5 VDC
- *Response time:* Aprox. 100 ms
- *Operating temperature:* –40°C to +40°C

4.4. OPTRONIC SPECTRORADIOMETER 745-O-PMT

This instrument determines global direct spectral irradiance (in $W cm^{-2} nm^{-1}$) in the range of 250 to 800 nm. The sampling is usually fixed to 1 nm by automatic integration. The FWHM (Full Width at Half Maximum) is 1.6 nm.

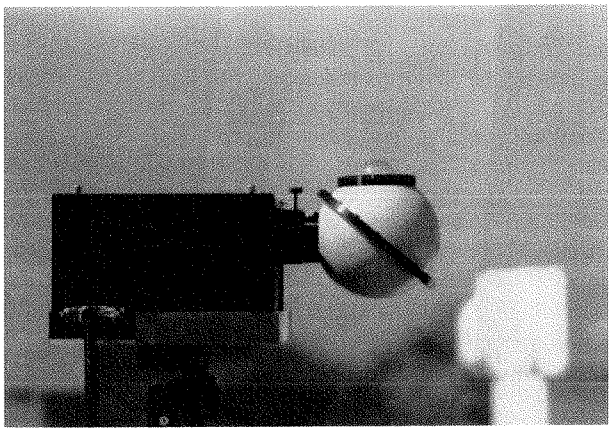

Fig. 13. View of a Optronic spectroradiometer.

The optical entrance optics consists of an integrating sphere, with diaphragms to eliminate the stray light, and covered with teflon and a quartz dome, to minimize the cosine effect, and a grating to minimize the radiation intensity. In case of direct irradiance measurement, the quartz dome is replaced by a collimator with an angle of view of 5.72. Before every measure it makes an automatic correction measuring the dark count.

The instrument consists of a double monocromator with focal distance 160 mm which consists of concave diffraction gratings with 1200 lines/mm. The sensor is an Optronic S-20 photomultiplier thermally stabilized.

The instrument is periodically calibrated with the system OL 752-10 consisting of 200 watts tungsten lamp NIST and of a stabilized power supply with a precision of ±0.01%.

The optronic is portable, with a weight of around 20 kg and for the direct irradiance measurements it is mounted on a tripod with three kneecaps at 120 (to point the sun manually).

The instrument is set up using a 4 watts fluorescent lamp for wavelength checking and a 5 watts filament tungsten lamp for gain checking.

4.5. SOLAR PHOTOMETER MICROTOPS II

This instrument can measure the total ozone column, total water vapour and aerosol optical thickness at 1 020 nm by measuring direct irradiance in five wavelengths, using five collimators with a 2.5° vision field and the respective photodiodes for each measured wavelength. The channels used are shown in the following table with their FWHM:

WAVELENGTH (nm)	FWHM (nm)
300.0 ± 0.3	2.4 ± 0.4
305.5 ± 0.3	2.4 ± 0.4
312.5 ± 0.3	2.4 ± 0.4
940.0 ± 1.5	10.0 ± 1.5
1 020.0 ± 1.5	10.0 ± 1.5

Ozone is measured taking into account the fact that the ozone content between the observer and the sun is proportional to the ratio of the radiation in two UV wavelengths, where the ozone absorption is bigger. Like the Dobson instrument, it measures in a third wavelength longitude to correct the dispersion for the aerosols and the diffuse radiation.

Fig. 14. View of a Microtops II.

The determination of the water vapour content is made starting from the intensity measurement at 940 nm, where there is a peak in the water absorption, and at 1 020 nm, where there is a slight absorption.

The aerosol optical thickness is determined by inverting the Lambert-Bouguert-Beer equation, which relates the spectral irradiance at ground level to the spectral irradiance and the optical thickness of the absorption and dispersion of the different components. For this, the irradiance measured at 1 020 nm and the content in water vapour and ozone determined with the other channels are employed.

This is an easy to handle portable instrument (it hardly weighs 600 g).

4.6. LI-COR 1800

The Li-Cor 1800 is a portable field spectroradiometer. The whole instrument weighs 6.4 kg, all the electronic and optical components are integrated in a box (16.3 × 20.1 × 36.0 cm). The electronic part consists of a ROM memory (24 Kb), the software of control is factory installed. A ROM memory (256 Kb) allows to store about 64 scans, but as this memory is divided, the access to its banks is not simple (there are 8 memory banks which have to be activated separately).

A 6 V internal battery made of Ni-Cd allows an autonomy of about 60 measurements. It is recharged by means of a simple connection to electric power. In standard operation (a measurement every 15 minutes, at 25ºC), the battery has an autonomy of 8 hours.

The diagram of the optics involved in the instrument is detailed in the figure 15. The solar light reaches a cosine receiver. This receiver follows the law of Lambert, or of the cosine, so that the irradiance transmitted in all directions is constant.

The light transmitted by the receiver (a teflon dome in the original version of the instrument), is directed by reflection in a mirror towards a filter wheel. This wheel contains seven filters, arranged according to the spectral interval they allow to pass, so that the transmitted light doesn't contain radiation in wavelengths that could cause interferences in the measurement, due to superior orders of diffraction. During a measurement, while the holographic grating is rotating, the internal microcontroller of the Li-Cor rotates in its turn the wheel of filters, selecting the filter that covers the spectral interval that is being measured. There are seven filters which transmit different spectral intervals, eliminating therefore the unwanted radiation. The wheel contains in an eighth position a black filter, used to determine the reading in darkcount of the instrument. This zero level is measured before and after each scan, so that the Li-Cor subtracts this darkcount level to the taken measurement, giving finally the corrected measurement.

The radiation then reaches the monocromator's input slit (a rectangular opening). The monocromator consists of both input/output slits and a disperser element among them which spectrally separates and projects the incident radiation on the output slit. By moving the disperser element, different wavelengths of the incident radiation in the output slit. Input and output slits determine the band width of the radiation that reaches the detector.

The disperser element of the Li-Cor's monocromator is a holographic grating. There are no descriptions in the instrument specifications that indicate that there is an internal optic in the monocromator. This implies that the grating is concave. This way, the incident radiation passes through the output slit of the monocromator, in the spectral interval of 300 to 1 100 nm. The grating moves by means of a step by step precision motor, following the orders of the microcontroller. The steps can be chosen among 1 nm, 2 nm, 5 nm or 10 nm. Nevertheless, the measurements described hereinafter have a step of 1 nm.

When the radiation comes out of the output slit of the monocromator, it is picked up by a detector, which consists of a silicon photodiode that produces an electric current proportional to the quantity of radiation that it receives. The current sign is amplified, then converted to tension and it passes through an analogical-digital converter that can be read by the internal microprocessor. In the later reading circuit there are some filters that eliminate possible fluctuations of the measurements due to interference of alternating current near sources.

Measuring a complete spectrum takes about 50 seconds since the order is sent from a PC. A software installed in it allows the communications with the instrument, discharge of

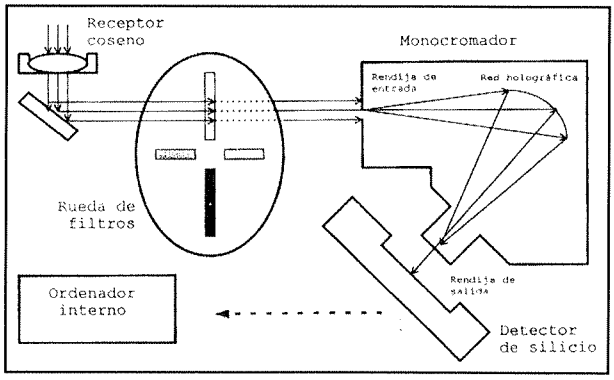

Fig. 15. Diagrammatic view of the Li-Cor 1800.

data, etc. The internal microprocessor of the Li-Cor takes charge of controlling scans, registering data, storing them in the banks, etc. Parameters such as the spectral interval on which it will be measured, the step, the number of scans to average, etc. can be controlled with the software. It is feasible to program a measurement schedule, according to the hour, so that up to ten measures in different hours and days, can be made. There is not much autonomy in it, because it doesn't allow to change the memory bank, and so, the restriction is that the measurements which can be held in a memory bank can be programmed.

The slit function (FWHM) is 6 nm according to factory. The Li-Cor can work with the entrance dome connected to the box, or through an optic fibre instead of this dome. At the end of the fibre there is a small receiving cosine. The optic fibre is an ideal system to measure the direct irradiance, since it facilitates the directibility of the instrument. However, it must be taken into account that when adding fibre to a system, smaller illumination will reach it. For this reason, the losses due to the fibre transmitance will reduce perceptibly the SNR of the system.

In both cases, to measure the direct irradiance, a collimator tube should be used, which allows the arrival to the receiving cosine of part of direct irradiance from the sun. For that, this tube constrainer should have at least, a FOV 1.08º, which is the solid angle that covers the sun from the earth.

This instrument must be calibrated every six months as minimum.

4.7. CIMEL 318A

The solar photometer Cimel Electronique 318A, manufactured in Paris, France, has a dual detector for the measurement of direct radiation from the sun with 1.2 degrees FOV, and aureole and sky radiation, with their respective 33 cm colimators, presenting a 10-5 stray light rejection. This means that the noise is very low, and scarcely affects the CIMEL. The head of the sensor is mounted in such a way that the optic is protected from the rain and the entrance of strange particles in the system in the standby position. The solar aureole colimator is protected by a quartz window allowing the observation with a silicon UV detector which allows spectral observations in the range from approximately 300 nm up to 1 020 nm. The colimator of the sky has the same illumination field, but an opening approximately 10 times to get better dynamic range in the measurement of the sky radiations. The head of the sensor is made of sealed rings, 8 interferential filters are placed in a filters wheel which is controlled by a step by step motor. A termistor measures the temperature of the detector allowing the compensation for any dependence with the temperature in the silicon detector.

There are step by step transmission motors which direct the head of the sensor in the azimuth and zenith with an accuracy of 0.05 degrees. A microprocessor calculates the position of the sun according to time and geographical coordinates, and directs the head of the sensor approximately one degree toward the sun, then a four quadrants detector points accurately to the sun just before every measurement. After completing a routine measurement, the instrument returns to the standby position, until the next measurement sequence. A humidity sensor exposed to rain will cancel any measurement sequence in progress.

The obtained data are collected by a DCP typically used in the system of geostationary telemetry satellites.

REFERENCES

Microtops II. User's Guide.

Kerr, J. B., C. T. McElroy and R. A. Olafson. Measurements of Ozone with Brewer Ozone Spectrophotometer. In Proceedings of the Quadrennial International Ozone Symposium, edited by J. London, pp. 74-79, Natl. Cent. For Atmos. Res., Boulder, Colo., 1981.

Komhyr, W. D. Observers' Manual. Dobson Ozone Spectrophotometer. U. S. Department of Commerce – NOAA, 1972.

Komhyr, W. D. Operations handbook – ozone observations with a Dobson spectrophotometer. 1980.

SCI-TEC, Brewer-MKIII pectrophotometer. Operator's Manual.

WMO/GAW publication No. 125. Instruments to Measure Solar Ultraviolet Radiation.

WMO/GAW publication No. 126. Guidelines for Site Quality Control of UV Monitoring.

Yankee Environmental System, Inc. UVB-1 Ultraviolet Pyranometer. Installation and User Guide.

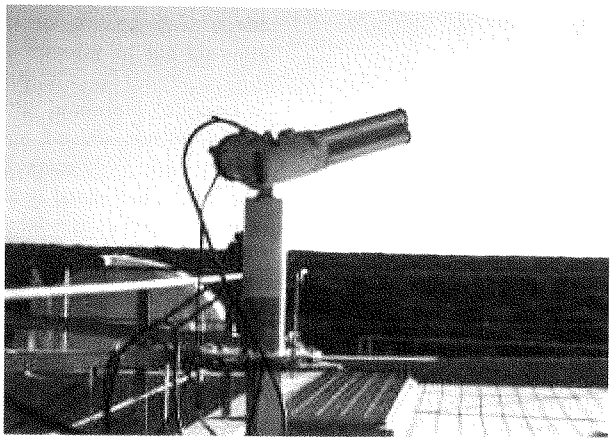

Fig. 16. *View of a Cimel photometer operative at "El Arenosillo".*

CHAPTER 5

IRRADIANCE ABSOLUTE CALIBRATION OF SPECTRORADIOMETERS IN LABORATORY

J. P. Díaz[1], F. J. Expósito[1], A. Redondas[2], V. Carreño[2], C. Torres[2] and A. M. Díaz[1]

[1] Departamento de Física, Universidad de La Laguna. 38200 La Laguna, S. C. de Tenerife, *jpdiaz@ull.es*

[2] Observatorio Atmosférico de Izaña, Instituto Nacional de Meteorología. 38071 Santa Cruz de Tenerife.

SUMMARY

The procedure followed to transfer the irradiance scale from two NIST traceable DXW 1 000 watt lamps during the I Iberian Intercomparison of UV instruments (INTA-CEDEA, El Arenosillo, Huelva) is described. The operational procedure followed in the laboratory uses a third DXW 1 000 watt seasoned lamp. We describe how this lamp is calibrated and used during the calibration of the instruments to increase the live-time of the standard lamps. The scheme of the designed laboratory to maintain the accuracy and precision of the distance between the optical input of the instruments with regard to the lamp, its vertical alignment, and the current throughout the calibration process is described. During the three days of calibration in laboratory the standard deviations varied from a minimum of ±0.0006 up to a maximum of ±0.0024 amperes (0.03% error with regard to the set-point current of 8 amperes).

5.1. INTRODUCTION

To evaluate the effects of UV radiation is fundamental to obtain reliable measurements of spectral irradiance. UV measurements gathered at different times and places must be expressed on an absolute scale of irradiance in order to be related to each other.

The quality of the measurements attained by the existing instrument is not better than about 5%. However, in many physical applications an accuracy of 1% is desirable.

The main methods employed to establish an absolute irradiance scale are: absolute cryogenic radiometry, synchrotron radiometry and black body cavity radiometry. These techniques are used in the national standards laboratories such us NIST (National Institute of Standards and Technology, USA), NPL (National Physical Laboratory, UK) and PTB (Physikalisch-Technische Bundesanstalt, Germany). In an operative way the absolute scale irradiance must be transferred to the field instruments via intermedial sources and detectors. At present the most widely method to transfer the calibration are the spectral irradiance lamps. It is very important to take into account that relative accuracies of 1% to 5% are attainable by well-maintained instrument, but absolute accuracies of better than 5% cannot presently be demonstrated due to the uncertainties introduced during the transfer of the absolute scale.

In this chapter we describe the procedure followed to transfer the irradiance scale during the intercomparison at CEDEA-INTA, El Arenosillo (Huelva) in 1999. This method employs two NIST traceable 1 000 watt lamps and a third one, which has been calibrated during the laboratory measurements.

5.2. LABORATORY DESCRIPTION

To calibrate a spectroradiometer using a spectral standard lamp is necessary to reproduce the same conditions in which the lamp was calibrated. Thus, it is extremely important to maintain the accuracy and precision of: the distance between the optical input of the instrument with regard to the lamp filament; its vertical alignment and the lamp current throughout the calibration process.

5.2.1. Optical bench

A scheme of the optical bench used in the laboratory is shown in figure 1. This set-up achieves the requirements with regard to the distance and alignment between the lamp filament and the optical input of the instrument. This set-up consists in a vertical bench with three holders, one for the calibration lamp, a second one in the top of the bench for a laser, and a third one on the bottom holds for a baffle (not shown in the figure). The instrument to calibrate is placed over a base with its sensor in the vertical of the lamp and laser. The holder of the lamp used is a 3D-axis holder, which can be adjusted by three micrometer screws.

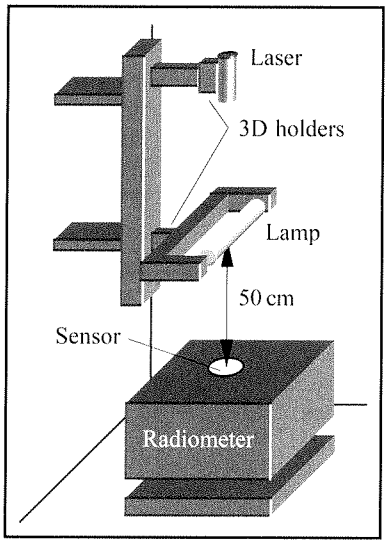

Fig. 1. Scheme of the optical bench set up.

The laser at the top of the bench is a 10 mW He-Ne laser, which permits the vertical alignment between the lamp and the optical input of the instrument. To ensure this alignment a small mirror is placed (in those equipments with a plane diffuser as input) over the diffuser. The lamp and the input of the equipment will be in the same vertical whether the glint of the laser light reaches the output window of the laser source.

One of the more important parameters in this set-up is the distance between the input of the instrument and the lamp filament. Note that following the distance square inverse law, a difference of 5 mm in 500 mm, which is the usual distance between the lamp and the sensor, gives an error of 2%. To fix this distance a non-deformable 50 cm bar has been used. All the fine adjustments were done with micrometer screws in the three space directions.

5.2.2. Control of the intensity

The current across the lamp is another of the main factor that is necessary to reproduce exactly to calibrate any instrument. This intensity must be accurately maintained during all the calibration period at the same value. Note that for a 1 000 W FEL lamp, an error of 1% in the current produces an error of 10% in the spectral irradiance at the wavelengths of 300 nm. In order to reproduce always the same intensity a current-control system has been developed (Figure 2).

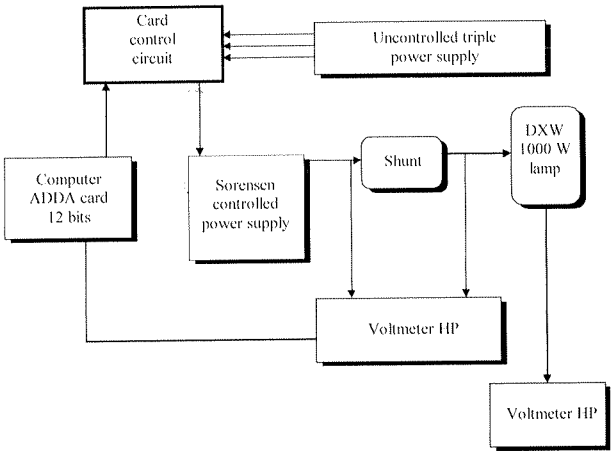

Fig. 2. Connection diagram for the intensity-control system.

A 1 800 watts Sorensen 150-12B supplies the power to the circuit. This source works between 0 and 150 V and it can be externally controlled by a control voltage (0–10 V) with a factor conversion of 1/15.

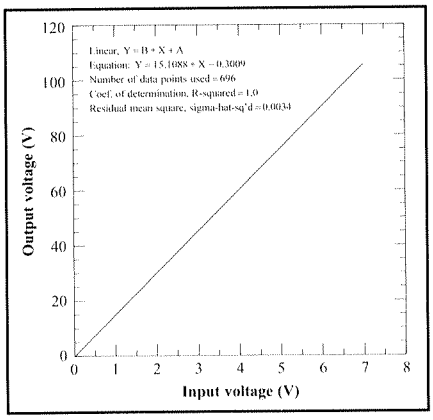

Fig. 3. Output voltage in the terminal of the Sorensen power supply versus the input control voltage.

This power supply can follow a voltage ±0.03% with variations in the charge. It has a response to the transients of 50 ms although this response decreases for frequencies lower than 60 Hz in a factor of $(60/f)^2$. Moreover it has a typical resolution of ±0.05%. The Sorensen source has two modes of work: voltage mode and current mode. In the first one the voltage is constant whereas the current varies with the charge. In the second one the voltage varies and the current is constant. The source can change automatically between both modes depending on the charge. In this current-control system the source has been controlled by an external voltage input, which it has permitted to change the set-point voltage in the voltage mode.

In order to control this power supply a dedicated PC with an analogical-digital/digital-analogical (ADDA) card has been installed. The ADDA card is a PCL-812PG with the next characteristics:

- 16 analogical input channels.
- 16 digital input channels compatible with TTL/DTL.
- 2 analogical output channels, which can generate voltages from 0 to 5 or from 0 to 10 V using the reference of the card (−5 or −10 V). Moreover it is possible to introduce external references to produce other voltage ranges.
- 12 bits converter (HADC574Z) with a maximum sample speed of 30 kHz in DMA mode.
- Different analogical input ranges: ±5 V, ±2.5 V, ±1.25 V, ±0.625 V and ±0.3125 V.
- 3 trigger modes: software, external trigger and programmable internal trigger.
- A programmable clock/counter INTEL 8253-5.

The analogical input (AD conversion) has a precision of 0.015% in a reading of ±1 bit, with a linearity of ±1 bit. The analogical output has a linearity of ±1/2 bit.

This card permits to send the appropriate voltage signal to the Sorensen to control the current of the lamp. This signal depends on the voltage measured by a precision voltmeter in the terminal of a high precision resistor (shunt). The voltmeter is 6 digits and half HP 34401A, with output HP-IB and RS-232. Following the Ohm's law, this instrument measures the current in the circuit via the shunt and continuously sends these data to the PC using the serial port. In order to check the ageing of the lamp it is important to record these data and the voltages in its ends. Moreover the analysis of these records will permit to validate the calibration because any abnormal variation in the irradiance must be follow by a variation in the current.

The precision resistor or shunt has a resistance of $0.010130 \pm 0.000001\ \Omega$ and is connected with the lamp in a serial way. This value is taken as constant for the Ohm's law so it is especially important to know this value accurately to obtain the current in the circuit.

As it has been noted before the ADDA card has 12 bit of resolution, which implies a resolution of 2.44 mV in the input signal to the power supply for a range between 0 and 10 V. This means about 2.7 mA of resolution in the current of the circuit. Nevertheless for a calibration of these characteristics is necessary to increase this resolution. With this aim has been developed an electronic device. Its main task is to change between the card output, 0-10 V, and a more precise output, 0-0.5 V, using an external reference. For it is necessary to send a specific control signal to a multiplexer (CMOS 4051B). This integrated circuit must switch between both signals. The logical scheme can be sawn in the next figure (figure 4).

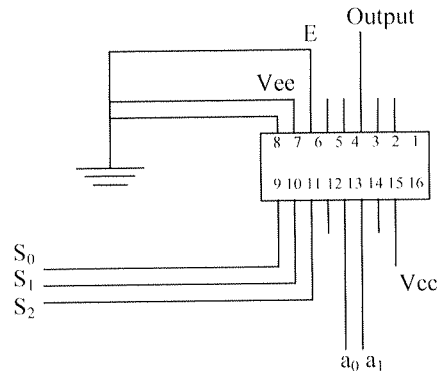

Fig. 4. Logical scheme of the electronic circuit developed to increase the resolution in the intensity control.

With this system the accuracy in the current increases up to 0.13 mA. Besides this circuit, it is necessary to use another power supply to produce a base voltage, which is added to the ADDA card to supply the input to the Sorensen. Obviously this second power supply must have an accurate better 0.5 V in a range of 0-10 V and a good stability. The second source used is a Hameg triple power supply HM8040.

The heart of the current-control system is the control software developed *ex-professo*. This software reads the voltage across the shunt and calculates the input signal to the Sorensen in order to reproduce the original calibration current across the filament of the lamp, keeping it constant during the whole calibration procedure. Besides this main task, this software has implemented other functions: increase the current gradually from 0 to the set-point in order to avoid shocks to the filament; warm up the lamp for a short time (20 minutes is usually enough) to get the stability of the standard irradiance and finally, decrease gradually the current when the spectroradiometer has finished its calibration procedure.

All this set-up is based in a feedback control system, whose scheme can be sawn in the figure 2.

The control has two main tasks: to control the fluctuations of the current across the lamp and to fix the set-point current.

Without any control, the intensity in the lamp varies around the setting current about $\pm 2.3 \cdot 10^{-3}$ A (see figure 5).

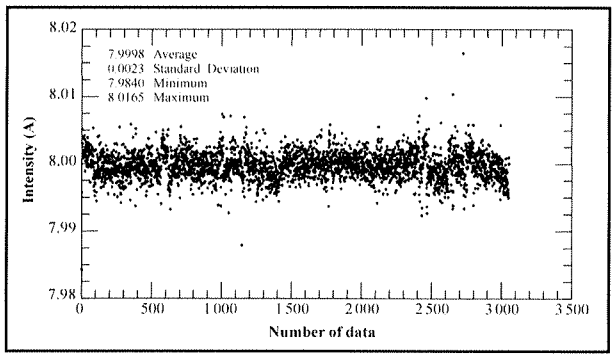

Fig. 5. *Intensity of the lamp without control.*

Due to different factors the current of the lamp shows oscillations with a random behaviour. The analysis of the intensity spectral power density confirms that the noise is really "white", without dominant spectral components (see figure 6).

Although it is impossible to eliminate this kind of noise the software can reduce the oscillation band. Moreover the current of the lamp usually changes with time due to several reasons like variations in the resistance of the filament or variations in the main. Nevertheless these variations belong to the slow ones, which can be easily controlled. Finally, external perturbations as drafts of air or small hits in the bench produce

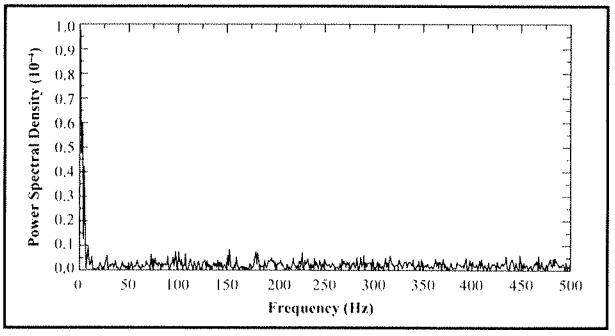

Fig. 6. *Power spectral density to the lamp intensity.*

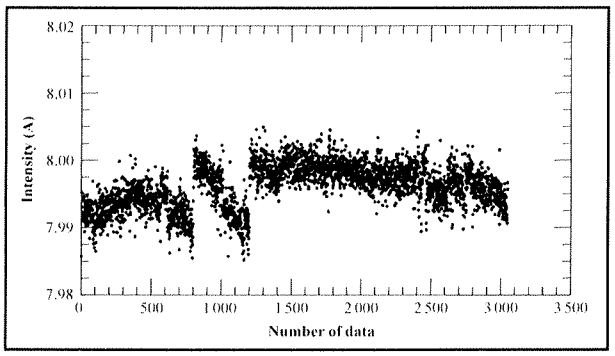

Fig. 7. *Intensity of the lamp without control and with external perturbations.*

sudden variations of the current that can also be controlled (figure 7).

On the other hand, such as it has been noted before there is a linear relation between the voltage control (0-10 V) and the voltage output of the Sorensen. Nevertheless this relation is not true whether a load (lamp plus shunt) is connected to the power supply. In this case the relation goes to be quadratic (see figure 8).

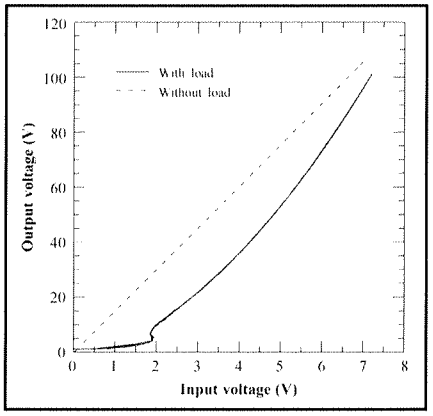

Fig. 8. *Output voltage of the Sorensen power supply with and without load.*

Note the variation in the output voltage about 2 volts in the voltage control, due to the change of resistance in the lamp when it starts the incandescence phase. This behaviour depends on the lamp so it is necessary that the program has the ability to learn how the input control signal to the DC controlled power supply must be changed to get the calibration current across the lamp filament. With this aim, during the initial ramp, the software saves a file with the input voltage sent to the Sorensen source and the measured voltage across the shunt. Doing a least square fit of these data to a second order polynomial the software knows which input value must be send to obtain the output voltage necessary to achieve the voltage across the shunt corresponding to the calibration current.

In the software used during this intercomparison the control is based in the last three voltage measured across the shunt. The command sent to the power supply tries to correct the difference between the setting current and the value measured using a weighted function of the last three differences. The weights are 60% for the last value, 25% for the value before the last and 15% for the first one. This strategy, although does not correct the white noise of the natural oscillations of the circuit, reduces the scattering of these data. The instruments used in the calibration setup are shown in Table 1.

Table 1. *Instrument used in the calibration set-up.*

Current source	Sorensen	150-12B
	Serial number	
Shunt resistor	Company	
	Calibration date:	
	Resistance: [Ω]	0.010130 ± 0.000001
Voltmeter	Hewlett-Packard	HP 34401A
	Calibration date:	
	Calibration factor:	
Lamp #85	Optronic Labs.	1 000 watt DXW
	Calibration date:	25/9/96
	Calibrated by:	Deborah Griffith
Lamp #95	Optronic Labs.	1 000 watt DXW
	Calibration date:	23/8/99
	Calibrated by:	Deborah Griffith

5.3. CALIBRATION SCHEDULE

The absolute calibration of the instruments was carried out during three days (natural days 249, 250 and 251) using two NIST traceable lamps (lamps #85 and #95) and a seasoned one (#04). The calibration schedule followed is shown in Table 2.

Table 2. *Calibration schedule.*

Date	*Instrument*	*Lamps*		
		85	*95*	*04*
6/9/99	ULL	✓	✓	✓
	IZ1		✓	✓
	IZ2	✓	✓	✓
7/9/99	UVO			✓
	UVL			✓
	BAL			✓
	VAL			✓
	GIO			✓
	MUB			✓
	COB			✓
	IZ2	✓	✓	✓
8/9/99	IZ2	✓		
	MAB			✓
	ZAB			✓
	POB			✓
	CAB			✓
	ARB	✓	✓	✓

In order to increase the lifetime of the expensive NIST traceable lamps were acquired five 1 000 watt DXW tungsten lamps. The stability of these lamps was checked at home measuring the current across the lamps during 24 hours. Lamp #04 showed the best stability and consequently was seasoned.

To calculate the spectral irradiance of the lamp #04 as accurately as possible and to recheck the stability, during the first day three instruments with double monochromator measured all the lamps. These three spectroradiometers (2 Bentham and 1 Brewer) were intercompared at Izaña Observatory previously, showing a relative response of ±2%. At last of each day during the intercomparison one of the double monochromator measured again the lamp #04, in order to check the stability of the lamp for that day.

The figures 9 and 10 show the data of intensity and voltage respectively, recorded for different instruments during the calibration. From these data the mean intensity changes from 7.9992 to 8.0025 for the three used lamps. The average for the lamp #4 was 8.0000 amperes during the three days of the measurements in the laboratory with a standard deviation of 0.0012 amperes, whereas for the lamp #85 was 8.001±0.0002 amperes and for the lamp #95 8.0000±0.0024 amperes.

Figures 11, 12, and 13 show the ratios of absolute irradiance between the lamps #4 (seasoned), #85 and #95 (standard lamps) and the ratios between the lamp #4 and the calibration measured by different instruments at laboratory.

Fig. 9 (part 1). *Intensity across the filament of the standard lamps. The instrument and the calibration lamp used appear in the top of the figure. Table 3 shows the numerical values.*

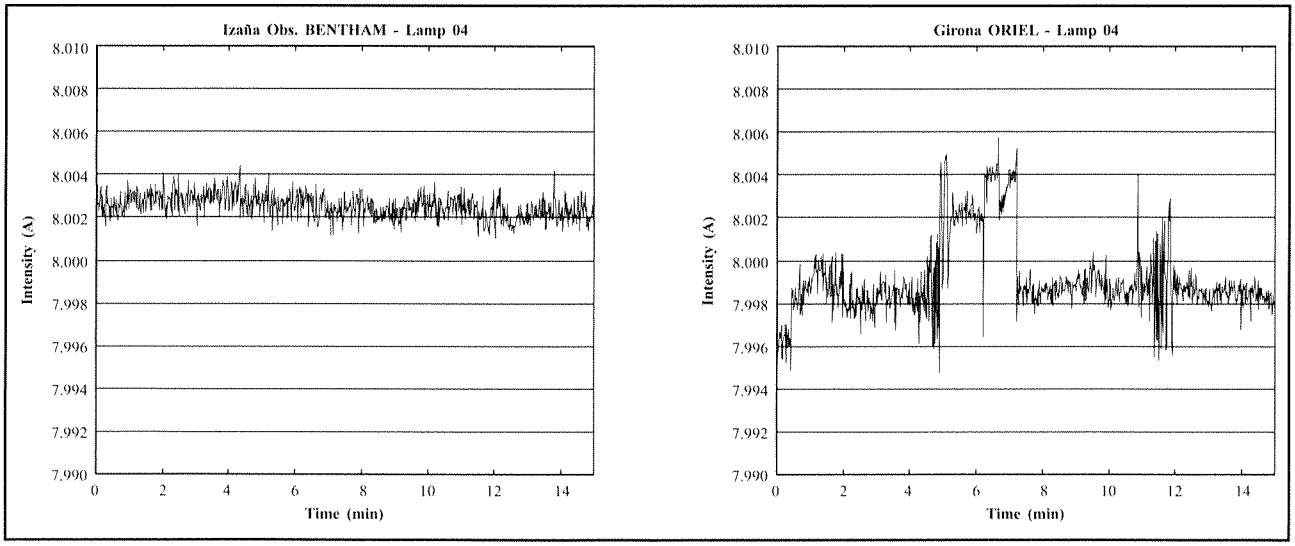

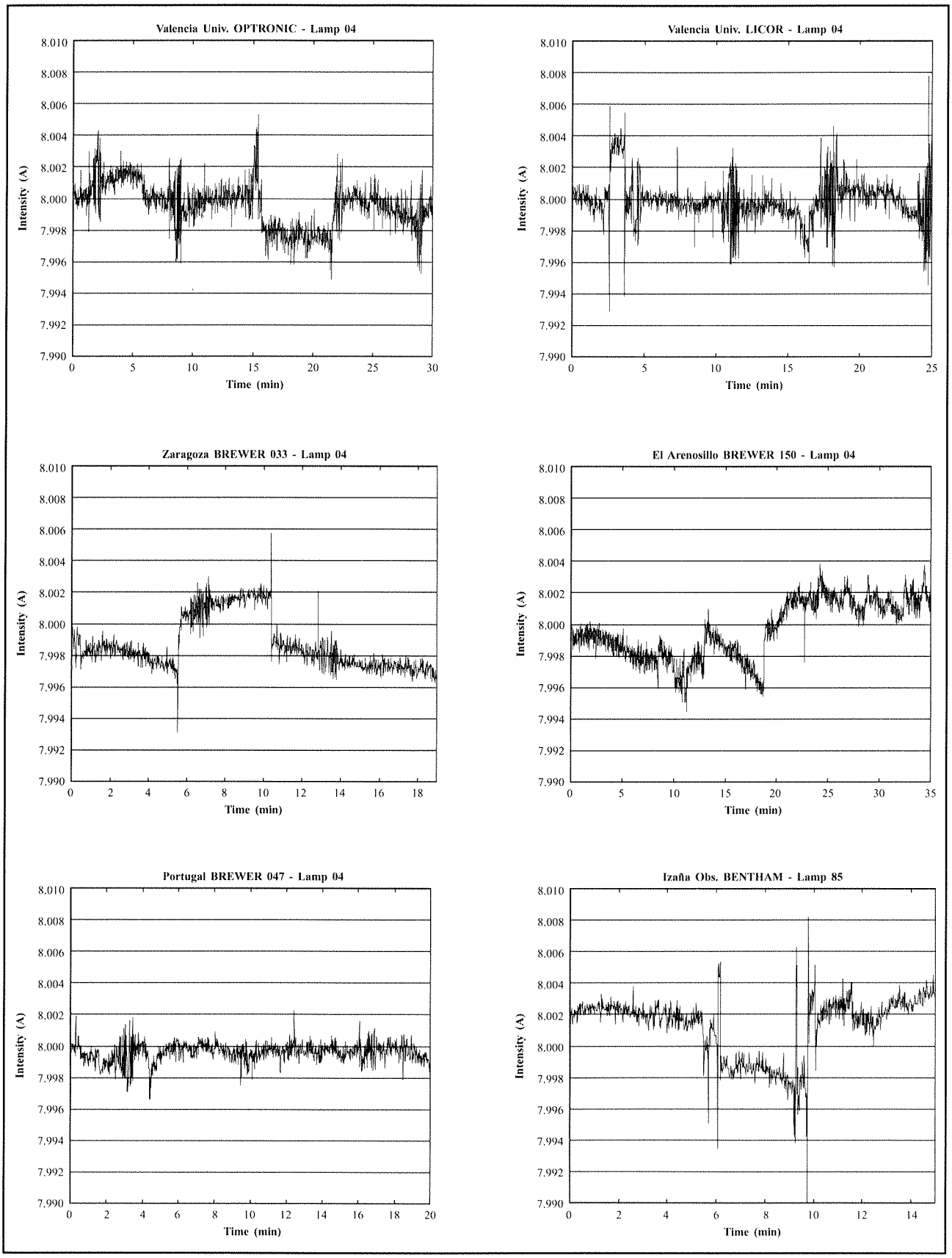

Fig. 9 (part 2). *Intensity across the filament of the standard lamps. The instrument and the calibration lamp used appear in the top of the figure. Table 3 shows the numerical values.*

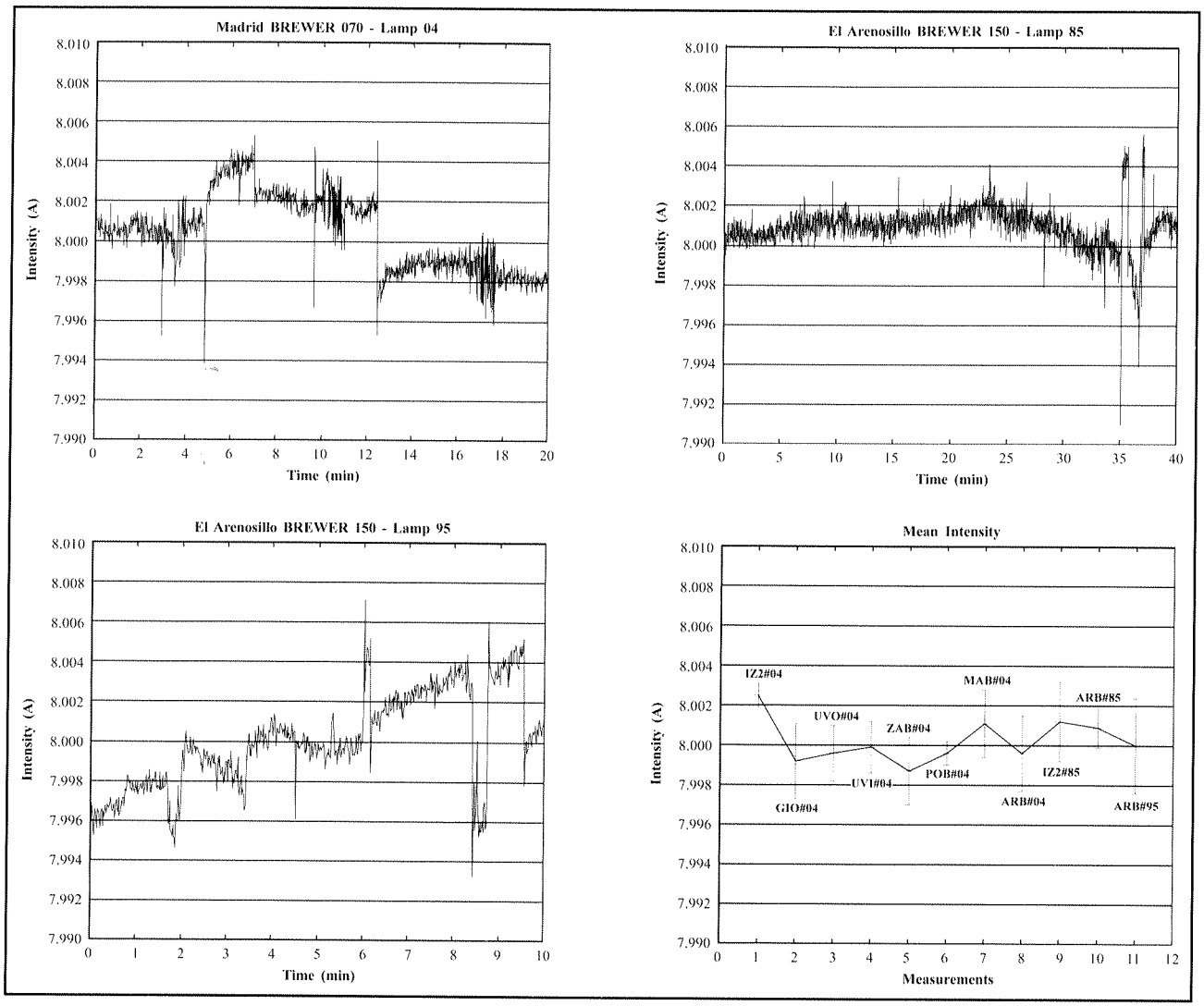

Fig. 9 (& part 3). *Intensity across the filament of the standard lamps. The instrument and the calibration lamp used appear in the top of the figure. The last figure shows the mean intensity and standard deviations for the three lamps (#4 –seasoned–, #85, and #95 –standard lamps–) during the three days of measurements in the laboratory. Table 3 shows the numerical values.*

Table 3. *Mean and standard deviation of the intensity recorded during the calibration of the instruments for the different lamps.*

Lamp 04	*Equipment*	*Date*	*Time* [min]	*Mean Intensity* [A]	*SD Intensity* (σ) [A]
	Bentham (Izaña Obs. INM)	06/09/99	15	8.0025	0.0006
	Oriel (Girona Univ.)	07/09/99	15	7.9992	0.0019
	Optronic (Valencia Univ.)	07/09/99	30	7.9996	0.0014
	LiCor (Valencia Univ.)	07/09/99	25	7.9999	0.0013
	Brewer 033 (Zaragoza INM)	08/09/99	19	7.9987	0.0017
	Brewer 047 (IM Portugal)	08/09/99	20	7.9996	0.0006
	Brewer 070 (Madrid INM)	08/09/99	20	8.0011	0.0017
	Brewer 150 (CEDEA-INTA Arenosillo)	08/09/99	35	7.9996	0.0019
Total Average				**8.0000**	**0.0012**

Lamp 85	*Equipment*	*Date*	*Time* [min]	*Mean Intensity* [A]	*SD Intensity* (σ) [A]
	Bentham (Izaña Obs. INM)	06/09/99	15	8.0012	0.0020
	Brewer 150 (CEDEA-INTA Arenosillo)	08/09/99	40	8.0009	0.0010
Total Average				**8.0011**	**0.0002**

Lamp 95	*Equipment*	*Date*	*Time* [min]	*Mean Intensity* [A]	*SD Intensity* (σ) [A]
	Brewer 150 (CEDEA-INTA Arenosillo)	08/09/99	10	8.0000	0.0024
Total Average				—	—

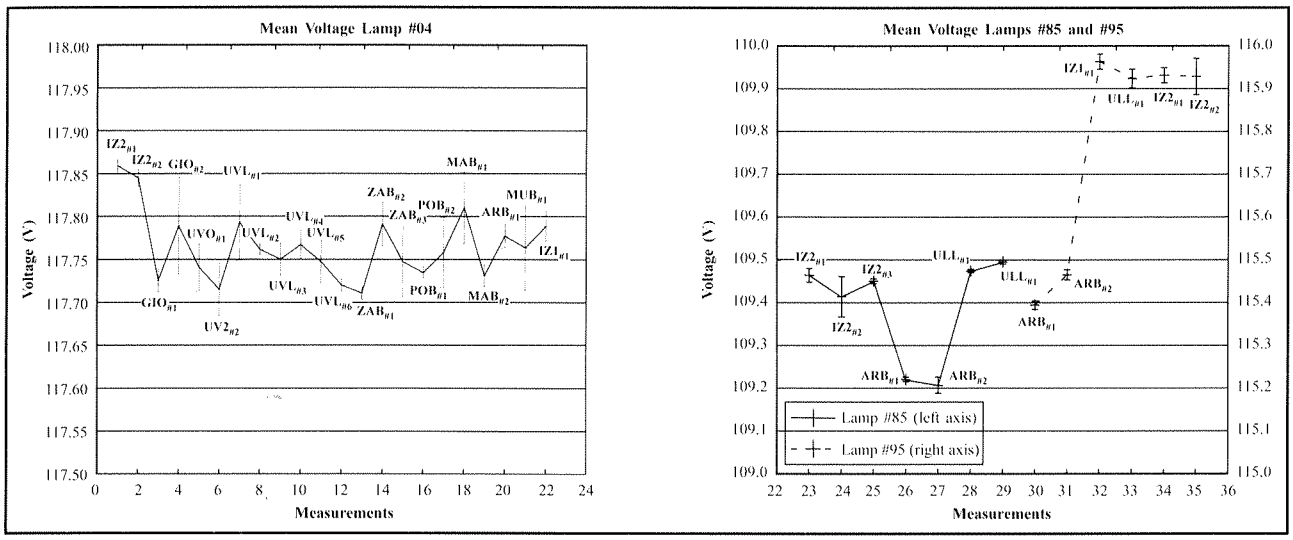

Fig. 10. *Voltage in the ends of the calibration lamps. The instrument and the calibration lamp used appear in the top of the figure. The last two figures shows the mean voltage and standard deviations for the three lamps (#4 –seasoned–, #85, and #95 –standard lamps–) during the three days of measurements in the laboratory. Table 4 shows the numerical values.*

Table 4. *Mean and standard deviation of the voltage recorded during the calibration of the instruments for the different lamps.*

Lamp 04	*Equipment*	*Date*	*Scan*	*Mean Voltage* [V]	*SD Voltage* (σ) [V]
	Bentham (Izaña Obs. INM)	06/09/99	#1	117.8590	0.0086
			#2	117.8449	0.0097
	Brewer (Izaña Obs. INM)	06/09/99	#1	117.7634	0.0176
	Optronic (Valencia Univ.)	07/09/99	#1	117.741	0.028
			#2	117.715	0.031
	LiCor (Valencia Univ.)	07/09/99	#1	117.793	0.044
			#2	117.7615	0.0068
			#3	117.750	0.019
			#4	117.767	0.017
			#5	117.747	0.025
			#6	117.7198	0.0076
	Oriel (Girona Univ.)	07/09/99	#1	117.725	0.014
			#2	117.789	0.057
	Brewer (Murcia INM)	07/09/99	#1	117.7634	0.0496
	Brewer 033 (Zaragoza INM)	08/09/99	#1	117.7106	0.0076
			#2	117.791	0.026
			#3	117.747	0.041
	Brewer 047 (IM Portugal)	08/09/99	#1	117.7345	0.0070
			#2	117.758	0.041
	Brewer 070 (Madrid INM)	08/09/99	#1	117.810	0.042
			#2	117.731	0.013
	Brewer 150 (CEDEA-INTA Arenosillo)	08/09/99	#1	117.777	0.014
Total Average				**117.765**	**0.039**

Lamp 85	*Equipment*	*Date*	*Scan*	*Mean Voltage* [V]	*SD Voltage* (σ) [V]
	Bentham (La Laguna Univ.)	06/09/99	#1	109.474	0.042
			#2	109.495	0.050
	Bentham (Izaña Obs. INM)	06/09/99	#1	109.464	0.016
			#2	109.414	0.047
			#3	109.4502	0.0056
	Brewer 150 (CEDEA-INTA Arenosillo)	08/09/99	#1	109.2205	0.0052
			#2	109.207	0.019
Total Average				**109.39**	**0.12**

Lamp 95	*Equipment*	*Date*	*Scan*	*Mean Voltage* [V]	*SD Voltage* (σ) [V]
	Bentham (La Laguna Univ.)	06/09/99	#1	115.924	0.022
	Brewer (Izaña Obs. INM)	06/09/99	#1	115.963	0.018
	Bentham (Izaña Obs. INM)	06/09/99	#1	115.931	0.0175
	Brewer (Izaña Obs. INM)	07/09/99	#1	115.928	0.0425
	Brewer 150 (CEDEA-INTA Arenosillo)	08/09/99	#1	115.394	0.010
			#2	115.465	0.012
Total Average				**115.430**	**0.050**

06/09/99

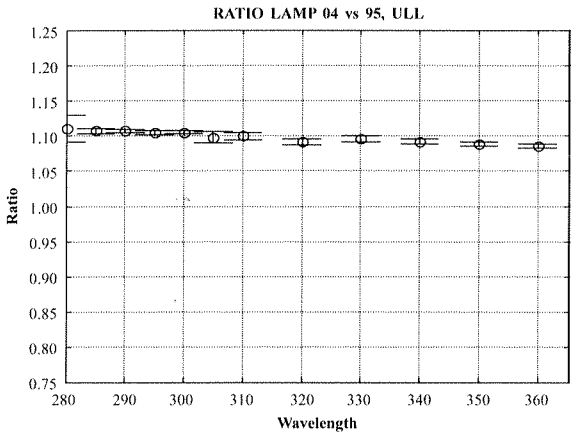

Wavelengths (nm)	Mean ratio	SD (σ)
2.8000000e+002	1.1104037e+000	1.8337646e−002
2.8500000e+002	1.1067764e+000	4.2868187e−003
2.9000000e+002	1.1067987e+000	2.4708464e−003
2.9500000e+002	1.1044880e+000	2.3497116e−003
3.0000000e+002	1.1050548e+000	1.7420701e−003
3.0500000e+002	1.0975858e+000	8.0175708e−003
3.1000000e+002	1.0994579e+000	5.1681357e−003
3.2000000e+002	1.0913032e+000	4.5396886e−003
3.3000000e+002	1.0962176e+000	4.4311719e−003
3.4000000e+002	1.0916177e+000	3.5723944e−003
3.5000000e+002	1.0885581e+000	3.2643352e−003
3.6000000e+002	1.0854035e+000	3.1900622e−003
3.7000000e+002	1.0826595e+000	2.4973155e−003
3.8000000e+002	1.0809028e+000	2.5847978e−003
3.9000000e+002	1.0781715e+000	3.2744407e−003
4.0000000e+002	1.0764100e+000	1.5643889e−003
4.1000000e+002	1.0745137e+000	1.1694695e−003
4.2000000e+002	1.0731064e+000	5.2412918e−004
4.3000000e+002	1.0706237e+000	9.5997217e−004
4.4000000e+002	1.0692749e+000	8.5502880e−004

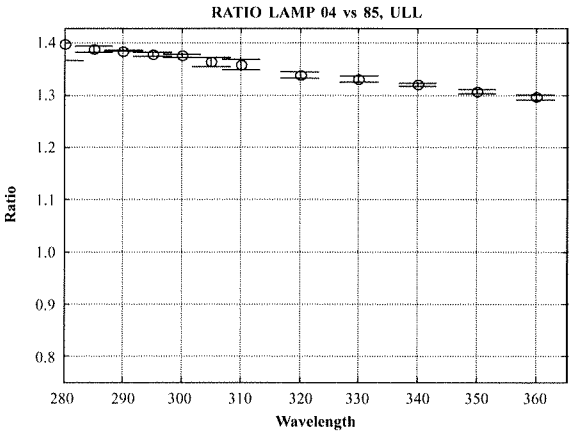

Wavelengths (nm)	Mean ratio	SD (σ)
2.8000000e+002	1.3986588e+000	3.0864162e−002
2.8500000e+002	1.3888669e+000	5.3444953e−003
2.9000000e+002	1.3856821e+000	1.6102692e−003
2.9500000e+002	1.3790349e+000	3.7846886e−003
3.0000000e+002	1.3765512e+000	3.0119626e−003
3.0500000e+002	1.3643496e+000	9.4548983e−003
3.1000000e+002	1.3586814e+000	1.0310527e−002
3.2000000e+002	1.3389290e+000	6.7084328e−003
3.3000000e+002	1.3315911e+000	6.0675510e−003
3.4000000e+002	1.3208897e+000	3.1851383e−003
3.5000000e+002	1.3077743e+000	3.7602658e−003
3.6000000e+002	1.2966410e+000	4.6876862e−003
3.7000000e+002	1.2877987e+000	4.9831319e−003
3.8000000e+002	1.2782087e+000	4.7349185e−003
3.9000000e+002	1.2678881e+000	5.8973344e−003
4.0000000e+002	1.2609527e+000	2.0462349e−003
4.1000000e+002	1.2529394e+000	2.9564496e−003
4.2000000e+002	1.2457008e+000	2.2875016e−003
4.3000000e+002	1.2373307e+000	2.4352753e−003
4.4000000e+002	1.2307238e+000	1.7932799e−003

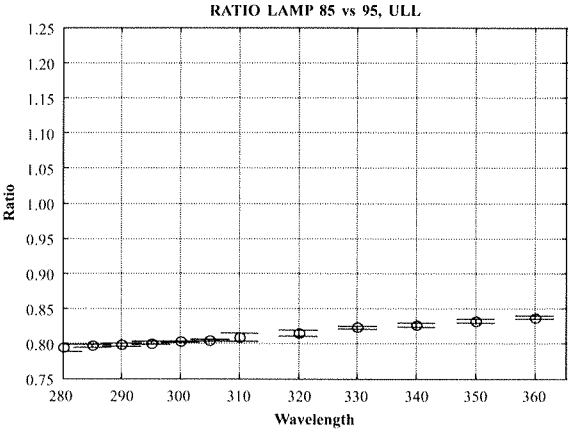

Wavelengths (nm)	Mean ratio	SD (σ)
2.8000000e+002	7.9398652e−001	5.2792469e−003
2.8500000e+002	7.9689493e−001	2.6052682e−003
2.9000000e+002	7.9874031e−001	2.0970997e−003
2.9500000e+002	8.0091813e−001	2.6265405e−003
3.0000000e+002	8.0277148e−001	6.7016808e−004
3.0500000e+002	8.0447494e−001	1.5526897e−003
3.1000000e+002	8.0924424e−001	6.2655719e−003
3.2000000e+002	8.1507156e−001	4.6321293e−003
3.3000000e+002	8.2324460e−001	2.7125049e−003
3.4000000e+002	8.2642826e−001	2.7031535e−003
3.5000000e+002	8.3238037e−001	3.3470696e−003
3.6000000e+002	8.3709302e−001	2.2353076e−003
3.7000000e+002	8.4071227e−001	2.4046651e−003
3.8000000e+002	8.4564417e−001	2.0896480e−003
3.9000000e+002	8.5037449e−001	1.8294299e−003
4.0000000e+002	8.5364925e−001	1.2841558e−003
4.1000000e+002	8.5759711e−001	1.4648698e−003
4.2000000e+002	8.6145056e−001	1.6575512e−003
4.3000000e+002	8.6527068e−001	1.1490991e−003
4.4000000e+002	8.6881915e−001	1.0908222e−003

Fig. 11 (part 1). *Ratios measured by the ULL instrument on 6/9/99 between the lamps #4 –seasoned–, #85, and #95 –standard lamps– and the lamps versus the calibration. Ratio of lamp #4 and calibration measured by IZ1 instrument on 6/9/99.*

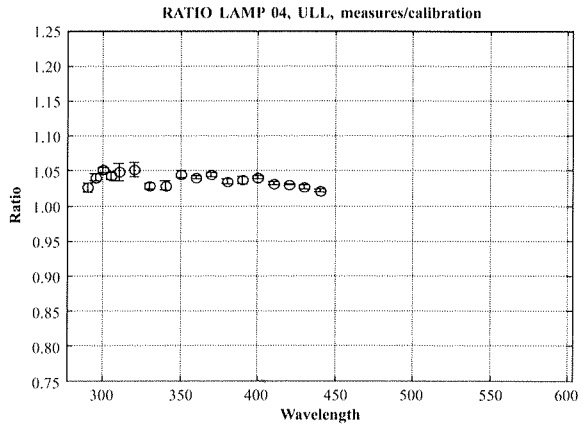

Wavelengths (nm)	Mean ratio	SD (σ)
2.9000000e+002	1.0263597e+000	6.6615782e−003
2.9500000e+002	1.0403647e+000	5.1283475e−003
3.0000000e+002	1.0512312e+000	3.1588409e−003
3.0500000e+002	1.0428737e+000	5.2643215e−003
3.1000000e+002	1.0483754e+000	1.2933029e−002
3.2000000e+002	1.0516290e+000	1.0463117e−002
3.3000000e+002	1.0282686e+000	4.3108385e−003
3.4000000e+002	1.0290057e+000	6.3809203e−003
3.5000000e+002	1.0450528e+000	4.8140137e−003
3.6000000e+002	1.0409150e+000	2.4987224e−003
3.7000000e+002	1.0444483e+000	2.8783895e−003
3.8000000e+002	1.0348869e+000	3.4153043e−003
3.9000000e+002	1.0370248e+000	5.3157122e−003
4.0000000e+002	1.0403592e+000	2.3210183e−003
4.1000000e+002	1.0318095e+000	2.1173767e−003
4.2000000e+002	1.0302552e+000	7.8374047e−004
4.3000000e+002	1.0269026e+000	2.5244568e−003
4.4000000e+002	1.0216688e+000	2.4347861e−003

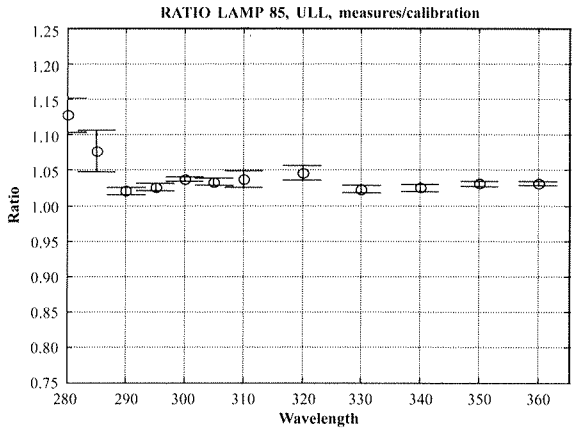

Wavelengths (nm)	Mean ratio	SD (σ)
2.8000000e+002	1.1277228e+000	2.3926478e−002
2.8500000e+002	1.0768503e+000	2.8790678e−002
2.9000000e+002	1.0205954e+000	5.6396962e−003
2.9500000e+002	1.0258316e+000	5.0346880e−003
3.0000000e+002	1.0366706e+000	2.8350078e−003
3.0500000e+002	1.0335011e+000	4.5218314e−003
3.1000000e+002	1.0369319e+000	1.1767620e−002
3.2000000e+002	1.0461138e+000	9.6154107e−003
3.3000000e+002	1.0231629e+000	5.2367728e−003
3.4000000e+002	1.0250609e+000	5.3806523e−003
3.5000000e+002	1.0307432e+000	3.1021732e−003
3.6000000e+002	1.0313899e+000	3.3745159e−003
3.7000000e+002	1.0337043e+000	4.2196352e−003
3.8000000e+002	1.0227842e+000	2.1892436e−003
3.9000000e+002	1.0251091e+000	5.3156829e−003
4.0000000e+002	1.0276913e+000	2.3514419e−003
4.1000000e+002	1.0194190e+000	2.2026231e−003
4.2000000e+002	1.0166856e+000	1.0449266e−003
4.3000000e+002	1.0143716e+000	2.1055677e−003
4.4000000e+002	1.0105756e+000	1.6549235e−003

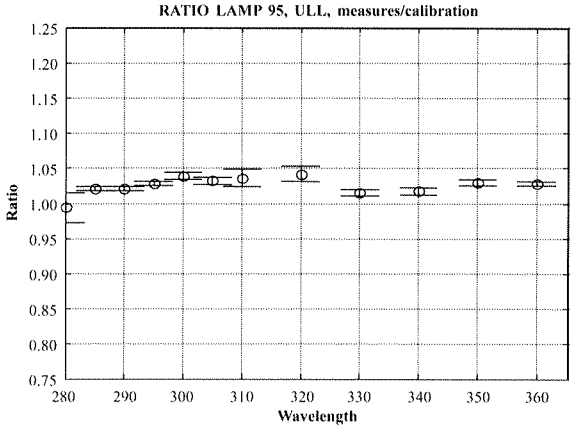

Wavelengths (nm)	Mean ratio	SD (σ)
2.8000000e+002	9.9441556e−001	2.0899432e−002
2.8500000e+002	1.0213238e+000	3.1434206e−003
2.9000000e+002	1.0217849e+000	2.9361329e−003
2.9500000e+002	1.0286703e+000	2.5639047e−003
3.0000000e+002	1.0391662e+000	5.3986720e−003
3.0500000e+002	1.0327458e+000	5.0935522e−003
3.1000000e+002	1.0363865e+000	1.2238376e−002
3.2000000e+002	1.0422471e+000	1.1172093e−002
3.3000000e+002	1.0155366e+000	4.9141725e−003
3.4000000e+002	1.0176788e+000	4.8662732e−003
3.5000000e+002	1.0299967e+000	3.8011289e−003
3.6000000e+002	1.0285656e+000	2.4239179e−003
3.7000000e+002	1.0265887e+000	2.6630128e−003
3.8000000e+002	1.0202510e+000	1.8264439e−003
3.9000000e+002	1.0219660e+000	5.5115096e−003
4.0000000e+002	1.0266691e+000	1.6364538e−003
4.1000000e+002	1.0185806e+000	2.4603249e−003
4.2000000e+002	1.0139769e+000	1.1015734e−003
4.3000000e+002	1.0078008e+000	3.5506458e−003
4.4000000e+002	9.9809593e−001	3.6214658e−003

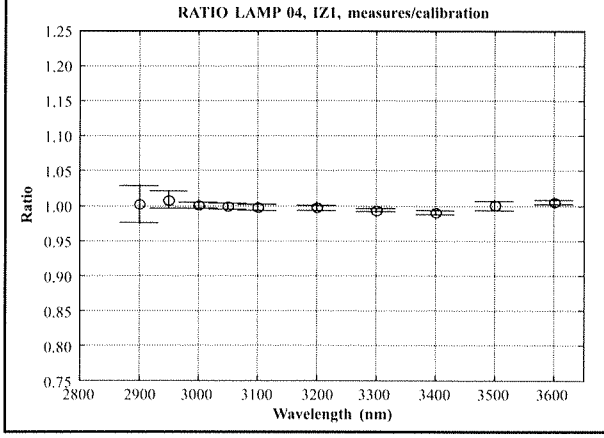

Wavelengths (nm)	Mean ratio	SD (σ)
2900	1.002E+000	2.67E−002
2950	1.009E+000	1.23E−002
3000	1.000E+000	4.10E−003
3050	9.988E−001	4.39E−003
3100	9.978E−001	4.47E−003
3200	9.973E−001	3.19E−003
3300	9.941E−001	2.22E−003
3400	9.906E−001	3.39E−003
3500	1.000E+000	6.48E−003
3600	1.005E+000	2.90E−003

Fig. 11 (& part 2). *Ratios measured by the ULL instrument on 6/9/99 between the lamps #4 –seasoned–, #85, and #95 –standard lamps– and the lamps versus the calibration. Ratio of lamp #4 and calibration measured by IZ1 instrument on 6/9/99.*

07/09/99

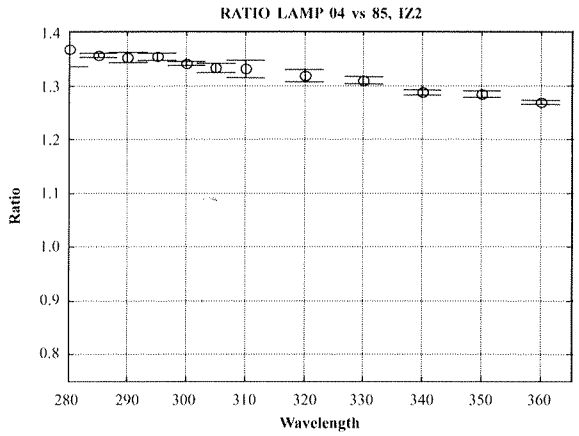

Wavelengths (nm)	Mean ratio	SD (σ)
2.8000000e+002	1.3685713e+000	3.2569780e−002
2.8500000e+002	1.3561160e+000	4.0686223e−003
2.9000000e+002	1.3530838e+000	9.0649060e−003
2.9500000e+002	1.3539252e+000	6.4083940e−003
3.0000000e+002	1.3409112e+000	4.0635064e−003
3.0500000e+002	1.3328824e+000	8.9088053e−003
3.1000000e+002	1.3308124e+000	1.5387567e−002
3.2000000e+002	1.3187939e+000	1.1669695e−002
3.3000000e+002	1.3093236e+000	6.3872809e−003
3.4000000e+002	1.2870314e+000	5.5254812e−003
3.5000000e+002	1.2836823e+000	6.0980148e−003
3.6000000e+002	1.2692844e+000	4.1426148e−003
3.7000000e+002	1.2626543e+000	6.2518574e−003
3.8000000e+002	1.2490935e+000	5.1420417e−003
3.9000000e+002	1.2427817e+000	4.0078435e−003
4.0000000e+002	1.2389042e+000	0.0000000e+000

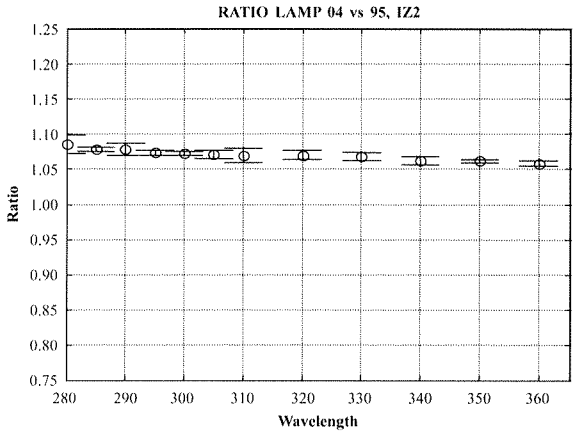

Wavelengths (nm)	Mean ratio	SD (σ)
2.8000000e+002	1.0853941e+000	1.3626867e−002
2.8500000e+002	1.0785963e+000	2.8638644e−003
2.9000000e+002	1.0781042e+000	8.1832703e−003
2.9500000e+002	1.0735529e+000	3.8305551e−003
3.0000000e+002	1.0726880e+000	3.1319396e−003
3.0500000e+002	1.0712310e+000	5.9924546e−003
3.1000000e+002	1.0698710e+000	1.0258824e−002
3.2000000e+002	1.0695564e+000	6.6410646e−003
3.3000000e+002	1.0683203e+000	5.9303256e−003
3.4000000e+002	1.0621977e+000	6.1831129e−003
3.5000000e+002	1.0615513e+000	2.7081059e−003
3.6000000e+002	1.0579022e+000	3.6953460e−003
3.7000000e+002	1.0585856e+000	5.0707585e−003
3.8000000e+002	1.0574413e+000	5.4795729e−003
3.9000000e+002	1.0555630e+000	2.5550459e−003
4.0000000e+002	1.0547771e+000	0.0000000e+000

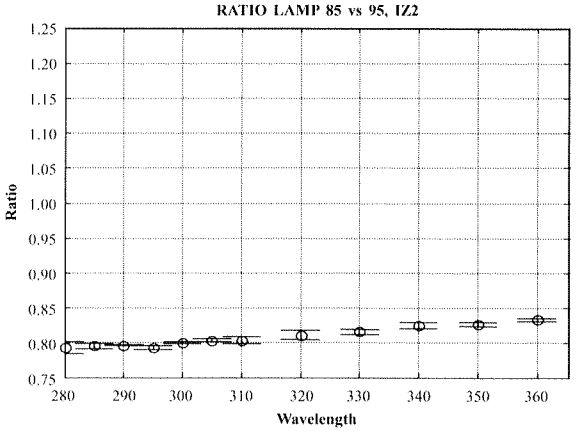

Wavelengths (nm)	Mean ratio	SD (σ)
2.8000000e+002	7.9325197e−001	8.8523227e−003
2.8500000e+002	7.9536208e−001	2.9763088e−003
2.9000000e+002	7.9677253e−001	1.3999117e−003
2.9500000e+002	7.9292533e−001	2.5928952e−003
3.0000000e+002	7.9997038e−001	1.2078773e−003
3.0500000e+002	8.0370207e−001	2.3145661e−003
3.1000000e+002	8.0395639e−001	5.6876748e−003
3.2000000e+002	8.1104913e−001	6.5292774e−003
3.3000000e+002	8.1593749e−001	3.5954852e−003
3.4000000e+002	8.2531591e−001	4.9591092e−003
3.5000000e+002	8.2696957e−001	3.2100668e−003
3.6000000e+002	8.3346669e−001	2.6409076e−003
3.7000000e+002	8.3838390e−001	1.9839395e−003
3.8000000e+002	8.4656836e−001	3.1125465e−003
3.9000000e+002	8.4935872e−001	1.8732077e−003
4.0000000e+002	8.5137912e−001	0.0000000e+000

Fig. 12 (part 1). *Ratios measured by the IZ2 instrument on 7/9/99 between the lamps #4 –seasoned–, #85, and #95 –standard lamps– and the lamps versus the calibration. Ratios of lamp #4 and calibration measured by different instrument on 7/9/99.*

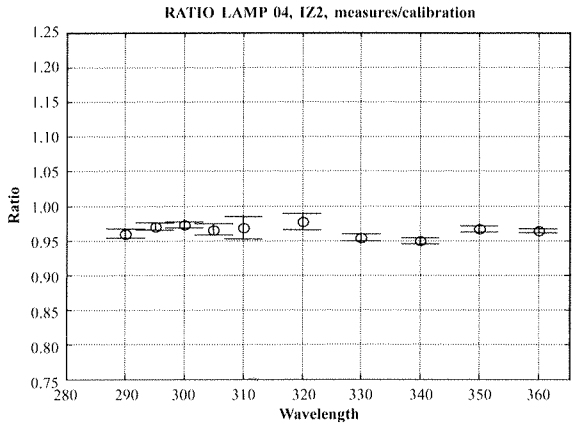

Wavelengths (nm)	Mean ratio	SD (σ)
2.9000000e+002	9.6049229e−001	6.3599341e−003
2.9500000e+002	9.7056152e−001	5.5911151e−003
3.0000000e+002	9.7247443e−001	4.3989547e−003
3.0500000e+002	9.6600183e−001	7.9359140e−003
3.1000000e+002	9.6826979e−001	1.6324287e−002
3.2000000e+002	9.7743380e−001	1.1602121e−002
3.3000000e+002	9.5466447e−001	5.6991882e−003
3.4000000e+002	9.4984346e−001	3.9503086e−003
3.5000000e+002	9.6678126e−001	4.0660265e−003
3.6000000e+002	9.6459300e−001	3.1663364e−003
3.7000000e+002	9.7393660e−001	4.3929925e−003
3.8000000e+002	9.6952332e−001	1.6030073e−003
3.9000000e+002	9.7776368e−001	9.7000459e−003
4.0000000e+002	9.8951925e−001	0.0000000e+000

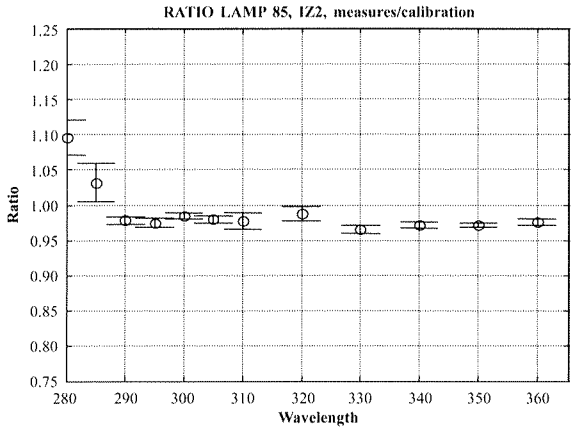

Wavelengths (nm)	Mean ratio	SD (σ)
2.8000000e+002	1.0955961e+000	2.4710317e−002
2.8500000e+002	1.0321454e+000	2.7040281e−002
2.9000000e+002	9.7812219e−001	4.8687039e−003
2.9500000e+002	9.7476290e−001	6.6284801e−003
3.0000000e+002	9.8449583e−001	4.3163566e−003
3.0500000e+002	9.7990592e−001	5.0374456e−003
3.1000000e+002	9.7773439e−001	1.1464772e−002
3.2000000e+002	9.8716730e−001	1.0211980e−002
3.3000000e+002	9.6607768e−001	5.8702700e−003
3.4000000e+002	9.7110486e−001	4.1658648e−003
3.5000000e+002	9.7144890e−001	3.5098933e−003
3.6000000e+002	9.7636691e−001	4.4507690e−003
3.7000000e+002	9.8310798e−001	2.7654369e−003
3.8000000e+002	9.8052541e−001	2.5646172e−003
3.9000000e+002	9.8603881e−001	8.5339421e−003
4.0000000e+002	9.9634963e−001	0.0000000e+000

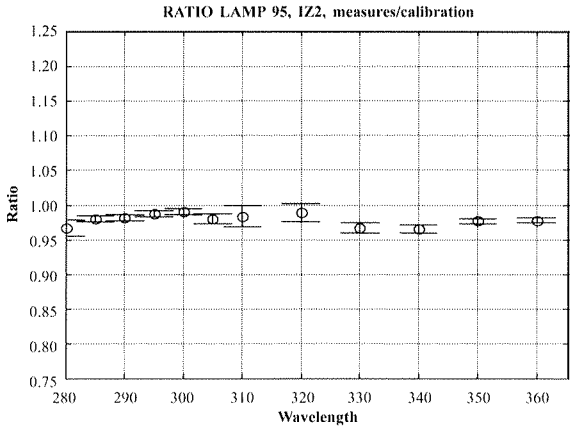

Wavelengths (nm)	Mean ratio	SD (σ)
2.8000000e+002	9.6687556e−001	1.1668342e−002
2.8500000e+002	9.8082733e−001	4.4983538e−003
2.9000000e+002	9.8168543e−001	4.2328146e−003
2.9500000e+002	9.8730850e−001	3.9867477e−003
3.0000000e+002	9.9031540e−001	4.6640700e−003
3.0500000e+002	9.8014388e−001	7.5121673e−003
3.1000000e+002	9.8368332e−001	1.5212211e−002
3.2000000e+002	9.8842863e−001	1.3185561e−002
3.3000000e+002	9.6747570e−001	6.9905910e−003
3.4000000e+002	9.6543462e−001	6.3578537e−003
3.5000000e+002	9.7709526e−001	3.7894461e−003
3.6000000e+002	9.7792992e−001	3.5447762e−003
3.7000000e+002	9.7905778e−001	3.5630247e−003
3.8000000e+002	9.7703663e−001	3.8039419e−003
3.9000000e+002	9.8418876e−001	8.3080834e−003
4.0000000e+002	9.9533190e−001	0.0000000e+000

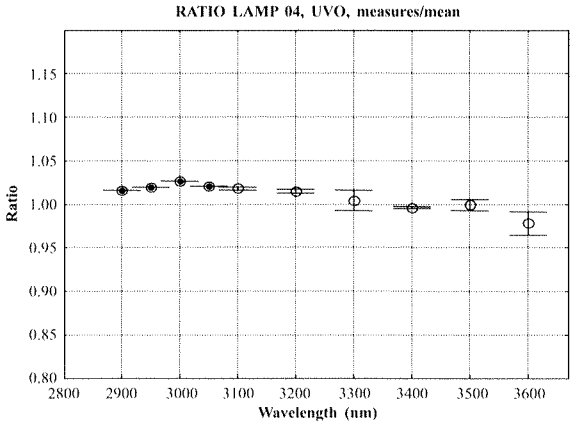

Wavelengths (Å)	Mean ratio	SD (σ)
2.9000000e+003	1.0159490e+000	0.0000000e+000
2.9500000e+003	1.0192340e+000	0.0000000e+000
3.0000000e+003	1.0266020e+000	0.0000000e+000
3.0500000e+003	1.0210450e+000	0.0000000e+000
3.1000000e+003	1.0175480e+000	1.1921820e−003
3.2000000e+003	1.0144850e+000	1.9233304e−003
3.3000000e+003	1.0041661e+000	1.1770358e−002
3.4000000e+003	9.9584145e−001	9.8973736e−004
3.5000000e+003	9.9905715e−001	6.7187165e−003
3.6000000e+003	9.7827885e−001	1.3404270e−002
3.7000000e+003	1.0052487e+000	2.3195012e−002
3.8000000e+003	1.0046613e+000	7.3959127e−003
3.9000000e+003	9.9838485e−001	6.5282219e−003
4.0000000e+003	9.8137465e−001	2.0106935e−002
4.1000000e+003	9.9563180e−001	6.6468037e−006
4.2000000e+003	9.9570390e−001	1.9772120e−003
4.3000000e+003	9.9172510e−001	3.3648383e−003
4.4000000e+003	9.9146730e−001	1.9386040e−003

Fig. 12 (part 2). *Ratios measured by the IZ2 instrument on 7/9/99 between the lamps #4 –seasoned–, #85, and #95 –standard lamps– and the lamps versus the calibration. Ratios of lamp #4 and calibration measured by different instrument on 7/9/99.*

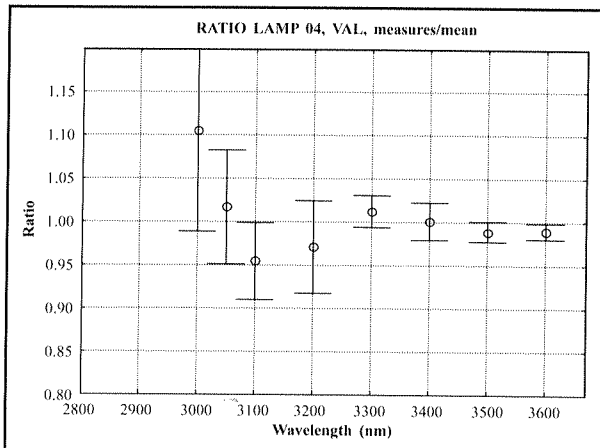

Wavelengths (Å)	Mean ratio	SD (σ)
3.0000000e+003	1.1058068e+000	1.1675211e−001
3.0500000e+003	1.0170454e+000	6.6097266e−002
3.1000000e+003	9.5462658e−001	4.4487486e−002
3.2000000e+003	9.7110257e−001	5.3653525e−002
3.3000000e+003	1.0123056e+000	1.7938938e−002
3.4000000e+003	1.0011733e+000	2.1266260e−002
3.5000000e+003	9.8921674e−001	1.1973398e−002
3.6000000e+003	9.8965616e−001	8.8147108e−003
3.7000000e+003	9.9822695e−001	2.8869119e−003
3.8000000e+003	9.9045002e−001	3.3733418e−003
3.9000000e+003	9.9210243e−001	3.0138608e−003
4.0000000e+003	9.8686535e−001	2.2483513e−003
4.1000000e+003	9.8564225e−001	1.7813430e−003
4.2000000e+003	9.8436259e−001	1.4043297e−003
4.3000000e+003	9.8366974e−001	9.1140472e−004
4.4000000e+003	9.8386994e−001	1.0162313e−003

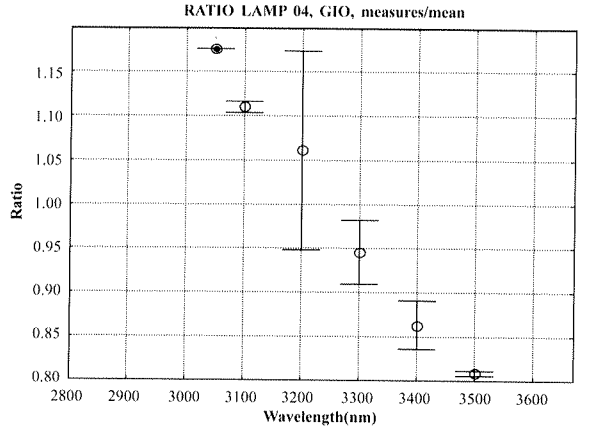

Wavelengths (Å)	Mean ratio	SD (σ)
3.0500000e+003	1.1754890e+000	0.0000000e+000
3.1000000e+003	1.1101960e+000	6.4276006e−003
3.2000000e+003	1.0609015e+000	1.1259056e−001
3.3000000e+003	9.4577795e−001	3.6096882e−002
3.4000000e+003	8.6270025e−001	2.7386741e−002
3.5000000e+003	8.0849550e−001	2.9185125e−003
3.6000000e+003	7.5066540e−001	3.1299940e−002

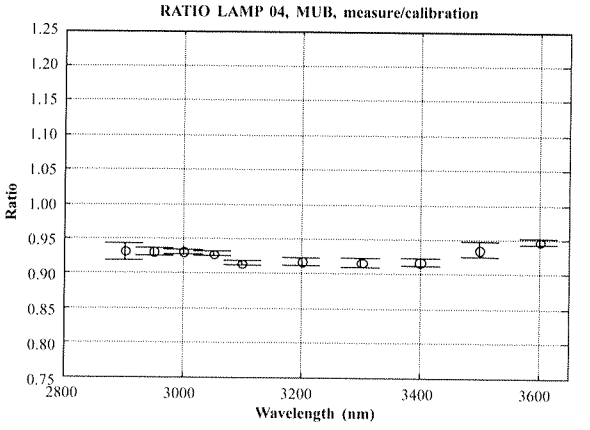

Wavelengths (Å)	Mean ratio	SD (σ)
2900	9.320E−001	1.19E−002
2950	9.308E−001	4.99E−003
3000	9.308E−001	3.31E−003
3050	9.288E−001	3.18E−003
3100	9.154E−001	3.89E−003
3200	9.172E−001	5.48E−003
3300	9.158E−001	6.94E−003
3400	9.173E−001	4.95E−003
3500	9.359E−001	1.12E−002
3600	9.476E−001	3.95E−003

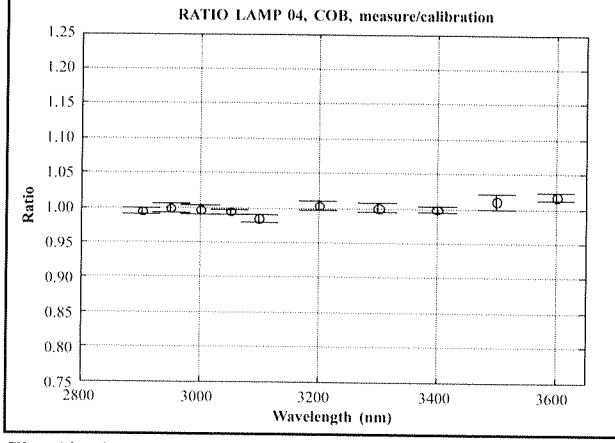

Wavelengths (Å)	Mean ratio	SD (σ)
2900	9.943E−001	3.92E−003
2950	9.983E−001	6.68E−003
3000	9.964E−001	7.42E−003
3050	9.943E−001	3.71E−003
3100	9.847E−001	5.06E−003
3200	1.003E+000	6.53E−003
3300	1.002E+000	6.12E−003
3400	9.993E−001	4.39E−003
3500	1.011E+000	1.03E−002
3600	1.018E+000	6.15E−003

Fig. 12 (& part 3). *Ratios measured by the IZ2 instrument on 7/9/99 between the lamps #4 –seasoned–, #85, and #95 –standard lamps– and the lamps versus the calibration. Ratios of lamp #4 and calibration measured by different instrument on 7/9/99.*

08/09/99

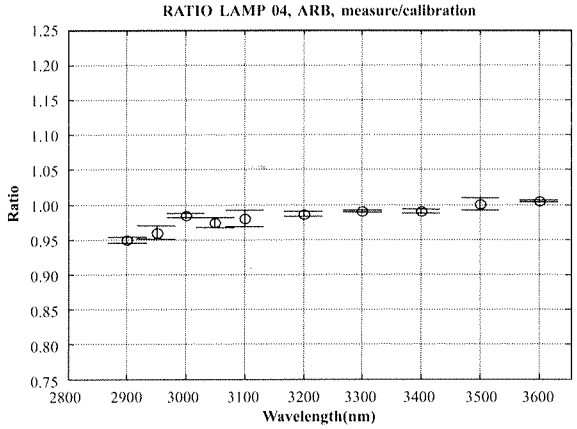

Wavelengths (Å)	Mean ratio	SD (σ)
2900	9.498E−001	4.79E−003
2950	9.603E−001	9.74E−003
3000	9.847E−001	3.55E−003
3050	9.748E−001	7.21E−003
3100	9.802E−001	1.12E−002
3200	9.864E−001	3.63E−003
3300	9.906E−001	2.04E−003
3400	9.906E−001	2.57E−003
3500	1.000E+000	8.49E−003
3600	1.005E+000	1.67E−003

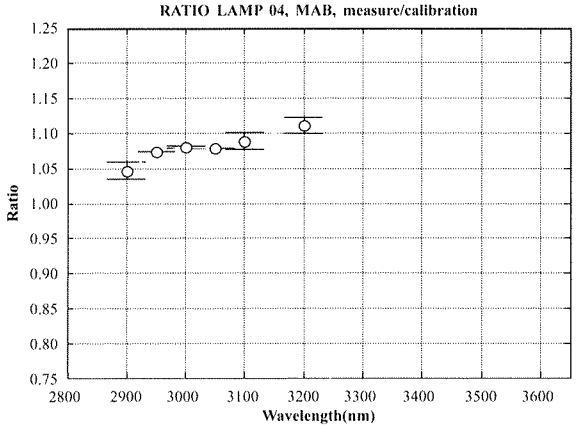

Wavelengths (Å)	Mean ratio	SD (σ)
2900	1.047E+000	1.22E−002
2950	1.073E+000	0.00E+000
3000	1.080E+000	1.49E−003
3050	1.079E+000	0.00E+000
3100	1.089E+000	1.29E−002
3200	1.111E+000	1.15E−002

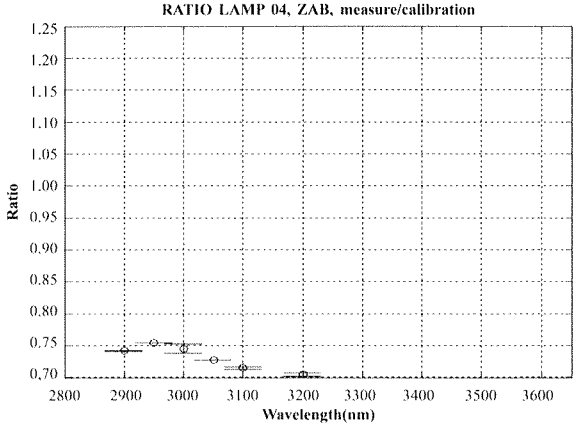

Wavelengths (Å)	Mean ratio	SD (σ)
2900	7.416E−001	5.00E−004
2950	7.538E−001	0.00E+000
3000	7.455E−001	7.07E−003
3050	7.272E−001	0.00E+000
3100	7.147E−001	2.51E−003
3200	7.045E−001	2.26E−003

Fig. 13 (part 1). *Ratios of lamp #4 and calibration measured by different instrument on 8/9/99.*

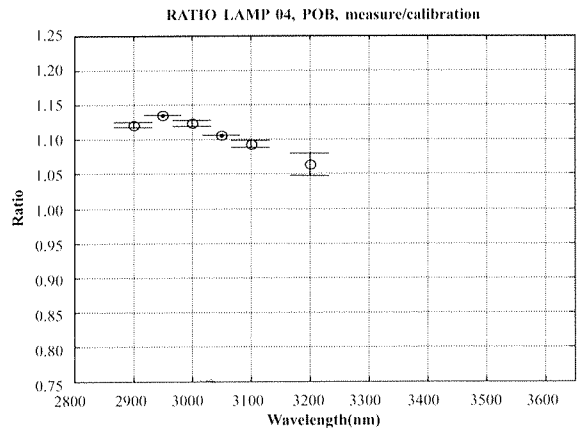

Wavelengths (Å)	Mean ratio	SD (σ)
2900	1.121E+000	3.01E−003
2950	1.135E+000	0.00E+000
3000	1.124E+000	4.18E−003
3050	1.106E+000	0.00E+000
3100	1.094E+000	4.92E−003
3200	1.064E+000	1.66E−002

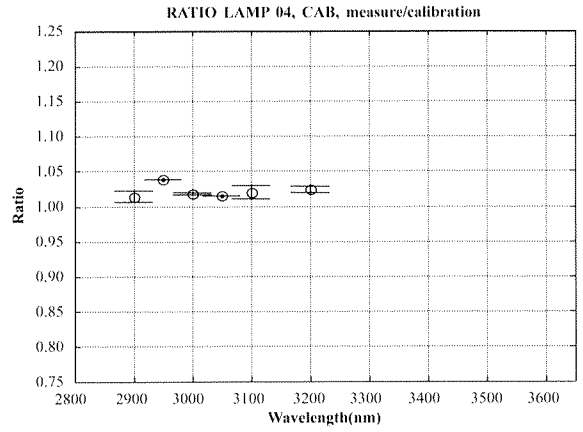

Wavelengths (Å)	Mean ratio	SD (σ)
2900	1.014E+000	8.32E−003
2950	1.038E+000	0.00E+000
3000	1.018E+000	1.77E−003
3050	1.015E+000	0.00E+000
3100	1.020E+000	9.37E−003
3200	1.024E+000	4.23E−003

Fig. 13 (& part 2). *Ratios of lamp #4 and calibration measured by different instrument on 8/9/99.*

5.4. REFERENCES

GARDINER, B. G. and P. J. KIRSCH (1995): "Setting standards for European ultraviolet spectroradiometers". Air Pollution Research Report 53. Commision of the European Communities, Luxembourg, Report EUR 16153, ISSN 1018 5593, ISBN 92 826 5405 2, 138 pp.

GARDINER, B. G. and P. J. KIRSCH (1996): "Intercomparison of ultraviolet spectroradiometers, Ispra, 24-25 May 1995". Report to the Commision of the European Communities, Directorate-General for Science, Research and Development, Bruxelles, Contract EV5V-CT93-0353. 84 pp.

REDONDAS, A. (1999): "Protocolo de calibración y control de calidad". Nota técnica presentada en la 1.ª Intercomparación de radiómetros UV en El Arenosillo (Huelva). Proyecto CICYT CLI97-0345-C05.

WALKER, J. H., R. D. SAUNDERS, J. K. JACKSON and D. A. MCSPARROW (1987): "Spectral irradiance calibrations". NBS Special Publication 250-20. U.S. Government Printing Office, Washington, DC, 102 pp.

WALKER, J. H., R. D. SAUNDERS, J. K. JACKSON and K. D. MIELENZ (1991): "Results of a CCPR intercomparison of spectral irradiance measurements by national laboratories". *J. Res. Natl. Inst. Stand. Technol.*, **96 (6)**, 647-668.

ACKNOWLEDGEMENTS

We thank to the CICYT projects CLI97-0453 and CLI97-0345-C05 for economical support during this work.

CHAPTER 6

INTERCOMPARISON OF SOLAR UV MEASUREMENTS: SPECTRAL AND BROADBAND INSTRUMENTS

A. Redondas[1], J. Gröbner[2], J. P. Díaz[3], F. J. Expósito[3], C. Torres[1], V. Carreño[1] and J. M. Vilaplana[4]

[1] Observatorio Atmosférico de Izaña, Instituto Nacional de Meteorología. 38071 Santa Cruz de Tenerife, *aredondas@inm.es*.

[2] International Ozone Services (IOS), Toronto, Canada. Present address: IHCP, Joint Research Centre, Ispra, Varese, Italy.

[3] Departamento de Física Básica, Universidad de La Laguna. 38200 La Laguna, S. C. de Tenerife.

[4] Instituto Nacional de Técnica Aeroespacial, Estación de Ozonosondeos de "El Arenosillo", Huelva.

SUMMARY

The first Iberian UV radiation intercomparison was held at "El Arenosillo" – Huelva station of INTA (Instituto Nacional de Técnica Aeroespacial) from 1st to 10th September 1999. Eleven spectroradiometers from Spain, one from Canada, and one from Portugal participated in the UV intercomparison. This intercomparison was developed in the frame of the research projects CLI97-0453 and CLI97-0345-C05, supported by the Spanish Government (Comisión Interministerial de Ciencia y Tecnología). The methodology of the solar intercomparison and the results are shown in this chapter. The procedure used on the campaign follows the methods used in recent European intercomparison. The results show that the measurements of the three reference instruments, ARB, IZ1 and ULL are in +/–1% agreement during both days of the campaign. The other two double monochromators are also on this 1% agreement, the IZ2 instrument during the first day, and the UVO instrument when wavelengths averages are considered. Regarding to the UVI data, the campaign probe that with the exceptions of the VAL and GIO instruments all the participating instruments provide accurate Ultraviolet Index with the 80% of the measurements accord with the reference and the 100% of valid measurements within +/–1 UVI.

6.1. INTRODUCTION

The solar UV radiation, due to its energy, can affect drastically all ecosystems in the biosphere. The radiative transfer of UV solar radiation in the Earth atmosphere is function of astronomical factors, total ozone concentration, clouds, surface albedo, and/or aerosols. The alarming reports about the ozone layer depletion, mainly at Antarctic region, have drawn attention to eventual increase of ultraviolet solar radiation at Earth's surface. In the latest year have been measured increases up to 70% in the erythemally-weighted UV radiation.

Due to the complexity of the radiative transfer modelling of the UV solar radiation, direct measurements are needed. To achieve the necessary accuracy and precision to can use the measurements in trends studies, several approaches can be used to improve the quality of UV data. One of most useful is the organization of joint intercomparison, both of calibrations set-ups and of spectroradiometers.

The first Iberian UV radiation intercomparison was held at the facilities of the Centro de Experimentación de El Arenosillo (CEDEA) of Instituto Nacional de Técnica Aeroespacial (INTA, Spain) from 1st to 10th September 1999. This station is located in Huelva and it is described in chapter 2 of this report. This campaign was organized in the frame of the research projects: Measurements and modelization of the space-time distribution of solar UV irradiance in Spain, and Investigation of the interrelations of the UV radiation levels with the radiative properties of the atmospheric aerosols and clouds, both supported by the Comisión Interministerial de Ciencia y Tecnología, Spanish Government, with references CLI97-0345-C05 and CLI97-0453, respectively. The main goal was to test the homogeneity and intercomparibility of the instrument of the Iberian UV network. This campaign brought together about 30 scientists from Spain, Portugal, Canada and Austria. The institutions providing UV data for the intercomparison were: Instituto Nacional de Técnica Aeroespacial-Spain (INTA, the host), Instituto Nacional de Meteorología-Spain (INM), Instituto Portugues de Meteorología (IPM), Universidad de La Laguna (ULL), Universidad de Valencia (UV), and Universidad de Girona (UV). The instruments are: 3 Brewer Mk-II, 3 Brewer MK-IV, 2 Brewer MK-III, 1 Optronic OL752, 1 Oriel MS257, 1 LICOR 1800, and 2 Bentham DM150. In table 1 appears the data for each instrument and institution.

The intercomparison campaign permits us to detect hidden characteristics of the instruments or in the measurements procedure, which will be very difficult to detect by other strategies. On the other hand, the exchange of experiences and knowledge between the participants is one most important valuable objective of these campaigns.

Table 1. *Spectral instruments participating in the First Iberian UV radiation intercomparison. In bold the instruments belonging to the INM network.*

Station measurements	*Instrument*	*Code*	*Institution*
Observatorio Atmosférico de Izaña (Tenerife)	**MK-III**	**IZ1**	**INM**
Observatorio Atmosférico de Izaña (Tenerife)	**Bentham DM 150**	**IZ2**	**INM**
A Coruña	**MK-IV**	**COB**	**INM**
Madrid	**MK-IV**	**MAB**	**INM**
Murcia	**MK-IV**	**MUB**	**INM**
Zaragoza	**MK-II**	**ZAB**	**INM**
El Arenosillo	**MK-III**	**ARB**	**INTA**
Azores	MK-II	POB	
Ozone Travelling Standard	MK-II	CAB	Instruments Ozone Service
La Laguna	**Bentham DM 150**	**ULL**	**Universidad de La Laguna**
Valencia	Optronic 752	UVO	Universidad de Valencia
Gerona	Oriel MS 257	GIO	Universidad de Girona

This chapter is divided into 13 points, from which 6 are appendixes. In the second point the methodology of the campaign is described, whereas the results are discussed in the next one following these 5 headers: wavelength shift, sky measurements results, UV index (UVI) intercomparison, detailed report and instrument review. The broadband results are shown in the part number 4. The conclusions are summarized in the 5, and the acknowledgments and references appear in the sections 6 and 7 respectively. The appendixes start in the point 8 and are: Slits function of the instruments, wavelength shift of the instruments, ratio for the different instruments versus the reference for the Julian day 246, the next one is the same but for the Julian day 247. Finally the UVI measurements for both days (246 and 247), and the detailed report for each instrument are described.

6.2. INTERCOMPARISON PROCEDURE

During the blind days the instruments used its own calibration and interchange of data between teams were avoided. To assurance the comparison of the data a common horizon and time synchronization had to be granted. For the common horizon the instruments were installed on the roof (figure 1) at the similar level, the main obstacle was a tower above the roof at 20 meters at south of the instruments (see Chapter 2 for details). The simultaneous measurements of spectral global irradiance from 290 to 365 nanometers with a step of 0.5 nm were used on the comparison. The scans were taken every full and half an hour, from the sunrise to the sunset, from 6:30 to 18:30 UTC. On the "blind days", days without information interchange between operators, every instrument measured the same wavelength at the same time. A time of three second between each wavelength step were decided in order to allow slow instruments could made synchronous measurements. This gives a scan time about 6 minutes during the measurements. The first quarter from every full and half hour, instruments intervention by the operators were forbidden to avoid shadows or interferences to the measurements. The irradiance data used for the comparison were submitted before the noontime of the next day.

The first day of the Intercomparison, 246/99, all the instruments took measurements but POB, with instrumental problems, missed this day, which was nearly clear (see meteorology in Chapter 3 for details). There was a general power failure at 9:45, which affected to all the instruments, and most of them lost the 10:00 scan. The second day was cloudy on the morning and clear at the afternoon, all the instruments could perform the entire scheduled program.

Fig. 1. Instruments location during the blind days, on the left the seven Brewers, on the right the two Bentham over wood boxes, Optronic, Oriel and Licor. The photo was taken from the tower, the main obstacle for the instruments.

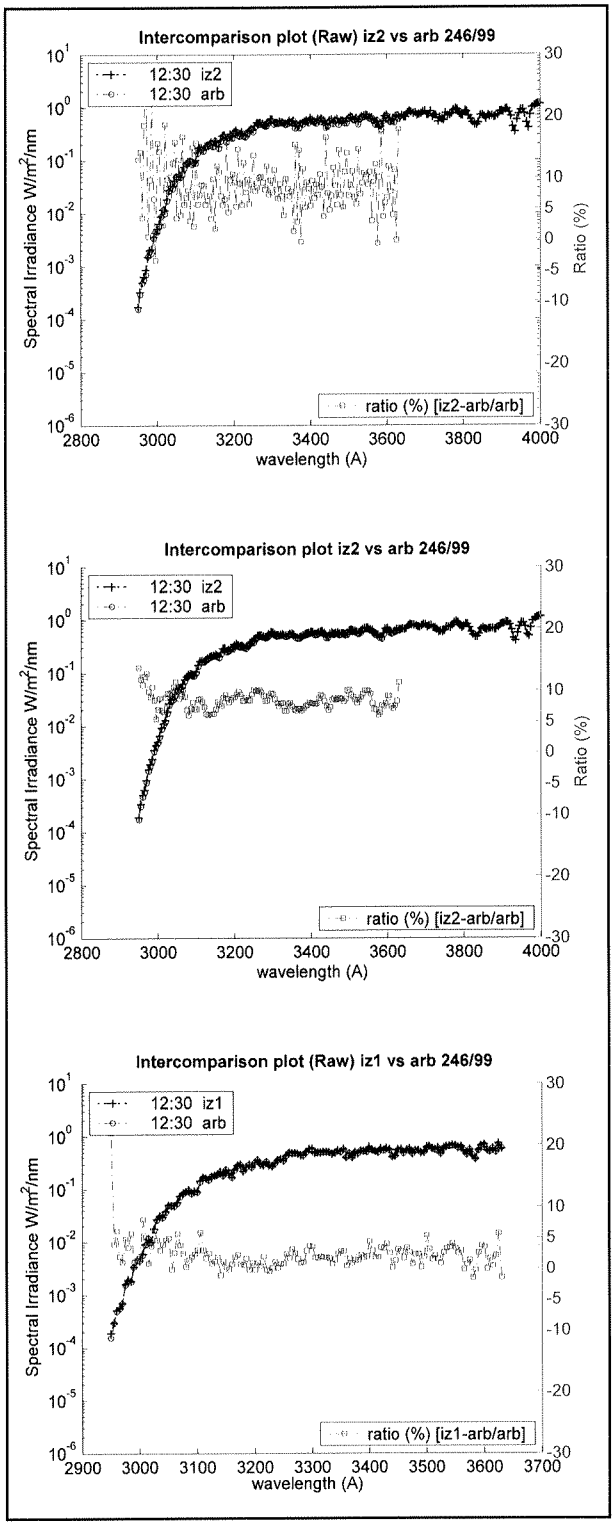

Fig. 2. Comparison of 12:30 scans, on the left axis the spectra irradiance of the two instruments on logarithmic scale, the first instrument in black crosses and the second one on blue circles. The percent ratios of one instrument versus the second one for each wavelength are showed on the right axis. The upper graph shows the comparison of the spectra of different instrument ARB Brewer MKIII vs. IZ1 Bentham DM-150, a characteristic scatter of the ratio. When comparing identical instruments, like the two double Brewers "ARB" and "IZ1" with similar slit functions, this scatter reduces significantly. The same effect with different instruments is achieved when use the "analysed spectra" for the instruments of the figure one.

When comparing different instruments the ratios of synchronous scans show a characteristic and sometimes-noisy wavelength pattern (Figure 2). These noisy patterns are caused by the different instrument characteristics, mainly due to its different slit function and wavelength alignment (Slaper, 1997). These noises obscure the interpretation of the results. With the experience of previous intercomparison campaigns as NOGIC 93, 97 and SUSPEN 97 a better comparison is achieved if an "analysed spectra", which correct these unwanted effects, is used. These "analysed spectra" or "normalized spectra" are post-processed spectra by the "SHICrivm" algorithm described on detail on Slaper (1995) and Slaper and Koskela (1997). Firstly, the process implements a wavelength shift correction.

The shift is calculated through comparison of the structure on the measured spectra, caused by the Fraunhofer lines, with the same structures on high-resolution extraterrestrial spectrum. The high resolution spectra used (obtained at Kitty Peak), has an error better than 0.005 nm (*Kurucz et al.*, 1984). The precision of the wavelength shift algorithm is estimated on 0.01 nm even in cloudy conditions (*Slaper*, 1997). Then the effect of the different slit function is corrected deconvolving the instrument spectra with the instrument slit function and convolving again with a common slit. This common slit has a triangular shape with a full wide half maximum (FWHM) of 1 nm. All these processes are implemented by SHICrivm 2.75 program developed by Slaper. The performance of the algorithm depends on the stability of the atmospheric transmission during the scan, the measurement noise, and the FWHM of the instrument.

For practical reasons, is better to establish a common reference to compare all the instruments. We can use a unique instrument, like in NOGIC 93 (*Koskela*, 1994) or Garmish 97 (*Seckmeyer*, 1998) campaigns but the problem arises if the reference instrument misses one record. Or we can use more sophisticated algorithms to select the reference with a mean of selected instruments like NOGIC 96 which try to select the most stable instruments (*Slaper and Koskela*, 1997) or the "objective algorithms" used on SUSPEN 97 (*Gardiner and Kirsch*, 1997). On the Iberian campaign we use the ARB instrument as the reference to rapid evaluation during the intercomparison and a mean of the five doubles monochromators: ARB, IZ1, IZ2, ULL and UVO on the final analysis. From this "arbitrary" reference we remove the UVO instrument due to the big wavelength shift error, which was bigger than the SCHIRIVM algorithm can correct (Figure 4 and 5). The IZ2 instrument was also removed of the mean on the second day due a big change on the instrument response latter described on this chapter. The reference calculated for the comparison should not be considered as the "true" irradiance at the ground. The agreement of an instrument with the reference should be considered like a relative measure because there is not an absolute irradiance standard of ultraviolet spectral irradiance to compare the instruments (*Bais et al.*, 2001).

The use of the code need the instrument slit function (see Appendix I for definitions), which was provided by the participants (Appendix I). On the case of the Brewers (ARB, CAB, COB, IZ1, MAB, MUB, POB, ZAB) the slit was determined on previous campaigns by measurement of the 325 nm line of HeCd laser, The instruments provide a slit function based on measures of 253 nm mercury line, (IZ2, ULL, UVO) and the HG 296 for the (GIO, VAL) who can not get the more intense 253 line. These slits functions used is far from the recommended slit function characterization (*Ann Web*, 1998), with five orders of magnitude between the base line and the peak maximum and 6 FWHM wide. Even the INM's Brewers, cannot reach this requirement because the laser does not provide enough power.

To check the irradiance scale all the instruments measured a common lamp at the laboratory on the subsequent days, as described in detail in chapter 5. This measure is used to obtain a lamp corrected measurements dividing the sky irradiance by the ratio of the lamp measure versus the certificate of the lamp (*Tapani et al.*, 1997). The lamp measurement required transporting the instrument from the roof to the calibration room. We can expect some changes on the instrument during transportation. Some operators take portable lamp measurements before and after the transportation to guarantee the stability of the instrument.

At the end we have three sets of data, the original provided by the participants referred as "raw spectra", the 'analysed spectra' by the SHICrivm and finally the "lamp corrected spectra" as described before.

6.3. INTERCOMPARISON RESULTS

6.3.1 Wavelength shift results

Wavelength shift analyses are shown on Appendix II for every day. It shows the wavelength and time dependence of the shift. Except one, all the instruments have a shift less than 0.1 nm during the two days. Due the shape of solar spectra an error of 0.15 nanometers gives an error of 3-5% on biologically weighted UV, so a shift of 0.05 nm is required to give a biologically weighted, like UVI, within 1% of error (*Slaper*, 1997). The precision of the algorithm reduces for low solar zenith angles due to the low signal, and with non-stable conditions. The noise on wavelength shift observed around 10 GMT (see Appendix II), with moving clouds, could be attributed to this algorithm limitation.

The Brewers (ARB, CAB, COB, IZ1, MAB, MUB, POB) show a very good and stable wavelength alignment with time. These instruments can perform a wavelength alignment by measuring an internal mercury lamp lines. On this campaign after and before each UV scan were programmed. This possibility allows realigning the instrument like the MAB instrument on day 246, which suffered a malfunction due to the power failure. On the Section 13.13 we can see how it has a 0.25 shift on the next scan after the cut, and the shift was corrected for the rest of the day.

This was not the case with the ULL Bent ham. This instrument changed dramatically the wavelength alignment from 0.05 to 2.5 nm produced by the power failure and maintained the wavelength shift during the rest of the day (Section 13.18). On the second day the shift of the ULL Bentham was constant and below 0.05 nm like the behaviour of the other Bentham IZ2. The UVO instrument has a big wavelength shift, even bigger than the Slaper's algorithm can correct. The time dependence suggests that the problem is caused by the temperature inside the instrument, which is not stabilized. GIO also shows soft time dependence and values around 0.1.

6.3.2. Sky measurements results

To have an idea of the performance of all instruments, the figure 3 shows together the ratio of the analysed measurements to the reference at noon on the second blind day. At that time all instruments were presented and the solar zenith angle was 35°. Most of the instruments show ratios within 10%, the same agreement achieve for other celebrated intercomparisons like NOGIG 96 (*Kjelstad et al.*, 1997) and SUSPEN 97 (*Bais et al.*, 2001).

With the exclusion of GIO and VAL which are not UV designed spectrometers, all the instruments are within 10% in the comparison with the submitted data and with the analysed data (Figure 3). Also with the exception of IZ2 and VAL all the instruments were very stables during the two days (Figure 8).

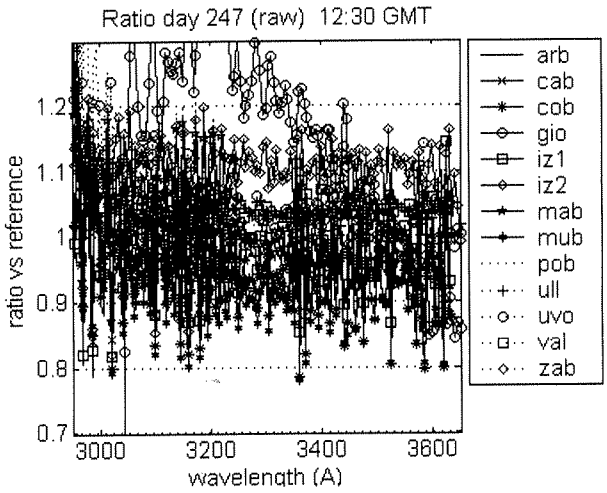

Fig. 3. Comparison of 12:30 spectral with the reference of with all the instruments present on the comparison. The plotted data are as submitted by the operators without any correction applied. Compare with the figure 4 witch data are the "analysed spectra" wavelength shift corrected, deconvolved with its slit function and convolved again with a common, 1 nm FHWM triangular one.

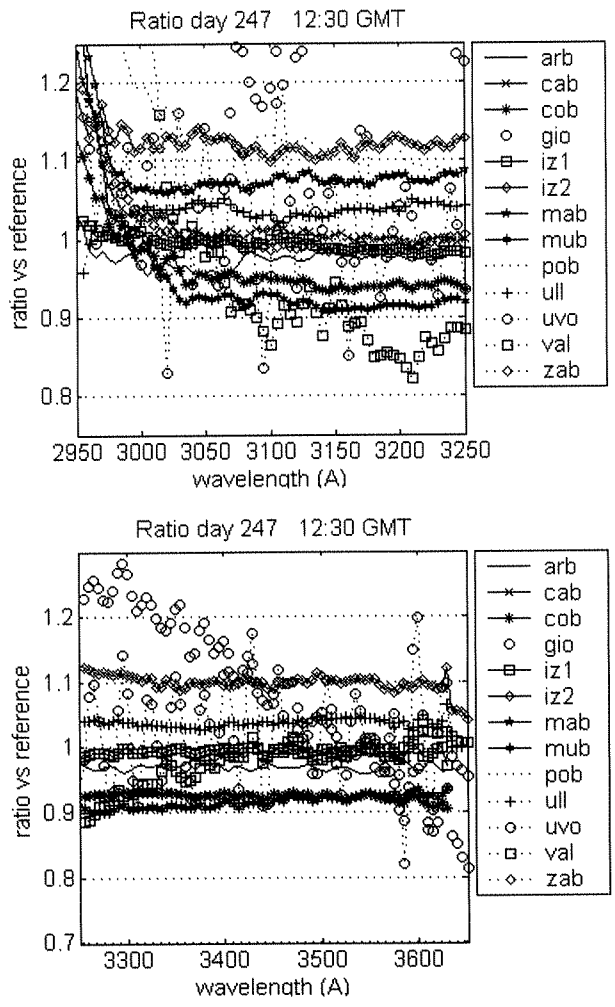

Fig. 4. Comparison of 12:30 analysed spectra, with the reference for all the instruments of the comparison. The upper graph shows the ratio for the 290-325 nm range (mostly UVB) and the lower one the data for the 325-360 nm (mostly UVA). The agreement is clearly better for the UVA range.

This general view of the intercomparison was dominated by single monochromators instruments. CAB, GIO, MAB, MUB, POB, VAL, and ZAB instruments show the stray light effect on lower wavelengths with overestimations on the 290-300 range. The concordance of the instruments is reduced on cloudy conditions like the morning of day 247. An extreme case, with moving clouds across the sun is showed on figure 5.

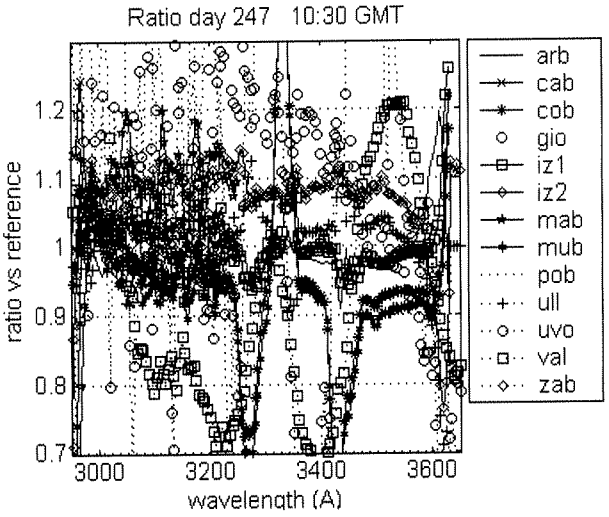

Fig. 5. Comparison during moving clouds conditions at 10:30 GMT on the second day. At some stage on the measure the cloud obscures the sun disk arising synchronizing problems.

Most of the instruments show a constant ratio with the wavelength except GIO, VAL and UVO. To quantify how the irradiance calibration affects it has been averaged the ratio of every instrument for the whole day on wavelength intervals and applied irradiance scale correction based on the laboratory measurements. The intervals are for 5 nm on the short wavelengths (290-310) and 10 nm for the longest. When the averages are done we smooth and lost some characteristics, but its use clarify the comparison (see Figure 6, Table 3).

Table 3. *Time averaged ratios, for the whole day, at wavelength intervals of 290-360, 295-360 and 300-360. For the last wavelength interval five instruments are agree on 5%. If we apply the lamp correction 8 instruments are inside the five percent interval.*

Day 247 – Ratios time and wavelength averaged						
	Irradiance/reference			*Irradiance (corr.)/reference*		
	R290-360	*R295-360*	*R300-360*	*R290-360*	*R295-360*	*R300-360*
ARB	0.98	0.98	0.99	1.00	1.00	1.00
CAB	1.13	1.03	1.01	1.11	1.01	0.99
COB	1.03	0.95	0.93	1.04	0.95	0.93
GIO	1.07	1.07	1.21	1.13	1.13	1.13
IZ1	0.99	0.99	0.99	0.99	0.99	1.00
IZ2	1.02	1.08	1.08	1.06	1.12	1.12
MAB	1.57	1.17	1.12	1.40	1.05	1.01
MUB	1.48	1.10	1.08	1.39	1.02	0.99
POB	0.93	1.08	0.94	0.99	1.17	1.02
ULL	1.01	1.02	1.02	0.97	0.98	0.98
UVO	1.05	1.04	1.04	1.03	1.02	1.02
VAL	17.12	1.51	0.95	0.94	0.94	0.94
ZAB	1.07	0.91	0.89	1.45	1.24	1.23

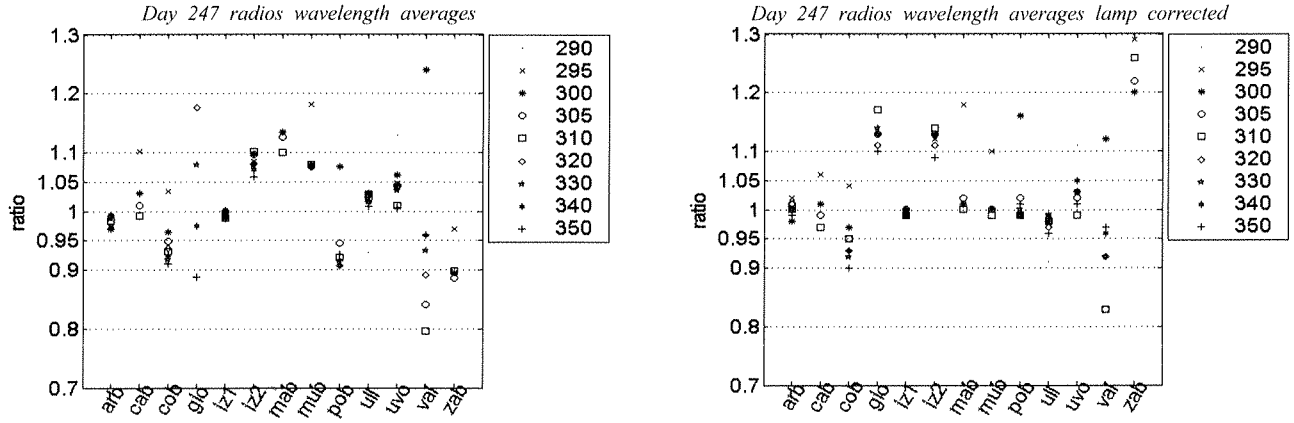

Fig. 6. Averaged ratios for the whole day at wavelength intervals. The intervals are for 5 nm for the 290-310 nm and 10 nm for the rest. The legend only shows the first wavelength of the average. If we take the ratios for wavelength longer than 300 nm, 5 instruments are within the five percent interval. With the lamp correction 8 instruments are inside the five percent interval.

6.3.3. Ultraviolet Index (UVI) intercomparison

Report the UVI (ultraviolet index) to the public is one of the main objectives of the project. The UVI is calculated by:

$$\int E(\lambda) \cdot w(\lambda)\, d\lambda$$

Where $E(\lambda)$ is the spectral irradiance and the $w(\lambda)$ is the erythemal weighted function based on the CIE action spectrum (*McKinlay and Diffey*, 1987). The UVI index is the above expression in W/m^2 plus 25, which gives an open ended index normally between 0 and 16.

The results reproduce (Figures 7, 8 and 9) the differences observed on the spectral measurements, however the different cosine response becomes evident on larger solar zenith angles. Take into account that any instrument performs cosine correction; the reference has the cosine characteristic of the mean of the reference instruments. As a result the reference cannot be considered the true. The big differences found on large solar zenith angles, can only say the cosine response of the instrument are different to the cosine response of the reference. In addition for large solar zenith angles the irradiance measured is low and small absolute differences give large relative differences. The UVI is reported to the public rounded to nearest integer, taken this into account, all instrument are within +/−1 UVI interval. For the 300 possible measures on day 247 of the twelve instruments the 80% are on the ref UVI, 15% are +/−1 UVI and 5% were lost. Surprisingly the VAL instrument, a visible spectrometer, gives very good results, the UVI depends strongly on the wavelength below 310 (Figure 9), therefore the UVI value result of the arbitrary selection of the irradiance values for the shorter wavelengths for which the instrument does not measure.

6.3.4. Detailed report

On the Appendix III and IV we can find the ratio of the instruments versus wavelength and time for both days of intercomparsion. To easy check the performance of each instrument alone we can consult the Appendix VI where for every instrument and for the two blind days we present the following information:

- 3-D representation of the spectral irradiance, "analysed spectra".
- Wavelength shift, wavelength dependence.

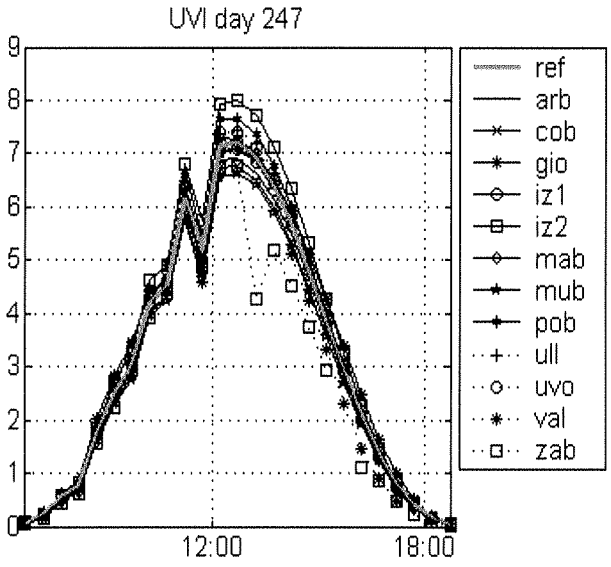

Fig. 7. UVI obtained for the participants during the second day of the Intercomparison. The entire instrument shows a good agreement with less than one unit of difference.

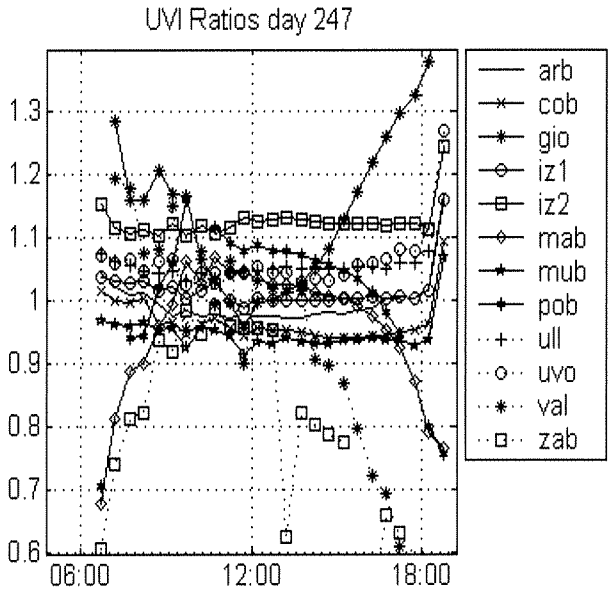

Fig. 8. Ratio of UVI with the reference of all participant instruments, the ratio with the reference with time.

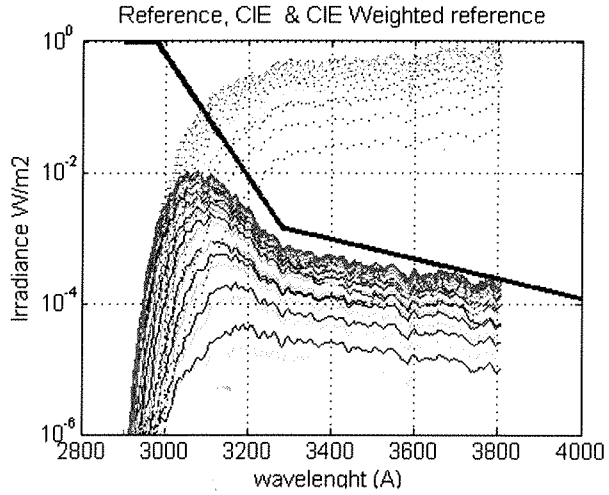

Fig. 9. Irradiance of the reference for 247 day is represented with points on logarithmic scale. The thick line is the CIE and the lines represent the CIE weighted reference. The main contribution to the UVI is on the 300-310 range which domain on the CIE comparison.

- Time dependence of the wavelength shift.
- Time dependence of the ratio of the instrument versus the reference for several wavelength average intervals.
- Contour plot representing the ratio between the "analysed" spectra and the reference.
- Daily mean ratio of wavelength averages, also the standard deviation. The ratio with the reference lamp (Lamp 04) and the agreement if the reference lamp correction is applied.
- Table 2: Wavelength average ratio for noon, 60° and 45° for the morning and afternoon the daily mean ratio of wavelength averages.

6.3.5 Instrument review

ARB: This instrument took part on the reference; its behaviour was stable with time and wavelengths during the two blind days.

CAB: The Brewer ozone travelling standard showed a good stability both days, with the behaviour of the single monochromators on the lower wavelength. The instrument ratio has a slightly dependence with time and wavelength, values at 45° sza in the afternoon are 2% lower than on the morning.

COB: The mark IV Brewer showed a 9% underestimation of the radiance. It was stable on both days and although the lamp calibration was very near to the certificate do not improve the results.

GIO: The instrument was stable during the two days. Like a single monochromators shows the problem of the stray light on shorter wavelengths. The instrument had an irregular irradiance calibration, with strong wavelength dependence. Also it showed time dependence. The lamp calibration did not improve the results, it could correct the wavelengths irradiance dependence but not the time dependence.

IZ1: This instrument took part on the reference. It behaved stable on wavelength and time during the two days.

IZ2: During the first day the instrument behaviour was very stable and similar to the ULL instrument, which shares a calibration lamp. During the second day the response of the instrument changed to overestimate about 10%. This unexpected change was explained on the laboratory by the influence of magnetic field of a refrigerator on the photomultiplier. On the measurements site could be caused due to the proximity of a monitor during the second day. This explanation is consistent with the fact that the instrument was stable in wavelength.

MAB: This Brewer is a MK-IV with the wavelength range of MK-II 290-325 nm. For the wavelengths over 300 nm overestimated 6-7% the same amount of the overestimation of the reference lamp.

MOB: This Brewer is a MK-IV and for the wavelengths over 300 nm underestimated 10% the same amount of the overestimation of the reference lamp, with the lamp correction.

POB: This Brewer MK-II was repaired during the first day. It showed wavelength dependence from 12% overestimation at 300 nm to 8% at 325 nm. The lamp measurements showed the same behaviour on the laboratory. As a result, the lamp corrected measurements were within 3% of the reference.

ULL: The ULL took part on the reference. It was affected by a power failure, which caused a shift on the first day but could be corrected by the Slaper's algorithm and did not affect to the performance of the instrument. The instrument was stable during the two days.

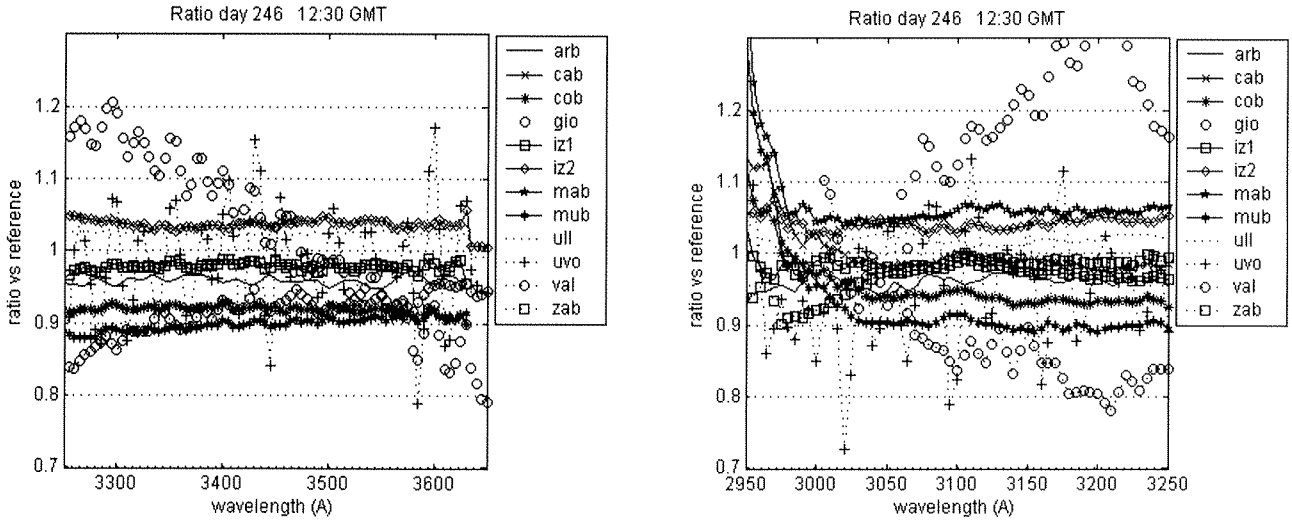

Fig. 10. Comparison of 12:30 measured spectra with the reference for the first day of intercomparison. On the upper graph for the 290-325 nm range and the second one the data for the 325-360 nm roughly the UVB and UVA range respectively.

UVO: It was very noisy mostly due to the SHICrivm algorithm failed correcting the wavelength shift, which reached the maximum correction of 1 nm. The ratios were less noisy without wavelength shift correction than with the correction applied. But the ratios were much better with the wavelength shift correction (Appendix II). When the wavelength averages were taken the noise disappeared and the calibration was 4% higher. With the lamp calibration the irradiance was agree to 2%.

VAL: This instrument with a broad FWHM of 6 nm is mainly used for visible and direct measurements. With this slit we cannot use the SHICrivm algorithm. The ratios were calculated with a different reference. This reference was convoluted with its wide slit. The instrument on the first day showed a constant 9% underestimation along the day. But on the second day had a clear solar zenith angle dependence of the ratios with 8-12% underestimation during the middle of the day, and went down up to 30%.

ZAB: It had a very good agreement with the reference for longer wavelengths during the first day and the first half of the second. On the second one had problems with the diffraction grating, which had to be repaired on the next days. We cannot conclude anything with the laboratory measurements because the instrument was completely different.

6.4. BROADBAND UVI INTERCOMPARISON

Four broadband instruments participated in the campaign, three Yankee UVB-1 and one NILU-UV6. Descriptions of these instruments can be found in chapter 4.

Table 4. *Participating broad band instruments.*

Instrument	Code	Location
Nilu UV6	Nilu	Antarctica
Yankee	y-izo	Izaña Atmos. Obs.
Yankee	y-ref	Network Reference
Yankee	y-mad	Network Travelling

The campaign was focused on the UVI comparison, and was not intending to use as a calibration of the broadband instruments. On these analysis all the instruments used the manufacturer calibration for the CIE weighted irradiance. We expected the calibration constants were correct since all the instruments were recently acquired. The Yankee instruments were purchased for the national UVI network of the INM and the NILU for the Antarctic network of the project CRACRUV ("Control de Calidad de la Red Antartica para la Caracterización de la Radiación UV"). Probably this lack of experience was the reason for the problems with the travelling instrument acquisition. Due to these problems on the blind days, we had only 8 simultaneous records on day 247 with all the instruments (spectral reference and the broad band).

All the instruments recorded every minute a one-minute averages dose rates. They were compared with the UVI calculated of CIE weighted spectra of the campaign "reference spectrum". Due to the six minutes scans of the reference, 6 minutes averages of the broadband were used in the numerical comparison showed on Table 5. As the table and the Figure 11 show, all the instruments are in the 10% range, and the entire broad band overestimates the UVI. The best agreement is achieved by the NILU with 4%, then Y-MAD with a 7% and the Y-IZO and Y-REF around 10%. Remark that the reference spectrum is not cosine corrected so it's difficult to establish conclusions for the measurements at lower sza where is relevant the angular dependence error.

For public UVI diffusion, the main purpose of the broadband instruments, the error is less than 1 UVI unit and in all cases is overestimated, which is not too bad for a public warning service.

Table 5. *Ratios between the broad band UVI and reference spectrum CIE weighted. The mean and standard deviation are calculated for clear sky values (> 12 hour).*

Time	Nilu	y-izo	y-ref	y-mad
10:30	1.099	1.133	1.136	1.180
11:00	0.948	1.061	1.065	1.029
11:30	0.986	1.052	1.057	1.036
12:00	1.047	1.120	1.127	1.096
12:30	1.040	1.100	1.108	1.073
13:00	1.042	1.095	1.104	1.074
13:30	1.041	1.093	1.103	1.074
14:00	1.038	1.080	1.089	1.064
14:30	1.033	1.089	1.095	1.075
Mean	3.88E-02	9.14E-02	9.98E-02	7.20E-02
Std	3.56E-03	7.50E-03	7.66E-03	4.53E-03

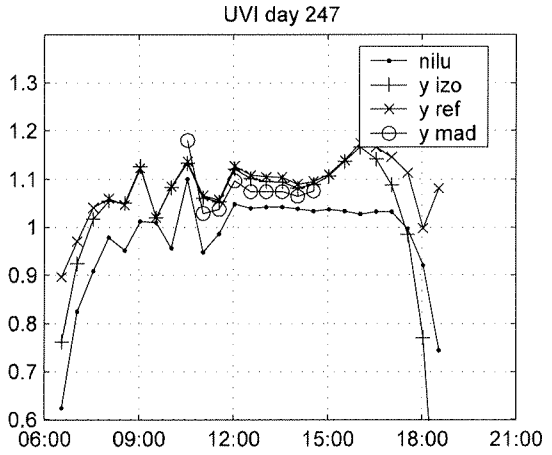

Fig. 11. *Ratio of UVI derived of broadband vs reference with time for day 247, second blind day.*

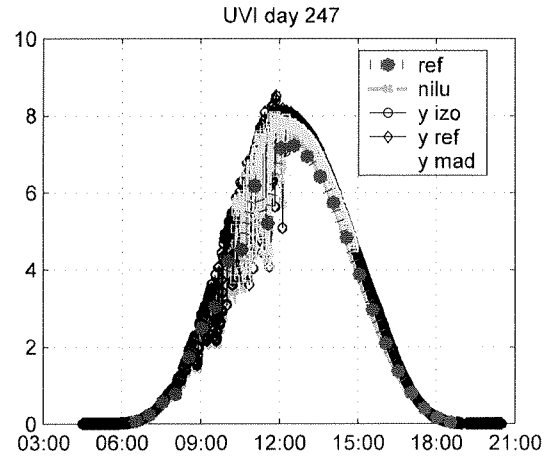

Fig. 12. *UVI index evolution on day 247, one-minute average are showed for five broadband instruments. Thick line indicates the reference calculated from spectral instruments every half an hour.*

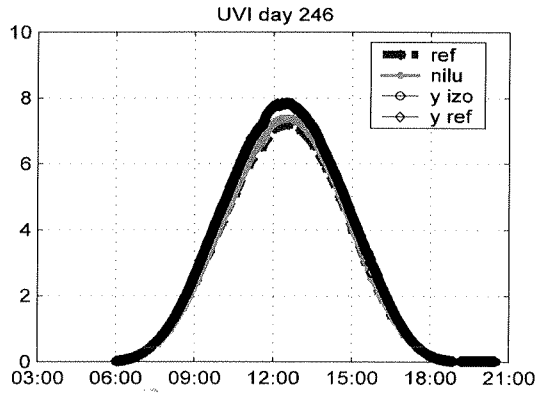

Fig. 13. UVI index evolution on day 246, one-minute average are showed for the broadband instruments, only the Nilu and two Yankees provided data on these day. The line with points shows the reference calculated from spectral instruments every half an hour.

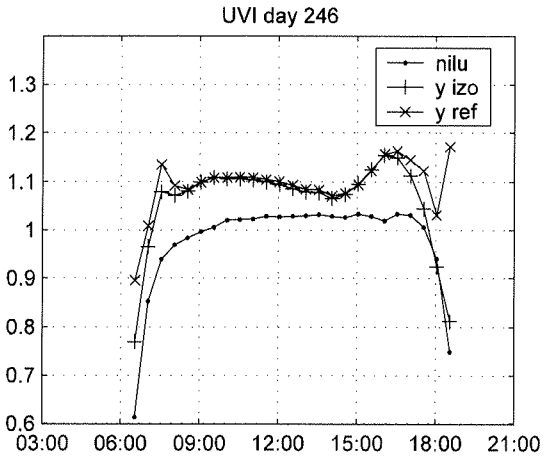

Fig. 14. Ratio of UVI derived of broadband vs reference with time for day 246 (first blind day).

6.5. CONCLUSIONS

The first ultraviolet Iberian Intercomparison was one of the first opportunities to interchange of knowing and information of UV measurements performed on the Iberian Peninsula. The exchange of information and experiences between the participating teams is the most valuable and perdurable result of the campaign above the scientific results.

The procedure used on the Intercomparison try to follow the methods used in recent European Intercomparison like NOGIG-96 and SUSPEN-97. On the analysis we use the SHICRIVM code to obtain the "analysed" spectra and lamp measurements to remove absolute calibration differences. An average of three double monochromators instruments was used as a reference on the intercomparison. The general agreement between all the instruments than accomplish the intercomparison is similar than other campaigns celebrated in Europe. The measurements of the three reference instruments, ARB, IZ1 and ULL are in +/−1% agreement during both days of the campaign. The other two double monochromators are also on these 1% agreement, the IZ2 instrument during the first day (during the second day show a sensitivity increase of 10 %), and the UVO instrument when consider wavelengths averages (the SHICRIVM algorithm could not correct the wavelength shift).

Single Brewers represents the half of the participants, with the lamp corrections applied and ignoring the 290-300 nm interval affected by the stray light four of the six instruments, CAB, MAB, MUB and POB are +/−3%. The other two ZAB and COB are on +/−10% interval.

VAL and GIO instruments show serious design limitations to provide measures on the UVB range.

The main objective of the research project, "Medida y Modelización de la Distribución Espacio-Temporal de la Irradiancia Solar Ultravioleta en España", CLI97-0345-C05-01, is to provide Ultraviolet Index measurements over the Iberian Peninsula These Intercomparison probe that whit the exceptions of the VAL and GIO instruments all the participating instruments provide accurate Ultraviolet Index with the 80% of the measurements accord with the reference and the 100% of valid measurements within +/−1 UVI.

ACKNOWLEDGEMENTS

We thank to the CICYT projects CLI97-0453 and CLI97-0345-C05 for economical support during this work. The authors are deeply grateful to all the instrument operators.

We would like to extend our sincere appreciation to Dr. Muniosguren for the coordination of the campaign, and to Dr. Benito de la Morena for the use of the *"El Arenosillo"* Laboratory facilities, and for the food and accommodation.

REFERENCES

Bais, A., B. Gardiner et al. (2001): SUSPEN intercomparison of ultraviolet spectroradiometers. *Journal of Geophisical Research*, **106**, 12509-12525.

Gardiner, B. and P. J. Kirsh (1997): Intercomparison of Ultraviolet Spectroradiometers, Advances in Solar Ultraviolet Spectroradiometry, Air Pollut Res, Rep. 63, edited by Ann Webb, European Commision, Luxembourg pp. 67-151.

Kjelstad, B., B. Jhonsson, T. Koskela (1997): The Nordic intercomparison of Ultraviolet and total ozone instruments at Izaña, October 1996, Final Report. Ed. B. Kjeldstad and T. Koskela, Finn. Meteorol. Inst., Meteorological Publications No. 36.

Koskela, T. et al. (1997): "Spectral Sky Measurments". The Nordic intercomparison of Ultraviolet and total ozone instruments at Izaña, October 1996, Final Report. Ed. B. Kjeldstad and T. Koskela, Finn. Meteorol. Inst., Meteorological Publications No. 36.

Koskela, T. (*ed.*) (1994): "The Nordic intercomparison of ultraviolet and total ozone instruments at Izaña from 24 October to 5 November, 1993". Final Report, Finnish Meteorological Institute, Meteorological Publications, No. 27, 123 p., Helsinki, Finland.

Kurucz et al. (1984): Solar flux atlas from 296 to 1300 nm, in National Solar Observatory Atlas 1, Harvard Univ. Press., Cambridge, Mass.

Mckinley, A., and B. Diffey (1987): A reference action spectrum for ultraviolet induced erytema in human skin. CIE Research Note, CIE Journal, Vol. 6, No. 1, 17-22.

Seckmeyer G., B. Mayer, and G. Bernhard (1988): The 1997 Status of Solar UV Spectroradiometry in Germany: Results from The National Intercomparison of UV Spectroradiometers, Garmish-Partenkirchen, Germany, Schriftenreihe of the Fraunhofer Institue for Atmospheric Enviromental Research, rep. 55, 166 p., Shaker Verlag, Frackfurt am Main, Germany, ISBN 3-8265-3695-9.

Slaper, H., H. A. J. M. Reinen, M. Blumtaler (1995): "Comparing ground level spectrally resolved solar UV measurements using various instruments: A technique resolving effect of wavelength shift and slit". *Geophys. Res. Lett.*, **22(20)**, 2721-2724.

Slaper, H. and T. Koskela (1997): "Metodology of intercomparing spectral sky measurements". The Nordic intercomparison of Ultraviolet and total ozone instruments at Izaña, October 1996, Final Report. Ed. B. Kjeldstad and T. Koskela, Finn. Meteorol. Inst., Meteorological Publications No. 36.

Web, Ann et al. (1999): Guidelines for Site Quality Control of UV Monitoring, WMO/GAW Report #126. World Meteorological Organization, Geneva.

6.6. APPENDIX I: INSTRUMENTS SLIT FUNCTIONS

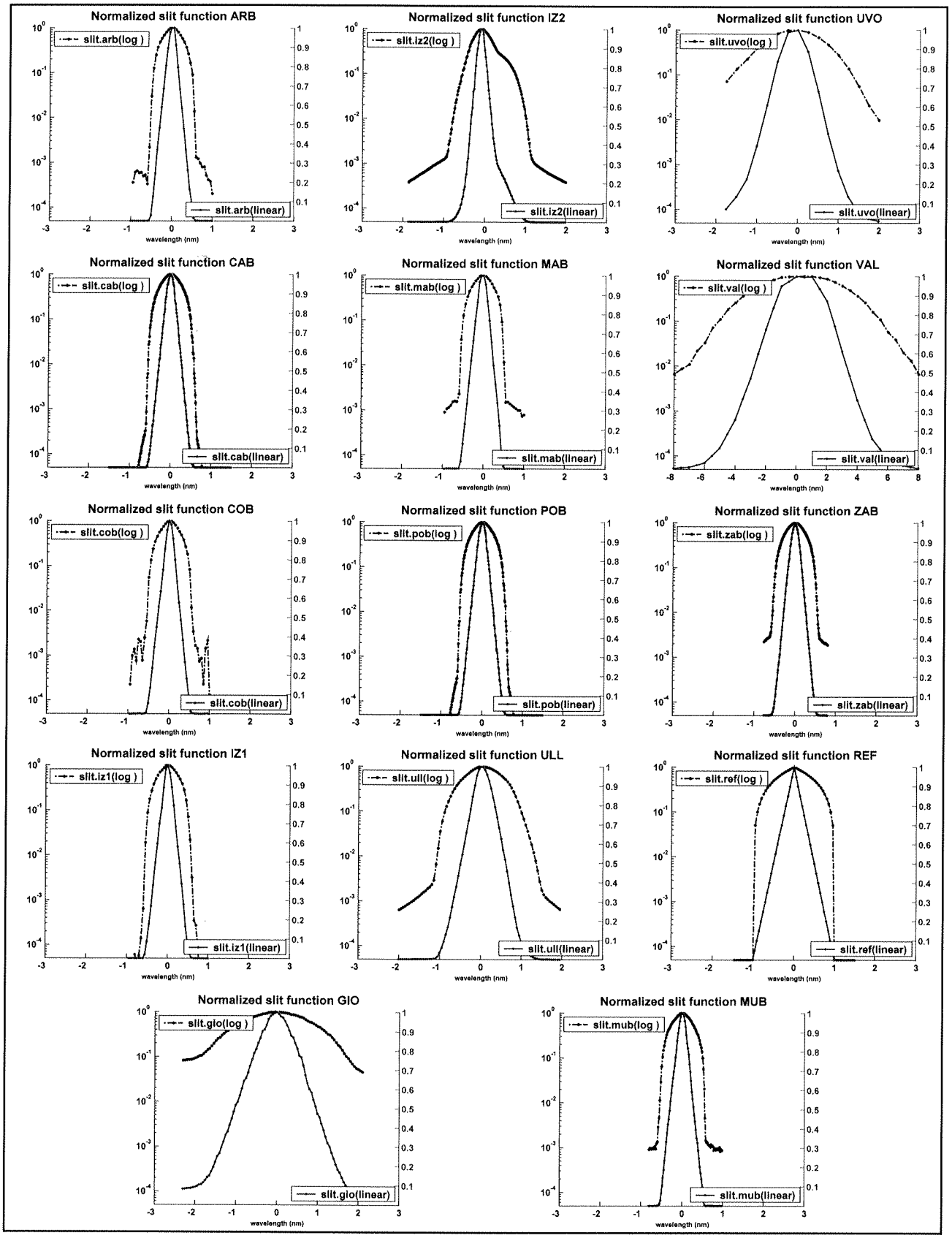

Fig. 15. Slit functions of the instruments provided by the operators. From upper left to down right the figures are sorted in alphabetical order of the instruments: ARB, CAB, COB, GIO, IZ1, IZ2, MAB, MUB, POB, ULL, UVO, VAL, ZAB, and finally the REF, the common slit used to normalize the measures on the "analysed spectra". REF is a triangular slit function with one nanometer of FWHM. The slit functions are normalized to the maximum intensity. On the left axis and in circles the slit function on logarithmic scale, on the right axis and in blue line the same on a linear scale.

6.7. APPENDIX II: WAVELENGTH SHIFT OF THE INSTRUMENTS

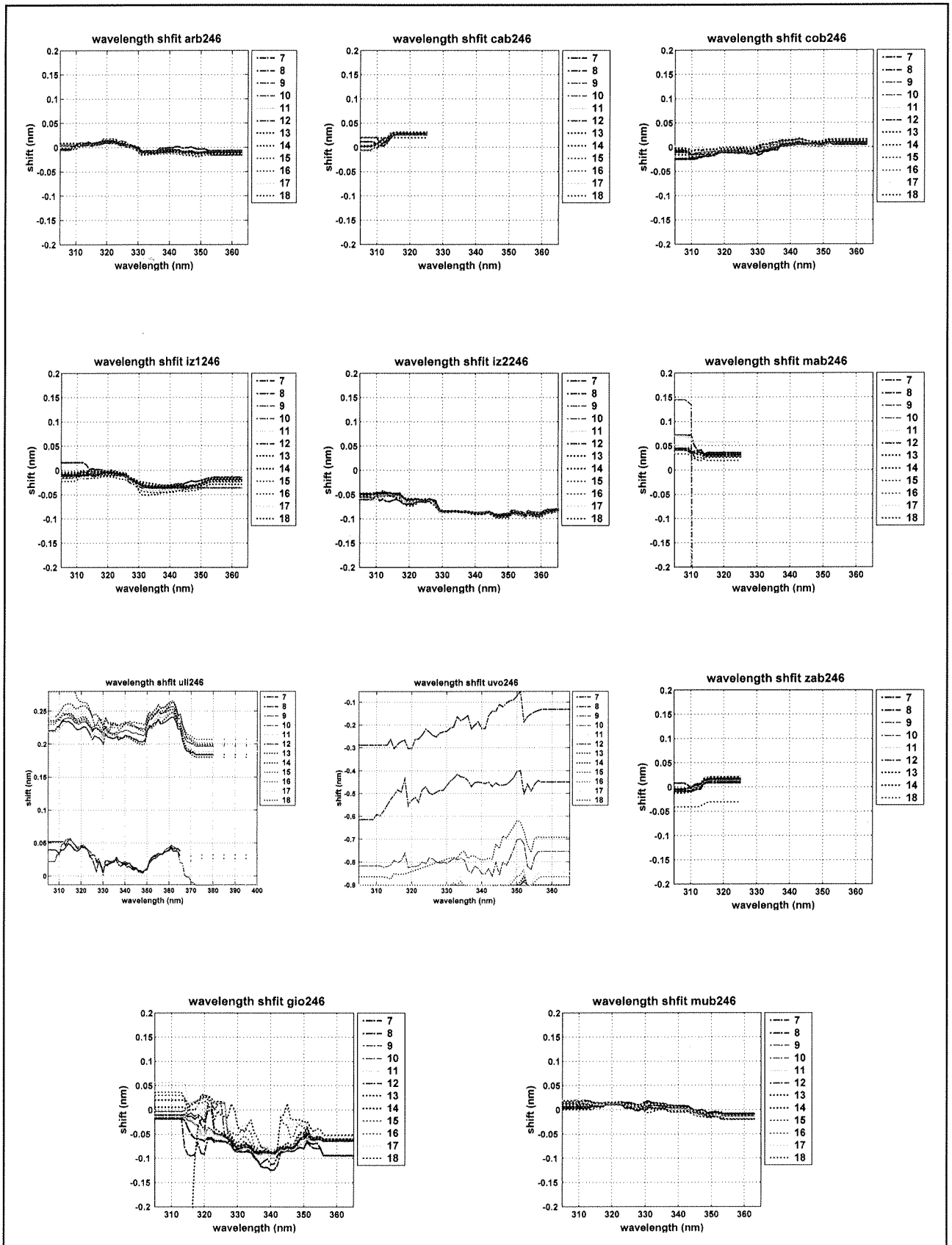

Fig. 16. Wavelength shift of the instruments during the first day of the intercomparison. Figures show the wavelength shift versus wavelength on the full hour scans along the day. From upper left to down right the figures are sorted in alphabetical order of the instruments: ARB, CAB, COB, GIO, IZ1, IZ2, MAB, MUB, POB, ULL, UVO, VAL and ZAB. With the exception of ULL and UVO, which graphs have extended scales, all the instruments have a shift lower than 0.1 nm over its spectral range.

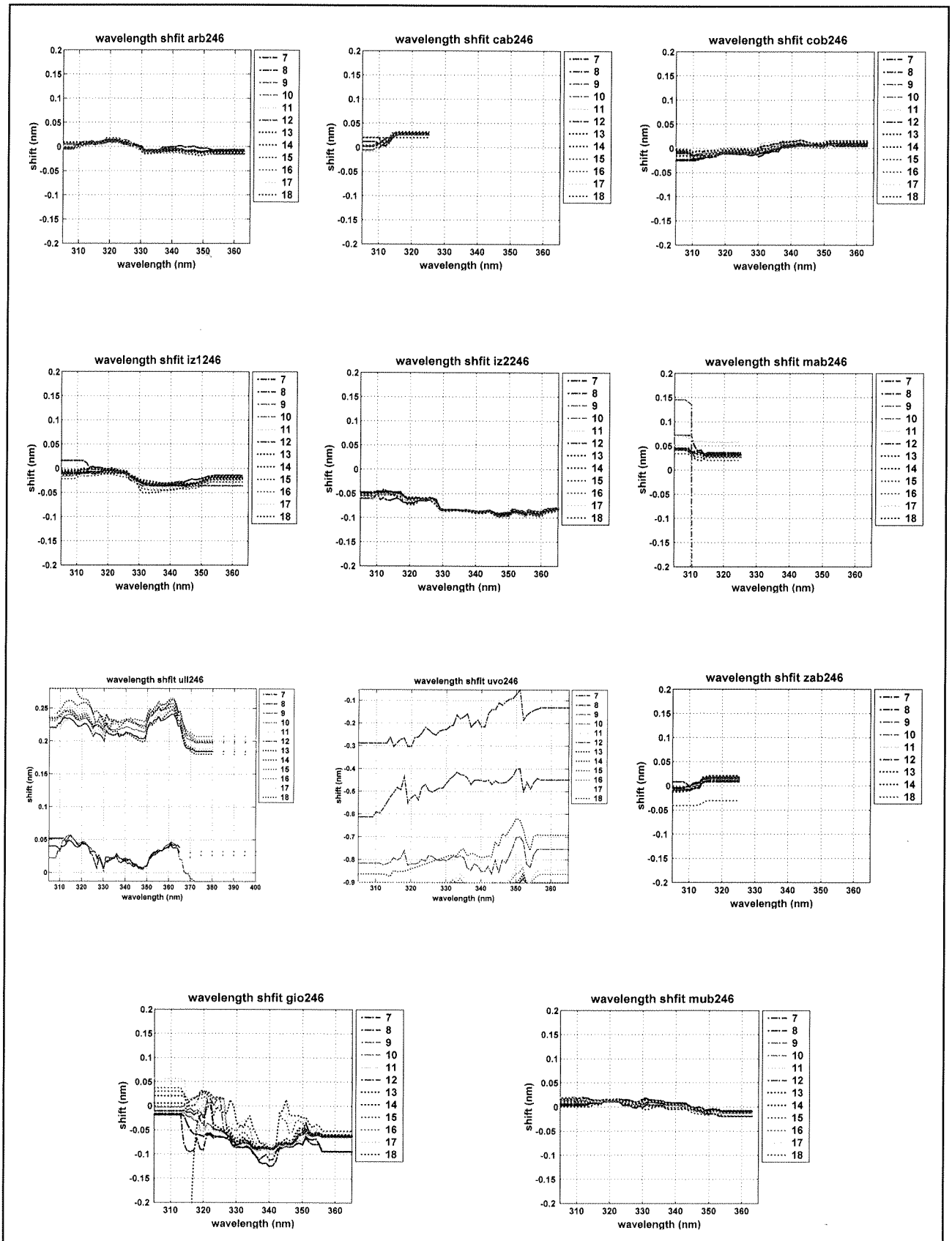

Fig. 17. Wavelength shift of the instruments during the first day of the intercomparison. Figures show the wavelength shift versus wavelength on the full hour scans along the day. From upper left to down right the figures are sorted in alphabetical order of the instruments: ARB, CAB, COB, GIO, IZ1, IZ2, MAB, MUB, POB, ULL, UVO, VAL and ZAB. With the exception of ULL and UVO, which graphs have extended scales, all the instruments have a shift lower than 0.1 nm over its spectral range.

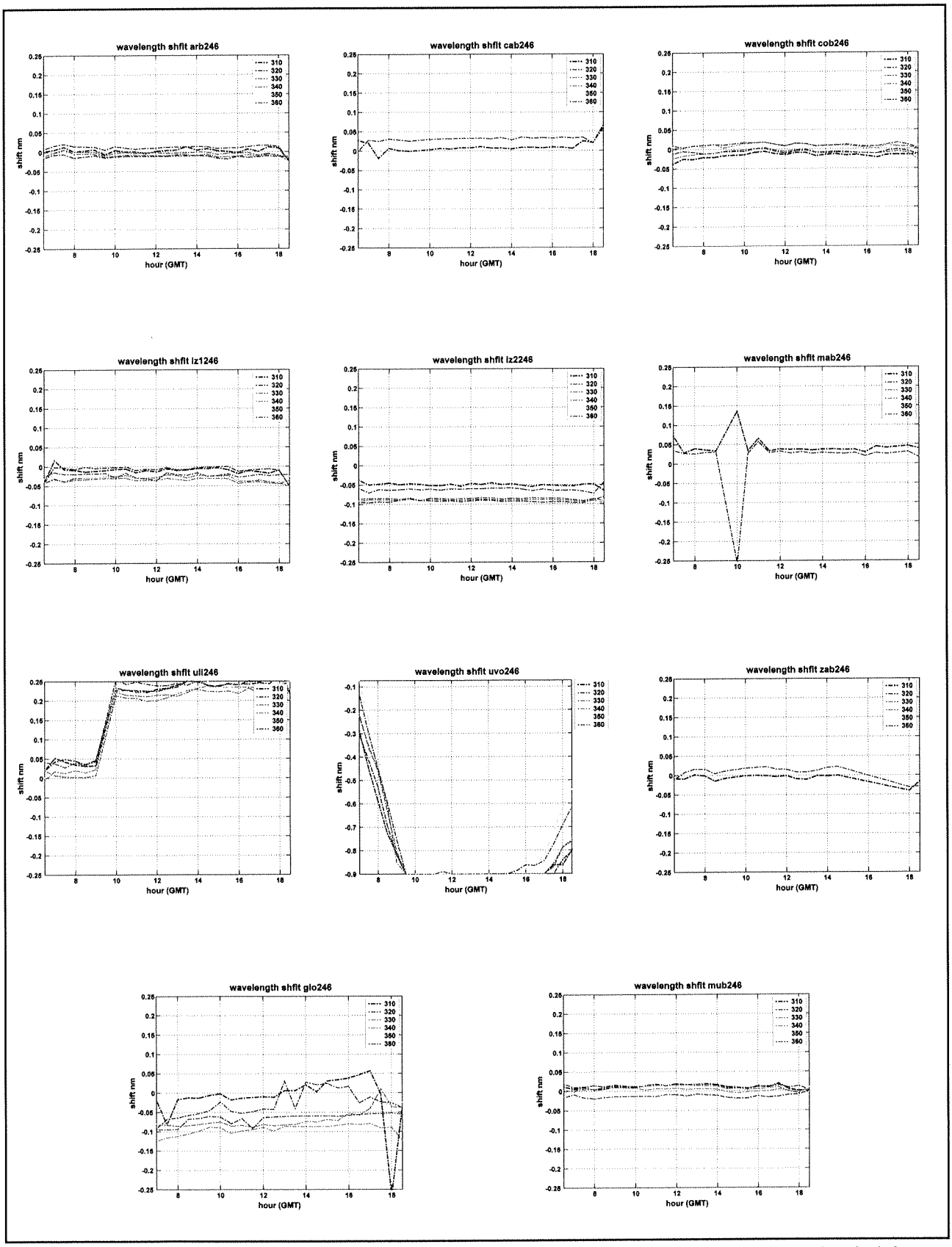

Fig. 18. *Wavelength shift of the instruments during the first day of the intercomparison. Figures show the wavelength shift versus time for five selected wavelengths from 310 to 360 every 10 nm. From upper left to down right the figures are sorted in alphabetical order of the instruments: ARB, CAB, COB, GIO, IZ1, IZ2, MAB, MUB, POB, ULL, UVO, VAL and ZAB. Some instruments were affected by the power cut at 9:30 like MAB and ULL and others show time dependence UVO and GIO probably due a temperature dependence.*

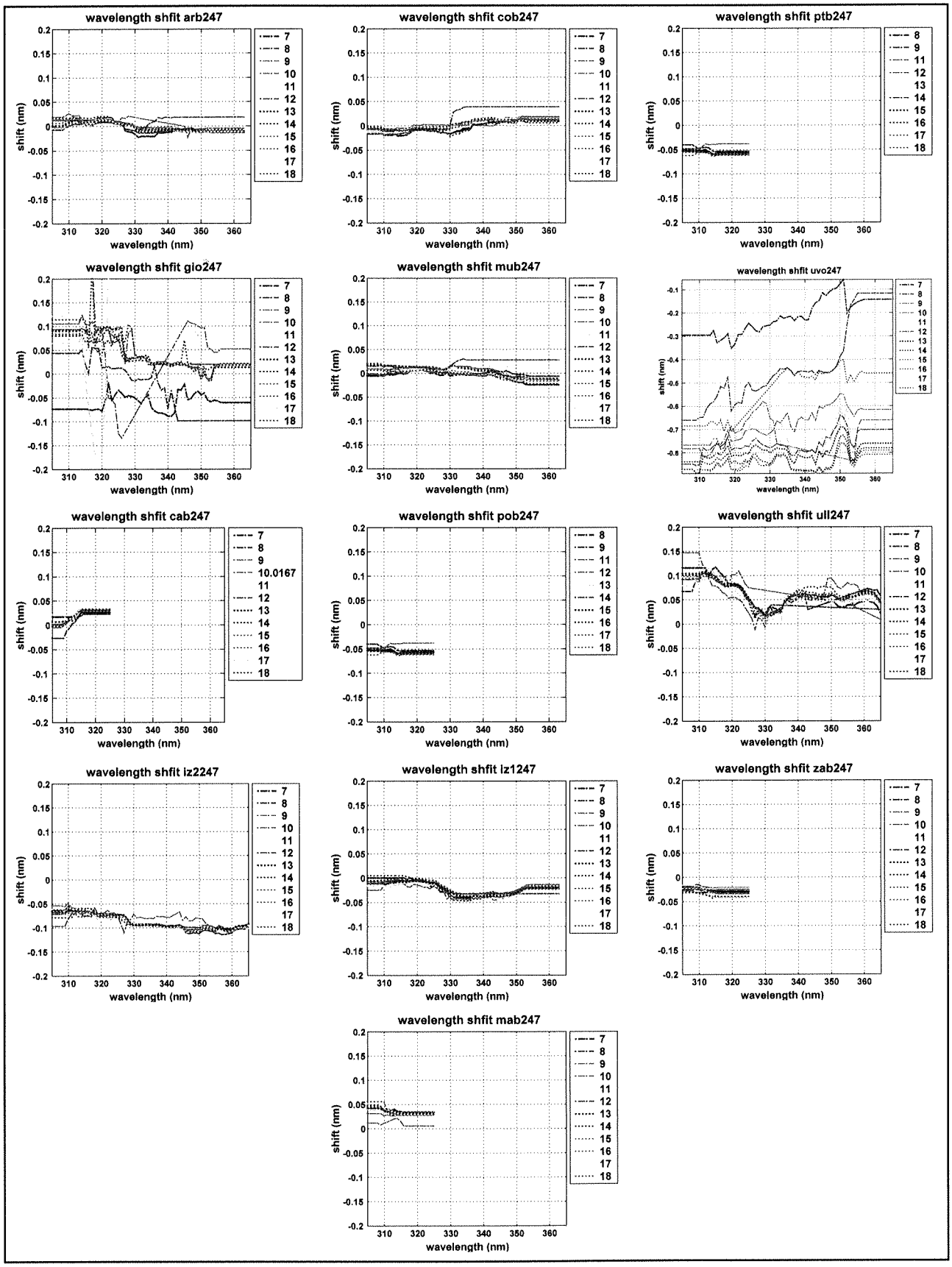

Fig. 19. *Wavelength shift of the instruments during the second day of the intercomparison. Figures show the wavelength dependence of the shift on the full hour scans along the day. From upper left to down right the figures are sorted in alphabetical order of the instruments: ARB, CAB, COB, GIO, IZ1, IZ2, MAB, MUB, POB, ULL, UVO, VAL and ZAB. UVO graphs have extended scales. All the instruments have a shift lower than 0.1 nm over its spectral range except UVO.*

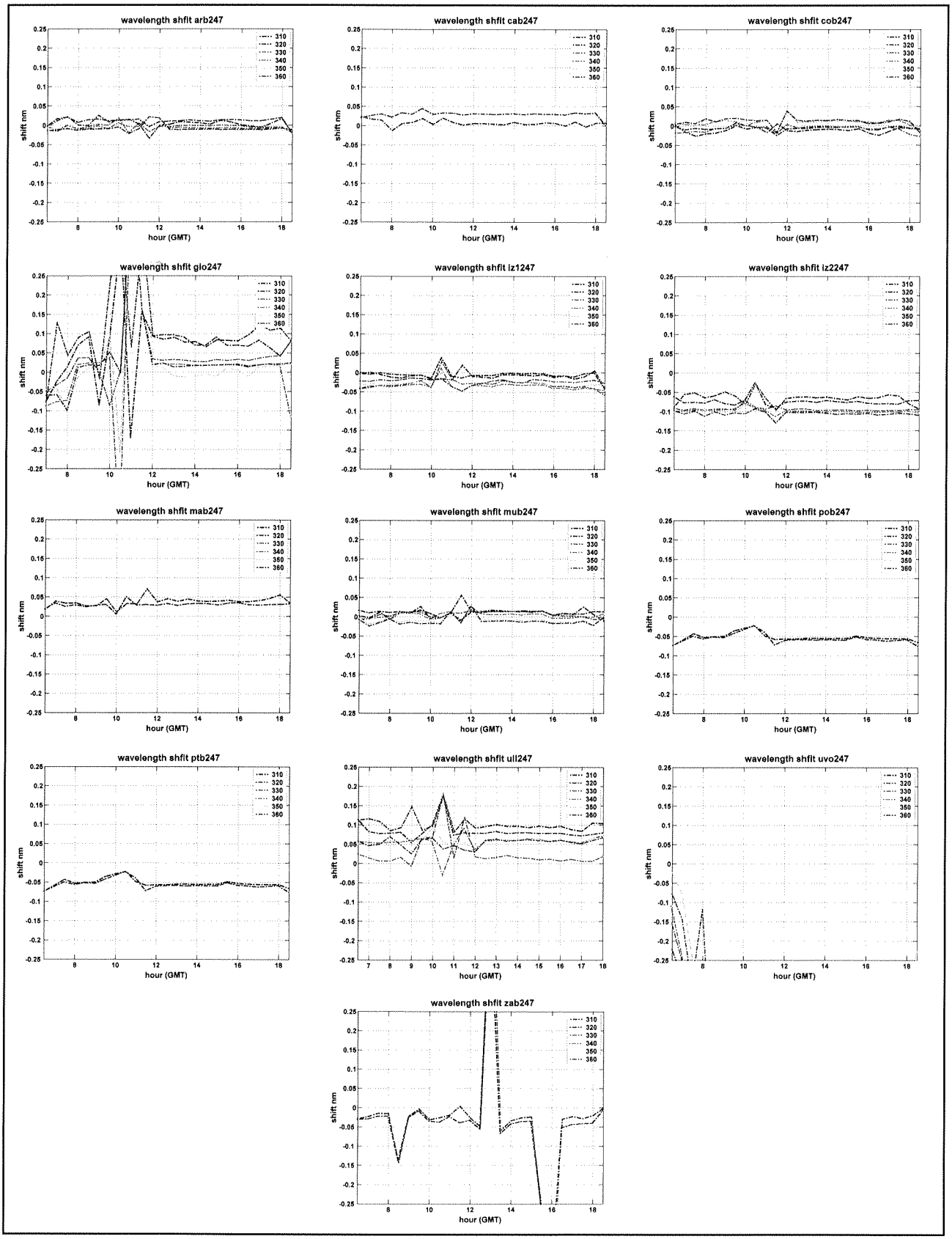

Fig. 20. *Wavelength shift of the instruments during the second day of the intercomparison. Figures show the time dependence of the shift for five selected wavelengths from 310 to 360 every 10 nm. From upper left to down right the figures are sorted in alphabetical order of the instruments: ARB, CAB, COB, GIO, IZ1, IZ2, MAB, MUB, POB, ULL, UVO, VAL and ZAB. Some instruments were affected by the power cut at 9:30 like MAB and ULL and others show time dependence (UVO and GIO) probably due to the temperature.*

6.8. APPENDIX III: RATIOS DAY 246

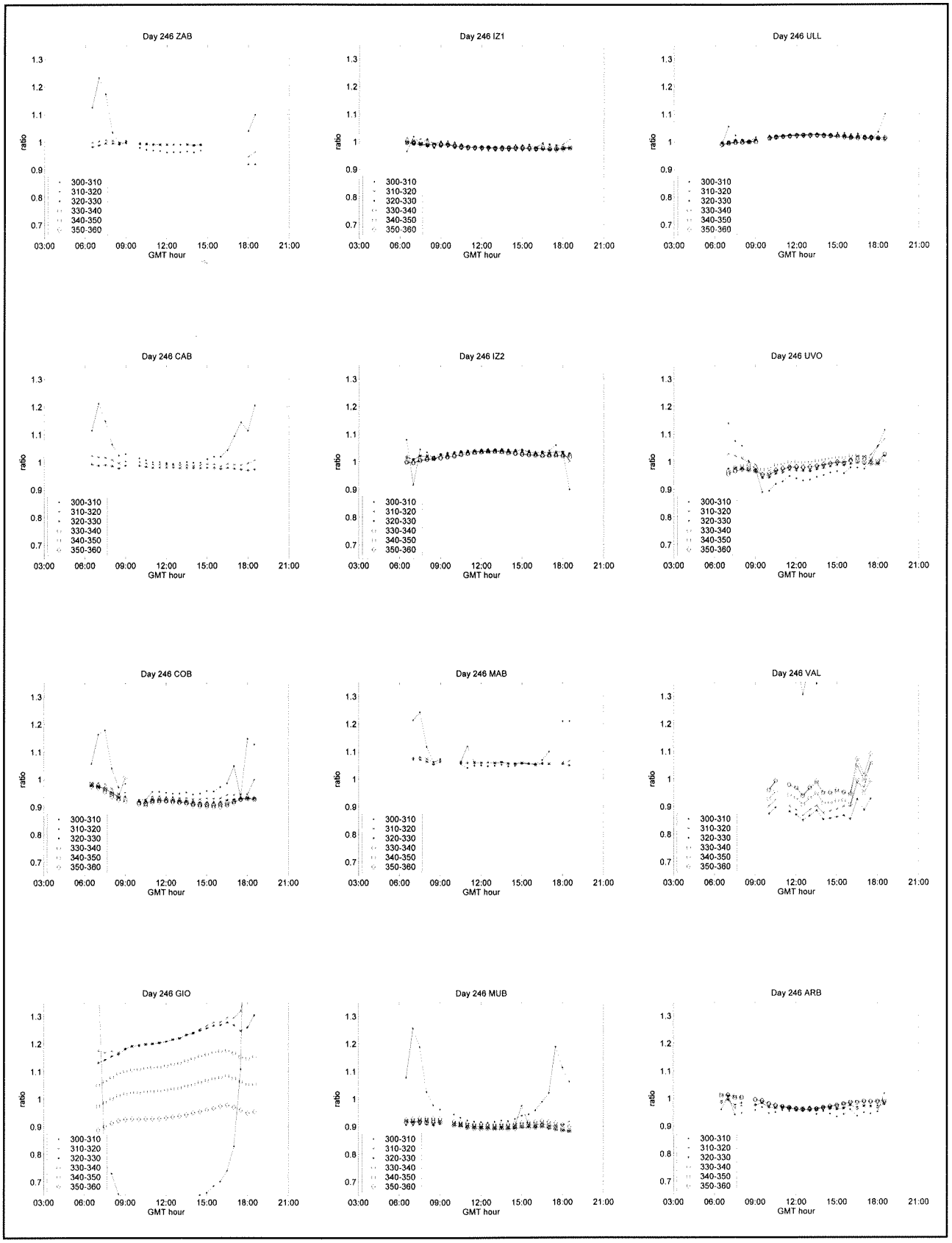

Fig. 21. *Ratio of the instruments with the reference, averaged on 10 nm wavelength intervals, during the first day of the intercomparison. Figures show the time dependence of the ratio averaged on five selected wavelengths intervals from 310 to 360 every 10 nm. From upper left to down right the figures are sorted in alphabetical order of the instruments: ARB, CAB, COB, GIO, IZ1, IZ2, MAB, MUB, ULL, UVO, VAL and ZAB. Some instruments loss the 10:00 scan due the power cut at 9:30. Single monochromators instruments show a characteristics overestimation for the first wavelength range 300-310 nm.*

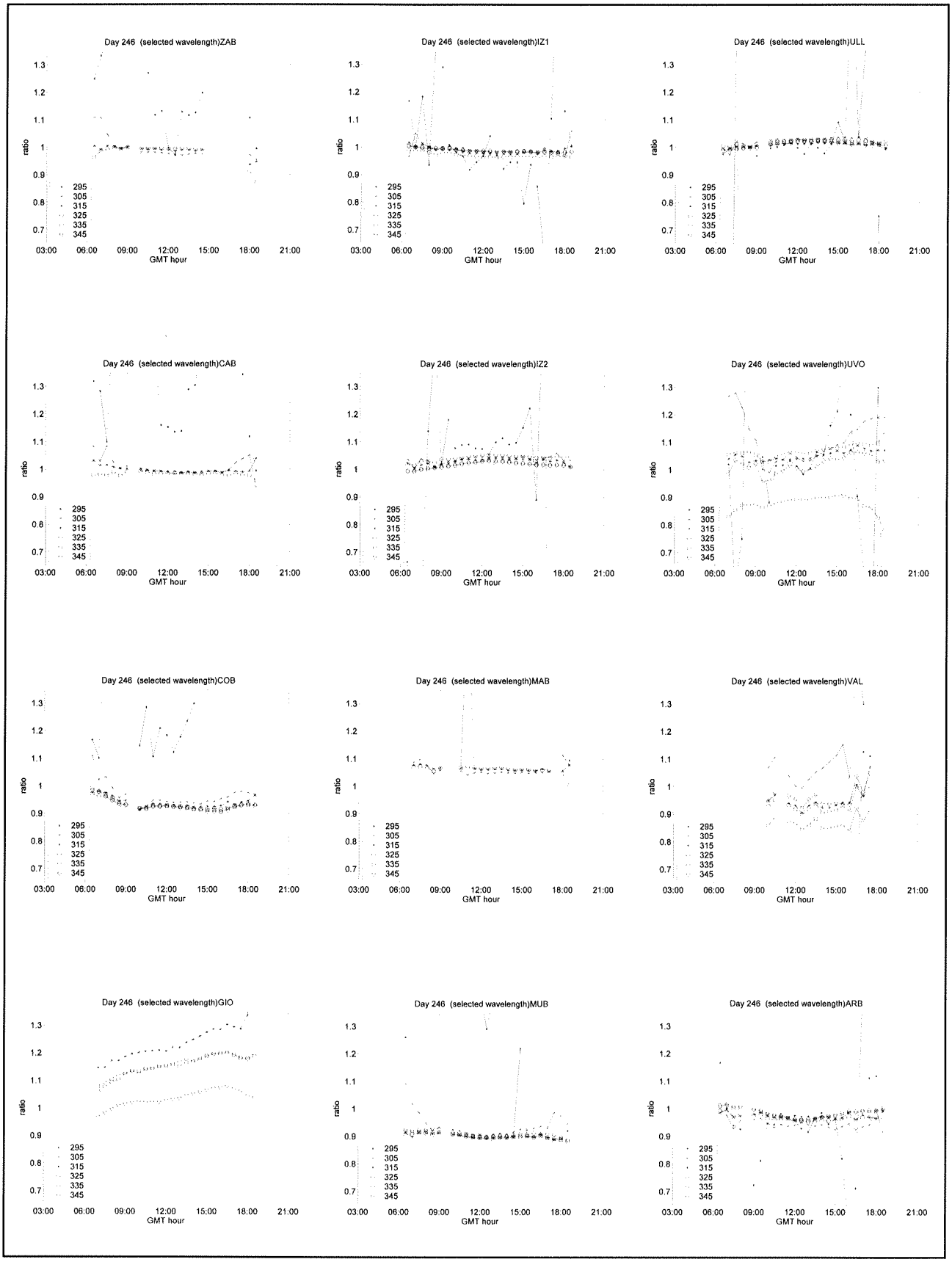

Fig. 22. *Ratio of the instruments with the reference, for certain wavelengths, during the first day of the intercomparison. Figures show the time dependence of the ratio on five selected wavelengths intervals from 295 to 345 every 10 nm. From upper left to down right the figures are sorted in alphabetical order of the instruments: ARB, CAB, COB, GIO, IZ1, IZ2, MAB, MUB, ULL, UVO, VAL and ZAB. Most of the instrument shows a constant behaviour with for wavelength greater than 295 except VAL and GIO.*

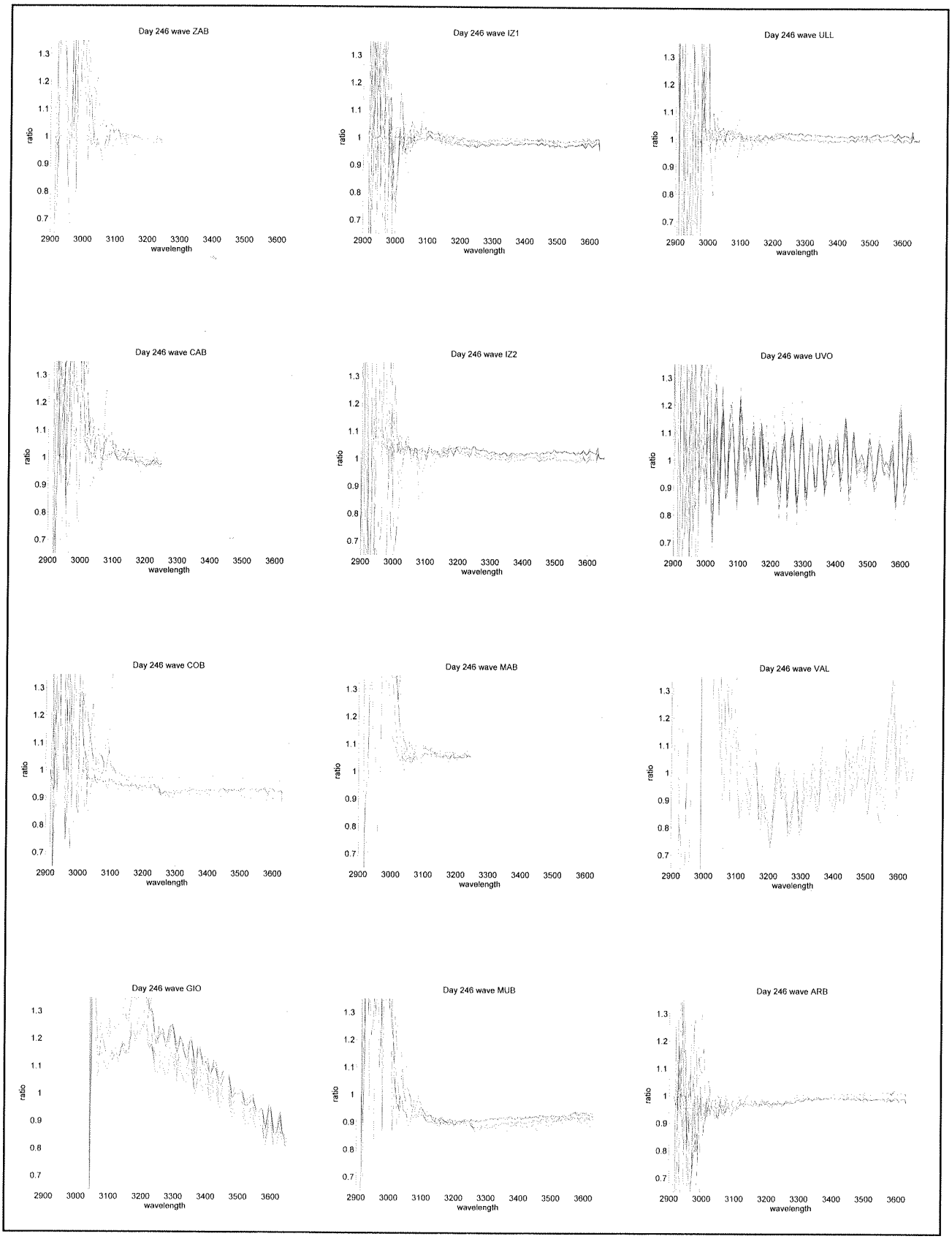

Fig. 23. *Ratio of the instruments using the "analysed spectra" with the reference, vs. wavelength during the first day of the intercomparison. Figures show the wavelength dependence of the ratio for all the measured scans, clear grey values correspond to scans near noon and dark grey lines corresponds with the measures with high zenith angles. From upper left to down right the figures are sorted in alphabetical order of the instruments: ARB, CAB, COB, GIO, IZ1, IZ2, MAB, MUB, ULL, UVO, VAL and ZAB. The VAL instrument can not be analysed due the FHWM of the instrument, ratio with the original data are displayed.*

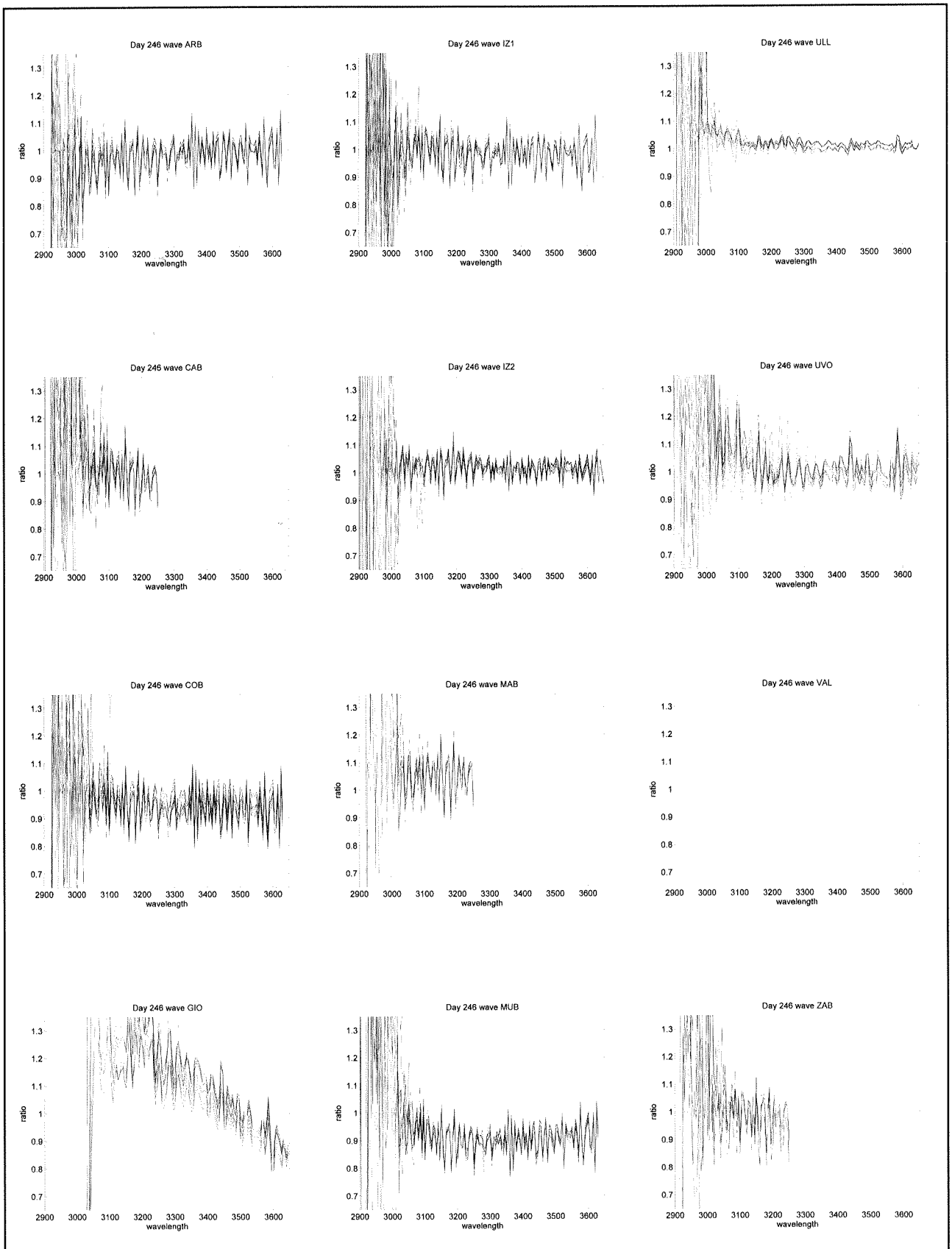

Fig. 24. *Ratio of the instruments using the original submitted data with the reference, vs. wavelength during the first day of the intercomparison. Figures show the wavelength dependence of the ratio for all the measured scans, clear grey values correspond to scans near noon and dark grey lines corresponds with the measures with high zenith angles. From upper left to down right the figures are sorted in alphabetical order of the instruments: ARB, CAB, COB, GIO, IZ1, IZ2, MAB, MUB, ULL, UVO, VAL and ZAB.*

6.9. APPENDIX IV: RATIOS DAY 247

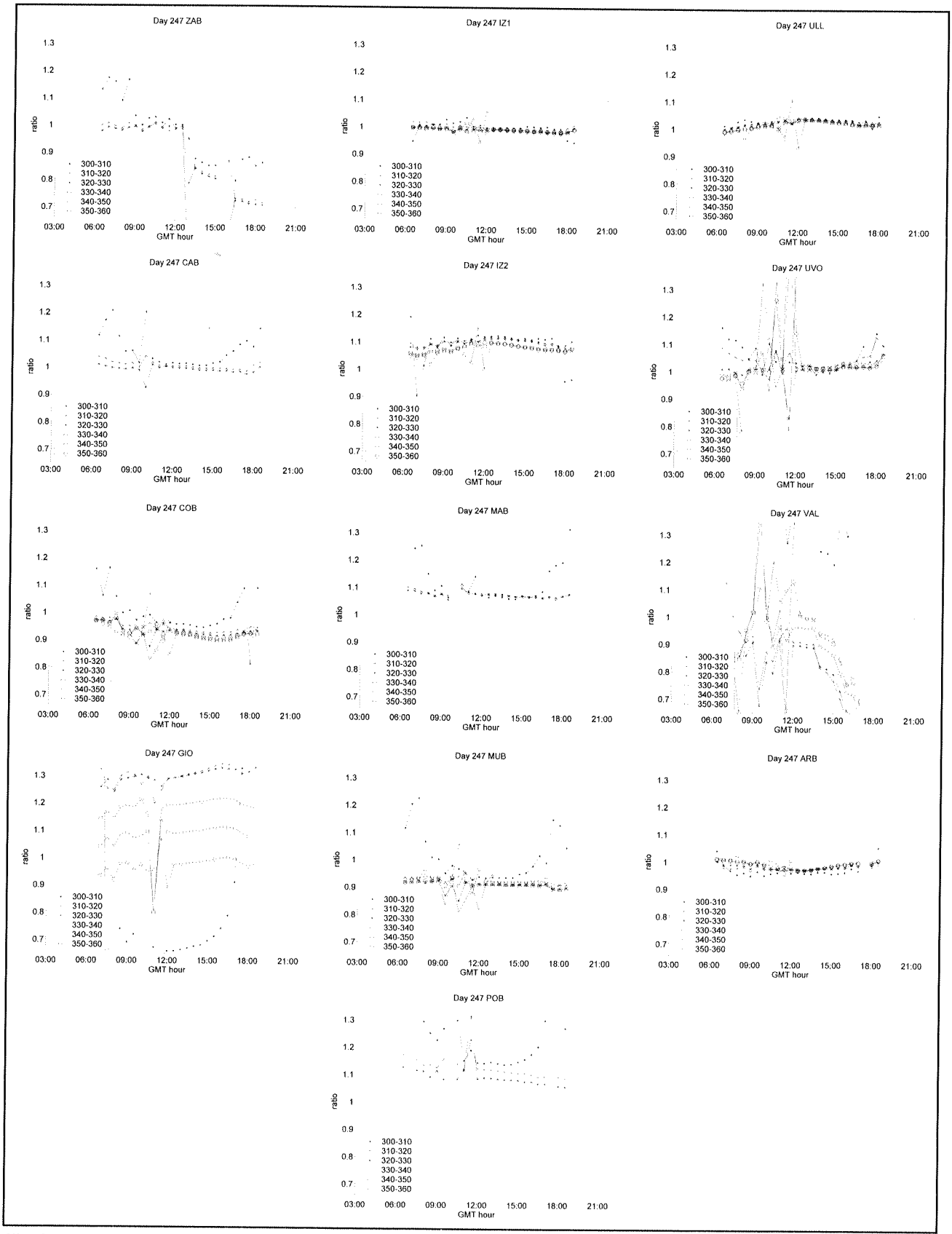

Fig. 25. Ratio of the instruments using the original submitted data with the reference, vs. wavelength during the second day of the intercomparison. Figures show the wavelength dependence of the ratio for all the measured scans, clear grey values correspond to scans near noon and dark grey lines corresponds with the measures with high zenith angles. From upper left to down right the figures are sorted in alphabetical order of the instruments: ARB, CAB, COB, GIO, IZ1, IZ2, MAB, MUB, POB, ULL, UVO, VAL and ZAB.

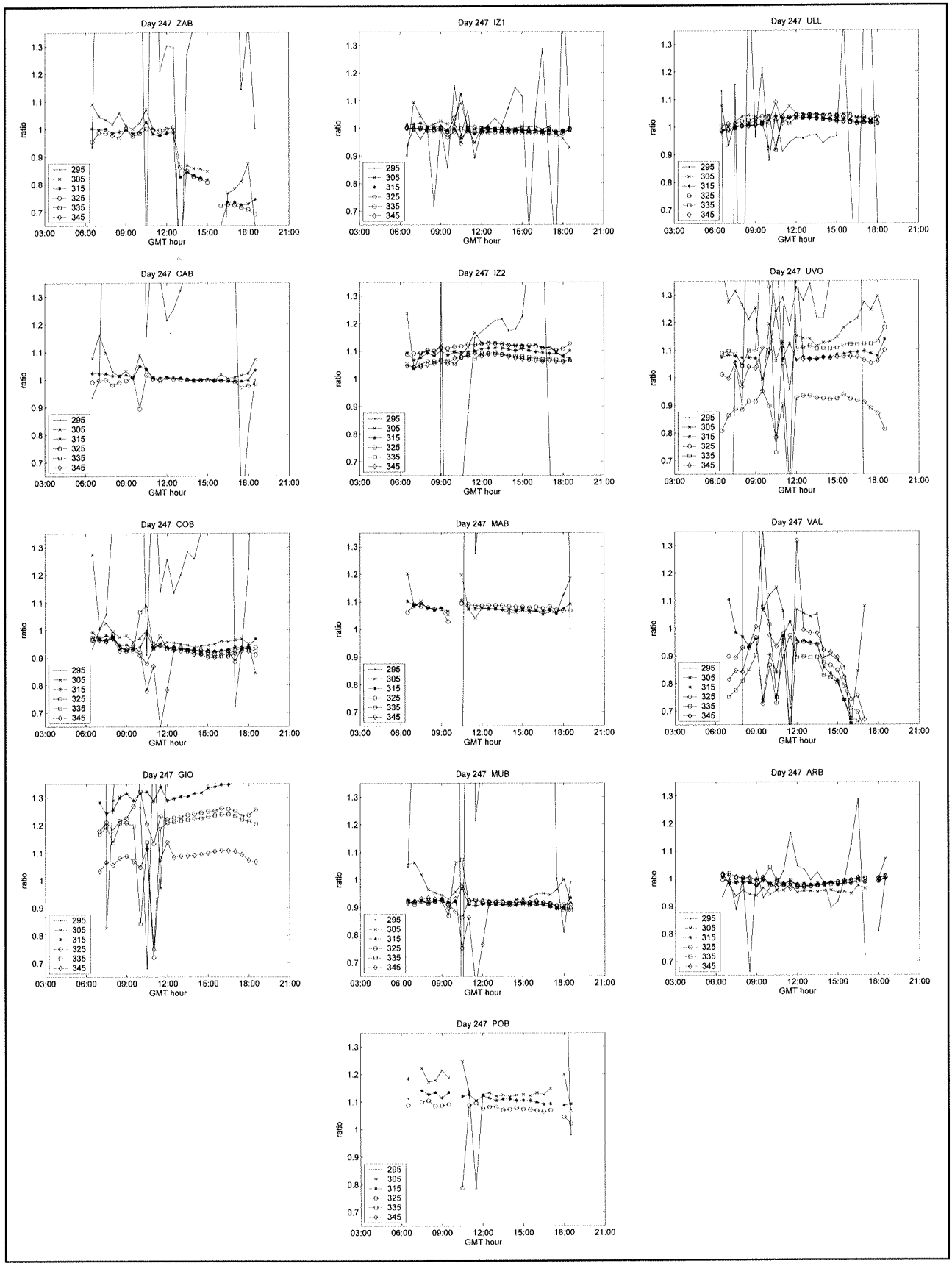

Fig. 26. *Ratio of the instruments with the reference, averaged on 10 nm wavelength intervals, during the second day of the intercomparison. Figures show the time dependence of the ratio averaged on five selected wavelengths intervals from 310 to 360 every 10 nm. From upper left to down right the figures are sorted in alphabetical order of the instruments: ARB, CAB, COB, GIO, IZ1, IZ2, MAB, MUB, POB, ULL, UVO, VAL and ZAB.*

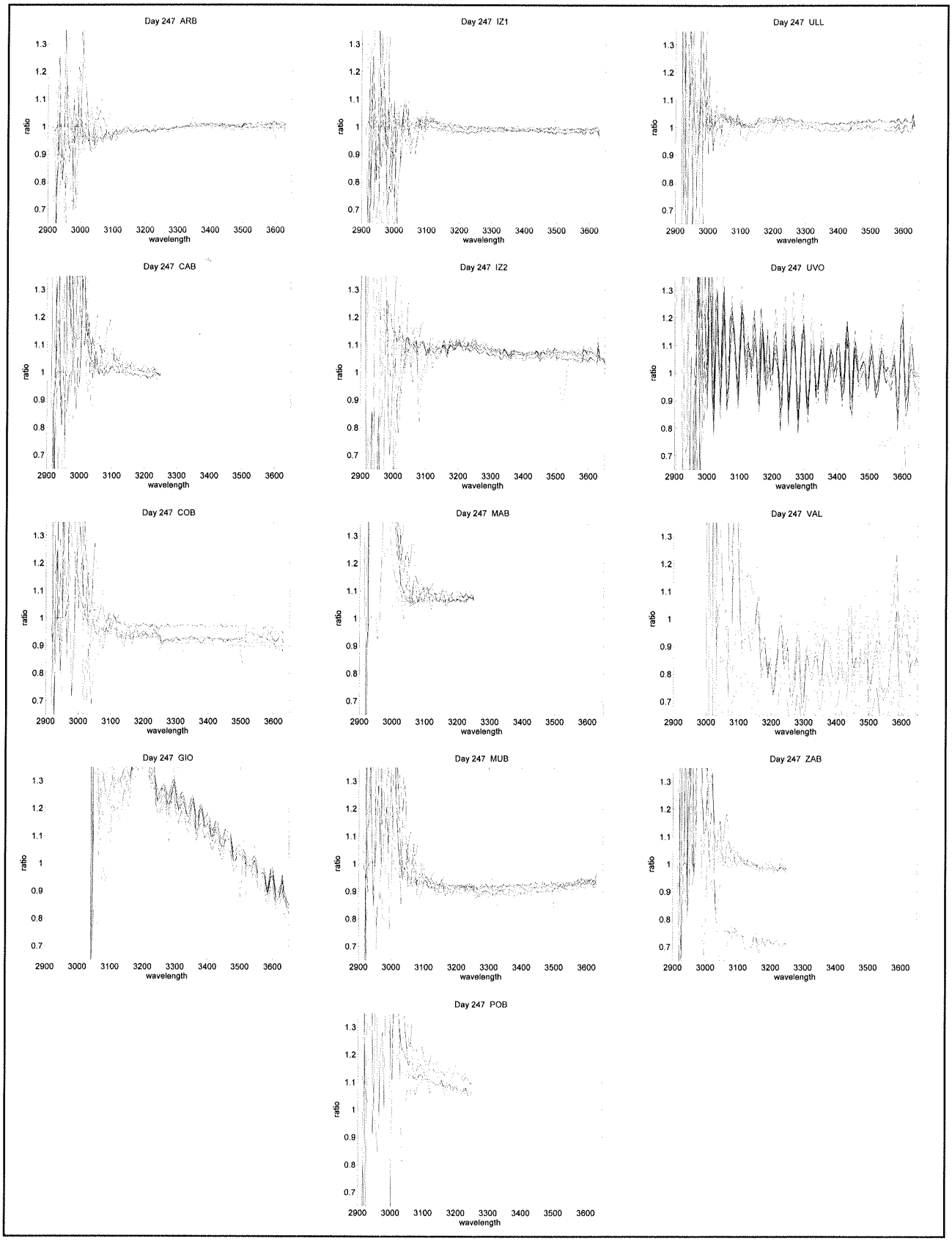

Fig. 27. *Ratio of the instruments using the "analysed spectra" with the reference, vs. wavelength during the first day of the intercomparison. Figures show the wavelength dependence of the ratio for all the measured scans, clear grey values correspond to scans near noon and dark grey lines corresponds with the measures with high zenith angles. From upper left to down right the figures are sorted in alphabetical order of the instruments: ARB, CAB, COB, GIO, IZ1, IZ2, MAB, MUB, ULL, UVO, VAL and ZAB. The VAL instrument can not be analysed due the FHWM of the instrument, ratio with the original data are displayed.*

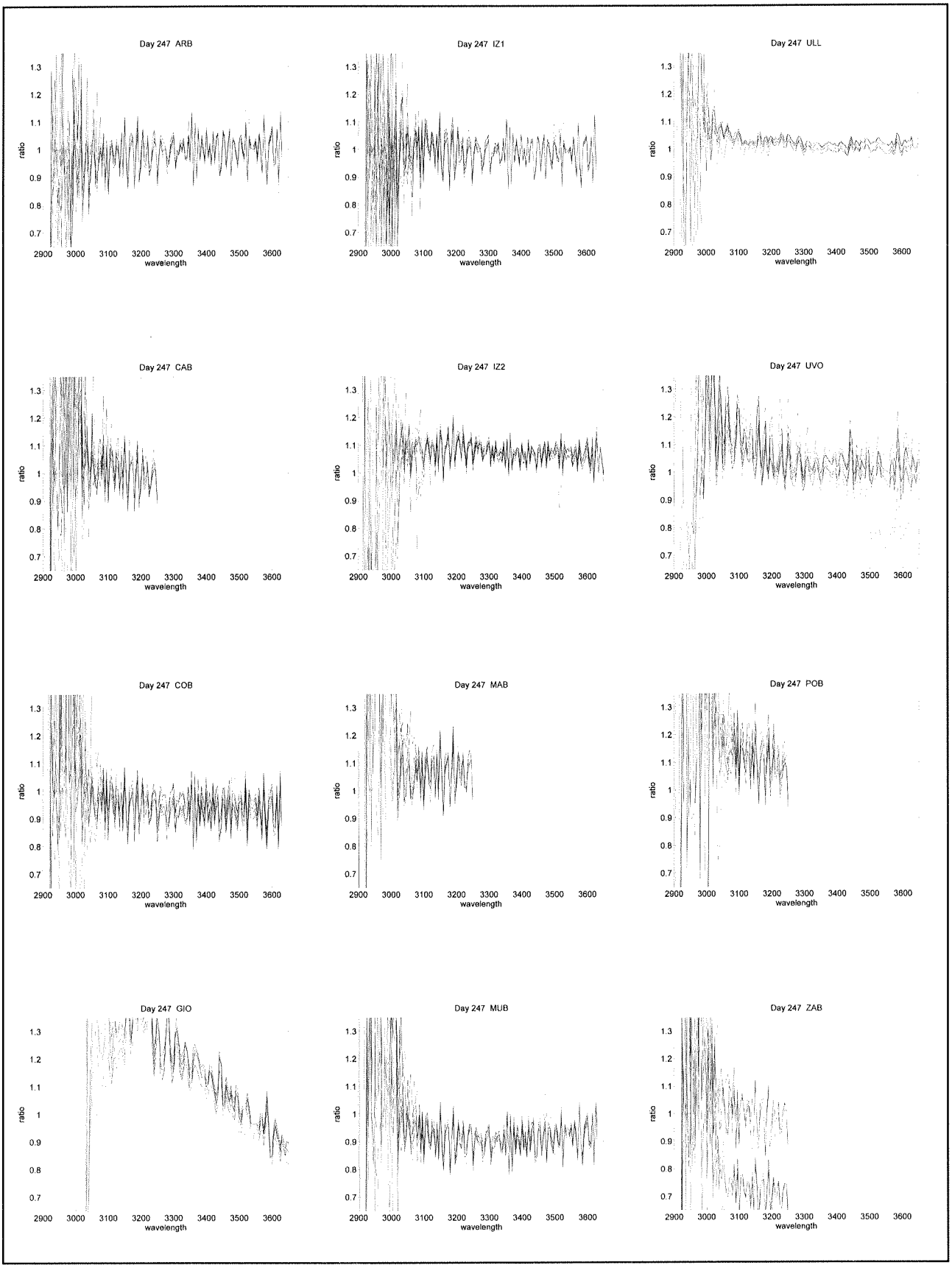

Fig. 28. *Ratio of the instruments using the original submitted data with the reference, vs. wavelength during the second day of the intercomparison. Figures show the wavelength dependence of the ratio for all the measured scans, clear grey values correspond to scans near noon and dark grey lines corresponds with the measures with high zenith angles. From upper left to down right the figures are sorted in alphabetical order of the instruments: ARB, CAB, COB, GIO, IZ1, IZ2, MAB, MUB, ULL, UVO and ZAB.*

6.10. APPENDIX V: UVI RESULTS

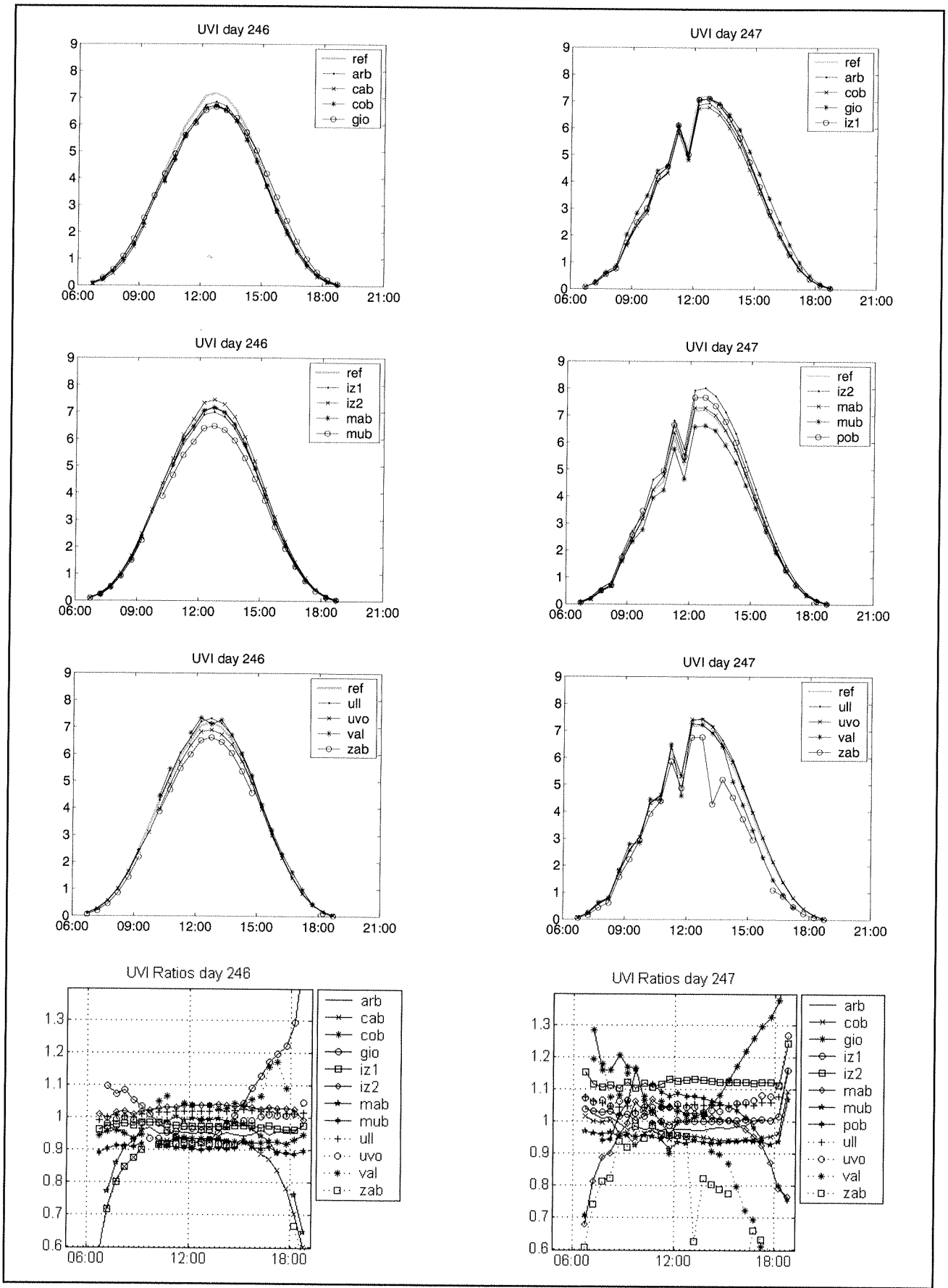

Fig. 29. UVI calculated by the spectroradiometers for the two blind days on the 3 first graphs of each column, the reference is showed by a thick grey line. The last figures show the ratios with the reference along the days.

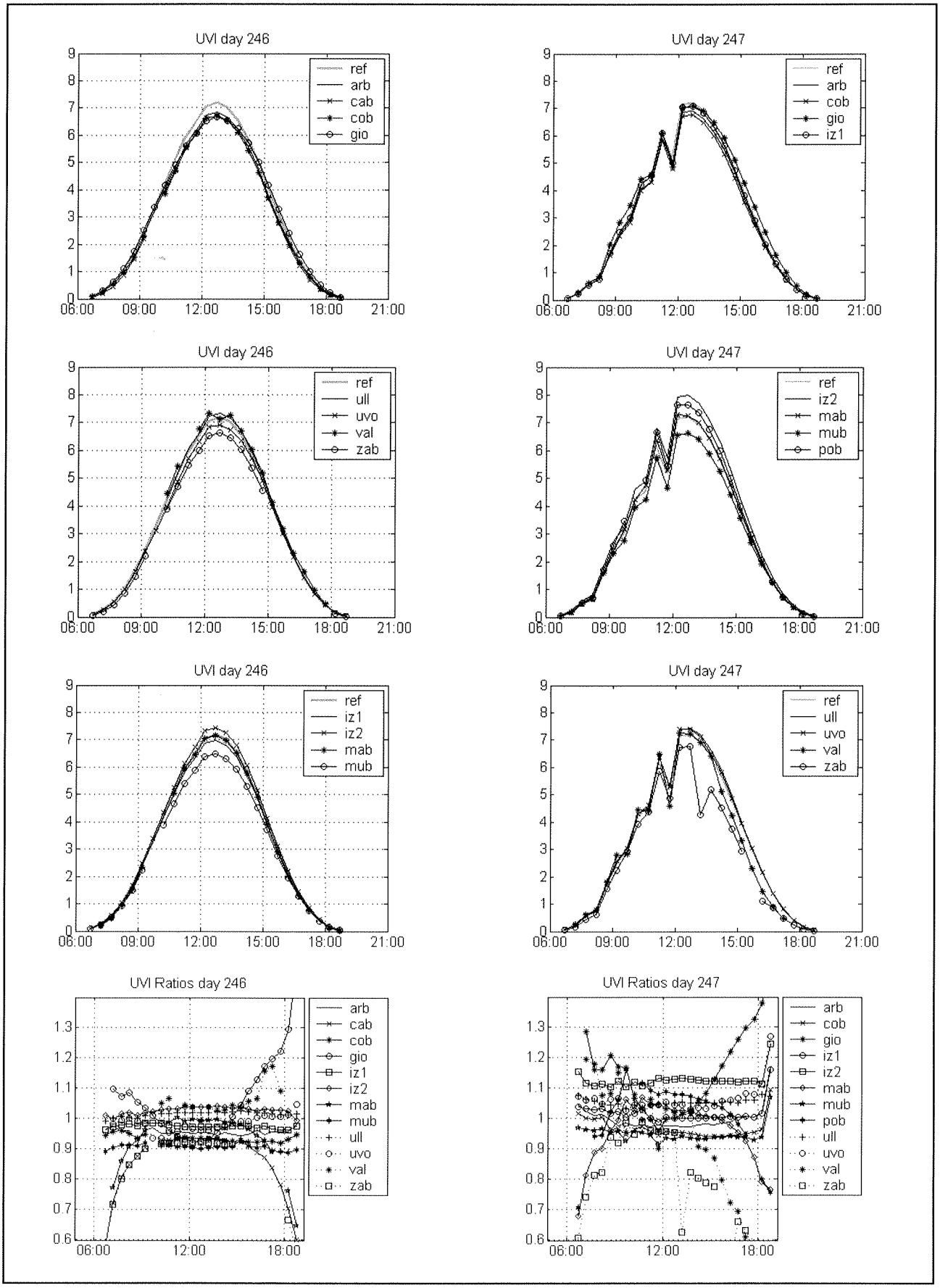

Fig. 30. *UVI calculated by the spectroradiometers for the two blind days on the 3 first graphs of each column, the reference is showed by a thick grey line. The last figures show the ratios with the reference along the days.*

CHAPTER 7
VISIBLE SOLAR IRRADIANCE MEASUREMENTS

J. A. Martínez-Lozano, M. P. Utrillas y R. Pedrós
Grupo de Radiación Solar, Departamento de Termodinámica, Universitat de Valencia. Dr. Moliner, 50. 46100 Burjassot, Valencia (Spain), *jmartinez@uv.es*

SUMMARY

This chapter presents the results of the analysis of the solar irradiance measurements in the visible range (400-700 nm), made in the framework of the First Iberian UV-VIS Instruments Intercomparison. These measurements correspond to four spectroradiometers; one Optronic 754 and three Licor 1800s equipped with different receiver optics. The analysis covers measurements of global irradiance on a horizontal plane made over a two day period as well as measurements of direct irradiance at normal incidence (obtained by using collimators with different fields of view) taken on a third day. Parallel studies have been carried out of the data given by the spectroradiometers with their original calibration file and of the same data corrected following in situ calibration of the instruments using a laboratory reference lamp. To compare the series of spectral data the relative values of MBD, MAD and RMSD have been used. The results obtained for the measurements of global irradiance show that the Licor 1800s presented very significant differences at the beginning and at the end of the day due to the influence of the cosine effect. This obliged us to limit the analysis of these measurements to solar altitude angles greater than 30°. At the same time the measurements of direct irradiance showed that in this case, even when considering the non-corrected data, the deviations are of the order of the precision of the instruments in the visible range (5%). If correction factors are considered these deviations are reduced to 3%, and when the Licors are compared with the Optronic, the deviations are less than 2%.

RESUMEN

En este capítulo se presentan los resultados del análisis de las medidas realizadas en el rango visible (400-700 nm), en el marco de the First Iberian UV-VIS Instruments Intercomparison. Se han utilizado cuatro espectrorradiómetros, 3 Licor 1800 (provistos de diferentes ópticas en cuanto al receptor) y un Optronic 754. Se analizan tanto las medidas de irradiancia global sobre un plano horizontal, registradas durante dos días de la intercomparación, como medidas de irradiancia directa en incidencia normal utilizando colimadores que presentan diferentes FOVs correspondientes a un tercer día. Se ha realizado un estudio paralelo tanto de los datos registrados por los espectrorradiómetros calibrados en origen, como de los datos corregidos tras la calibración de los instrumentos realizada in situ frente a una lámpara de referencia. Para la comparación de las series de datos espectrales se han utilizado los valores relativos del MBD, MAD y RMSD. Los resultados obtenidos del análisis de las medidas de irradiancia global muestran que los Licor presentan discrepancias muy importantes en las horas extremas del día, debido a la influencia del efecto coseno, lo que nos ha obligado a limitar el análisis de estas medidas para alturas solares superiores a 30°. A su vez, los resultados obtenidos del análisis de las medidas de irradiancia directa muestran que las desviaciones, aún en el caso de considerar los datos no corregidos, son del orden de la precisión de los instrumentos en el rango visible (5%). Caso de considerar los factores correctores, éstas se reducen al 3%. Cuando se comparan los Licor con el Optronic, si se consideran los valores corregidos, las desviaciones son inferiores al 2%.

7.1. INTRODUCTION

This chapter presents the results of the analyses of the measurements made in the visible range in the framework of the First Iberian UV-VIS Instruments Intercomparison, carried out in September 1999 at the installations of the INTA (Instituto Nacional de Técnica Aeroespacial) in El Arenosillo (Huelva, Spain). All the results refer to the spectral range 400-700 nm. Although the instruments used do permit the acquisition of data in part of the near infra red (IR) range it was decided not to include this in the analysis for two reasons: *a)* the IR interval is small, reaching, in the best case, up to 1 100 nm, so the results could not be considered as very representative of the IR range, *b)* the limit of the IR range of the different instruments is not the same, so if we wanted to draw conclusions that are valid for all the instruments we would have to limit the spectral interval at 800 nm anyway.

Three Licor 1800s and one Optronic 754 spectroradiometers have been used. The Licors have the serial numbers RS-312 (Universitat de Barcelona), RS-415 (Universitat de Valencia) and RS-487 (Universidad de Valladolid). The first two are provided with a Teflon diffuser at the entrance to the detector, whilst the instrument of the University of Valladolid uses a remote cosine sensor with a fiber optic probe. In the following text these instruments are referred to as BAL (Barcelona Licor), UVL (Universitat Valencia Licor) and VAL (Valladolid Licor). The Optronic 754 has the serial number 98202085. It is operated by the Universitat de Valencia and is equipped with an integrating sphere for the measurement of global irradiance. In the following this instrument is referred to as UVO (Universitat Valencia Optronic). These instruments are all described in Chapter 4. All of them have also been used for irradiance measurements in the UV spectral range (300-400 nm) and the results of these analyses are given in Chapter 6. Finally the characteristics of the measurement site are shown in Chapter 2, and the overall meteorological conditions during the measurement campaign are described in Chapter 3.

As indicated above, the objective of this chapter is to compare, in the visible range, the measurements of solar irradiance made by these spectroradiometers on both horizontal planes as well as at normal incidence. The instruments used differ in their full width at half maxima (FWHM), in their

wavelength steps, and also in the receiver optics. Furthermore the radiance limiters (collimators) used for measuring direct irradiance at normal incidence have different fields of view (FOV).

To our knowledge there have been no previous intercomparison exercises such as this, based on solar irradiance in the visible range, since the instruments that are usually used for spectral irradiance measurements in this range are normally calibrated against a laboratory reference lamp (Kiedron et al., 1999). Although a similar intercomparison exercise was carried out for Licor 1800 spectroradiometers at SERI (Solar Energy Research Institute) in 1987 (Riordan et al., 1990), their results are not available. In this work we have followed, as far as possible, the procedures used in the UV spectroradiometer intercomparison campaigns carried out in recent years (Gardiner and Kirsch, 1995; Webb, 1997; Seckmeyer et al., 1998; see also Redondas et al., in Chapter 6 of this book).

Although the instruments used are described in detail in Chapter 4, together with the other instruments used in the intercomparison, for convenience their most relevant characteristics are summarised again here. The Licor 1800 is a spectroradiometer equipped with a single monochromator that allows measurements in the 300-1 100 nm range, with a FWHM of approximately 6 nm and a wavelength step of 1 nm. The receiver of the Valencia and Barcelona Licors is a Teflon diffuser and that of the Valladolid Licor is a remote cosine sensor with a fiber optic probe. Several papers have studied the uncertainty of this kind of spectroradiometer (Riordan et al., 1989; Nann and Riordan, 1991; Lorente et al., 1994; Cachorro et al., 1998). The error of measurements with these instruments depends on the spectral region considered. The greatest errors (around 20%) correspond to the UV range due to the greater calibration error in this band and the degradation of the Teflon diffuser. In the visible and near-infrared regions (400-1 000 nm) the error of measurements, governed mainly by the calibration uncertainty, is 5%, while in the range between 1 000 and 1 100 nm the error can increase significantly because of the sensitivity of the spectroradiometer to temperature.

The Optronic 754 is equipped with a double monochromator, with a spectral range that extends from 250 nm to 800 nm, with a FWHM of 1.6 nm allowing measurements to be made with a minimum wavelength step of 0.05 nm. The measurements made during the campaign showed that, in the UV range, there was a wavelength shift of nearly 1 nm through the day due to temperature variations. This effect, which has been previously reported by other authors (Slaper, 1997; Seckmeyer et al., 1998), is due to the dilations that occur in the holographic diffraction gratings which are not temperature stabilised, unlike the detector which is stabilised for the Peltier effect. This wavelength shift has been considered when comparing the measurements in the visible range.

7.2. EXPERIMENTAL MEASUREMENTS

During 3 and 4 September 1999 global solar irradiance on a horizontal plane was measured every 15 minutes from 6:30 to 17:45 GMT. On the first day all four instruments were used. On the second day the Optronic 754 was used just to measure UV irradiance with a higher precision wavelength step, so measurements are only available for the three Licor 1800 instruments for this day. Three days later, in the afternoon of 7 September, once all the instruments had been recalibrated against a reference lamp, direct solar irradiance at normal incidence was measured with the Valladolid and Valencia Licor 1800s and the Optronic. For these measurements collimators were used which, as indicated above, had different FOV. The collimators of the Licor 1800s were designed and constructed by each of the groups that operate them, and have FOVs of 4.7° (Valencia) and 4.2° (Valladolid). The Optronic collimator was supplied with the instrument by the makers and has an FOV of 5.7°. For direct measurements all spectroradiometers were positioned manually. This pointing accuracy was not quantified.

The results are presented under two different headings referring to the measurements of global irradiance on a horizontal plane and to direct irradiance at normal incidence respectively. For each case a distinction is made between the data corresponding to before and after the corrections carried out following the in situ calibration. In all cases the results are shown for the intercomparison of the Licors and for the comparison of each of the Licors with the Optronic. In all the comparisons the slit function values determined in the laboratory for all the different instruments has been taken into account.

To compare the series of spectral data the relative values of MBD (mean bias difference), MAD (mean absolute difference) and RMSD (root mean square difference) has been used. The analytical expression for each of these parameters is given in the Appendix at the end of the chapter. To condense the results only the averages of the differences for each spectral measurement series are presented. These average values were obtained from the 300 values corresponding to each wavelength step between 400 and 700 nm. As an example of the initial spectral data Figures 1 to 3 show some uncorrected experimental values obtained by these instruments over the whole measurement range, although as has already been noted, the subsequent analysis only considers the values in the visible spectral range, 400-700 nm. Figure 1 shows the values of global solar irradiance on a horizontal plane registered by the three Licors at 12:00 GMT on 03/09/99. Figure 2 shows, for the same day and time, the values obtained by the Optronic for the whole of this instrument's spectral range. Finally, Figure 3 shows the measurements of direct irradiance at normal incidence at 14:00 GMT on 06/09/99 made by the Valladolid and Valencia Licors.

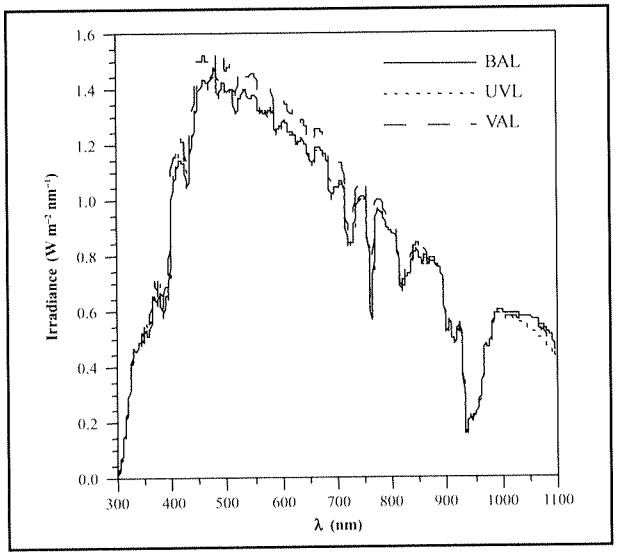

Figure 1. *Spectral horizontal global solar irradiance. 12:00 GMT, 03/09/99. BAL: Barcelona Licor; UVL: Valencia Licor; VAL: Valladolid Licor.*

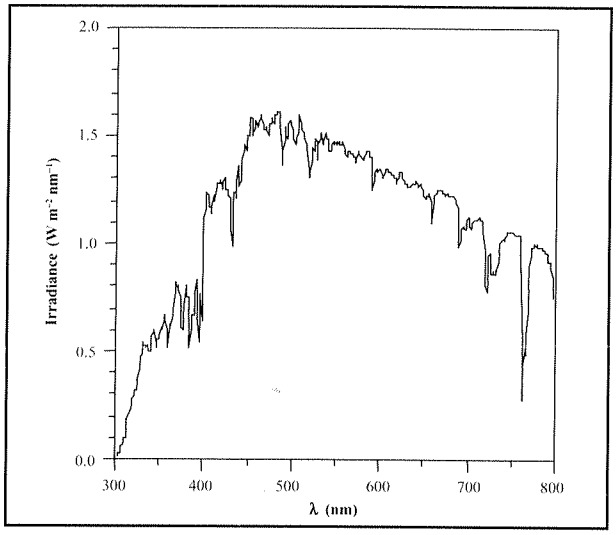

Figure 2. *Spectral horizontal global solar irradiance. 12:00 GMT, 03/09/99. Optronic 754.*

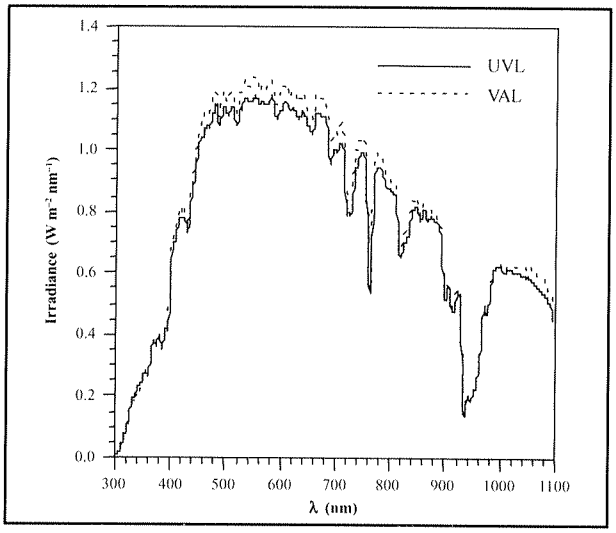

Figure 3. *Spectral direct solar irradiance at normal incidence. 14:00 GMT, 07/09/99. UVL: Valencia Licor; VAL: Valladolid Licor.*

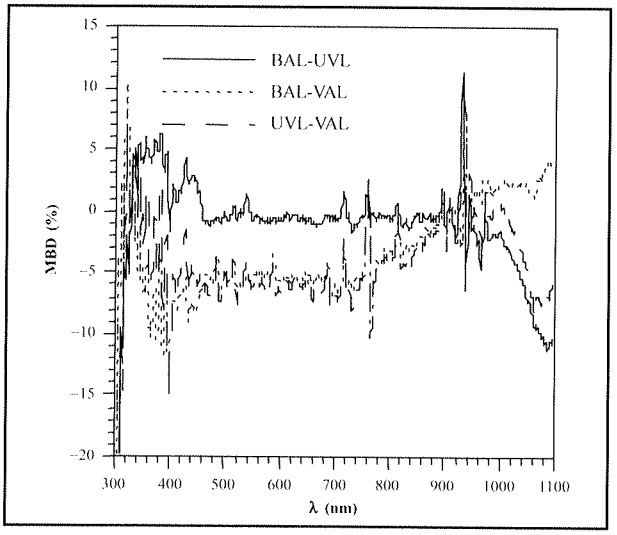

Figure 4. *Values of MBD obtained from global horizontal irradiance in the whole range of the Licors. BAL: Barcelona Licor; UVL: Valencia Licor; VAL: Valladolid Licor.*

7.3. RESULTS FOR HORIZONTAL GLOBAL IRRADIANCE

The first comparison made was between the data for global solar irradiance on a horizontal plane registered by the spectroradiometers with their respective original calibration files during the 3 and 4 September. The results from all the Licors have been compared and each of these has been compared in turn with the Optronic 754. From these data values of MBD, MAD and RMSD have been obtained for each wavelength (300 values between 400-700 nm). As an example of these spectral values Figures 4 and 5 show the MBD and MAD respectively resulting from the comparison of the measurements of global solar irradiance registered by the three Licors at 12:00 GMT on 03/09/99. These figures confirm that the biggest differences are found in the UV and IR, ranges for which, as noted previously, these instruments have lower precision. Nevertheless in the following analysis only the 400-700 nm range is considered, where the differences are smaller and uniform.

7.3.1. Intercomparison between the Licor 1800s

a) Uncorrected experimental values

The two days (03/09/99 and 04/09/99) for which measurements of the global horizontal irradiance were made have been analysed separately. Figures 6 (a-c) and 7 (a-c) show the daily evolution of the average values of MBD, MAD and RMSD for these days. These values were obtained from spectral values in the range 400-700 nm. In these figures it can be seen how at the beginning of the morning and at the end of the afternoon the values of MAD and RMSD are much higher than in the middle of the day. This is due basically to the error introduced by the cosine effect in the global irradiance measurements on a horizontal plane for low solar altitude angles.

From these average values of MBD, MAD and RMSD we have obtained representative statistical indicators of these parameters for each of the days. In this calculation we have ignored the extreme hours, focussing on the interval between 08:00 and 16:00 GMT, in order to avoid the distortions introduced by the cosine effect. On these days 08:00 GMT corresponded to a solar altitude of 23° and 16:00 GMT to a solar altitude of 30° (equivalent to an optical mass of

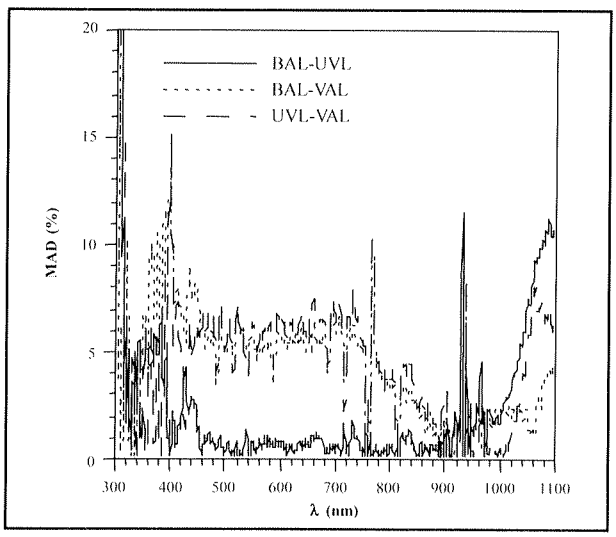

Figure 5. *Values of MAD obtained from global horizontal irradiance in the whole range of the Licors. BAL: Barcelona Licor; UVL: Valencia Licor; VAL: Valladolid Licor.*

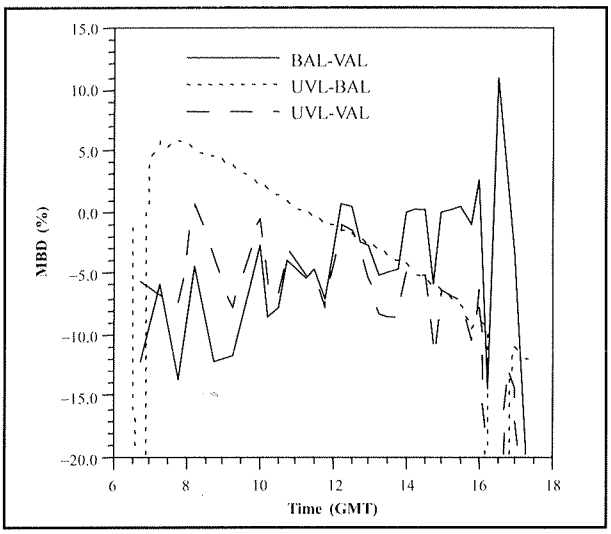

Figure 6a. *Daily evolution of the MBD (%) on 03/09/99. Horizontal global irradiance. Comparison Licor-Licor. BAL: Barcelona Licor; UVL: Valencia Licor; VAL: Valladolid Licor.*

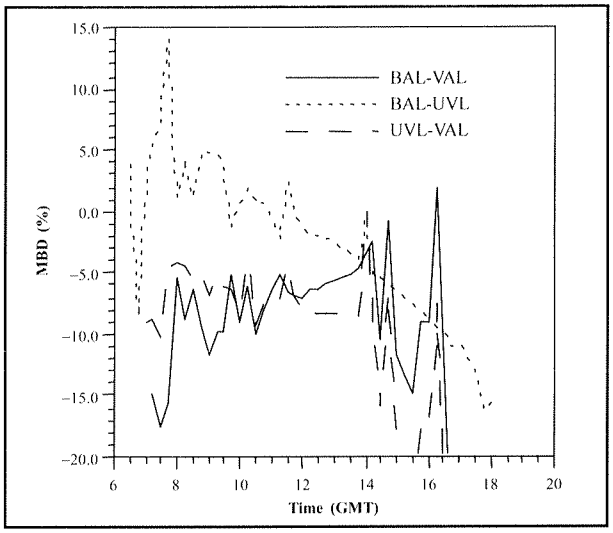

Figure 7a. *Daily evolution of the MBD (%) on 04/09/99. Horizontal global irradiance. Comparison Licor-Licor. BAL: Barcelona Licor; UVL: Valencia Licor; VAL: Valladolid Licor.*

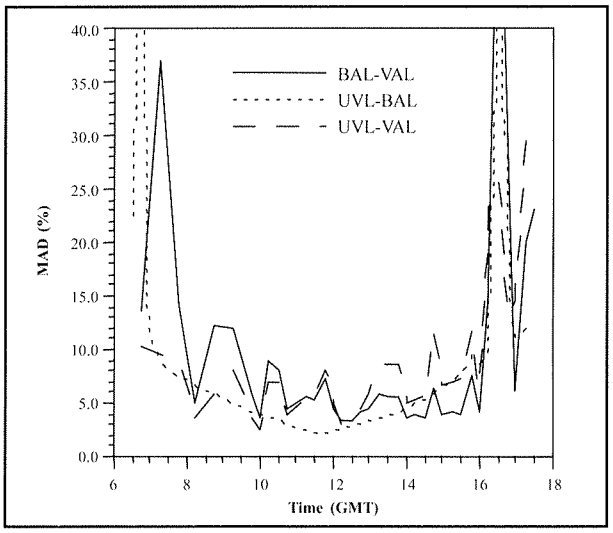

Figure 6b. *Daily evolution of the MAD (%) on 03/09/99. Horizontal global irradiance. Comparison Licor-Licor. BAL: Barcelona Licor; UVL: Valencia Licor; VAL: Valladolid Licor.*

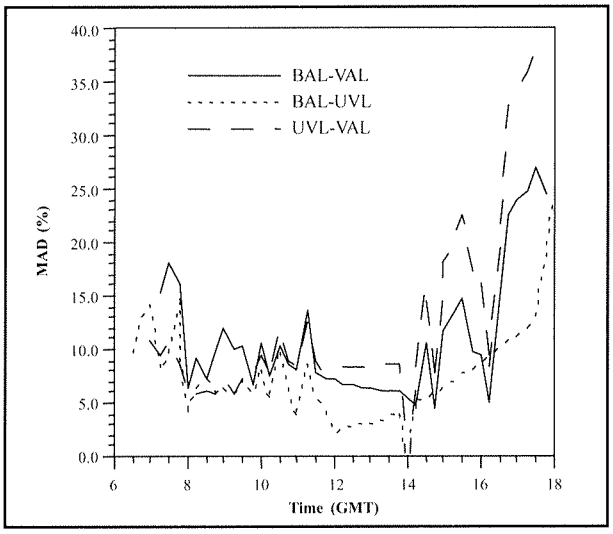

Figure 7b. *Daily evolution of the MAD (%) on 04/09/99. Horizontal global irradiance. Comparison Licor-Licor. BAL: Barcelona Licor; UVL: Valencia Licor; VAL: Valladolid Licor.*

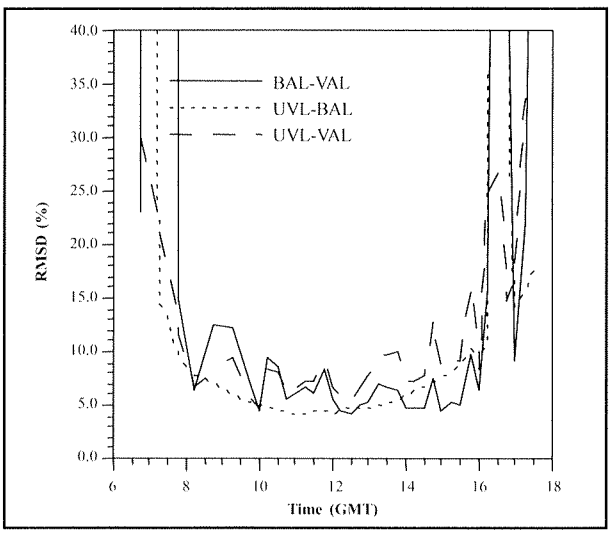

Figure 6c. *Daily evolution of the RMSD (%) on 03/09/99. Horizontal global irradiance. Comparison Licor-Licor. BAL: Barcelona Licor; UVL: Valencia Licor; VAL: Valladolid Licor.*

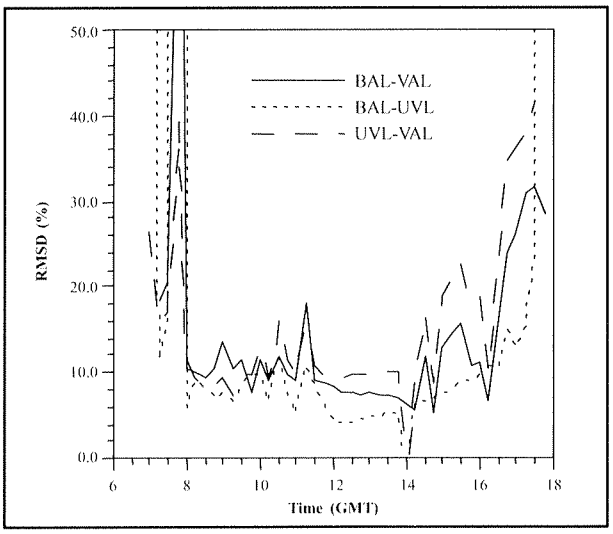

Figure 7c. *Daily evolution of the RMSD (%) on 04/09/99. Horizontal global irradiance. Comparison Licor-Licor. BAL: Barcelona Licor; UVL: Valencia Licor; VAL: Valladolid Licor.*

approximately 2). We have applied this criterion to all the irradiance measurements on a horizontal plane analysed in this chapter, so all the conclusion will only be valid for optical masses less than this value. Table I (03/09/99) and Table II (04/09/99) summarise the results for the uncorrected experimental data for this solar altitude interval. The tables give for each day the minimum and maximum values of MBD, MAD and RMSD as well as the average and the median of these parameters.

Table I. *Horizontal global irradiance on 03/09/99.*

	UVL-BAL		
	MBD(%)	MAD(%)	RSMD(%)
Minimum	−8.2	0.8	1.2
Maximum	8.7	8.7	8.8
Mean	−0.2	4.1	4.3
Median	−0.2	3.8	4.0
	UVL-VAL		
	MBD(%)	MAD(%)	RSMD(%)
Minimum	−14.4	1.1	1.4
Maximum	3.4	14.4	14.5
Mean	−6.8	7.1	7.2
Median	−7.2	7.2	7.3
	VAL-BAL		
	MBD(%)	MAD(%)	RSMD(%)
Minimum	−12.9	0.9	1.2
Maximum	2.0	12.9	13.0
Mean	−5.9	6.1	6.2
Median	−5.8	5.8	5.9

Table II. *Horizontal global irradiance on 04/09/99.*

	UVL-BAL		
	MBD(%)	MAD(%)	RSMD(%)
Minimum	−8.6	0.9	1.1
Maximum	9.1	10.7	14.8
Mean	−0.1	5.3	5.9
Median	−0.8	5.4	5.8
	UV-VAL		
	MBD(%)	MAD(%)	RSMD(%)
Minimum	−26.2	3.0	3.3
Maximum	−1.0	26.2	26.2
Mean	−10.8	11.1	11.7
Median	−10.0	10.0	10.5
	VAL-BAL		
	MBD(%)	MAD(%)	RSMD(%)
Minimum	−19.0	4.5	4.6
Maximum	−4.5	19.0	19.0
Mean	−10.7	10.9	11.2
Median	−10.1	10.2	10.5

The tables show, firstly, that 03/09/99 presented more stable atmospheric conditions than 04/09/99 since the variations in the values of MBD, MAD and RMSD are much smoother. The results seem to indicate that on 04/09/99 there were intervals of high clouds. This hypothesis is corroborated with the data acquired by the Brewers spectroradiometers but which is not analysed in this chapter. Since these instruments take 20 minutes to measure each spectral series they allow variations in atmospheric transmisivity to be detected, as peaks in the series, during these time periods.

With reference to the results obtained when comparing each pair of instruments, and focussing on the median, we see that the differences are within the overall margin of error expected for each (5% in the visible range) and are greater when one of the instruments is the Valladolid Licor. This could be due either to the use of the fiber optic probe or the manual operation of the instrument. On these days the Barcelona and Valencia Licors acquired data in automatic mode, being static throughout the measurement time, whilst the Valladolid Licor operated in manual mode, measuring alternatively global irradiance and direct irradiance. We think that this measurement procedure could have led to variations in the measurements of global irradiance due to possible inaccuracies in the horizontal alignment of the remote cosine sensor, in addition to those that could come from the movement of the fiber optic probe. Such variations would account for the sawtooth patterns that occur in the daily evolutions shown in figures 6 and 7 in which the curves corresponding to UVL-BAL are always smoother.

Whatever the case, the results indicate that these instruments are adequate for measuring global irradiance in the visible range and that they give comparable values, for optical air masses less than 2, even with different optics in the receiver and different measurement procedures and even without considering the results of the in situ calibration against a reference lamp.

b) In situ calibration of the Licor spectroradiometers

As already noted the results given in the previous section correspond to the data given by each spectroradiometer using their respective original calibration files, each of which had been established previously by the group that usually operates each sensor. Due to the displacement of the instruments to the intercomparison site the instruments could have suffered alterations in their calibration. For this reason it is normal in this type of campaigns to carry out a recalibration, in situ, against a reference lamp. The procedure followed for this intercomparison and the results for each of the instruments is given in Chapter 5. Here we present just a summary of the most relevant results for the three Licors. Figure 8 (a-c) shows the spectral response curves of these instruments against the reference lamp (three measurements in each case). Figure 9 shows the differences in the response of each of the Licors, with the original calibration, with respect to the lamp.

From the lamp standard and the measurements of the spectroradiometers corrections factors have been calculated to apply to the experimental data. These factors are presented in Figure 10. The smallest deviations from the original calibration correspond to the Valladolid Licor, with a median value of approximately 1.0%, whilst the values corresponding to the Barcelona and Valencia instruments were 5.4% and 3.5% respectively.

The instruments are calibrated by measuring the radiation of a calibration lamp placed at the calibration distance from the radiometers' entrance optics. The exact measurement of this distance is critical in the calibration process. In the VAL case, due to the configuration of the optics, this measurement is easily made. However this is not the case for the other two Licors due to the geometry of the Teflon dome. Because the Teflon diffuser is curved it is not obvious to which point inside the entrance optics the distance should be measured. This could cause significant uncertainty (depending on the calibrated distance) in the spectroradiometer's calibration factor (Bernhard and Sheckmeyer, 1997). This could therefore explain why the measurements made with the UVL and BAL instruments deviate considerably more from the expected values than those of the VAL and why they require greater correction factors.

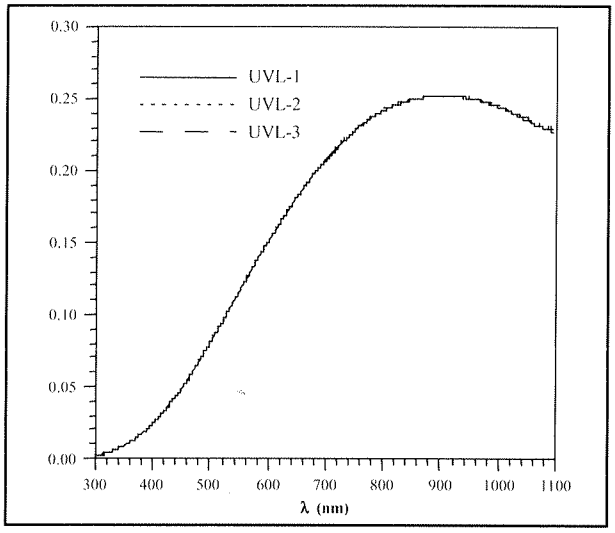

Figure 8a. *Spectral response, measured in laboratory against reference lamp, of the Valencia Licor (UVL).*

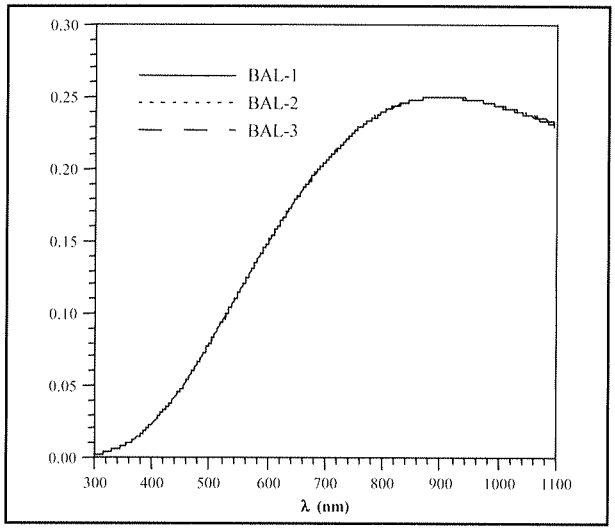

Figure 8b. *Spectral response, measured in laboratory against reference lamp, of the Barcelona Licor (BAL).*

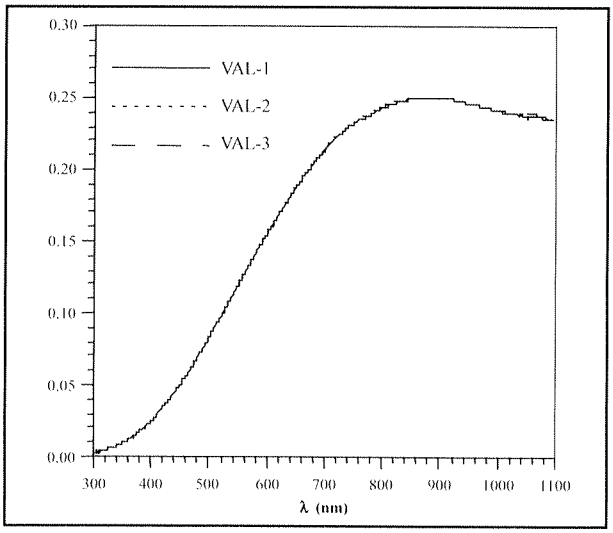

Figure 8c. *Spectral response, measured in laboratory against reference lamp, of the Valladolid Licor (VAL).*

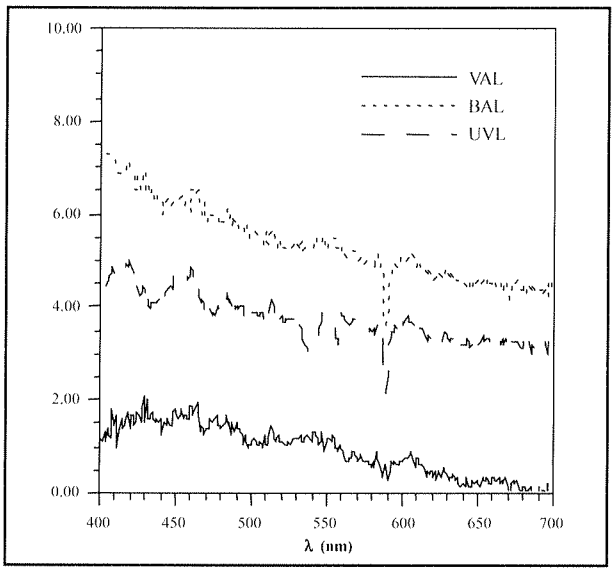

Figure 9. *Deviations of the response of each of the Licors with respect to the reference lamp. BAL: Barcelona Licor; UVL: Valencia Licor; VAL: Valladolid Licor.*

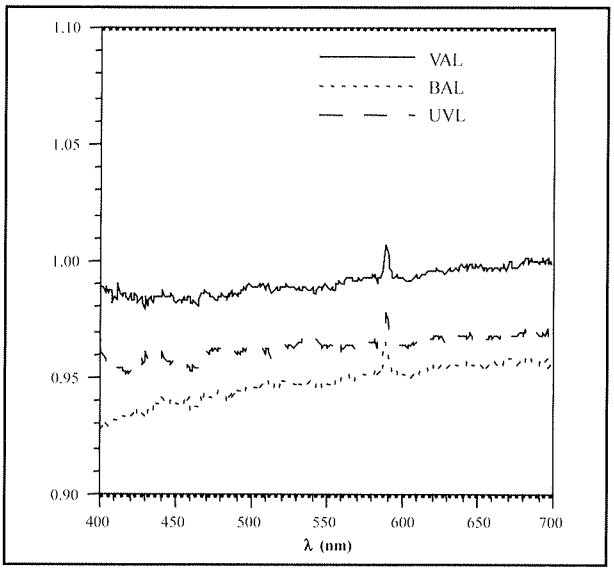

Figure 10. *Correction factors obtained from the reference lamp used for the intercomparison. BAL: Barcelona Licor; UVL: Valencia Licor; VAL: Valladolid Licor.*

c) Corrected experimental values following in situ calibration

Once the calibration factors have been established, Figure 10, these have been used to correct the experimental data analysed in section III.1.a) before repeating the analysis of the differences described in that section. Thus figure 11 (a-c) and figure 12 (a-c) are analogous to figures 6 (a-c) and 7 (a-c), presenting the daily evolution of the average values of MBD, MAD and RMSD for 03/09/99 and 04/09/99 after correcting the experimental values.

Following the same criterion that was used with the uncorrected values (reduction of the data set to those data corresponding to solar elevations above 30°), Tables III (03/09/99) and IV (04/09/99) summarise the average values of MBD, MAD and RMSD for the corrected experimental values.

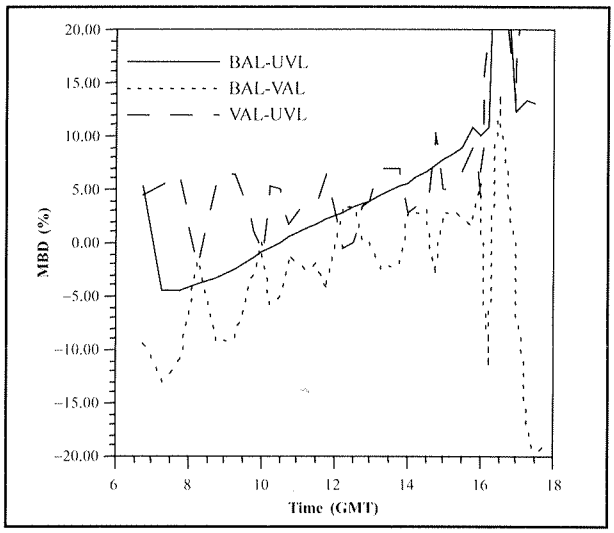

Fig. 11a. *Daily evolution of MBD (%) for 03/09/99. Corrected horizontal global irradiance. Comparison Licor-Licor. BAL: Barcelona Licor; UVL: Valencia Licor; VAL: Valladolid Licor.*

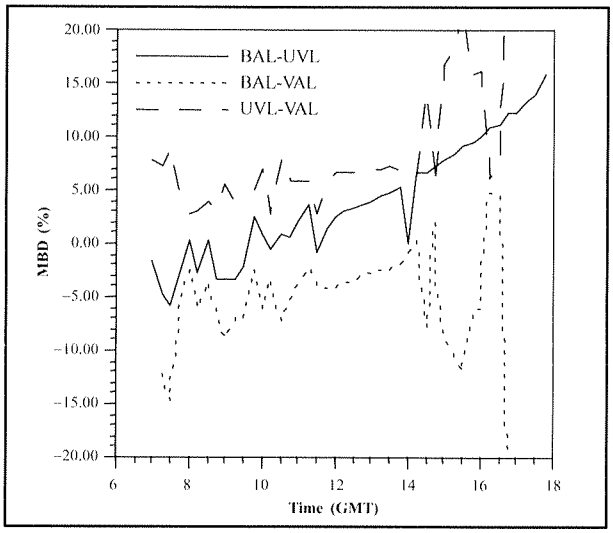

Fig. 12a. *Daily evolution of MBD (%) for 04/09/99. Corrected horizontal global irradiance. Comparison Licor-Licor. BAL: Barcelona Licor; UVL: Valencia Licor; VAL: Valladolid Licor.*

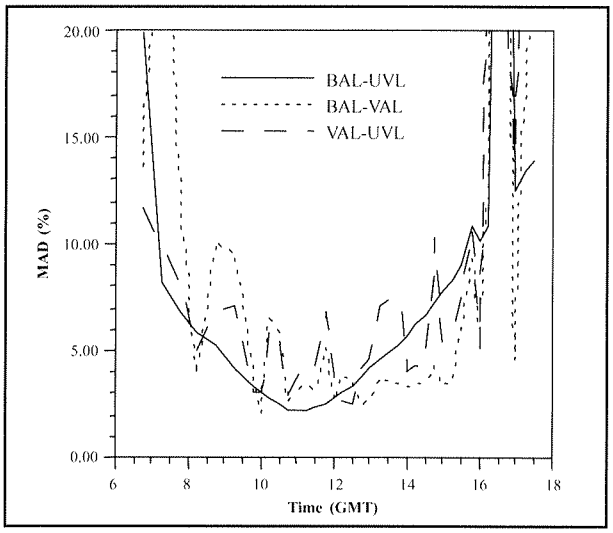

Fig. 11b. *Daily evolution of MAD (%) for 03/09/99. Corrected horizontal global irradiance. Comparison Licor-Licor. BAL: Barcelona Licor; UVL: Valencia Licor; VAL: Valladolid Licor.*

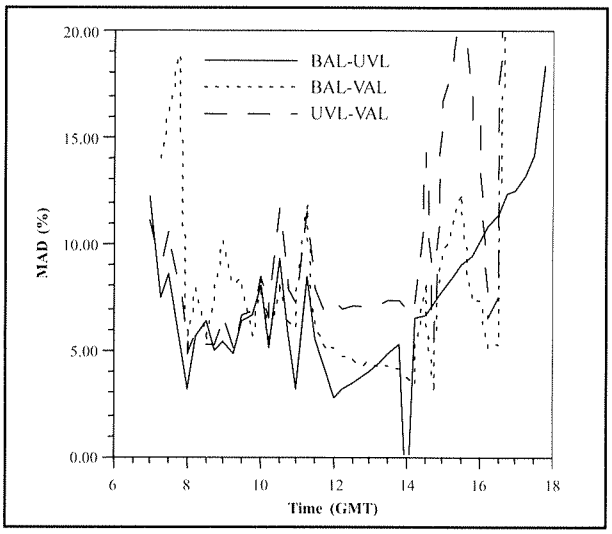

Fig. 12b. *Daily evolution of MAD (%) for 04/09/99. Corrected horizontal global irradiance. Comparison Licor-Licor. BAL: Barcelona Licor; UVL: Valencia Licor; VAL: Valladolid Licor.*

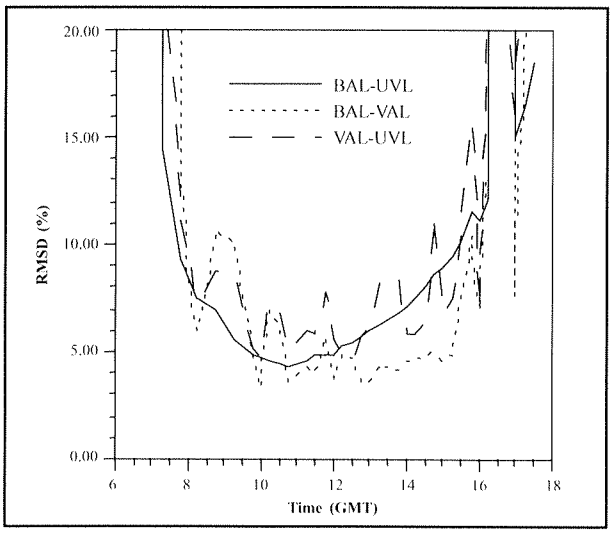

Fig. 11c. *Daily evolution of RMSD (%) for 03/09/99. Corrected horizontal global irradiance. Comparison Licor-Licor. BAL: Barcelona Licor; UVL: Valencia Licor; VAL: Valladolid Licor.*

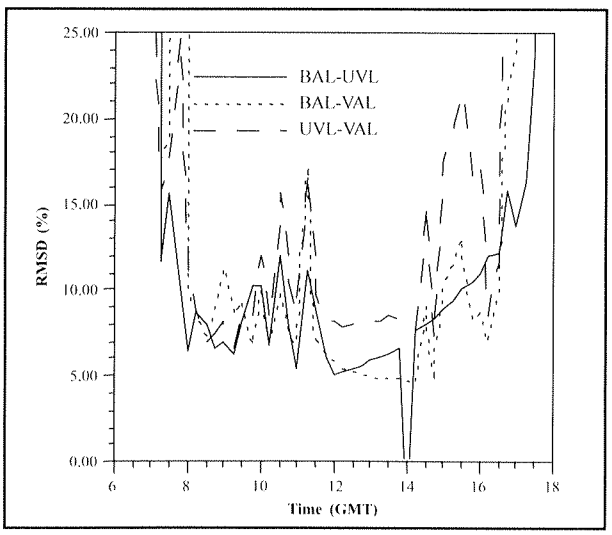

Fig. 12c. *Daily evolution of RMSD (%) for 04/09/99. Corrected horizontal global irradiance. Comparison Licor-Licor. BAL: Barcelona Licor; UVL: Valencia Licor; VAL: Valladolid Licor.*

Table III. *Corrected horizontal global irradiance for 03/09/99.*

	UVL-BAL		
	MBD(%)	MAD(%)	RSMD(%)
Minimum	−6.4	0.9	1.2
Maximum	9.9	9.9	10.0
Mean	2.5	4.4	4.5
Median	2.5	3.9	4.0
	UVL-VAL		
	MBD(%)	MAD(%)	RSMD(%)
Minimum	−6.2	0.7	1.1
Maximum	11.6	11.6	11.7
Mean	3.9	4.6	4.8
Median	4.3	4.4	4.6
	VAL-BAL		
	MBD(%)	MAD(%)	RSMD(%)
Minimum	−8.4	0.8	1.2
Maximum	6.5	8.4	8.5
Mean	−1.5	3.3	3.4
Median	−1.3	2.7	2.8

Table IV. *Corrected horizontal global irradiance for 04/09/99.*

	UVL-BAL		
	MBD(%)	MAD(%)	RSMD(%)
Minimum	−7.4	1.0	1.4
Maximum	10.3	10.8	14.8
Mean	1.8	5.6	6.2
Median	2.5	5.7	6.4
	UV-VAL		
	MBD(%)	MAD(%)	RSMD(%)
Minimum	−1.8	1.1	1.4
Maximum	23.4	23.4	23.5
Mean	8.0	8.8	9.4
Median	7.2	7.6	8.0
	VAL-BAL		
	MBD(%)	MAD(%)	RSMD(%)
Minimum	−14.5	0.5	0.7
Maximum	0.0	14.5	14.5
Mean	−6.3	6.6	7.0
Median	−5.7	5.9	6.7

We can see that, as when uncorrected values were used, the deviations for 03/09/99 were significantly lower that those corresponding to 04/09/99, which would appear to confirm the presence of greater atmospheric instability on the second day. On the other hand, whilst the results of the comparison of UVL-BAL remain practically unchanged, the comparisons involving VAL improve significantly, by about 3% in the value of the median. At the same time the curves given in figures 11 and 12 show that the variations in the differences throughout the day continue to be smoother for UVL and BAL and less stable for VAL, especially on 03/09/99.

In summary, Table V presents the median values for MAD and RMSD for the uncorrected (UC) and corrected (C) experimental values for each of the measurement days. We can see that if we consider MAD as an indicator of non-systematic deviations, then in no case do the corrected values pass 8%, even on 04/09/99, indicating the adequacy of the Licors for this type of measurement so long as the optical mass is less than 2.

Table V. *Horizontal global irradiance measurements. Deviations (in %) corresponding to the median.*

	Day 03/09/99			
	MAD (UC)	RSMD (UC)	MAD (C)	RSMD (C)
UVL-BAL	3.8	4.0	3.9	4.0
UVL-VAL	7.2	7.3	4.4	4.6
BAL-VAL	5.8	5.9	2.7	2.8
	Day 04/09/99			
	MAD (UC)	RSMD (UC)	MAD (C)	RSMD (C)
UVL-BAL	5.4	5.8	5.7	6.4
UVL-VAL	10.0	10.5	7.6	8.0
BAL-VAL	10.2	10.5	5.9	6.7

7.3.2. Comparison of the Licor 1800s with the Optronic 754

We present here the results obtained by comparing the measurements made with the Optronic 754 with those from each of the Licors. The procedure has been totally analogous to that described in section III.1, but limited only to 03/09/99. For 4 September no data were available for the Optronic because it was used for measuring values in the UV band (290-365 nm) with a 0.5 nm wavelength step. It was not possible to extend the measurements to the visible because in this case the time used for each spectral series would have made it impossible to maintain the measurement frequency fixed in the procedure for the intercomparison of all the spectroradiometers in the UV range. As for the previous case we present separately the results obtained from the uncorrected data and those obtained once the data had been corrected using the calibration factor obtained in the laboratory against a reference lamp.

a) Experimental uncorrected values

Figure 13 (a-c) shows the daily evolution of the average values of MBD, MAD and RSMD on 03/09/99. The curves that appear in these figures show some significant differences with respect to those in figures 6, 7, 11 and 12, corresponding to the intercomparisons of the Licors. Firstly the differences in the early and late hours is smoother, partly because in this case the values range from 07:00 to 17:00, but also because the symmetry that was found in the previous case disappears. Instead there is a tendency to increase through the day in the cases of UVL and BAL. In fact we see the Licors of Valencia and Barcelona behaving differently from that of Valladolid.

The curves corresponding to UVL and BAL are smoother, as occurred when the Licors were compared amongst themselves, which could again confirm the possible influence of the fiber optic probe on the stability of the measurements through the day. On the other hand the values of MAD and RMSD of the VAL stay within a narrower margin over the length of the day than the values for the other two which tend to increase. This asymmetry around midday cannot be interpreted solely in terms of the cosine effect and must necessarily be due to other causes. One possible explanation could be found in the "temperature effect" which may be considered to be cumulative over the length of the day. We analyse this effect below when we consider the corrected values.

Table VI shows the relative values of the median of MBD, MAD and RMSD, corresponding to the comparisons of each of the Licors against the Optronic. As in the previous tables, in order to determine the differences only those values corresponding to optical air masses of less than 2 have been considered. The table shows that, although all the values could be considered as acceptable, those corresponding to VAL were

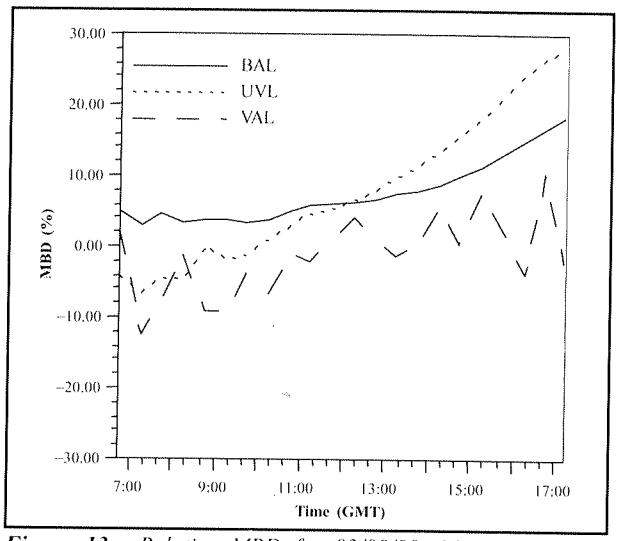

Figure 13a. *Relative MBD for 03/09/99. Measurements of horizontal global irradiance. Comparison Optronic-Licor. BAL: Barcelona Licor; UVL: Valencia Licor; VAL: Valladolid Licor.*

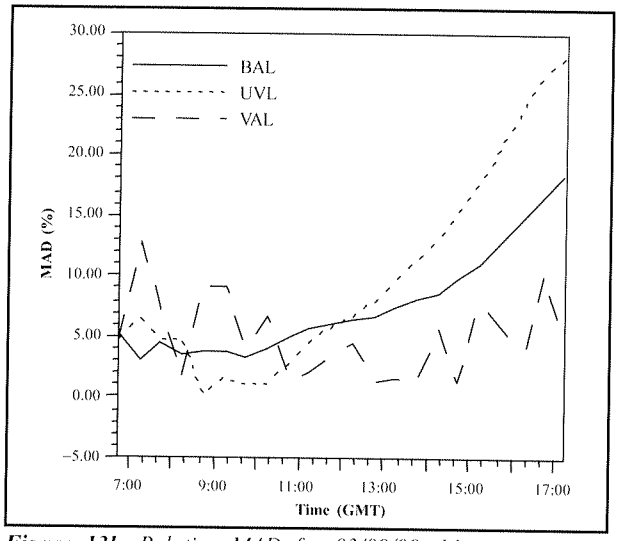

Figure 13b. *Relative MAD for 03/09/99. Measurements of horizontal global irradiance. Comparison Optronic-Licor. BAL: Barcelona Licor; UVL: Valencia Licor; VAL: Valladolid Licor.*

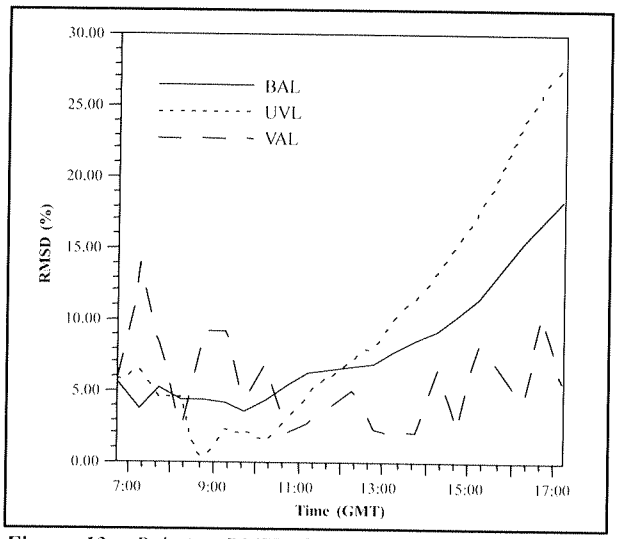

Figure 13c. *Relative RMSD for 03/09/99. Measurements of horizontal global irradiance. Comparison Optronic-Licor. BAL: Barcelona Licor; UVL: Valencia Licor; VAL: Valladolid Licor.*

significantly lower that those for UVL and BAL (about 30% lower). Furthermore, in the cases of these latter two instruments the differences were not uniform through the day, a fact that is not reflected in the table. If only the experimental values corresponding to the morning are considered (till 12:00 GMT) then the MAD (in %) is reduced to 3.8 for the BAL and to 4.5 for the UVL. This confirms that there is some time dependent external parameter that is not related to the solar altitude which influences the differences between these two instruments and the Optronic.

Table VI. *Measurements of horizontal global irradiance for 03/09/99. Comparison Optronic-Licor (uncorrected values). Median values.*

Licor	MBD (%)	MAD (%)	RSMD (%)
VAL	−1.1	4.2	4.9
UVL	3.6	6.6	6.7
BAL	5.5	6.1	6.5

b) In situ calibration of the Optronic 754

In section III.1.b) the spectral responses of each of the Licor against the reference lamp are shown (Figure 8) together with the corresponding calibration factors that have been used to correct the experimental data acquired by these spectroradiometers (Figure 10). A similar process was followed in the laboratory to characterise the Optronic 754. Figure 14 shows the spectral response, measured in the laboratory against the reference lamp, of the Optronic 754. In this case the average deviations of the three measurements was 0.4%. Figure 15 shows the correction factor obtained from these laboratory measurements.

As noted previously, the measurements made with the Optronic during the intercomparison in the UV range indicated that this instrument suffered a wavelength shift, close to 1 nm, because of the sensitivity of the spectroradiometer to temperature. Given that in the UV measurement range a wavelength step of 0.5 nm is used it is absolutely essential to correct for this wavelength shift to avoid introducing serious errors in the comparison. In the UV range the algorithm of Slaper et al (1995) was used with a reference spectrum for extraterrestrial spectral irradiance obtained from the SUSIM instrument (Van Hoosier et al., 1988).

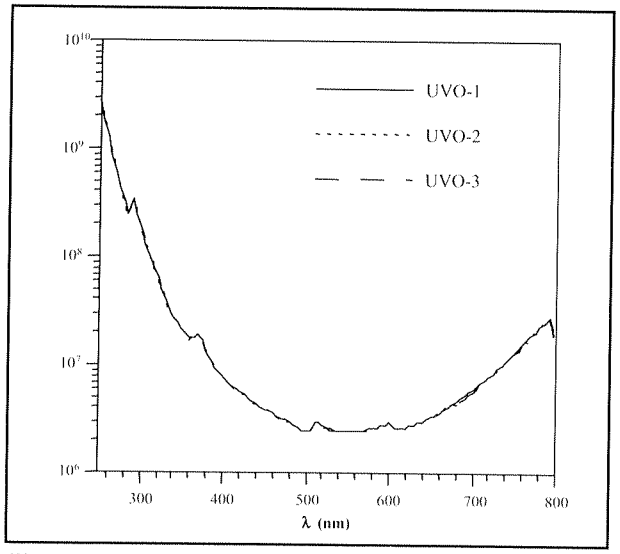

Figure 14. *Spectral response, measured in laboratory against reference lamp, of the Optronic 754.*

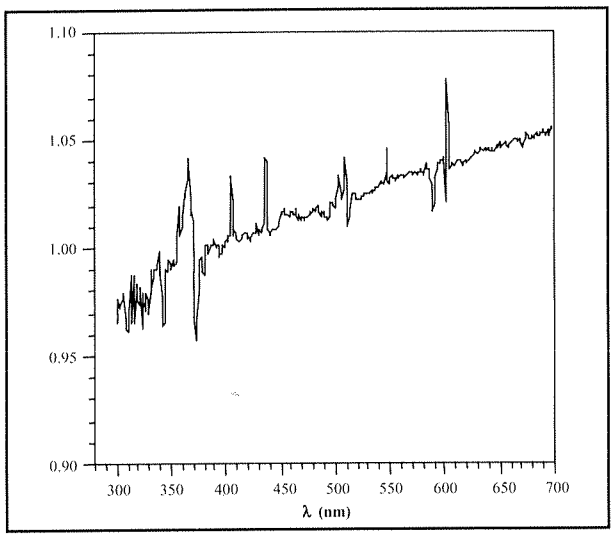

Figure 15. *Correction factor for the Optronic 754 obtained from the reference lamp used in the intercomparison.*

In order to determine whether a correction of this sort was needed in the visible range the method for wavelength shift determination proposed by Slaper was used, analysing the evolution over the length of the day of the $R_M(\lambda)$ factor in the visible interval. The $R_M(\lambda)$ factor is defined as the ratio of measurements at wavelength λ with two close neighbouring wavelengths. In Figure 16 (a and b), by way of example, the values of this parameter are shown for two measurement series, taken with a time difference of more than 7 hours, in the UV (16a) and the visible (16b). As can be seen this parameter has considerably higher values in the UV than in the visible range. The comparison of these values with the ratio of extraterrestrial measurement at wavelength λ with two close neighbouring wavelengths, $R_M(\lambda+\delta)$, showed that in the visible range the wavelength shift never reached 1 nm. Given that the measurements of the Optronic were made in this spectral interval with a wavelength step of 1 nm, and that the resolution of the Licor is very much less than this value, it was considered unnecessary to introduce this correction when comparing the Optronic measurements with those of the Licor.

a) Corrected experimental values following in situ calibration

Using the calibration factors of the Licors (Figure 10) and the Optronic (Figure 15) the experimental values were corrected and the analysis of the previous section III.2.a) was repeated. In figure 17 (a-c), as for figure 13, the daily evolution of the relative average values of MBD, MAD and RMSD obtained from the corrected experimental data can be seen for 03/09/99. Table VII shows the values of the median for these three parameters for each of the instruments compared with the Optronic. The values in this table were calculated, as in the previous cases, using only the experimental data corresponding to solar altitudes of greater than 30°.

Table VII. *Measurement of horizontal global irradiance on 03/09/99. Comparison Optronic-Licors (corrected values). Median values.*

Licor	MBD (%)	MAD (%)	RSMD (%)
VAL	1.2	4.0	5.1
UVL	4.1	7.1	7.0
BAL	3.3	3.8	4.1

As can be seen in figure 17, apart from the variations in the measurements of the VAL already noted in the sections above, the asymmetry between the morning and afternoon remains for the UVL and BAL, although overall the results for the latter instrument improve considerably with respect to the uncorrected data. All this appears to indicate that in these spectroradiometers, and particularly in the one from Valencia, in addition to the cosine effect, already detected during the intercomparison of the Licors, there is another effect that has not been taken into account so far. In our opinion this effect, temporal and asymmetric, has to be a consequence of the effect of temperature on the Licors and the Optronic, although in this case it ought to effect the VAL also. One possible explanation of why this effect is much less noticeable in the Valladolid instrument could be the following. As has already been noted, on 03/09/99 and 04/09/99 the UVL and BAL Licors operated automatically, exposed to the sun throughout the day on their tripod mountings. The VAL Licor was operated manually with a fiber optic probe. The VAL remote cosine sensor was located on a tripod whilst the Licor itself remained at ground level.

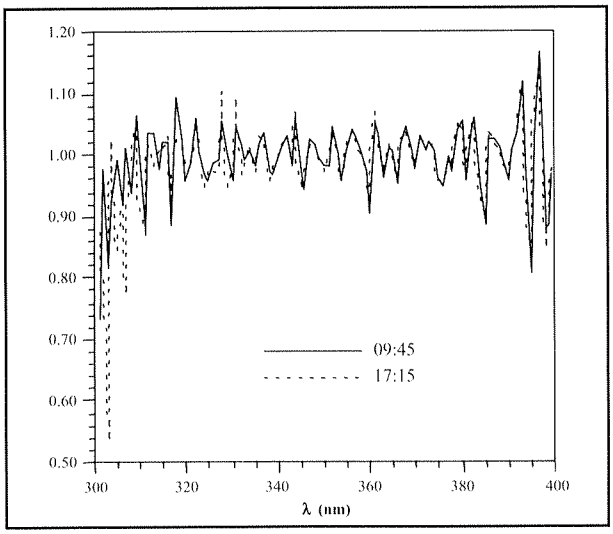

Figure 16a. *Values of the radio of measurements at wavelength λ, $R_M(\lambda)$, in the UV range. Optronic 754. 03/09/99.*

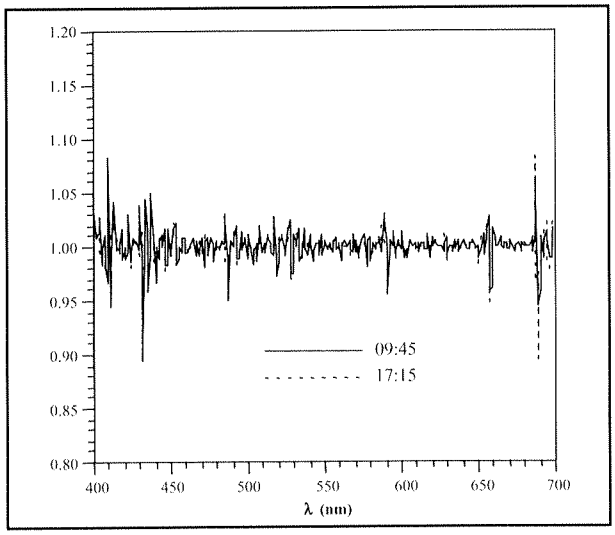

Figure 16b. *Values of the radio of measurements at wavelength λ, $R_M(\lambda)$, in the Visible range. Optronic 754. 03/09/99.*

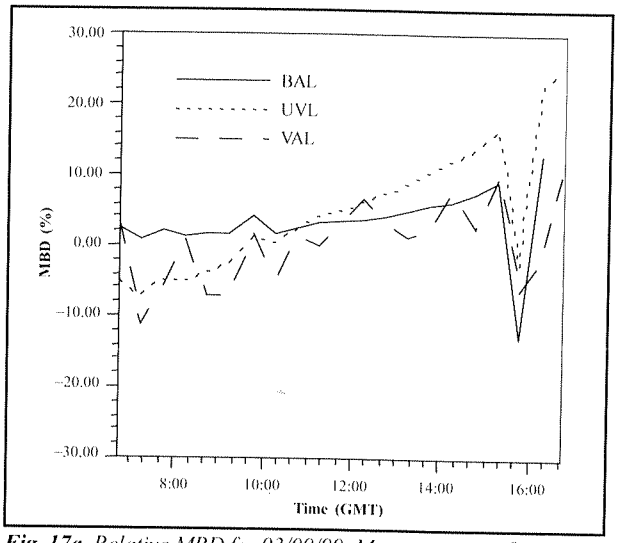

Fig. 17a. Relative MBD for 03/09/99. Measurements of corrected horizontal global irradiance. Comparison Optronic-Licor. BAL: Barcelona Licor; UVL: Valencia Licor; VAL: Valladolid Licor.

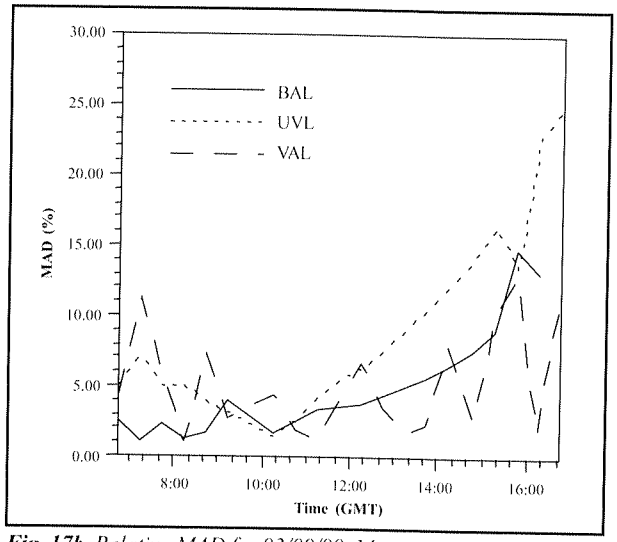

Fig. 17b. Relative MAD for 03/09/99. Measurements of corrected horizontal global irradiance. Comparison Optronic-Licor. BAL: Barcelona Licor; UVL: Valencia Licor; VAL: Valladolid Licor.

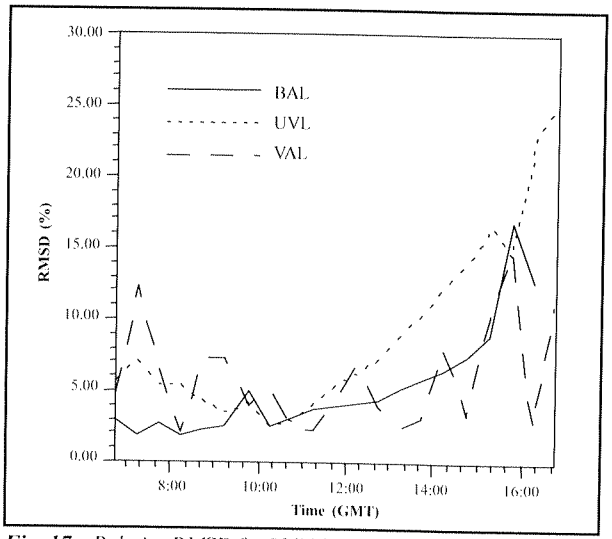

Fig. 17c. Relative RMSD for 03/09/99. Measurements of corrected horizontal global irradiance. Comparison Optronic-Licor. BAL: Barcelona Licor; UVL: Valencia Licor; VAL: Valladolid Licor.

The operational procedure consisted of the acquisition of the direct and global measurements alternately. This meant the presence of at least one, and for much of the time, two operators from the University of Valladolid standing close to the Licor to handle the remote cosine sensor. In this way although the VAL was not expressly protected from the Sun's rays it is very likely that during some of the time it was in shadow. Thus the use of the fiber optic probe had two effects: on the one hand it introduced variations in the MAD of up to 7% between consecutive measurements, but on the other hand, given the method of operation of the instrument during the campaign, it could have favoured the protection of the detector from the temperature effect.

7.4. RESULTS FOR DIRECT IRRADIANCE

The measurements of direct irradiance were only made in the afternoon of a single day, 07/09/99. Although the VAL measured direct irradiance during all the days of the intercomparison exercise, simultaneously with the measurements of global irradiance, the UVL and the Optronic 754 only measured direct irradiance on this day. The BAL registered only measurements of global irradiance throughout the campaign, and no other instrument present during the intercomparison registered measurements of direct irradiance in the visible range. Therefore the results analysed in this section refer only to the UVL, VAL and UVO.

It is important to point out that the measurements of direct irradiance were affected by an additional factor leading to inaccuracies: the fact that the different instruments used radiance limiters that have different FOVs. The FOV of the VAL is 4.2°, that of the UVL is 4.7° whilst that of the Optronic is 5.7°. Furthermore, for direct measurements all spectro-radiometers were positioned manually, though this pointing accuracy was not quantified. These circumstances lead us to consider the results set out in this section as merely orientative, pending clarification in a future intercomparison campaign.

An important difference with respect to the measurements of global irradiance is that in this case, and given the effect that temperature had on the Optronic was then known (a first analysis of the intercomparison of the measurements in the UV was available), an attempt was made to protect the instruments as far as possible from direct exposure to the Sun's rays. During the whole measurement period the UVL and the UVO were protected with reflecting plastic. Furthermore, and since their operation was manual in this case, they were kept in the shade between measurements. The results suggest that these protective strategies were sufficient to limit in the main the temperature effect.

The procedure followed to analyse the results was the same as described previously for the horizontal global irradiance. The only difference is that in this case all the available measurements were used, without the limitation related to the solar altitude, since the cosine effect is irrelevant when measuring direct irradiance. We present first the comparison of the two Licors and then the results of the comparison of these instruments with the Optronic. Similarly to the case of global irradiance the results obtained from the uncorrected data are analysed separately from those obtained after correcting for the calibration factors obtained in the laboratory against a reference lamp.

7.4.1. Intercomparison of the Licor 1800s

a) Uncorrected experimental values

Figure 18 shows, as an example, the spectral values of MBD (%) and MAD (%) at 14:30 GMT calculated from the

uncorrected values. It can be seen that the values are quite uniform except in the UV zone where the precision of these instruments is less. The peaks in the rest of the range coincide with the limits of the filter wheels of these instruments. As for the case of global irradiance, we have only analysed the values corresponding to the interval 400-700 nm. Table VIII presents the maximum and minimum values as well as the average and the median of MBD, MAD and RMSD parameters. The calculations were made based on the spectral difference UVL-VAL, so the negative values of MBD indicate that the values registered for the VAL were systematically greater than those registered for the UVL. This result appears to contradict the fact that the FOV of the collimator of the VAL is slightly larger than that of the UVL. Nevertheless the differences are of the same order as the accuracies that are usually assigned to these instruments in the visible range (5%). In some cases they are less than those found for measurements of global irradiance, despite the differences in the FOVs. This allows us to affirm, with the caveat given at the start of this section, that the Licors are adequate instruments for measuring direct solar irradiance, and the results that they give are comparable, even when the optics of the receiver and the FOV of the collimator are different.

Table VIII. *Measurements of direct irradiance on 07/09/99. Comparison UVL-VAL (uncorrected values). Median values.*

	MBD (%)	MAD (%)	RSMD (%)
Minimum	−8.8	1.6	1.6
Maximum	−1.6	8.8	8.9
Mean	−4.9	4.9	5.3
Median	−5.1	5.1	5.4

b) Corrected experimental measurements following in situ calibration

In this case we just present a summary table of the results which were obtained in a similar way to those shown in Table VIII. The results summarise in Table IX show a reduction of nearly 50% with respect to the uncorrected values, with the average RMSD of the order of 3% for the entire visible range, which is the most used by the Licor. It can also be seen that on average the value of MBD is positive, indicating that the values registered by the UVL were greater than those for the VAL. This is a more logical result than the previous one since the collimator of the UVL has a larger FOV and a greater contribution from the circumsolar irradiance would be expected.

Table IX. *Corrected measurements of direct irradiance on 07/09/99. Comparison UVL-VAL (uncorrected values). Median values.*

	MBD (%)	MAD (%)	RSMD (%)
Minimum	17.8	1.1	1.6
Maximum	36.3	6.0	6.3
Mean	29.3	2.3	3.0
Median	28.8	2.4	3.0

Figure 19 shows the evolution over the measurement period of the relative average values of MAD and RMSD obtained from the uncorrected and corrected experimental data. It can be seen that the values remain quite stable except for the measurements made between 14:00 and 15:00 GMT. This could be due either to the incorrect alignment of one of the Licors or the presence of high cloud bands.

7.4.2. Comparison of the Licor 1800s with the Optronic 754

a) Uncorrected experimental values

Figure 20 (a-c) presents the evolution of the relative average values of MBD, MAD and RMSD, corresponding to the comparison of the two Licors and the Optronic, obtained always from the spectral differences Optronic-Licor. In the representation of the MBD it can be clearly observed how the UVL data overestimated those of the Optronic whilst those of VAL underestimated them. The differences between the values given by the three instruments are practically constant except around 14:00 to 14:30 GMT at which time there appeared a pronounced peak with no obvious explanation. This peak was also apparent when the two Licors were compared. Table X gives the median values of MBD, MAD and RMSD of the two Licors in comparison with the Optronic. A very good agreement is seen in both cases, exceptionally so for the UVL.

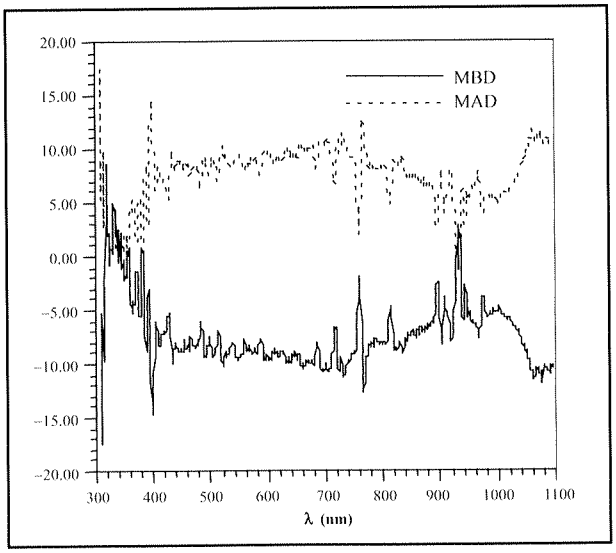

Fig. 18. *Relative MAD and MBD for 14:00 GMT on 07/09/99. Measurements of direct irradiance. Comparison UVL-VAL.*

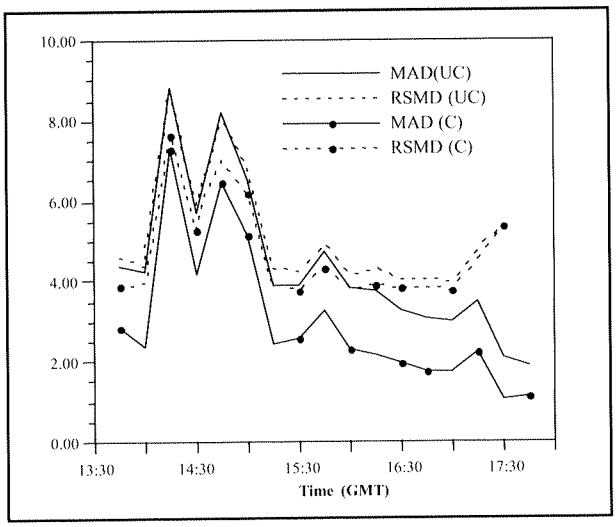

Fig. 19. *Relative MAD and RSMD for 07/09/99. Measurements of direct irradiance. Comparison Licor-Licor. (UC) Uncorrected values. (C) Corrected values.*

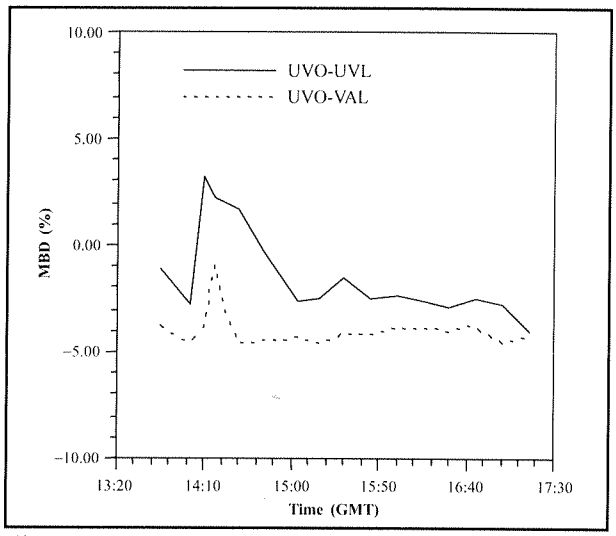

Figure 20a. *Relative MBD for 07/09/99. Uncorrected values of direct irradiance. Comparison Optronic-Licor. UVL: Valencia Licor; VAL: Valladolid Licor.*

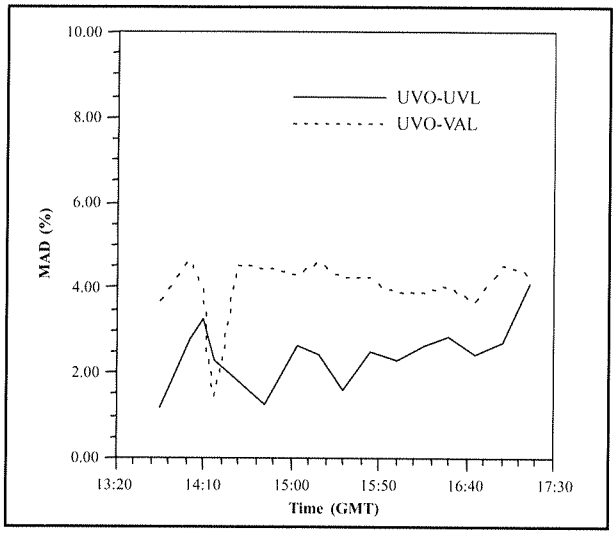

Figure 20b. *Relative MAD for 07/09/99. Uncorrected values of direct irradiance. Comparison Optronic-Licor. UVL: Valencia Licor; VAL: Valladolid Licor.*

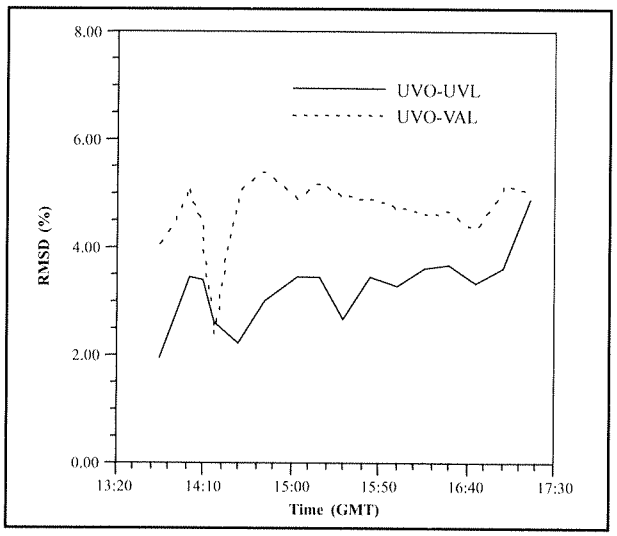

Figure 20c. *Relative RMSD for 07/09/99. Uncorrected values of direct irradiance. Comparison Optronic-Licor. UVL: Valencia Licor; VAL: Valladolid Licor.*

Table X. *Measurements of direct irradiance for 07/09/99. Comparison Optronic-Licors (uncorrected values). Median values.*

Licor	MBD (%)	MAD (%)	RSMD (%)
VAL	−3.2	5.2	4.1
UVL	1.3	1.6	2.2

b) Corrected experimental values following in situ calibration

Figure 21 presents the daily evolution of the relative average values of MBD, MAD and RMSD corresponding to the comparison of the corrected experimental values of the two Licors with the Optronic. Table XI shows the average daily values of MBD, MAD and RMSD. All the differences, as for the case of the uncorrected values, are of the same order or less than the instruments' accuracies, so it is not possible to draw valid conclusions with respect to one or the other instrument. However it is interesting to note that the drift in time of the value of the differences, observed in the measurements of global irradiance, is not seen in the direct irradiance. This allows us to reaffirm our hypothesis that they were due to the temperature effect and that they were not seen in this case because of the protective measures taken. Furthermore, the variations in time in form of a sawtooth that appeared in the global irradiance measurements from the VAL do not appear either, which seems to confirm that they could have been caused by horizontal alignment errors of the remote cosine sensor.

Table XI. *Measurements of direct irradiance for 07/09/99. Comparison Optronic-Licors (corrected values). Median values.*

Licor	MBD (%)	MAD (%)	RSMD (%)
VAL	−1.1	1.6	3.1
UVL	1.0	1.9	3.1

7.5. CONCLUSIONS

We have analysed the results obtained from the measurements of solar irradiance (global and direct) in the visible range (400-700 nm), registered during the first Iberian UV-VIS instruments intercomparison, which took place from 31 August to 10 September 1999 in the Centro de Experimentación de El Arenosillo (CEDEA) of the Instituto Nacional de Técnica Aeroespacial (INTA). The instruments used were three Licor 1800 spectroradiometers; RS-312 (Universitat de Barcelona, BAL), RS-415 (Universitat de Valencia, UVL) and RS-487 (Universidad de Valladolid, VAL), and one Optronic 754 spectroradiometer; 98202085 (Universitat de Valencia, UVO). On 3 and 4 September 1999 measurements were made of global solar irradiance on a horizontal plane every 15 minutes from 06:30 till 17:45 GMT. On the afternoon of 7 September direct solar irradiance at normal incidence was measured using the UVL and VAL Licors and the Optronic. To compare the series of spectral data relative values of MBD, MAD and RMSD were used.

The results of the analysis of the measurements of global irradiance showed that the Licor measurement suffered significant distortions at the beginning and end of the day due to the cosine effect. This forced us to limit the analysis to the measurements corresponding to solar altitudes of higher than 30°. For this range, the results of the intercomparison between the Licor instruments, before their in situ calibration, showed differences that were within the overall error margins expected for these instruments (5% in the visible range) and that were greater when one of the instruments was the VAL. We think

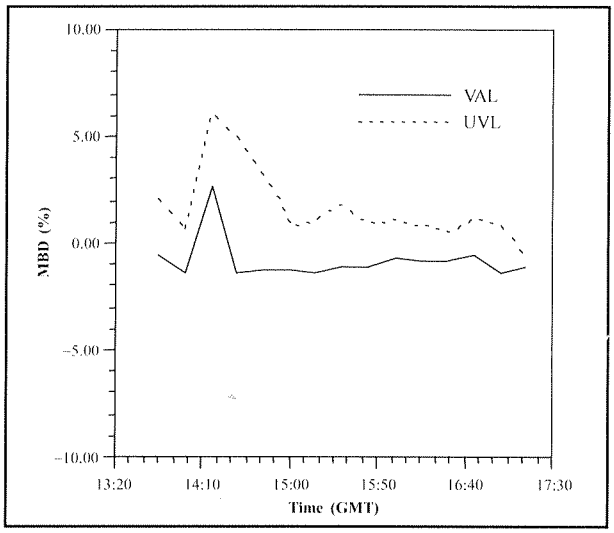

Figure 21a. *Relative MBD for 07/09/99. Corrected values of direct irradiance. Comparison Optronic-Licor. UVL: Valencia Licor; VAL: Valladolid Licor.*

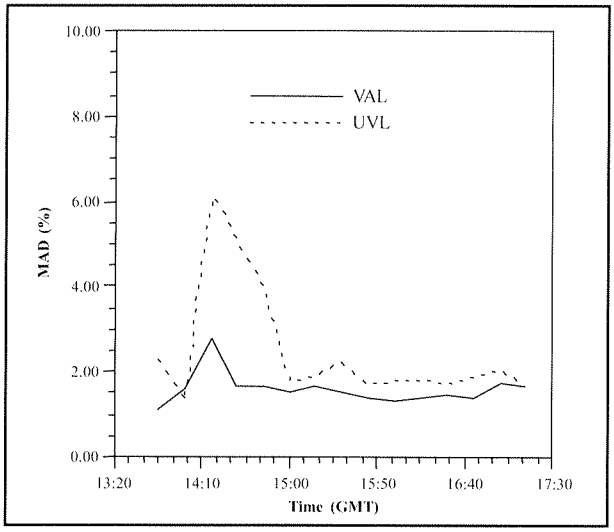

Figure 21b. *Relative MAD for 07/09/99. Corrected measurements of direct irradiance. Comparison Optronic-Licor. UVL: Valencia Licor; VAL: Valladolid Licor.*

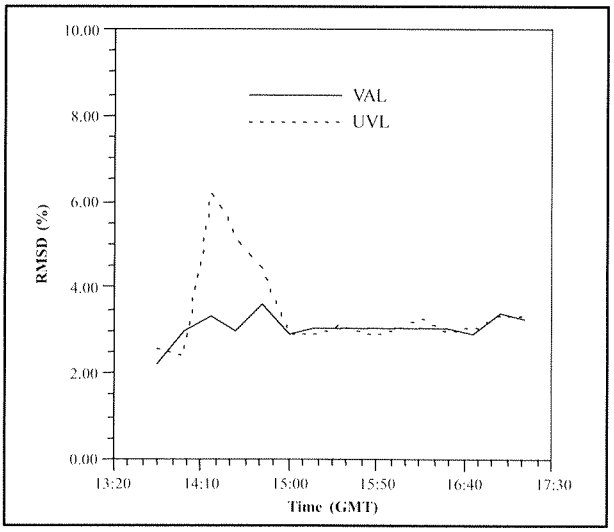

Figure 21c. *Relative RMSD for 07/09/99. Corrected measurements of direct irradiance. Comparison Optronic-Licor. UVL: Valencia Licor; VAL: Valladolid Licor.*

that the greater discrepancy between this and the other two instruments could be due to a combination of the use of the fiber optic probe and the manual operation of the instrument.

Once the calibration factors obtained against a reference lamp had been applied, the results related to the VAL improved noticeably, to around 3%, whilst those of the BAL-UVL remained practically unchanged. These results could be related to the procedure used during the laboratory calibration because the Teflon diffuser has a curved geometry which could lead to significant uncertainty in the calibration factor.

The comparison between the Licors and the Optronic, using uncorrected data from in situ calibration, showed an asymmetry between the morning and afternoon results for the BAL and UVL, possibly due to the temperature effect. The results with the VAL were noticeably better, perhaps due to differences in the measurement procedure. Although the VAL continued to show the variations noted previously the average difference was less. Once the calibration factors obtained from the reference lamp were applied the results from the BAL improved significantly whilst those of the UVL and VAL remained practically unchanged. This suggests that the UVL is subject to a temperature effect similar to the Optronic, but so far this effect has not been quantified.

During the measurements of direct irradiance an attempt was made to protect the UVL and UVO instruments from direct exposure to the Sun's rays. The results indicate that the measures taken were sufficient to remove the temperature effect. The results of the analysis of the measurements of direct irradiance showed that, even when considering uncorrected data, the differences between the Licors were of the order of the accuracy of these instruments in the visible range (5%). When correction factors are considered the differences reduced to 3%. The comparisons with the Optronic gave figures of 5% for the VAL and 2% for the UVL, for uncorrected data. After correcting the data the average differences were less than 2% in both cases. These results could be considered as exceptional given that the instruments are each mounted with collimators with different FOVs and each has different optics in the receiver. In our opinion these results justify the use of the Licors for the acquisition of highly reliable measurements of direct irradiance in the visible range.

Although they are ideal for acquiring direct irradiance measurements they suffer a number of problems when measuring global irradiance which should be taken into account. For solar altitudes of less than 30° the deviations caused by the cosine effect can invalidate the measurements. A detailed laboratory studied of each instrument is required to quantify this effect. It would also be useful to quantify how much the temperature affects these instruments, especially the Licor of the Universitat de Valencia.

ACKNOWLEDGEMENTS

This work was financed by the Spanish CICYT, through the CLI97-0345-C05-04 project. We would like to thank the colaboration of the members of all the participating groups in the intercomparison campaign, particularly to J. Lorente and V. Cachorro who provided the data of the Licors from Barcelona and Valladolid respectively, and to A. Redondas, of the INM at Izaña, who were responsible for the intercomparison in the UV range, that initially determined the drift of the Optronic with temperature. We would also like to show our thanks to J. P. Díaz of the Universidad de La Laguna and to R. Vergaz of the Universidad de Valladolid, for the useful discussions related to various aspects of this work. Finally we want to thank B. de la Morena for all the facilities put at our disposal in the El Arenosillo installations and to thank L. Sánchez-Muniosguren for being able to coordinate a project that would have seemed impossible only a few years ago.

APPENDIX

To analyse the solar radiation data in the visible waveband three statistical indicators were used: MBD (Mean Bias Difference), MAD (Mean Absolute Difference) and RMSD (Root Mean Square Difference). These figures are quoted in either absolute or relative values. The expressions for each are the following:

Absolute values:

$$\mathrm{MBD} = \frac{\sum_{i=1}^{N} [(measured\_licor_1)_{\lambda i} - (measured\_licor_2)_{\lambda i}]}{N}$$

$$\mathrm{MAD} = \frac{\sum_{i=1}^{N} |(measured\_licor_1)_{\lambda i} - (measured\_licor_2)_{\lambda i}|}{N}$$

$$\mathrm{RMSD} = \sqrt{\frac{\sum_{i=1}^{N} [(measured\_licor_1)_{\lambda i} - (measured\_licor_2)_{\lambda i}]^2}{N}}$$

Relative values (in %):

$$\mathrm{MBD}\ (\%) = \frac{\sum_{i=1}^{N} [(measured\_licor_1)_{\lambda i} - (measured\_licor_2)_{\lambda i}]}{(measured\_licor)_m}$$

$$\mathrm{MAD}\ (\%) = \frac{\sum_{i=1}^{N} |(measured\_licor_1)_{\lambda i} - (measured\_licor_2)_{\lambda i}|}{(measured\_licor)_m}$$

$$\mathrm{RMSD}\ (\%) = \sqrt{\sum_{i=1}^{N} \left(\frac{(measured\_licor_1)_{\lambda i} - (measured\_licor_2)_{\lambda i}}{(measured\_licor)_{m\lambda i}} \right)^2}$$

REFERENCES

Bernhard, G. and G. Sheckmeyer (1997): "New entrance optics for solar spectral UV measurements", *Photochem. Photobiol.*, **65**, 923-930.

Cachorro, V. E., M. P. Utrillas, V. Vergaz, P. Durán, A. De Frutos and J. A. Martínez-Lozano (1998): "Determination of the atmospheric-water-vapour content in the 940-nm absorption band by use of moderate spectral-resolution measurements of direct solar irradiance", *Appl. Opt.*, **37**, 4678-4689.

Gardiner, B. G. and P. J. Kirsch (1995): "Setting standards for European ultraviolet spectroradiometers". European Commission. Air pollution research report 53. Luxembourg.

Van Hoosier, M. E., J. D. F. Bantee, G. E. Braeckner and D. K. Prinz (1988): "Absolute solar spectral irradiance 120-400 nm results from the SUSIM experiment on board Spacelab-2", *Astrophys. Lett. Comm.*, **27**, 163-168.

Kiedron, P. W., J. J. Michalsky, J. L. Berndt and L. C. Harrison (1999): "Comparison of spectral irradiance standards used to calibrate shortwave radiometers and spectroradiometers", *Appl. Opt.*, **38**, 2432-2439.

Lorente, J., A. Redaño and X. De Cabo (1994): "Influence of urban aerosol on spectral solar irradiance", *J. Appl. Meteorol.*, **33**, 406-414.

Nann, S. and C. Riordan (1991): "Solar spectral irradiance under clear and cloudy skies: measurements and a semiempirical model", *J. Appl. Meteorol.*, **30**, 447-462.

Riordan, C., D. Myers, M. Rymes, M. Hulstrom, W. Marion, C. Jennings and C. Whitaker (1989): "Spectral solar radiation data base at SERI", *Solar Energy*, **42**, 67-79.

Riordan, C., D. Myers and R. L. Hulstrom (1990): "Spectral solar radiation data base documentation", SERI/TR-215-3513A, Golden, CO.

Seckmeyer, G. et al. (more than 20 authors) (1998): "The 1997 status of solar UV spectroradiometry in Germany: Results from the national intercomparison of UV spectrradiometers". Garmish-Partenkirchen, Germany. Shaker-Verlag, AAchen.

Slaper, H. (1997): "Methods for intercomparing instruments", Advances in solar ultraviolet spectroradiometry, 155-164. European Commission. Air pollution research report 63. Luxembourg.

Slaper, H., H. A. J. M. Reinen, M. Blumthaler, M. Huber and F. Kuik (1995): "Comparing ground level spectrally resolved solar UV measurements using various instruments: A technique resolving effects of wavelength shift and slit width", *Geophys. Res. Lett.*, **22**, 2721-2724.

Webb, A. R. (1997): "Advances in solar ultraviolet spectroradiometry", European Commission. Air pollution research report 63. Luxembourg.

CHAPTER 8

TOTAL OZONE INTERCOMPARISON OF BREWER SPECTROPHOTOMETERS AND OTHER INSTRUMENTS

E. Cuevas[1], K. Lamb[2], A. Redondas[1], C. Torres[1], V. Carreño[1], J. Gröbner[3], J. P. Díaz[4] and J. M. Vilaplana[5]

[1] Observatorio Atmosférico de Izaña, Instituto Nacional de Meteorología. C/ La Marina, 20; 38071 Santa Cruz de Tenerife, Spain, *ecuevas@inm.es*.

[2] International Ozone Services (IOS), Toronto, Canada.

[3] Institute for Health and Consumer Protection (IHCP), Joint Research Centre, Ispra, Varese, Italy.

[4] Departamento de Física Básica, Universidad de La Laguna (ULL), Tenerife, Spain.

[5] Estación de Sondeos Atmosféricos "El Arenosillo", INTA/División de Ciencias del Espacio, Huelva, Spain.

SUMMARY

During the First National Spectroradiometer Intercomparirison Campaign that was held in the "El Arenosillo" station (Huelva), managed by the Instituto Nacional de Técnica Aeroespacial (INTA) in September 1999, a total ozone intercomparison of the Brewer spectrophotometers #033, #070, #117, #150, #151 and #157 was performed. These instruments form the national Brewer network of the Instituto Nacional de Meteorología (INM). The total column ozone values obtained through direct sun (DS) measurements have been intercompared with those obtained with the traveling reference instrument Brewer#017 from the "International Ozone Services" (IOS), Toronto-Canada. This instrument was, in turn, calibrated against the triad of Brewer spectrophotometer (international world reference of Brewer instruments) located at the Meteorological Service of Canada (former AES) in Toronto, before and after the "El Arenosillo" intercomparison. Total ozone has also been determined with the Brewer spectrophotometers using global spectral UV measurements and the UQ routine. During this campaign total ozone was determined with the Bentham DM150 from La Laguna University (ULL), with the multichannel moderate bandwidth filter radiometer NILU-UV6#010 from INM-Izaña, with a Microtops-II portable filter sunphotometer from INM-Izaña and with the Dobson Spectrophotometer #120 located at the "El Arenosillo" station (INTA). In this chapter the results obtained with all these instruments and the corresponding relative differences against the Brewer#017 (IOS) are shown and discussed.

RESUMEN

Durante la Primera Campaña Nacional de Intercomparación de Espectrorradiometros que tuvo lugar en la estación de "El Arenosillo"(Huelva), del Instituto Nacional de Técnica Aeroespacial (INTA) en septiembre de 1999, se llevó a cabo una intercomparación de ozono total de los espectrofotómetros Brewer #033, #070, #117, #150, #151 y #157 que conforman la red nacional Brewer del Instituto Nacional de Meteología (INM). Las medidas de ozono total realizadas mediante medidas directas al sol con los Brewer fueron comparadas frente al instrumento de referencia Brewer#017 de "International Ozone Services" (IOS), Toronto-Canadá, que fue calibrado frente a la triada de espectrofotómetros Brewer del Servicio Meteorológico de Canadá (antiguamente AES) en Toronto, antes y después de esta intercomparación. Se determinó también ozono total con los espectrofotómetros Brewer a partir de las medidas de radiación UV espectral global mediante la rutina UQ. Durante la campaña se tuvo la oportunidad de medir ozono total en columna con el espectroradiómetro Bentham DM150 de la Universidad de La Laguna (ULL), con el radiómetro multicanal de ancho de banda moderada NILU-UV6 #010 del INM-Izaña, con un fotómetro de filtros portátil Microtops-II del INM-Izaña y con el espectrofotómetro Dobson #120 de la estación de "El Arenosillo" (INTA). En este capítulo se muestran y discuten todos los resultados obtenidos con estos instrumentos y las diferencias registradas frente al Brewer#017 (IOS).

8.1. INTRODUCTION: BACKGROUND AND GENERAL CONSIDERATIONS

This intercomparison, performed at the *"El Arenosillo"* station (Huelva, Southwestern Spain), managed by the Instituto Nacional de Técnica Aeroespacial (INTA), has been the first national intercomparison campaign of sun spectroradiometers. However, the Izaña Observatory (Instituto Nacional de Meteorología, INM, Spain) hosted four international UV and ozone instrument intercomparisons in previous years:

"The Nordic Intercomparison of ultraviolet and total ozone instruments" (NOGIC-93 campaign) was held at the Izaña Observatory from October 25 to November 5, 1993. The Nordic Ministry Council and the INM financed this. Thirteen Spectroradiometers and eight filter-radiometers were intercompared (*Koskela*, editor, 1994).

"The 12th WMO ozone commission Dobson calibration and intercomparison", financed by the World Meteorological Organization (WMO), the National Oceanic and Atmospheric Administration (NOAA-USA) and the INM was held at the Izaña Observatory on June 14-30, 1994. Dobson instruments from Argentina, Peru, Brazil, USA, Portugal, Spain and Germany were used in that campaign, as were the reference Brewer#017 (Canada), a SAOZ from the CNRS (France), two M-183 from Russia and Cuba, respectively, and the Brewer#033 (INM).

The CASCUM-95 campaign financed by the European Commission was held at the Izaña Observatory on July 12-20, 1995. Spectroradiometers from Austria, Great Britain, Greece and Spain were intercompared in this campaign.

In the NOGIC-96 campaign, seventeen UV spectro-radiometers and nine UV filter-radiometers from Finland,

Sweden, Norway, Denmark, Iceland, Canada, Greece, Holland, Estonia and Spain were intercompared at the Izaña Observatory on October, 8-21, 1996. This intercomparison was financed by the Nordic Ministry Council and the INM. Results of the campaign can be found in *Kjeldstad et al.* (ed.) (1997).

INM operates a national Brewer spectrophotometer network (Figure 1), partially financed by the National R+D Plan of the Ministry of Science and Technology. The Brewer at the *"El Arenosillo"* station, financed by the Andalusian Regional Government, is managed by INTA. This network provides total ozone and spectral UV that is monitored real-time through the INM's intranet. The information is stored and validated in a centralized database.

Total ozone daily means are submitted daily to the WMO Northern Hemisphere Daily Ozone Mapping Centre run by the Laboratory of Atmospheric Physics at the Aristotle University of Thessaloniki (Greece) and to the WOUDC (World Ozone and UV Data Center, Toronto-Canada).

Evaluated and refined total ozone data from the Madrid, Murcia and Izaña stations are periodically submitted to the WOUDC database. The Brewers (#033 and #157) at the Izaña Observatory have been intercompared with the international traveling reference Brewer#017 every year since 1991.

Since November 1999 the Brewer network has performed a common measurement schedule (ozone and spectral UV) on a daily basis. This information is stored in the centralized INM database.

To have an idea of the total column ozone content (DU) over the Iberian Peninsula during the *"El Arenosillo"* intercomparison campaign (from Day 244 to Day 251), daily ozone plots from the TOMS (Total Ozone Mapping Spectrometer) are shown in Figure 2. On September 1, 4 and 5 very high ozone values can be seen to the west of Portugal, coincident with the low pressure observed at high levels (700 hPa and 500 hPa) in this position (*Cuevas et al.*, this Report, Chapter 3, 2003). High ozone is found north-west of Iberian Peninsula, moving just as the low pressure does. The high ozone is the result of a sinking of the tropopause associated to the cut-off-low development. On September 3 a sharp ozone gradient is observed just over the *"El Arenosillo"* station produced by a jet stream found at about 250 hPa (*Cuevas et al.*, this Report, Chapter 3, 2003). Total ozone values over the *"El Arenosillo"* station are significantly lower on September 7 and 8 compared to those observed on previous days.

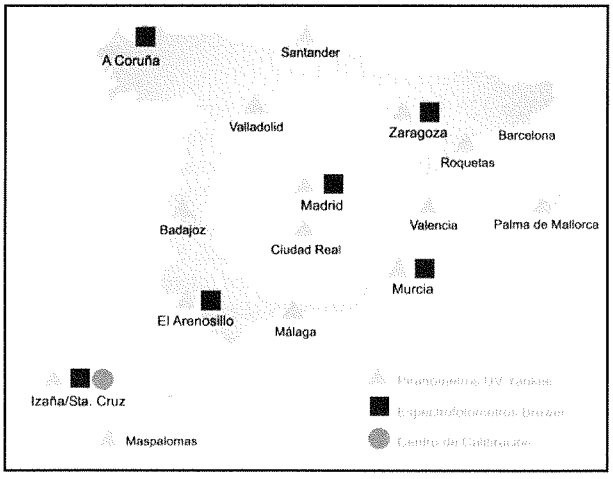

Figure 1. *National UV broadband radiometer and Brewer spectrophotometer network.*

8.2. MATERIAL AND METHODS

Instruments

At the *"El Arenosillo"* total ozone intercomparison the instruments indicated in Table 1 participated. There were a total of eight Brewer Spectrophotometers (two of them double monochromators, #150 and #157), one Dobson, one Bentham DM150 Spectroradiometer and two filter-radiometers.

Table 1. *Instruments that participated in the total ozone intercomparison at the "El Arenosillo" campaign.*

Instrument	Station	Location	Type	Institution
Brewer#017	World travelling reference	——	MK-II	IOS Canada
Brewer#033	Zaragoza	42°N, 1°W	MK-II	INM
Brewer#047*	Azores	39°N, 27°W	MK-II	IM Portugal
Brewer#070	Madrid	40°N, 4°W	MK-IV	INM
Brewer#117	Murcia	38°N, 1°W	MK-IV	INM
Brewer#150	*"El Arenosillo"*	37°N, 6.44°W	MK-III	INTA
Brewer#151	A Coruña	43°N, 8°W	MK-IV	INM
Brewer#157	Izaña	28°N, 16°W	MK-III	INM
Dobson#120	*"El Arenosillo"*	37°N, 6.44°W	——	INTA
Bentham DM150	Tenerife	28°N, 16°W	——	ULL
NILU-UV6 #010	Tenerife Antarctica	28°N, 16°W 78°S, 34.6°W	6-Ch.	INM
Microtops-II	Tenerife	28°N, 16°W	5-Ch.	INM

* *Due to technical problems this Brewer did not participate in the ozone intercomparison.*

Methods

The ozone intercomparison took place in the period 1-8 September 1999 (natural days 244-251) at the *"El Arenosillo"* station (Huelva, 37°N, 6.44°W) managed by INTA. During the intercomparison the Brewer owners (INM and INTA) had hired with International Ozone Services Inc. (IOS) to perform servicing and calibration checks. This calibration was performed by Ken Lamb and Julian Gröbner, and all the Brewers were compared against the travelling standard Brewer#017.

The Brewer#017 obtained 375 good ozone measurements, as well as timed simultaneous UV scans on each half hour over the eight days. The daily mean total ozone results of Brewer#017 for this period are in Table 2, which will be used as reference ozone data in the intercomparison.

Table 2. *Total ozone daily means obtained by the travelling reference Brewer#017 during the campaign.*

Day	Total ozone (DU)	SD	SO_2 mm-atm	SD	#of good obs.	#of total obs.
244	309.8	4.0	−0.3	0.6	34	69
245	301.4	1.7	0.0	0.3	55	72
246	308.8	3.1	0.5	0.5	38	55
247	316.8	2.7	−0.1	0.4	48	84
248	316.2	3.9	−0.1	0.6	64	81
249	325.4	2.7	0.0	0.4	68	81
250	310.8	4.1	0.3	0.7	52	68
251	302.9	0.9	0.0	0.4	36	47

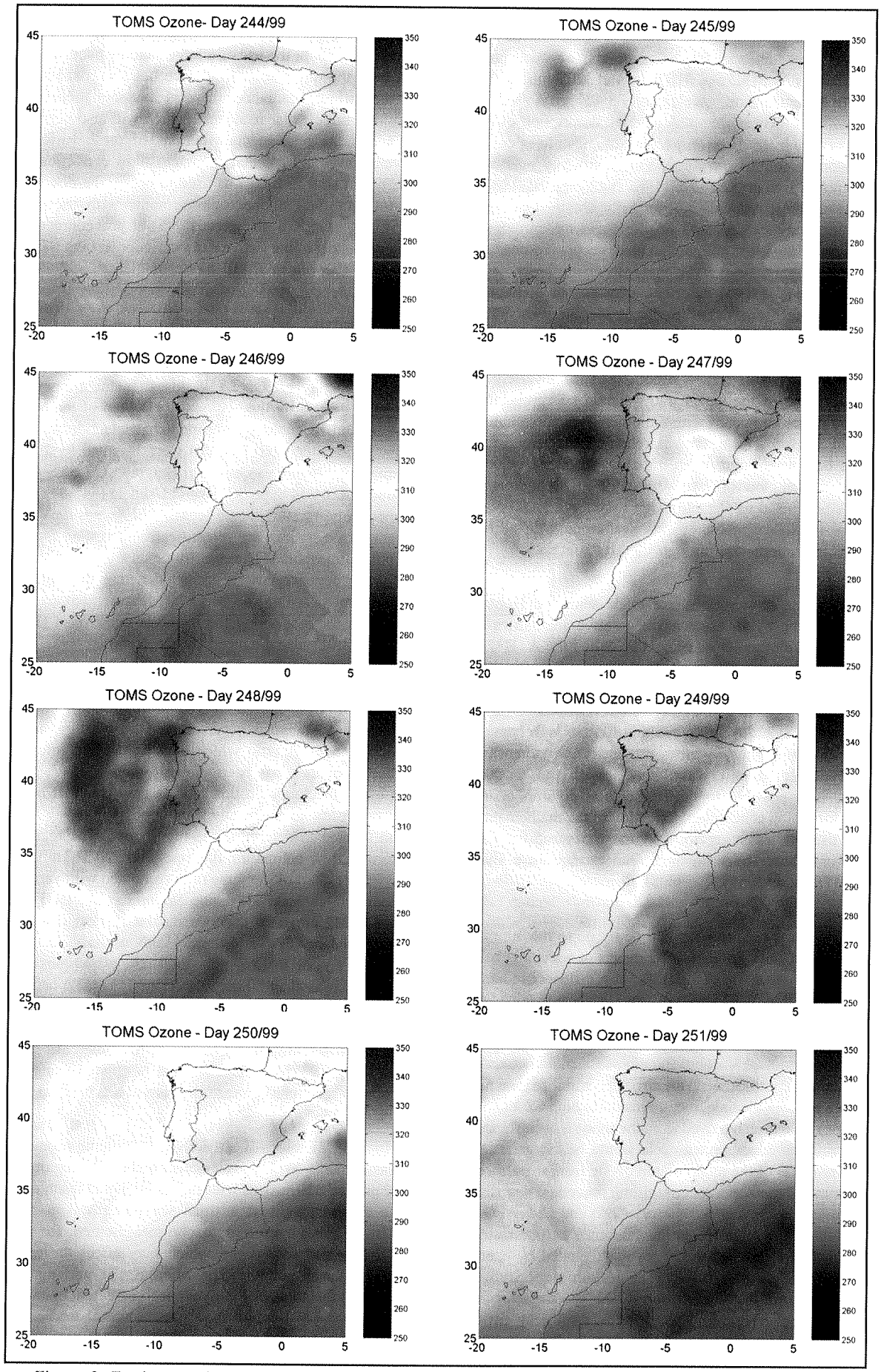

Figure 2. *Total ozone from TOMS over the Iberian Peninsula for the period September 1-8 (Days 244-251).*

Brewer

The Brewer spectrophotometer measures the intensity of light in UVB absorption spectrum of ozone at five wavelengths (306.3 nm, 310.1 nm, 313.5 nm, 316.8 nm and 320.1 nm) with a resolution of 0.6 nm, a sixth wavelength of 302.1 nm is used for calibration with a mercury lamp. A detailed description of the methodology used by the Brewer spectrophotometer to calculate the total ozone amount from direct sun, zenith sky or moon measurements is given in (*Kerr et al.*, 1983 and *Kerr et al.*, 1984). Accurate total ozone amounts are normally obtained through direct sun measurements. Tenths of direct sun measurements performed every day is the normal and more accurate procedure to obtain total column ozone with this instrument.

Stamnes et al. (1991) describes a method to derive the total ozone column from global irradiance measurements. The method is based on the comparison of measured irradiance ratios at two wavelengths in the UV region of the spectrum with a synthetic chart of this ratio computed for a variety of ozone values. One of the wavelengths should be appreciably absorbed by ozone compared with the other. Typically choices are 305 and 340 nm. The method is reliable under cloud free conditions, but increasingly overestimates the ozone column for optically thicker clouds (*Meyer et al.*, 1998). This alternative method has been used in this campaign to retrieve total ozone from global irradiance measurements performed with all the Brewer spectrophotometers through the UQ routine.

Dobson

Total ozone observations are made with the Dobson spectrophotometer by measuring the relative intensities of selected pairs of ultraviolet wavelengths, called the A, B*, C, C', and D wavelength pairs, emanating from the sun, moon or zenith sky. The A wavelength pair, for example, consists of the 305.5 nm wavelength that is highly absorbed by ozone, and the more intense 325.4 nm wavelength that is relatively unaffected by ozone. Thus, by measuring the relative intensities of suitably selected pair wavelengths with the Dobson instrument, it is possible to determine total column ozone. Detailed information concerning derivation of the mathematical equations used in reducing total ozone measurement data obtained from observations on direct sun or moon are given elsewhere (Dobson, 1957).

Bentham DM-150

The Bentham spectrometer can be set up to measure the global and diffuse solar irradiance by means of a shadow band which is moved over the diffuser for the diffuse irradiance measurement. The direct solar irradiance is then obtained by subtracting the diffuse irradiance from the global irradiance measurement. Since the whole procedure to obtain one direct spectrum takes about 20 minutes there is substantial uncertainty about attributing a specific time to the direct spectrum. To minimize this uncertainty about the time, measurements at high SZA (Solar Zenith Angle) have been removed from the analysis as the change in SZA during the measurement cycle would be too great.

The retrieval of the total column ozone from these direct solar spectrum is based on a spectral fitting procedure described in some works (*Mayer and Seckmeyer*, 1997, and *Huber et al.*, 1995). Essentially, a high-resolution reference extraterrestrial spectrum in the range 300 nm-350 nm is attenuated by ozone, Rayleigh scattering and aerosols. The resulting spectrum is then convolved with the slit function of the spectrometer and compared to the measured spectrum. A nonlinear fitting procedure with three free parameters, one for total column ozone and two for the aerosol optical depth minimizes the sum of the squares of ratio of model spectrum to measured spectrum.

Due to the above-mentioned uncertainty about the reference time for the direct spectrum as well as to the uncertainty about the use of a large shadow band which blocks not only the direct solar irradiance but also a substantial part of the diffuse irradiance, there is a systematic error in the resulting direct solar irradiance which will also depend on the SZA. As the relative contributions of these various effects have not been investigated enough to allow corrections of them, a constant shift in time was used to obtain the best agreement in total column ozone measurements with the co-located travelling standard Brewer#017. This procedure essentially removed most of the fictive daily variation at high SZA without affecting the values at the shorter angles.

NILU-UV6

The NILU-UV6 instruments measure global radiation at five UV channels and PAR. A radiative transfer model is used to calculate the total ozone content, cloud transmittance and the biologically effective UV doses. In the framework of a project financed by the National R+D Plan of the Ministry of Science and Technology, three multichannel moderate bandwidth filter radiometers (NILU-UV6) were installed by INM at the permanent Argentinean bases of Belgrano (77°52'S, 34°37'W), Marambio (64°14'S, 56°37'W) and Ushuaia (54°48'S, 68°19'W), respectively, in 1999, just after the *"El Arenosillo"* campaign. The selected stations are scientifically interesting for the study of polar atmosphere. These instruments are part of the Spanish Antarctic network now coordinated within the framework of the joint INTA-INM's "MAR" (Measurement of Antarctic Radiance for monitoring the ozone layer) Project (REN2000-0245-C02-01) also financed by the National R+D Plan.

The irradiance is measured by the NILU-UV6 instrument at five bands (305, 312, 320, 340 and 380 nm), all with a bandwidth of approximately 10 nm. The ratio of irradiances at 320 nm and 312 nm is very sensitive to variations in the total ozone amount. A ratio which may be used to infer the total ozone amount. It has been shown (*Stamnes et al.*, 1991) that the effect of clouds on this ratio is very small. It is therefore not necessary to make any corrections for clouds when this ratio is used to determine the total ozone. The total ozone is determined by comparing the measured 320/312 nm ratio with a synthetic chart of the same ratio computed with various ozone amounts (Dahlback, 1996, and *Stamnes et al.*, 1991). Because the 320/312 nm ratio depends on the vertical distribution of ozone for large SZA and the Signal/Noise ratio in the 312 nm channel is poor for low sun, total ozone becomes unreliable for SZA larger than 80 degrees. The NILU-UV6 had just been calibrated against the Bentham DM-150 from INM at the Izaña Observatory in August 1999, one week before the *"El Arenosillo"* campaign. In this previous calibration the coefficients for each channel were calculated using the INM Bentham spectroradiometer as reference.

Microtops-II

The Microtops-II can derive total column ozone by taking measurements at 3 wavelengths in the UV region (305 nm, 312 nm and 320 nm), as with the traditional Dobson instrument. The measurement at a third wavelength is used by the Microtops-II to correct its ozone measurement for particulate scattering and stray light, which may affect the readings of ozone column amount. The Microtops-II will display three readings for total column ozone: corrected ozone column measurement [03(corr)], the ozone column based on the ratio of channels 1 and 2 [03(1/2)], and the ozone column based on the ratio of channels 2 and 3 [03(2/3)]. A detailed description of the Microtops-II can be found in *Morys et al.* (1996).

8.3. TOTAL OZONE BREWER SPECTROPHOTOMETER INTERCOMPARISON

Blind ozone measurements and servicing

On September 1 the campaign began at "El Arenosillo" with the start of almost simultaneous ozone measurements with Brewers #033, #070, #117, #151, #157 and the travelling standard Brewer #017. Brewer #151 arrived on September 2 and started measurements in the afternoon. All users were advised to correct their instrument ETC constants according to Standard Lamp ratios if they had changed more than 10 units from the last calibration. It was done for all applicable instruments except Brewers #033 and #117.

On September 3 and 4, intensive ozone and UV measurements were performed from sunrise to sunset to obtain representative data for a large range of airmass. These days were used for the UV "blind" intercomparison. Brewer schedules were modified to prioritize spectral UV measurements. In addition, sun scan tests were performed to define the optimal ozone measurement position slit wavelengths. Even though moving clouds in the morning of September 4 slightly perturbed the measurements, a large set of simultaneous ozone measurements could be obtained. All instruments continued collecting data automatically on September 5. On September 6, mercury, cadmium and zinc spectral discharge lamps were used on the Brewers to characterize their wavelength alignment for UV scanning.

As can be seen in Figure 3, the ozone measurements of four of the five INM Brewers on September 2 (Day 245) were in good agreement with travelling standard Brewer #017, with maximal deviations before any adjustments of less than 4 DU. The Brewer#117 was low by about 4% and its ETC constants had to be re-established.

The spectrometer on the Brewer#033 was found to need grating re-alignment, probably as one of its mounting blocks had to be re-attached after it was moved to Zaragoza last year. This was done on the evening of September 3, and then the calibration step position had to be re-adjusted 3 steps the next day. The optimal ozone measuring position (calibration step) of the other four Brewers were in good agreement with the results from the sun scans and no changes were necessary. This result also implied that the ozone absorption coefficient used by those Brewers was still correct. Small changes to the extraterrestrial constants mostly based on change in the standard lamp ratios since the last calibration visit (1998), were implemented.

New constants had to be established for Brewer#033 due to the spectrometer re-alignment. Apart from the re-alignment and complete checkout of Brewer#033, the other Brewers only received the standard maintenance checks, cleaning and lubrication.

Results of the blind ozone measurements are summarized in Figure 4, where ozone relative differences for each day between each Brewer (when available) and reference Brewer#017 are shown. Brewer #070, #150, #151 and #157 show a good agreement. On the other hand, Brewer#033 and #117 turned out to be off.

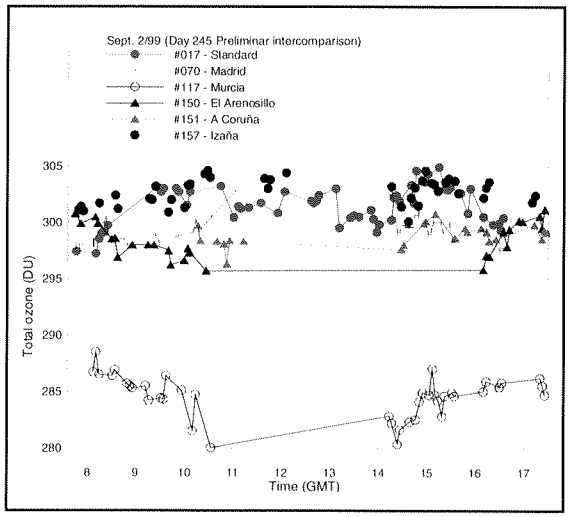

Figure 3. *Blind intercomparison. Total ozone obtained with the Brewer spectrophotometers before any correction on September 2, 1999 (Day 245).*

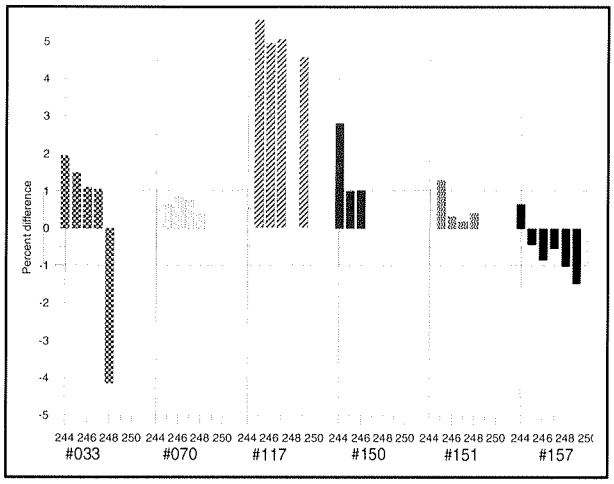

Figure 4. *Daily total ozone percentage differences of each Brewer against the travelling reference Brewer#017 with no corrections.*

Results after corrections: conclusions

Old and new ETC absorption coefficients and Cal. Step numbers are shown in Table 3. After corrections the analysis of the data showed the Brewer results improved and were within ±1%, which is the certified accuracy of Brewer spectrophotometers (Figure 5).

Table 3. *Brewer calibration constants.*

Brewer	ETC O_3/SO_2 Initial Final	O_3/SO_2 Abs. Coeff. Initial Final	Cal. Step-No. Initial Final
#033	3370/3645 3458/3654	0.3397/1.1300 0.3356/1.1393	133 136
#070	3010/3030	0.3403/1.1173	159 159
#117	2820/2740 2820/2740	0.3410/1.1423 0.3410/1.1423	286 286
#150	1548/221 1540/240	0.3376/1.1363 0.3418/1.1458	284 287
#151	3356/3672 3346/3730	0.3422/1.1434 0.3422/1.1434	288 288
#157	1551/185 1565/210	0.3420/1.1500 0.3420/1.1500	285 285

Figure 6 shows the total ozone results of all the Brewers for September 6 (Day 249) using final constants.

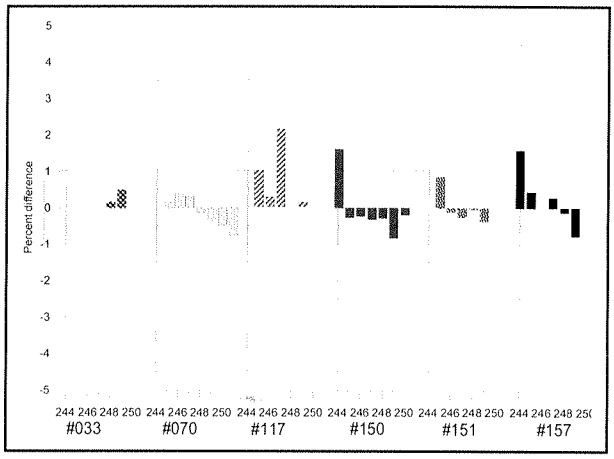

Figure 5. *Daily total ozone percent differences of each Brewer against the travelling reference Brewer#017 once corrections have been applied.*

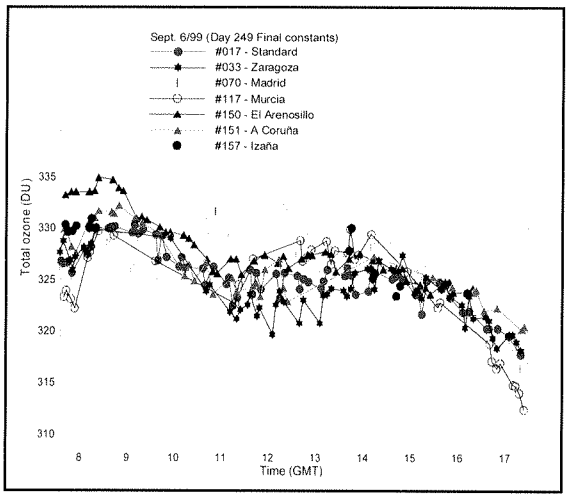

Figure 6. *Total ozone obtained with the Brewer spectrophotometers after correction on September 6, 1999 (Day 249).*

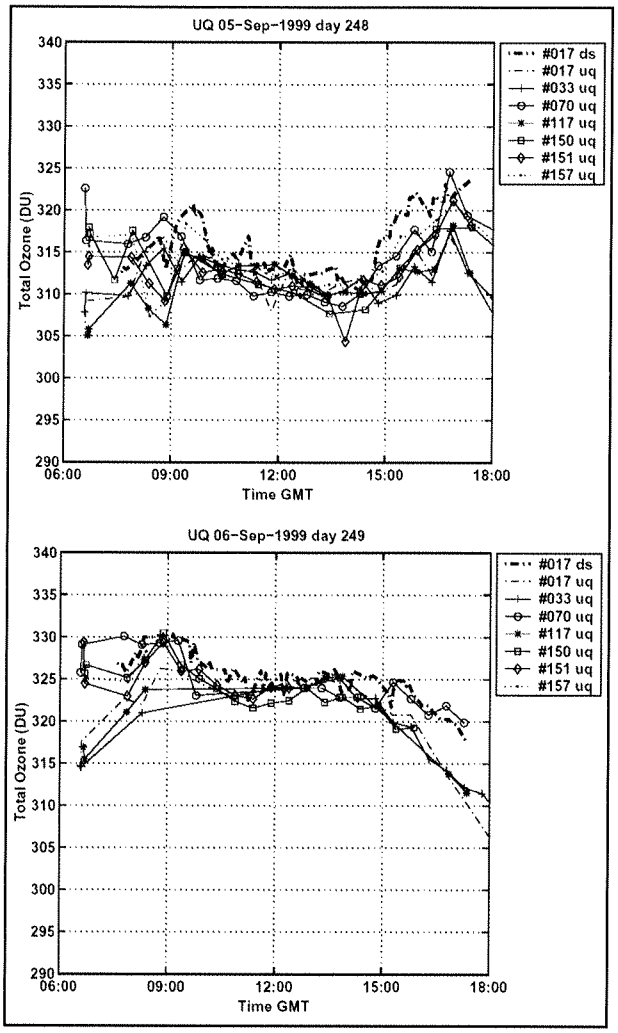

Figure 7. *Total ozone obtained with the Brewer spectrophotometers (in blue) from global UV measurements using the UQ routine compared with direct sun total ozone from the travelling reference Brewer#017 (in black) for September 5 and 6.*

Ozone determination using the UQ routine

Total ozone has been derived from global UV measurements for each Brewer using the UQ routine. An excellent agreement is achieved with total ozone obtained through direct sun with the travelling reference Brewer#017, as shown in Figure 7.

Diurnal total ozone course is well tracked on, both, September 5 and 6. Relative differences are within 1%. Notice that on September 5, cloudiness is significant in the afternoon and that, however, the total ozone calculation from global UV measurements is not affected tracking the total ozone increase observed well. This method is revealed as a very powerful alternative to direct sun measurements for days and/or sites with persistent cloudiness. Of course, the error is not acceptable for high airmasses.

8.4. OZONE INTERCOMPARISON WITH OTHER INSTRUMENTS

As was expected, the Dobson#120 measures total ozone amounts for each day of the campaign which are quite close to those obtained with the reference Brewer#017 (relative differences within 1%) as is shown in Figure 8.

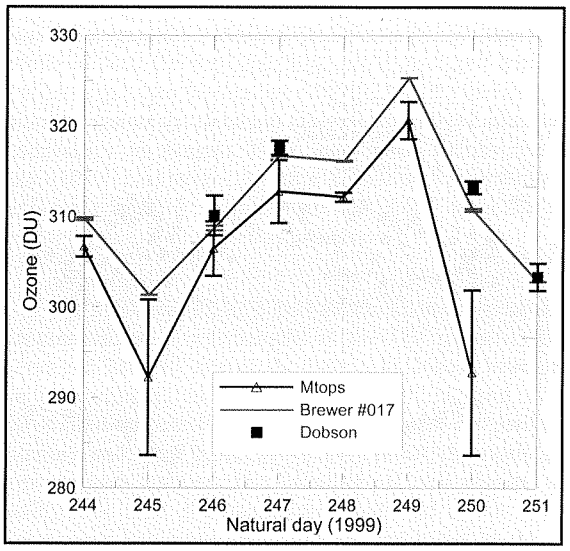

Figure 8. *Daily mean total ozone from the Dobson #120, the Microtops-II and the travelling reference Brewer#017 during the intercomparison (September 1-8).*

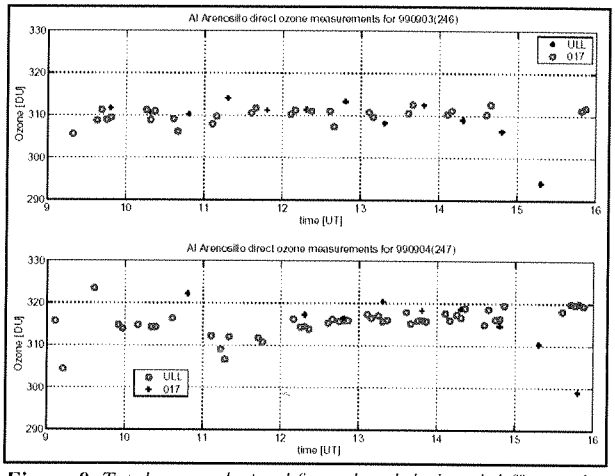

Figure 9. *Total ozone derived from the global and diffuse solar irradiances obtained with the Bentham spectroradiometer from La Laguna University (red open circles) compared with total ozone from the Brewer#017 for September 3 and 4, respectively.*

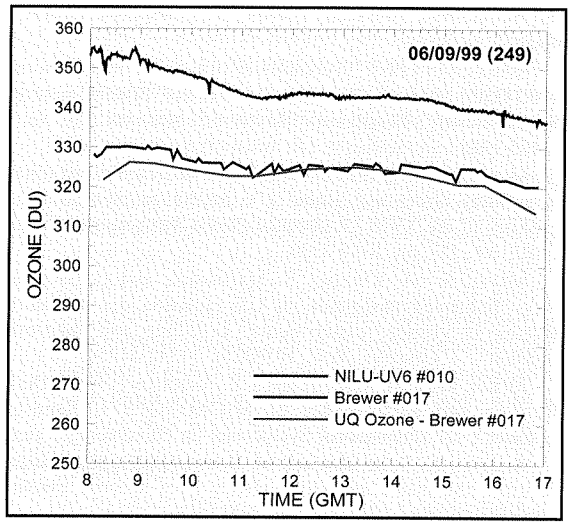

Figure 10. *Total ozone derived from the NILU-UV6 #010 compared with the ozone obtained by the Brewer #017 using, both, direct sun and global UV measurements.*

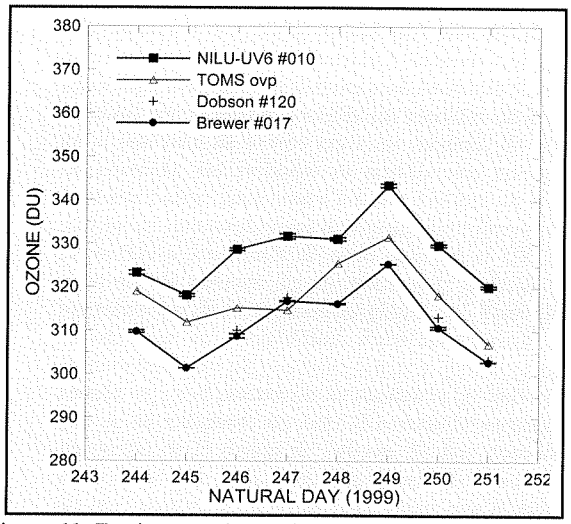

Figure 11. *Total ozone obtained around noon (hourly average of 1-minute values) with the NILU-UV6 #010 compared with the daily mean ozone obtained by the Brewer #017 and Dobson #120, and the TOMS overpass for the period September 1-8.*

Concerning the total ozone calculated with the Bentham spectroradiometer the results are surprisingly good, considering the uncertain time stamp of the measurements which is reflected in the deviations at airmasses above 1.4 (around 15 GMT). The agreement with Brewer#017 is within a few DU as can be observed in Figure 9.

Figure 10 shows the diurnal variation of total ozone calculated with the NILU-UV6#010 instrument compared with that obtained with the reference Brewer#017 using direct sun and global UV measurements for September 6. A constant offset of about 5% can be observed, the same found during the other days of the campaign (Figure 11).

Previous comparisons performed at the Izaña Observatory (ten days before this campaign) showed an excellent agreement between the NILU-UV6 #010 and the Brewer#157. This agreement was again achieved some weeks after the *"El Arenosillo"* campaign at the Izaña Observatory, which confirms that the measurements were affected by humidity inside the instrument. This problem might have been caused during its transportation to *"El Arenosillo"*. This instrument has shown itself to be capable of providing accurate total ozone if systematic corrections are performed to the irradiance measurements through periodical (2 weeks) external lamp tests (*Torres et al.*, 2002). Unfortunately during the campaign no standard lamp test was performed.

As has already been reported (*Köhler*, 1999) the Microtops-II might provide reasonably good total ozone measurements if the observations are carefully performed with a tripod. Figure 8 shows the daily mean total ozone record during the campaign obtained with this instrument and compared with the Brewer#017 and the Dobson#120. The day-to-day total ozone variations are well tracked by the Microtops-II, showing relative differences within 1%-3% compared to the Brewer#017.

A summary of daily total ozone means obtained by different instruments during the campaign are shown in Table 4.

Table 4. *Daily total ozone from different instruments and corresponding standard deviation.*

Natural day	Brewer #017	Dobson #120	Bentham DM150	*NILU UV#010	MTops II
244	309.8 ± 4.0	——		323.4 ± 0.5	306.7 ± 2.3
245	301.4 ± 1.7	——		318.2 ± 0.3	292.2 ± 17.2
246	308.8 ± 3.1	310.2 ± 4.4	310.6 ± 1.9	328.8 ± 0.3	306.5 ± 6.0
247	316.8 ± 2.7	317.2 ± 1.6	317.5 ± 2.6	331.8 ± 0.6	312.8 ± 6.9
248	316.2 ± 3.9	——		331.2 ± 0.4	312.2 ± 1.0
249	325.4 ± 2.7	——		343.6 ± 0.4	320.6 ± 4.1
250	310.8 ± 4.1	313.3 ± 1.4		329.8 ± 0.3	292.8 ± 18.2
251	302.9 ± 0.9	303.4 ± 3.0	305.6 ± 6.4	320.2 ± 0.3	——

* *Total ozone obtained around noon (hourly average of 1-minute values).*

8.5. CONCLUSIONS

The scatter in ozone values for all the Brewers that participated in this intercomparison was quite low, and similar to that of the ozone intercomparison performed in NOGIC-93 and NOGIC-96. Ozone calculation using global UV measurements with the Brewers is excellent. This alternative method is non-sensitive to cloudiness, although it fails for high airmasses.

The Dobson#120 shows the same agreement and scattering as the Brewers compared to the Brewer#017. Dobson and Brewer, as is now recognized worldwide, are both the only instruments capable of high-accuracy long-term ozone monitoring programs.

The Bentham DM-150 shows quite good results when compared with Brewer#017. However, it presents some problems of time synchronization, meaning that total ozone is only acceptable for airmasses lower than 1.4.

A regular (every one or two weeks) and long term external lamp test procedure is extremely important to obtain accurate total ozone with the NILU-UV6. Detected instrument instabilities or offsets could have been corrected if regular lamp checks, as indicated by *Torres et al.* (2002), had been performed during the campaign.

The Microtops-II is a reliable instrument for intensive campaigns and for detecting, in a first stage, malfunctions in a spectrophotometer network if regular ETC corrections are made through Langley Plots performed in high mountain stations.

ACKNOWLEDGEMENTS

The research has been funded by CICYT under Project CLI97-0345-CO5-05. The authors are deeply grateful to all the instrument operators. Special thanks are extended to Ms María Cascón, then at the Complutense University (Madrid), who joined the Tenerife group and performed most of the hard measurements with the INM's Microtops-II.

We would like to extend our sincere appreciation to Dr. Muniosguren for the coordination of the campaign, and to Dr. Benito de la Morena for the use of the *"El Arenosillo"* Laboratory facilities, and for the food and accommodation.

REFERENCES

Dahlback, A. (1996): "Measurements of biologically effective UV doses, total ozone abundances, and cloud effects with multichannel, moderate bandwidth filter instruments", *Appl. Opt.*, Vol. **35**, No. 33, 6514-6521.

Dobson, G. M. B. (1957): "Observers' handbook for the ozone spectrophotometer", in *Annals of the International Geophysical Year*, **V**, Part 1, 46-89, Pergamon Press.

Cuevas, E., C. Torres, V. Carreño and A. Redondas (2003): "Meteorological conditions during de First National Spectroradiometer Interconparison Campaign", this Report, Chapter 3.

Huber, M., M. Blumthaler and W. Ambach (1995): "Total atmospheric ozone determined from spectral measurements", *Geophys. Res. Lett.*, **22**, 53-56.

Kjeldstad, B., B. Johnsen and T. Koskela (*ed.*) (1994): "The Nordic intercomparison of ultraviolet and total ozone instruments at Izaña, October 1996". Final Report, Finnish Meteorological Institute, Meteorological Publications, No. 36, 186 p., Helsinki, Finland.

Koskela, T. (*ed.*) (1994): "The Nordic intercomparison of ultraviolet and total ozone instruments at Izaña from 24 October to 5 November, 1993". Final Report, Finnish Meteorological Institute, Meteorological Publications, No. 27, 123 p., Helsinki, Finland.

Kerr, J., C. McElroy and W. Evans (1983): "The automated Brewer spectrophotometer for measurement of SO_2, O_3 and aerosols", Proc. of the WMO/AMS/CMOS Symposium on Meteorological Observations and Instrumentation, Toronto, pp. 470-472.

Kerr, J., C. McElroy, D. Wardle, R. Olafson and W. Evans (1984): "The automated Brewer spectrophotometer", Proc. Quadrennial Ozone Symposium, Halkidiki, Greece, in Atmospheric Ozone, pp. 396-401.

Köhler, U. (1999): "A comparison of the new filter ozonometer MICROTOPS II with Dobson and Brewer Spectrometers at Hohenpeissenberg". *Geophysical Research Letters*, vol. 26, No. 10, pp. 1385-1388.

Mayer, B. and G. Seckmeyer (1997): "Retrieved ozone columns from spectral direct and global UV irradiance measurements", proceedings of the XVIII Quadrennial Ozone Symposium, L' Aquila, Vol. 102, No. D7, pp. 8719-8730.

Mayer, B., A. Kylling, S. Madronich, and G. Seckmeyer (1998): "Enhanced absorption of UV radiation due to multiple scattering in clouds: experimental evidence and theoretical explanation", *J. Geophys. Res.*, **103(D23)**, 31241-31254.

Morys, M., F. M. Mims III and S. E. Anderson (1996): "Design, calibration and performance of MICROTOPS II hand-help ozonometer". 12th International Symposium on Photobiology, Vienna.

Stamnes, K., J. Slusser and M. Bowen (1991): "Derivation of total ozone abundance and cloud effects from spectral irradiance measurements", *Appl. Opt.*, **30**, pp. 4418-4426.

Torres, C., A. Redondas, E. Cuevas, K. Lakkala, P. Taalas, M. Yela, H. Ochoa and G. Deferrari (2002): "Correction and validation of total ozone data series from an Antarctic multichannel filter radiometer solar UV network", 27th General Assembly of the European Geophysical Society (Nice, France), 21-26 April.

CHAPTER 9

DETERMINATION, MONITORING AND COMPARISON OF ATMOSPHERIC COMPONENTS: AEROSOL PARAMETERS (AEROSOL OPTICAL DEPTH AND RADIATIVE PROPERTIES) AND WATER VAPOR

V. Cachorro, R. Vergaz and A. M. de Frutos
Grupo de Óptica Atmosférica GOA-UVA.
Dpto. de Óptica y Física Aplicada. Facultad de Ciencias, 47071, Valladolid.
Dpto. de Física Aplicada. ETSI Agrarias de Palencia, 47071, Palencia, chiqui@baraja.opt.cie.uva.es.

SUMMARY

The determination, monitoring and comparison of the spectral aerosol optical depth (AOD) and water vapor content has been carried out by various instruments of different characteristics and performances, during the First Iberian Intercomparison Campaign in "El Arenosillo" (Huelva). This determination is based on measurements of the direct component of solar irradiance. Our Li-Cor1800 AOD data has been compared with those given by other Li-Cor during a afternoon. Three Brewers have reported the aerosol optical depth at the five UV ozone wavelengths based on two different methods. Two photometers, the MicrotopsII and the CIMEL318A, of very different performance have also reported data of AOD's at different wavelengths and water vapor. Microtops gives AOD at 1020 nm and the Cimel photometer woks at four wavelengths: 440, 670, 850, 1020. All these measurements were carried out manually except those of Brewer spectroradiometers and Cimel photometer. Generally these measurements were taken during the meantime between global irradiance measurements but the specific time is not exactly the same for all instruments, however a temporal comparison can be carried out. Good agreement is obtained in the comparison of the aerosol optical depth in the visible-infrared range between the two Li-Cors and also in the UV with the three Brewers. The comparison at 320 nm between the three Brewers and the two Li-Cors also shows a relatively good agreement, taking into account the deficiencies showed by the Li-Cors at these lower UV wavelengths. Based on the data of our Li-Cor spectroradiometer the Ångström turbidity parameters were also determined and monitored given their importance for UV global irradiance modeling. These parameters were determined at different spectral intervals to observe their variability. In order to characterise as much as possible the aerosols we have also determined their physical and optical (radiative) properties as the effective radius, single scattering albedo, w_o, and the asymmetry parameter, g, which are also relevant for UV modelling. Finally, the other atmospheric component that was studied has been the columnar water vapor content, CWV. This determination is based on the absorption features of the 940 nm band, but great differences have been found depending on the contribution of "continuum absorption" and the aerosols. The method employed by us is more consistent than the current differential absorption technique used by photometers because it makes use of the whole band-shape absorption features. The water vapor content data has been compared with those given by Microtops and Cimel, with relevant differences. The results about water vapor determination suggest that much research is needed in this area.

RESUMEN

Se ha determinado, monitorizado y comparado el espesor óptico de aerosoles (AOD) y el contenido de vapor de agua en la vertical con varios instrumentos de diferentes características durante la Primera Campaña de Intercomparación de Espectrorradiómetros que ha tenido lugar en la estación de "El Arenosillo" en Huelva. Esta determinación está basada en las medidas de la componente directa de la irradiancia solar. Los datos de AOD de nuestro espectrorradiómetro Li-Cor1800 han sido comparados con los de otro Li-cor durante una tarde de medida y durante varios días con los de tres espectrorradiómetros Brewer, a las 5 longitudes de onda de trabajo de determinación del ozono, usando dos métodos diferentes. Dos fotómetros, el MicrotopsII y el CIMEL318A, de muy diferentes características permiten también comparar el AOD a diferentes longitudes de onda y el vapor de agua. Microtops trabaja en 1 020 nm y el fotómetro Cimel en cuatro longitudes de onda (440, 670, 850, 1020). Todas las medidas son manuales excepto las medidas de los Brewers y el Cimel. Estas medidas fueron tomadas normalmente en el intervalo de tiempo entre las medidas de la irradiancia global, por lo que el momento exacto de todas ellas no coincide, sin embargo es posible una correcta comparación. El acuerdo obtenido de esta comparación es bastante bueno, tanto entre los dos Li-Cors en el visible y UV como con los Brewers en el UV. La comparación a 320 nm es sorprendentemente buena entre Brewers y Li-Cors dada las deficiencias que estos últimos presentan para la medida a longitudes de onda baja, en el UV. Tomando los datos de nuestro espectrorradiómetro Li-Cor se han determinado también los parámetros de turbiedad de Ångström durante la campaña, dada su importancia para la modelización de la irradiancia global UV. Estos fueron determinados en diferentes intervalos espectrales, con el fin de observar su variabilidad. Para caracterizar adecuadamente a los aerosoles, también se han determinado y monitorizado sus propiedades físicas y ópticas (o radiativas), como el radio efectivo, el albedo de single "scattering" simple, w_o, y el parámetro de asimetría, g; importantes en la modelización del UV. Finalmente, la otra componente que se ha estudiado ha sido el contenido vertical de vapor de agua, CWV. Esta determinación está basada en la absorción de la banda de 940 nm. Se han encontrado grandes diferencias en los resultados al tener en cuenta la contribución de la llamada "absorción del continuo", así como la contribución de los aerosoles. El método empleado por nosotros es teóricamente mejor que el método de absorción diferencial, pues este tiene en cuenta todas las longitudes de onda de la banda y por tanto la forma de esta. El contenido de vapor de agua atmosférico ha sido comparado con el determinado por los fotómetros Microtops y Cimel, con diferencias importantes. Los resultados muestran, por tanto, que es preciso seguir investigando en este tema de determinación del vapor de agua.

9.1. INTRODUCTION

The inherent spatial-temporal variability of atmospheric constituent (ozone, aerosol, water vapor, etc.) requires routine measurements over extended periods, where quality control data can be only given by specific standard protocols of instrument measurements and methods. Therefore intercomparison campaigns are necessary (*Gardiner and Kirsch*, 1993).

Intercomparison procedures applied to global irradiance data (and direct irradiance data) are the main goal of the intercomparison campaigns for assessing instrument comparative performances. However this task must be complemented with the comparison of derived or extracted data, as aerosol optical depth, ozone, water vapor, or other atmospheric parameters, due to the fact that different instrument have different characteristics and usually require different methods.

The aim of this chapter is the determination, monitoring and comparison of atmospheric components, as aerosol (optical depth and optical properties) and water vapor content in the vertical, by different spectroradiometers and instruments, during the First Iberian Intercomparison Campaign of Spectroradiometer held in "El Arenosillo" station belonging to INTA (Instituto Nacional de Técnica Aeroespacial) in Huelva (Spain), in September 1999.

Monitoring of aerosol parameters such as turbidity indices, spectral AOD, physical (effective radius, etc.) and radiative (single scattering albedo, asymmetry factor, etc.) vertical properties are necessary for climatologic and environmental studies (*WCP112*, 1986; *D'Almeida et al.*, 1992; *National Research Council*, 1996). Concerning this campaign aerosol are of interest to analyse their influence on UV irradiances. On the other hand this is a good oportunity to compare and assess the determination of different atmospheric parameter, as the aerosol optical depth and water vapor.

The necessity of measurements to report ozone depletion and hence higher level of UV radiation has been increasing during last years. Major focus on the aerosol optical depth (hereafter AOD or AOT, aerosol optical thickness) and aerosol characteristics at UV wavelengths has been carried out to assess the contribution of aerosol on UV irradiances. However, there is not abundance of measurements reporting AOD and aerosol properties at these wavelengths (*Bais*, 1997; *Marenco et al.*, 1997; *Carvalho and Henriques*, 1998). Much of the information of aerosol for UV modelling has been extrapolated from the behaviour in the visible and near infrared regions by means of aerosol models and measurements (*Wang and Lenoble*, 1996; *Mayer et al.*, 1997). Developing instruments for aerosol optical depth measurements in the UV region is generally linked to ozone content determination.

Here we are interested in the determination of the AOD and derived aerosol properties and columnar water vapor content retrieved by using different instruments and methods.

Water vapor is known to be a key parameter in atmospheric and climate studies from the hydrological cycle and biosphere-atmosphere interactions to energy budgets and climate change. In the specific case of radiative transfer problems, water vapor acts as an absorbing atmospheric component regulating the transmittance of the atmosphere, therefore accurate integrated content and vertical profiles are needed.

The methods and data discussed here could be of interest for monitoring purposes and validation of efficient procedures and approaches for determining AOD, aerosol optical properties and atmospheric water vapor content retrieval, mainly using ground-based instrument but also for assessing and validation satellite remote sensing techniques.

9.2. EXPERIMENTAL MEASUREMENTS

During the the First Iberian Intercomparison Campaign of Spectroradiometer held in "El Arenosillo" station, a given schedule of global UV horizontal irradiances measurements was carried out for Brewer spectroradiometer intercomparison. The other participating spectroradiometers like, Bentham, Optronic, Oriel and Li-Cors followed this schedule as much as possible, given the different characteristics between them, but this have been described in earlier chapters. Here we will focus on direct normal spectral irradiances in order to determine aerosol and water vapor content atmospheric constituents during the campaign, once spectral irradiances intercomparison between the different spectroradiometers were established.

Direct solar normal irradiance measurements were carried out by the "Grupo de Optica Atmosférica" of the University of Valladolid, GOA-UVA" with the Li-Cor1800 (serial number RS-487, assigned as VAL) during all the available days of the campaign. These measurements were taken practically in systematic way, in the meantime of global irradiance measurements that were taken every 15 minutes. Bear in mind that Li-Cor1800 spectroradiometer takes 40 seconds to record a spectrum for 300 to 1 100 nm. Therefore to get both direct and global irradiance data manual operation were required.

A Cimel photometer, model 318A of (GOA-UVA and LOA-Lille University) working at 4 wavelengths for aerosols: 440, 670, 850 and 1 020 nm allows us to determine the aerosol optical depth at these wavelengths. This instrument also determines the columnar water vapor (CWV) by means of the 936 nm channel.

Direct spectra measurements with Brewer instruments were also registered for ozone content determination but here we only report data of three Brewer: the Brewer #157 of group of INM (Izaña - Canary Island); Brewer #150 of INTA (El Arenosillo) and Brewer #47 of INM of Portugal. These data will be used to determine the AOD at the same wavelengths used to determine the ozone content. Specific time comparison of direct irradiance measurements were also performed during the morning on 7 September with the Li-Cor (serial number 312, assigned as UVL) of the Group of Solar Energy of the University of Valencia, which has similar characteristics that our Li-Cor. The difference is that our Li-Cor works with an optic fiber and remote receptor cosine and the FOV (Field-Of-View) of both collimators are slightly different (FOV=4.3 for VAL and FOV=3.6 for UVL).

Also, during the campaign Microtops measurements of the AOD at 1 020 nm and water vapor content were performed by the Group of the INM of Izaña, in a nearly systematic way. All these measurements for all the instruments were semi-automatic (manually tracking) except those of Brewer spectrometers and Cimel photometer. The different characteristics of these different instruments give rise to use different methods that are suited for each instrument, in order to determine the atmospheric constituents, hence the process of comparison is of great interest.

Vertical water vapor content (CWV) was determine by our measurements of Li-Cor1800 spectroradiometer (*Cachorro et al.*, 1998) and compared with those given by the Microtops and Cimel data at specific days.

9.3. METHODS TO DETERMINE THE SPECTRAL AEROSOL OPTICAL DEPTH

Spectral aerosol optical depth in the visible and near-infrared retrieved from the Li-Cor1800 spectroradiometer

We determine the experimental spectral aerosol optical depth AOD of the atmosphere from absolute calibrated direct

normal solar irradiance (W/m^2 nm) measurements at ground level with the Li-Cor1800 instrument using the Beer-Lambert law as follows

$$F(\lambda) = F_0(\lambda) \exp(-\tau(\lambda) M)$$

where $F_0(\lambda)$ is the irradiance at the top of the atmosphere corrected for the sun-earth distance; $\tau(\lambda)$ is the total optical depth of the atmosphere at wavelength λ and m the air mass, given by $m = (1/\cos(SZA))$ with SZA is the solar zenith angle. Usually the experimental AOD, $\tau_a(\lambda)$, is obtained by removing from the total atmospheric optical depth the contribution due to Rayleigh scattering, $\tau_R(\lambda)$ (scaled by the term P/P_o where P the pressure at the site of measurements and P_o the standard pressure (1 atm)) and the absorption of atmospheric gases, $\tau_g(\lambda)$, in the spectral range of interest according to

$$\tau_a(\lambda) = \tau(\lambda) - \tau_R(\lambda) - \tau_g(\lambda)$$

The expression used to removed the Rayleigh scattering is given by Bates (1988)

$$\tau_R(\lambda) = \frac{1}{117.2594\lambda^4 - 1.3215\lambda^2 + 0.00032 - 0.000076\lambda^{-4}}$$

Therefore AOD can be easily obtained in wavelengths of non-absorption. For wavelengths and region of atmospheric absorption gases the vertical contents of ozone, water vapor, etc. needs to be known before using this method, which will be referred as the "direct method". This ancillary data can be obtained from Dobson ozone measurements, radiosonde, satellite data, etc. or other available sources or methods. We have used this method in earlier works (*Cachorro et al.*, 1989; *Vergaz*, 1996; *Martínez-Lozano et al.*, 1998) using different spectral ranges in the visible and near-infrared.

Here we can use the direct method to determine the AOD removing ozone absorption by the data given by the Brewer spectrometer (see the chapter 8 about ozone determination) but water vapor can not be removed because these data are unknown and also need to be retrieved.

The moderate-high spectral resolution of the measured direct solar irradiance spectrum by the Li-Cor1800 instrument allows us selecting spectral windows of non-absorption where the AOD is calculated according the described procedure. Observing the spectral features of Rayleigh scattering and absorption by atmospheric gases in our spectral range

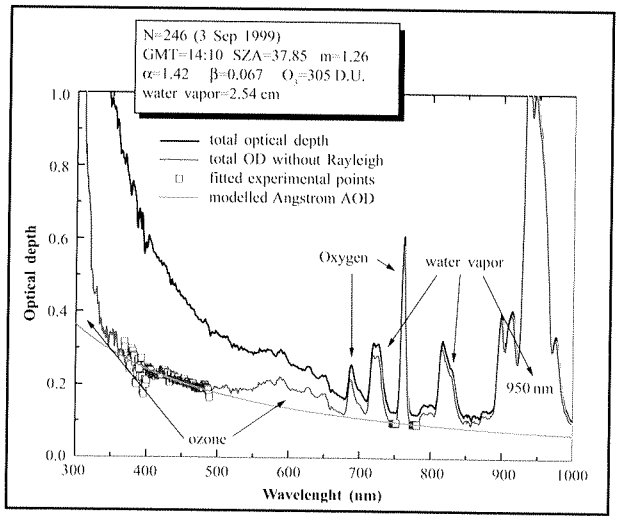

Figure 1. *Experimental optical depths due to the different atmospheric constituents with (black line) and without (green line) the Rayleigh scattering. Modelled aerosol optical depth by Ångström formula (blue line). (See text).*

(300-1 000 nm) (see figure 1) we have chosen three spectral windows of non-absorption: A(370-490 nm), B(748-757 nm) and C(776-782 nm). In the "A" spectral window we have not considered the weak absorption by NO_2 because of the high contribution of Rayleigh scattering and the associated error of the measured spectrum. The narrow windows B and C correspond to both sides of the strong 762 O_2 A-band. The experimental AOD points are fitted according to the Ångström formula.

$$\tau_a(\lambda) = \beta \lambda^{-\alpha}$$

A linear weighted fit, in a log-log plot of the AOD versus the wavelength permits the determination of the Ångström parameters α and β and so model the experimental AOD. The α parameter characterises the spectral features of aerosols and is related to the size of the particles while the β parameter is related to particle concentration and represents the AOD at 1 μm.

Figure 1 shows the experimental total optical depth of the atmosphere, that removing the Rayleigh contribution (solid line) and ozone contribution for a measured spectra at SZA = 37.85 degrees. The ozone, oxygen and water vapor absorption bands given by their optical depths can be easily observed. Also we can see the experimental points (square points) used to fit the Angstrom formula and the smoothed line which represent the modelled AOD. The obtained values for α and β parameters are depicted in the figure.

The evaluation of the modelled AOD by the window method will allow us in a subsequent step the determination of ozone content (*Cachorro et al.*, 1996) and water vapor content (*Cachorro et al.*, 1998). However, here, as ozone content is available, only water vapor will be determine as we will describe below.

Obviously the Ångström formula as better as shorter is the spectral range where it is applied. Therefore, the obtained α and β parameters are dependent on the selected spectral range. This is an inherent problem with the determination of these parameters. Therefore direct comparison between different sets of Ångström turbidity parameter must be made with care.

In spite of this, we will show later, the capacity of these parameters to retrieve the aerosol properties and to model direct and global spectral irradiances in the visible and near-infrared as well as their behaviour in the UV region (280-400 nm).

AOD determination in the UV region

Our research group is currently using the described procedure to determine AOD in visible and near-infrared region with Li-Cor1800 data, and is called by us "window" (*Cachorro et al.*, 1998; *Cachorro* 2000a, b). In the UV region we have follow the same procedure but in this case we evaluated the AOD at all the wavelengths from 300 nm to 400 nm, because only ozone absorption is considered and their vertical content is taken form Brewer spectrometer data. Figure 2 shows the procedure followed in the UV region, from 300 to 400 nm.

An Ångström fit at the spectral range 350-400 nm (the experimental points are depicted in the figure by the black squares) determines the α and β parameters. In this figure 2 the value of $\alpha = 3.5$ given by this UV fit and the value obtained with visible-infrared fit by the "window nmethod" ($\alpha = 1.42$) are shown. As can be seen in the figure the removed ozone below 320 nm give rise to a strong decrease of AOD which seem not realistic. However we must assess the errors of irradiance measurements and hence AOD error determination due to the characteristics of the Li-Cor1800 instrument, mainly their limitations to measure spectral UV radiation.

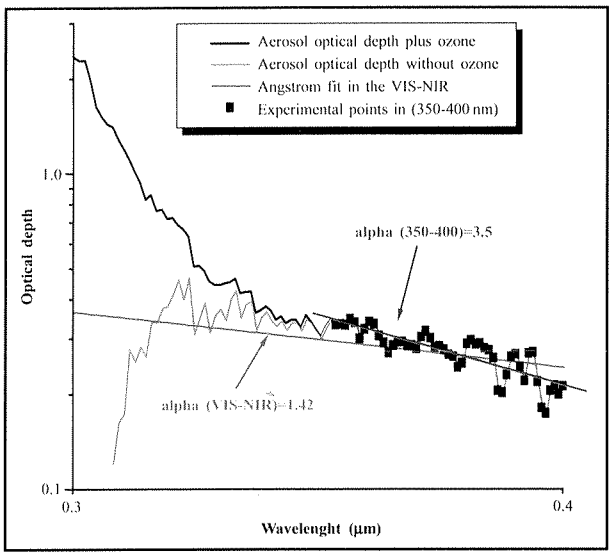

Figure 2. *Experimental total optical depths without Rayleigh contribution (black line). Orange line is the aerosol optical depth because the ozone absorption is removed from the latter. Ångström fit at the visible-infrared wavelengths by the "window method" (blue line) and the fit at UV wavelengths 350-400 nm (red line) (see text).*

AOD determination by the other instruments

The determination of the AOD by the other instruments is based on different methodologies according the characteristic of each instrument. Brewer spectroradiometers have followed two different methods. Brewer #157 (INM of Izaña) has taken the method developed by (*Kerr*, 1995) that is based on the determination of the solar constant by the Langley method at the five wavelengths used by this spectroradiometer to determine the ozone content. The special atmospheric conditions at the INM Observatory of Izaña allow the use of this method. Brewer #47 (INM-PT) and #150 (INTA) used another method developed by *Carvalho and Henriques* (2000) to obtain the AOD, also at the five wavelengths where the Brewer instrument makes the measurements of the direct component of solar radiation.

AOD Microtops data at 1 020 nm is based on the current methodologies used by this photometer (*Solar Light Company User's Guide*, 1996; *Morys et al.*, 2000).

Photometer calibration procedure (*Schmid et al.*, 1998) requires a constant of calibration for each filter wavelengths. These constants can be determined also by the Langley method or by comparison with a "Reference" photometer. However, the Microtops is a hand held photometer of low performance compared with Cimel photometer and hence gives rise to higher uncertainties on their retrieved data (*Schmid et al.*, 2000). Precisely, this type of Intercomparison Campaign helps us to know the accuracy and limitation of this different type of instruments.

Cimel photometer also requires the calibration constants of its filters. The characteristics of this instrument were described in Holben et al. (1986). The Cimel photometer was calibrated at the GSFC (Goddard Space Flight Center) of (NASA) just for this campaign of "El Arenosillo99" and now is installed there, belonging to the AERONET network (Web:www.aeronet.gsfc.nasa.gov:8080). The data here obtained are given by the procedures and method of AERONET.

Errors in the AOD determination

We must estimate the error associated with the determination of the AOD by our Li-Cor1800 spectroradiometer. The error of the retrieved experimental AOD, τ_a, is given by the error of total optical depth τ, Rayleigh error and the modelling of the other optical depths, including absorption coefficients and absorbing content values. However errors due to absorbing components have been not considered. The error of the total optical depth of the atmosphere, τ, is given by the irradiance measurements, extraterrestrial irradiance and air mass m (according Beer law), but this error has been estimated assuming that the error is only due to irradiance measurements F (the other factors can be neglected). By means of the propagation error theory the relative error of τ is given by

$$\varepsilon(\tau) = \varepsilon(F)/\tau m$$

Therefore we have establish the error of F based on error calibration and other uncertainties linked with the measurements process. As we have described elsewhere (*Cachorro et al.*, 1998) the error of the measured irradiance with our Licor1800 spectroradiometer was estimated as 5% from 370 to 1 000 nm. The uncertainties linked with the calibration method and between two successive calibrations are about 3% from 370 to 1 000 nm. This result has been also verified during the calibration and field measurements of this intercomparison campaign between the different Li-Cor spectroradiometers and other instruments (see chapter 7 for details).

The behaviour of the Li-Cor1800 in the range 370-320 nm is reasonably good but it fails below 320 nm wavelength. Furthermore the use of the optical fiber shows a high unstability in the measurements compared when it is not used. This behaviour has been observed during the calibration process and it can be analysed by figure 3. This figure 3 shows the measured spectrum of the calibration lamp #4 in the spectral region 300-370 nm given by Brewer #150 (INTA) and the three Li-Cors belonging to the University of Barcelona (serial number RS-415, BAL), Valladolid and Valencia respectively. The relative differences between our Licor and Brewer #150 decreases from −10% to 10% from 300 nm to 320 nm, falling to 3% at 330 nm and maintaining this 3% at 360 nm, however the standard deviation have the values ±20% from 300 to 320 nm, decreasing to 10% at 330 nm and 3% at 360 nm. The other two Licors have lower values due to the mentioned problem of the optical fiber.

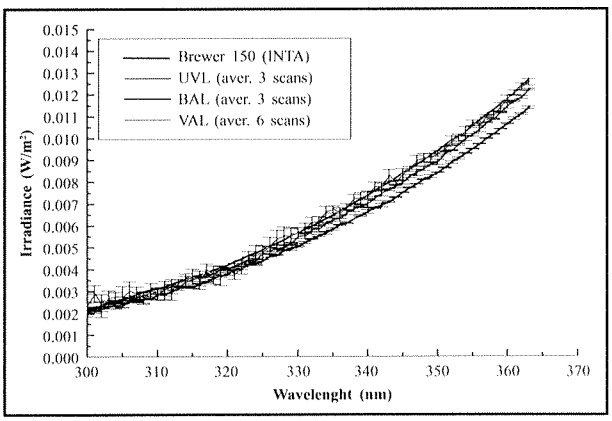

Figure 3. *Irradiance (W/m²) measured by the Brewer #150 (INTA) and the three Li-Cors belonging respectively to the Universities of Valencia UVL, Barceloba BAL and Valladolid VAL for the calibration lamp #4.*

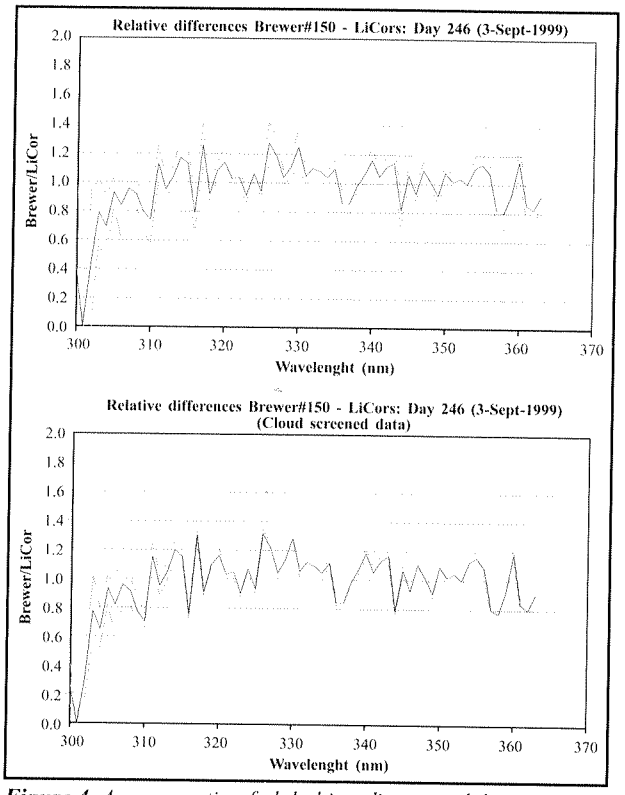

Figure 4. *Average ratio of global irradiance and their standard deviation between Brewer #150 (INTA) and Li-Cor of the GOA-UVA, VAL, for all measured spectra of day 246 including irradiance spectra measured under cloud conditions (top) and removing them, called cloud screening (bottom).*

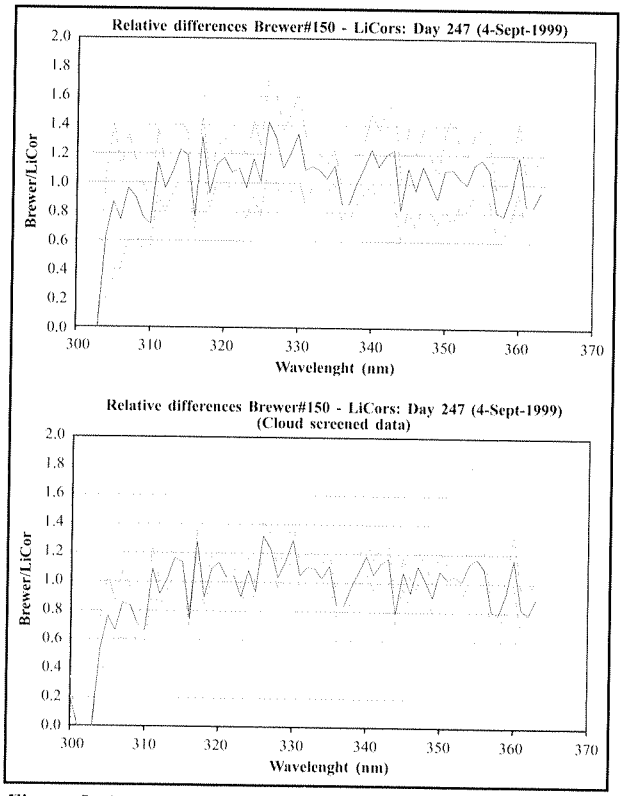

Figure 5. *Average ratio of global irradiance and their standard deviation between Brewer #150 (INTA) and Li-Cor of the GOA-UVA, VAL, for all measured spectra of day 247 including irradiance spectra measured under cloud conditions (top) and removing them (bottom).*

The comparison of our Li-Cor1800 spectroradiometer with the Brewer #150 (INTA) during the field measurements campaign have assessed the behaviour and performances of our spectroradiometer in the UV region. An illustrative example of this comparison can be seen in figures 4, 5 and 6. We have evaluated the ratio between Brewer and Li-Cor instruments taking all the global irradiance spectra measured each day. In figure 4 we depicted this average ratio and their standard deviation for day 246 without cloud screening (top) and with it (bottom). The same appears in figure 5 for day 247 spectra where cloud screening is more evident. The best agreement is about a 20% of difference in day 246 under cloud screening for wavelength greater than 320 nm, but differences as high as 40% can be observed in day 247.

Figure 6 shows this evaluation for specific wavelengths behaviour as a function of daytime evolution. As can be observed wavelength 330 nm has a bad behaviour than 320 nm, but in general below 320 nm the behaviour of the Li-Cor spectroradiometer is very unstable and we recommend to be not used. At 320 nm the behaviour of the system is still reasonable (see later figure 10). Obviously fields measurements gives higher differences than those of laboratory.

Concerning to AOD error, we must note that error propagation theory gives lower errors for high air masses, but these cases generally correspond to lower values of irradiance measurements, which yield greater uncertainties. Also considering the error of calibration the values of the AOD at high air masses gives lower error that at low air masses (see figure 8). This behaviour seems to be confusing and not realistic, but it has observed systematically from other sets of data.

We have evaluated the error for the AOD (including the Rayleigh error) at 500 nm resulting in values about 4-28% assuming an error for the irradiance of 5%. The same evaluation at 350 nm gives about 1-17% assuming an error of 10% for the irradiance. On the other hand we have evaluated the differences between the AOD determined during the days of the campaign (see results paragraph) taking the calibration of our Li-Cor at the arrival of the campaign and the calibration carried out during it (see figure 8). This figure 8 confirms the fact that the AOD determination is better at high air masses in spite of the fact of lower irradiance values and that the error is lower at visible wavelengths than at UV and infrared wavelengths.

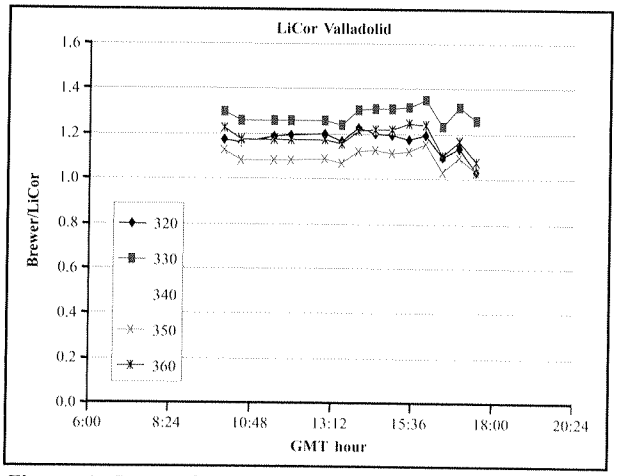

Figure 6. *Ratio of global irradiance between Brewer #150 (INTA) and Li-Cor of the GOA-UVA, VAL for specific wavelength at 320, 330, 340, 350 and 360 nm for all measured spectra during day 246 with cloud screening.*

9.4. RESULTS: MONITORING AND INTERCOMPARISON OF THE AEROSOL OPTICAL DEPTH

The atmospheric conditions during the days of the campaigns were in general very good, with clear skies that allowed a lot of spectral irradiance measurements for a good intercomparison process. Therefore, the monitoring of different atmospheric parameters has been carried out. The days used for the comparison were 3, 4, 5, and 8 September (Julian days: 246, 247, 250 and 251). Morning of day 247 days showed episodes of clouds but the other days were wonderful clear days.

These cloudy situations are very interesting because they allow the analysis of the influence of clouds on UV spectral irradiances, mainly if simultaneous measurements are carried out with Li-Cor1800 and Brewer spectroradiometers, with very different time scanning.

In figure 7(a-d) we show the evolution of the aerosol optical depth at the wavelengths: 320, 350, 500, 550, 670, 865 and 1 000 nm during the days 3, 4, 7 and 8 September of 1999 respectively.

Taking the AOD at 500 nm as a reference turbidity index, this parameter shows high values during day 3 September from 0.3 to 0.2 with slight lower values in the afternoon of day 4 September. About 0.2 in the afternoon of day 7 September and 0.1 during practically all the 8 September day with increasing values during last hours in the afternoon. We must note that the decreasing of AOD when the wavelength increases: i.e. 500 nm respect to 1 000 nm.

UV wavelengths at 320 nm and 350 nm show higher variations, mainly the day 3 September, but both wavelengths have equal values and follow a similar evolutions and tendencies. The similar behavior during these days allow us to model and predict UV radiation and UVI index taking the AOD at one wavelength and assuming practically not dependence on wavelength. This assumption is very good for effective irradiance and UVI index but less good for UVA modeling. As we have seen between 350 and 400 nm the variation of the AOD can be significant. Note however, their higher values compared with those at visible wavelengths and also the bad behaviour of 320 nm at high air masses.

In figure 8 we show the differences of the whole determined AOD data set (given in figure 7) at different wavelengths based on the calibration factor before (the factor at the arrival to the campaign) and after the "in situ" calibration of the campaign. The differences range from 0 to 2% at 670 nm wavelength; 0-5% at 350 nm and 0-7% at 500 nm, but at 320 nm these differences reach values about 20%. As can be seen these differences are the lowest at high air masses (low SZA), which is certainly very surprising.

Comparison between Li-Cors of Valladolid and Valencia

Figure 9 (top) shows the comparison between three measured spectra of the aerosol optical depth given by the Li-Cors of the University of Valladolid and Valencia, which were compared during the afternoon of day 250 (see also day 250 of figure 10). The differences in percentage of the three above spectra are depicted in figure 9 (bottom), being under 20% in the spectral range 400-1 000 nm.

The behaviour of the instrument at wavelengths greater than 1 000 nm shows a strong dependence on the temperature, which can explain the differences at these wavelengths.

The differences in the visible range are lower, falling about 10% as maximum, due to the non-existence of strong absorption band, like those of water vapor in the near-infrared. However, these relative differences seem to depend on the solar zenithal angle, and obviously on the values of the AOD.

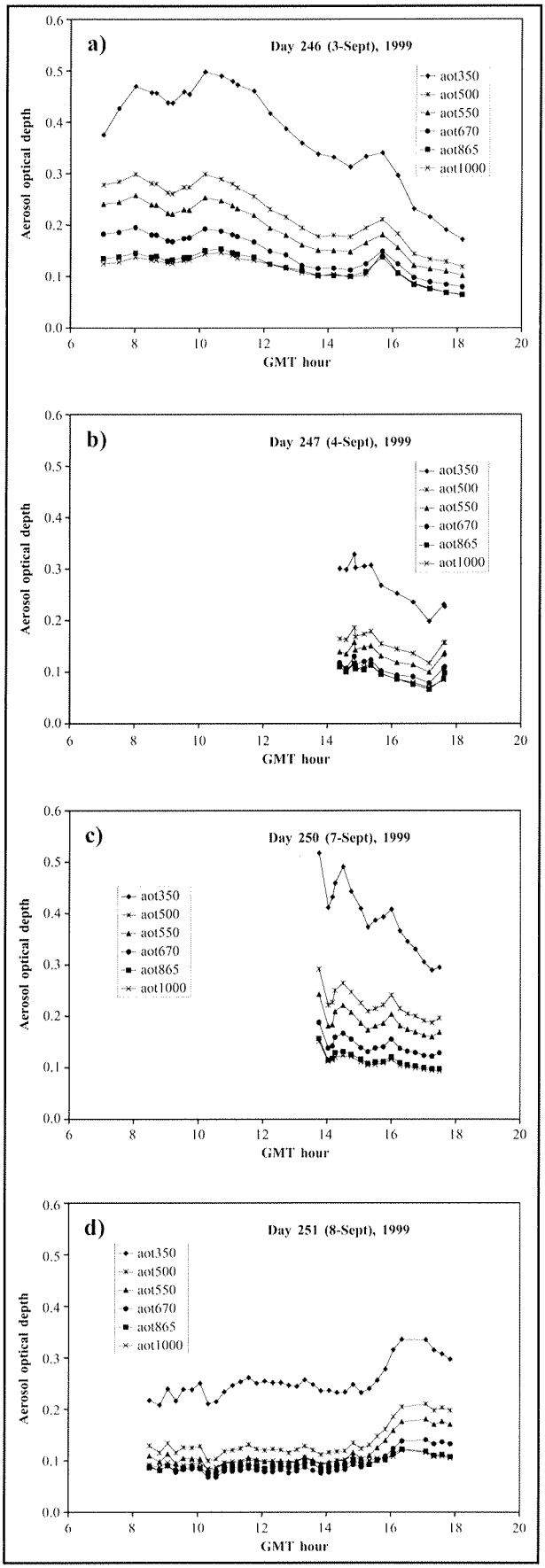

Figure 7(a-d). *Temporal evolution of experimental aerosol optical depths at different wavelengths during the days 246, 247, 250 and 251 of the intercomparison campaign given by the Li-Cor1800 (VAL) spectroradiometer.*

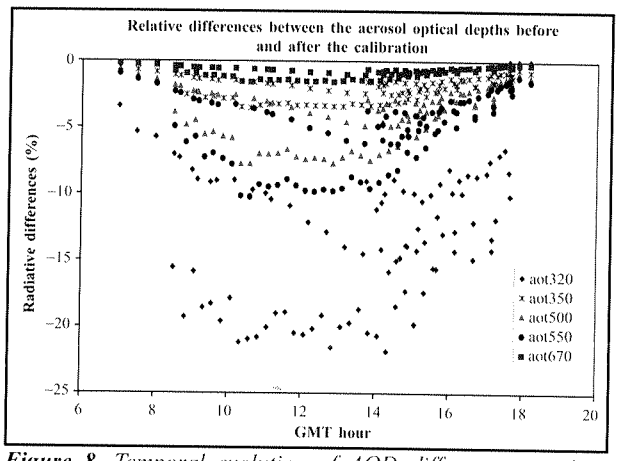

Figure 8. *Temporal evolution of AOD differences at given wavelengths of the whole data set before and after the "in situ" calibration at the intercomparison campaign for the GOA-UVA Li-Cor1800 spectroradiometer.*

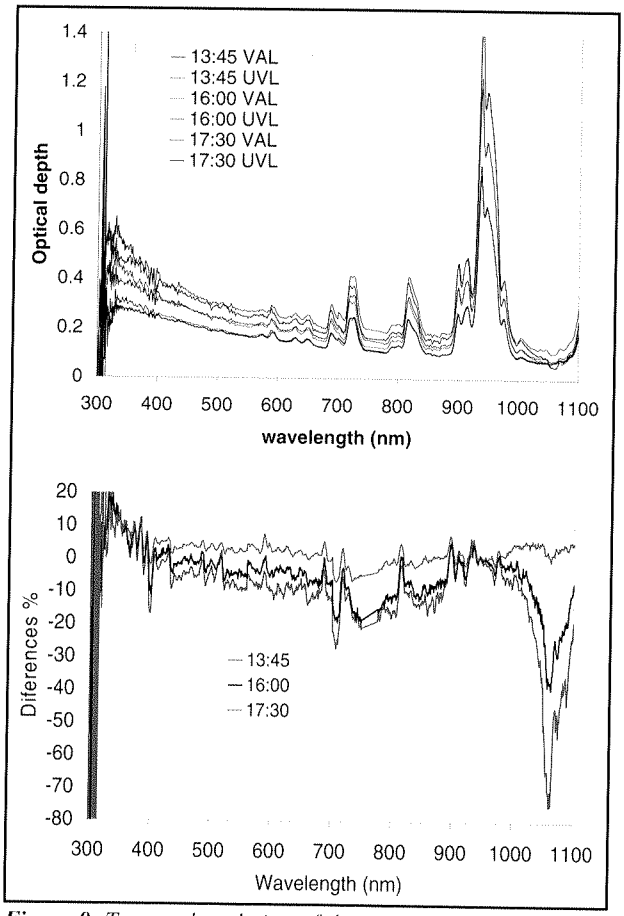

Figure 9. *Temporal evolution of three spectra of the AOD for Li-Cors of Valladolid (VAL) and Valencia (UVL) (top) and their corresponding relative differences (bottom).*

Comparison Li-Cor-Brewers

Figure 10 shows the comparison between the values of the AOD at 320 nm wavelength given by Li-Cor1800 of the GOA-UVA and the Brewer #150 (INTA), #157 (INM-Izaña) and #47 (INM-Portugal) during three days of the campaign, 246, 247 and 250. In the afternoon of Julian day 250 the Li-Cor of the group of the University of Valencia is also included. The agreement is very good taking into account the different characteristics of these instruments and the three methods involved. Brewer #47 is a simple monochromator and the other two have double monochromator (MKIV system, see Chapter 3). Brewers #47 and #150 used the method of Carvalho and Henriques (2000) while Brewer #157 use the standard method (*Kerr*, 1995). Also it can be observed that the measurements are not carried out exactly at the same time but the elapsed time between them allows a correct semi-quantitative comparison.

In day 246 very similar evolution in the values of the AOD at 320 nm can be observed between the two Brewers of double monochromator and the GOA-UVA Li-Cor. The differences between the two Brewers are greater than those with Li-Cor and are about 20%, except at high air masses. Morning of day 247 presented episodes of clouds, which are clearly observed in the scatter points between the three Brewers. The afternoon had better atmospheric conditions but no good agreement was obtained. However a very good agreement can be observed in day 250 between all the compared spectroradiometers. Again, we observed as the values of the two Li-Cors differ with those of Brewers at high air masses.

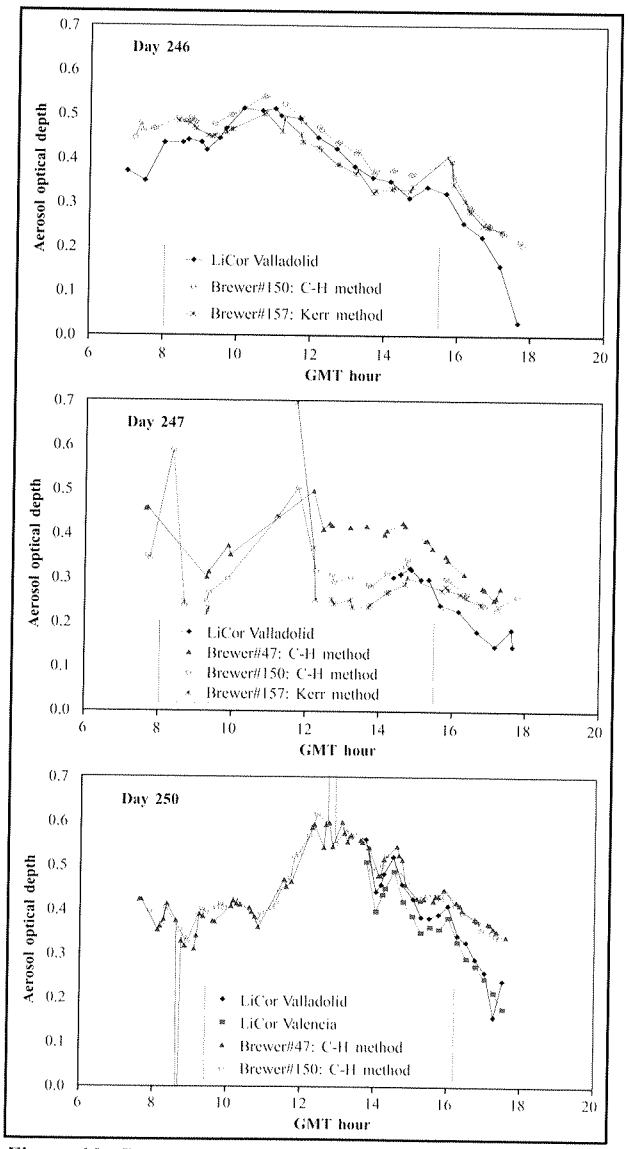

Figure 10. *Comparison of the evolution of the AOD at 320 nm between three Brewer and two Li-Cors during the Julian days 246 (3 Sep.), 247 (4 Sep.) and 250 (7 Sep.) derived using different methods.*

Comparison Li-Cor, Microtops and Cimel

From the various days of the campaign we show AOD's intercomparison at visible and infrared wavelengths between Microtops, Cimel and Li-cor1800. Microtops (belonging to the INM-Izaña) only has AOD data at 1 020 nm and hence the comparison with the Li-Cor and Cimel of GOA-UVA is carried out at this wavelength. We must note that the values of Li-Cor were evaluated at 1 000 nm but in this case the differences can be neglected. Usually three (or four) measurements are performed for one datum for Microtops, hence we show the average value and the standard deviation (vertical bars). These results can be seen in figure 11 (top) for Microtops and Li-Cor for all the available data of the campaign, where Julian day 247 was excluded for cloud screening of Microtops. We must note that the AOD is very low at this wavelength. Generally Microtops gives higher values than Li-Cor, observing values as high as 0.3.

As can be seen great scatter is obtained in many measurements, which appear as bad data. In figure 11 (bottom) only the data of day 3 September are compared, where we can observe more clearly the differences, with a better agreement in the afternoon.

In Figure 12, corresponding to 8 September we have added to the data of the two earlier instruments the available data of Cimel photometer. The figure 12 shows in general a good agreement.

We depict in figure 13 the comparison between our Li-Cor and Cimel for day 8 September where the AOD are given at 850 nm, 670 nm and 440 nm wavelengths. As can be seen a relative good agreement is found at 850 nm but significant differences is found at 670 nm and 440 nm, with values differing as twice. These high differences at the two lower filters can not be explained because so high can not be due to the interference of absorption. Furthermore at these wavelengths a better behaviour is generally expected respect to that at infrared wavelengths. The absolute error of Cimel AODs is about 0.01-0.02 at these wavelengths given rise to a maximum relative error of 8-20% for these AOD (*Holben et al.*, 1998).

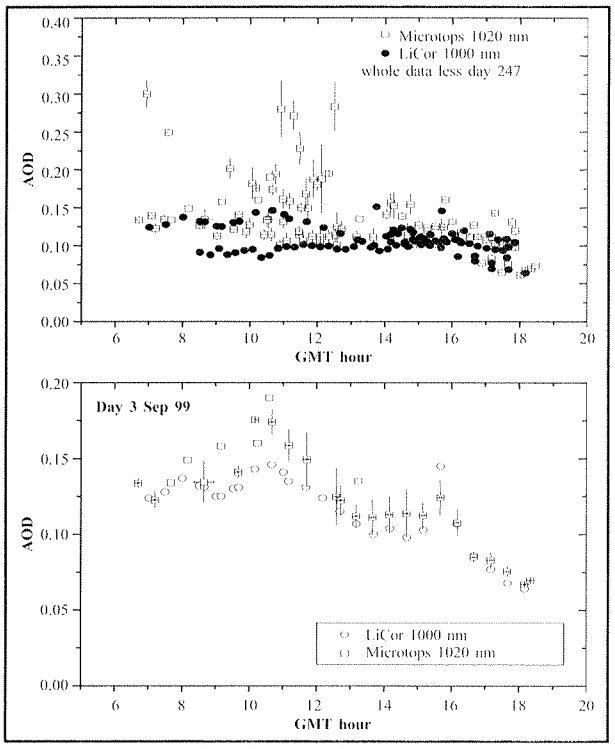

Figure 11. *Temporal evolution of the AOD given by the Li-Cor (1000 nm) of Valladolid and Microtops of INM-Izaña (1 000 nm) for the whole data set (247 was excluded) of the campaign (top) and during day 3 September (246 day) (bottom).*

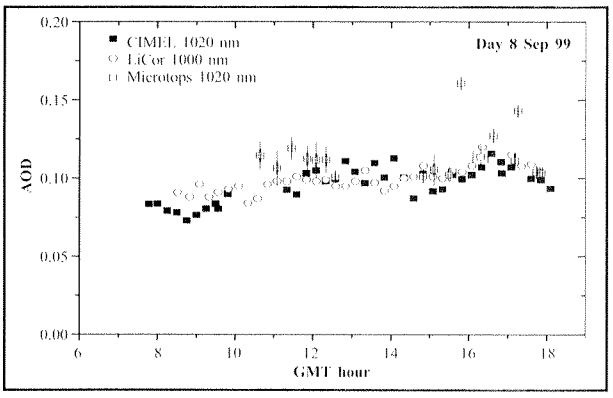

Figure 12. *Temporal evolution of the AOD during day 8 September for the Li-Cor (1 000 nm) and Cimel (1 020 nm) of Valladolid and Microtops of INM-Izaña (1 020 nm).*

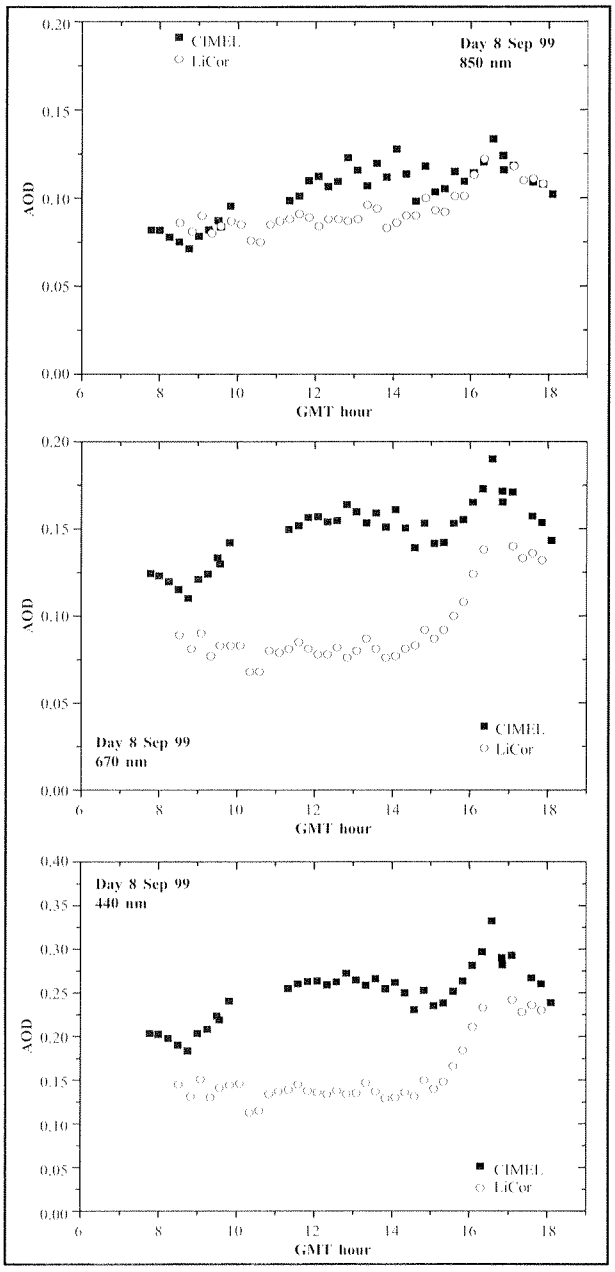

Figure 13. *Temporal evolution of the AOD during day 8 September (251 day) for the Li-Cor and Cimel of GOA-UVA for 850 nm, 670 nm and 440 nm wavelengths.*

9.5. RETRIEVAL OF THE ANGSTROM PARAMETERS

From the above explained window method for the Li-Cor1800 we have derived the modelled aerosol optical depth and the Ångström turbidity parameters α and β. In figure 14 we depicted the values of α for all the available data of the campaign. The values of Julian days 246 and 250 fall between 1.2-1.5 and those of 247 and 250 between 1.0-1.3 with not high variations during the day.

Figure 15 shows the α parameter for Julian days 246 and 250 obtained by the fit at three different spectral intervals: the spectral interval used by the window method, the visible 400-670 nm interval and in the UV 350-400 nm interval. As can be seen the α values determined using the two visible intervals give expected similar values but those of UV are very different. Furthermore the high differences at central hour of the day contrasts with the more similar values at high air masses. This behaviour of UV α values seems to be dependent on the solar zenithal angle but we can not assess this dependence. At high air masses the AOD is very difficult to determine and due to multiple scattering contribution of molecules, which is not accounted for, hence we have a great uncertainty. In the bibliography there is not current α values determined in the UV region, therefore the difficulty to assess these values.

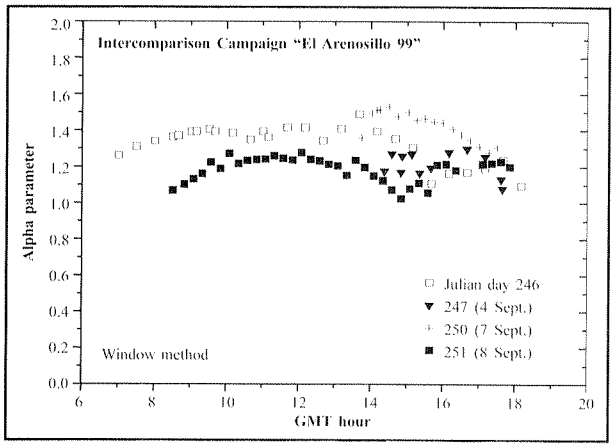

Figure 14. *Temporal evolution of the* α *parameter derived from data of Li-Cor of Valladolid by the window method during the campaign.*

9.6. RETRIEVAL OF THE AEROSOL OPTICAL PROPERTIES BY THE AOD SPECTRAL FEATURES

The columnar physical and optical properties of aerosol: effective radius, volume, single scattering albedo, asymmetry factor, etc., have been obtained by means of the derived Ångström parameters during four days of the campaigns.

The method have been described in detail elsewhere (*Cachorro et al.*, 2000b) and is based on the retrieval of the columnar aerosol particle size distribution function $\eta_c(r)$. This is carried out by the Mie scattering theory, which relates the AOD $\tau_a(\lambda)$ with $\eta_c(r)$ according to

$$\tau_a(\lambda) = \int_{r_1}^{r_2} \pi r^2 Q_e(n, x)\, \eta_c(r)\, dr$$

where $\eta_c(r)$ is normalised to the total vertical content of particles N_c (in cm^{-2}); $Q_e(n, x)$ is the Mie extinction efficiency factor for spherical particles and depends on the particle refractive index $n = n_R - n_I i$ and on the particle Mie size parameter $x = 2\pi r/\lambda$; r is the particle radius and r_1, r_2 are the lower and upper limits of the particle size distribution function.

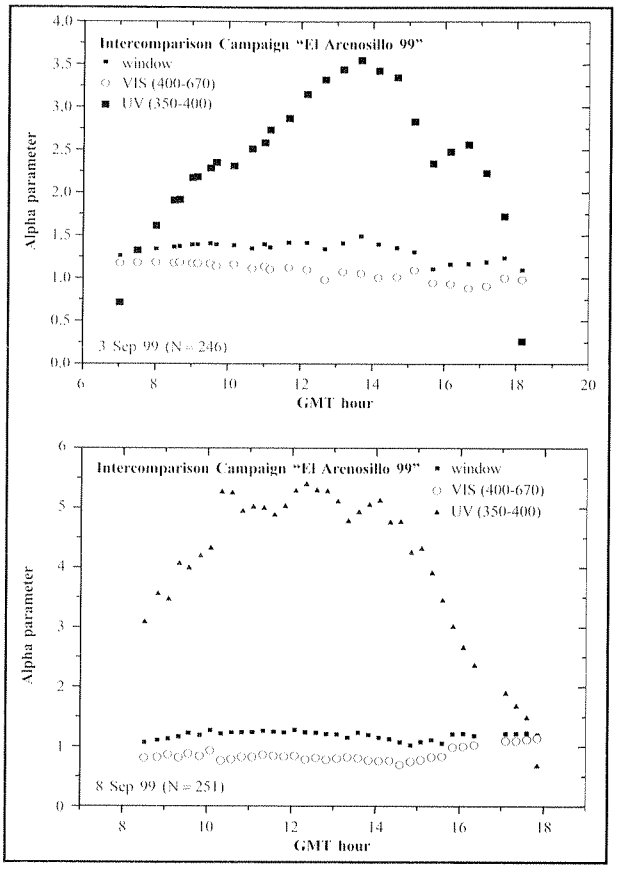

Figure 15. *Temporal evolution of the* α *parameter during days 3 (top) and 8 of September (bottom) derived from the Li-Cor of Valladolid by three different spectral fit procedures.*

The method used here to retrieve the $\eta_c(r)$ function is not a classical inversion method but a minimization technique between "experimental" and theoretical values (*Vergaz*, 1996). This means that we must assume a given particle size distribution function $\eta_c(r)$. We have selected a single monomodal lognormal function because it seems to be adequate based on current aerosol models. This function is defined by the mean geometrical radius or median radius r_g and the geometrical standard deviation σ. The r_g parameter is obtained based on the spectral features of the AOD (the AOD spectrum is normalised to area 1) and N_c on their absolute value, but previously we need to assume a given value for σ. The choice of a value for σ equal to 2.5 was based on the expected climate characteristics of the aerosols in our area of study and taking into account the values given in current aerosol models. However it is easily observed from the method that the retrieved r_g values are dependent on this choice. Greater σ values give lower r_g values and viceversa. Another parameter we also need as input in the retrieval is the particle refractive index n of atmospheric aerosols, which was taken as $n = 1.5\text{-}0.01i$.

Once the particle size distribution is determined we can evaluated their moment to characterize their properties. The moments, M_k, of a particle size distribution function $\eta_c(r)$ are given by

$$M_k = N_c \int_{r_1}^{r_2} r^k\, \eta_c(r)\, dr$$

that for the case of a lognormal function gives

$$M_k = r_g^k \exp\left(\frac{1}{2} k^2 \ln^2 \sigma\right)$$

Therefore, if r_g and N_c and σ parameters are known it is easy to compute the effective radius r_{eff}, the volume v (μm) or surface s and the mass loading M of atmospheric aerosols (for the latter an assumption over the average atmospheric density of aerosols is needed). Together with these physical properties, also the radiative properties must be evaluated, like the parameter of asymmetry $g(\lambda)$, the single scattering albedo ω_o and the single scattering phase function. For details of the procedure and retrieval of these parameters see *Cachorro et al.* (2000b).

The single scattering albedo, ω_o, is the ratio between the scattering and the extinction volume coefficients and is given in part by our assumption about the choice of the particle refractive index in the pseudo-inversion procedure. The asymmetry parameter g gives the scattering properties of the aerosols. It is defined according to

$$g(\lambda) = \frac{N_c}{\sigma_{sc}(\lambda)} \int_{r_1}^{r_2} \pi r^2 g(n, x) Q_{sc}(n, x) \eta_c(r) dr$$

where $\sigma_{sc}(\lambda)$ is the volume scattering coefficient. Both parameters, g and ω_o, will be necessary as secondary parameters to model global spectral irradiances in the UV, visible, near infrared ranges (*Cachorro et al.*, 2000d).

In figure 16 we show the evolution of the effective radius and the single scattering albedo ω_o and asymmetry parameter g for the above four referred days of the campaign. No great variations are observed during these days of similar atmospheric conditions: the effective radius ranges about 0.1 μm, g is about 0.6 and 0.93 for ω_o.

The determination of g and ω_o are also of interest for assessing UV modeling although these parameters are of second order of importance respect to the ozone absorption and aerosol optical depth contribution.

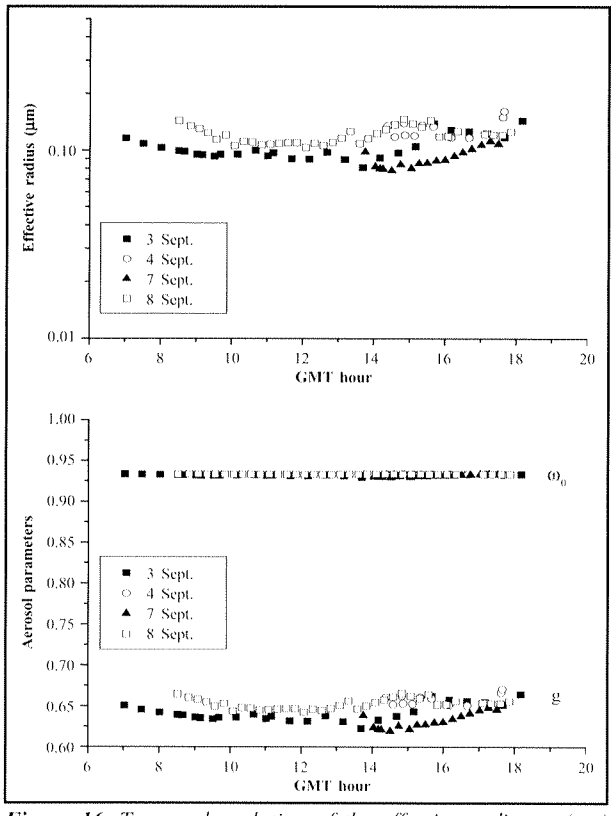

Figure 16. *Temporal evolution of the effective radius r_g (top) and the single scattering albedo ω_o and asymmetry parameter g (bottom) for various days of the campaign.*

9.7. RETRIEVAL OF THE COLUMNAR WATER VAPOR CONTENT (CWV)

The vertical (columnar) water vapor content w (CWV) (in cm, cm-pr units or g/cm^2) has been determined taken the same direct spectral data measured by the Li-Cor1800 by a method described elsewhere (*Cachorro et al.*, 1998). Comparative data with Cimel and Microtops have been carried out. Theoretically the three instruments use the 940 nm absorption band to determine the water vapor content, but the methods are different. Cimel and Microtops use the differential absorption method taking two spectral filters, one in the absorption band and the other at a window of non-absorption.

Li-Cor1800 uses another method based on the form of the whole absorption band. The quantitative derivation of a unique water vapor value is made by curve fitting of measured to modelled data by an iterative non-linear square fitting technique. This method can be applied using either the absolute or relative irradiance or transmittance values, but here we have used absolute values because we have previously evaluated absolute aerosol and Rayleigh contributions with the procedure already described.

Generally, the vertical integrated water vapor amount or the columnar water vapor (CWV) (also precipitable water vapor) w is distinguished from the equivalent absorbed water vapor amount w* but both are linearly correlated. We determined this correlation (*Cachorro et al.*, 1998) using the six atmospheric model profiles of *McClatchey et al.* (1972) obtaining $w = 1.16\, w^* + 0.063$ (correlation coefficient equal to 0.99).

Water vapor transmittance function in the 940 nm absorption band follows the LOWTRAN7 Code formulation

$$T_{H_2O}(\lambda) = \exp(-[C_{H_2O}(\lambda)\, w\, m]^a)$$

where $C_{H_2O}(\lambda)$ are the corresponding water vapor absorption coefficients taken from the current version of LOWTRAN7 and a is a constant which varies depending on the absorption band. These coefficients do not contain the absorption by continuum, which is considered by means of other multiplicative transmittance. To do this, a procedure was developed to parameterise the LOWTRAN7 continuum absorption transmittance in an easy and operational way, where the same functional form as above was assumed (but with $a = 1$) to obtain the continuum absorption coefficients. Therefore we have determined the water vapor content, considering the continuum absorption contribution and without it. The differences are significative, as can be observed in figure 17 for the four days of measurements during the campaign. The relative differences can reach values as high as 50% if we consider that the values of water vapor determined with the continuum are the reference values.

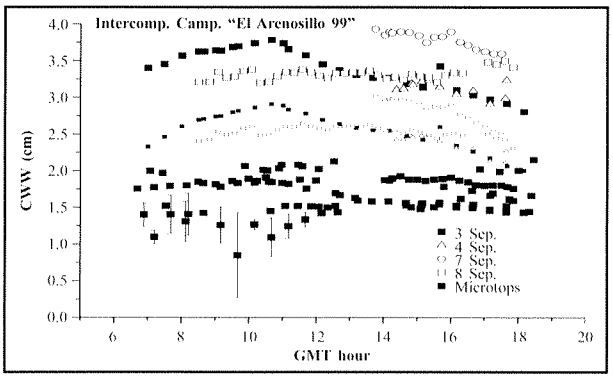

Figure 17. *Temporal evolution of the columnar water vapor without the continuum absorption and considering it, with the turbidity parameters determined by the window method at the visible-infrared spectral region, for various days of the campaign. These data are retrieved from Li-cor1800 VAL. Also added the Microtops data.*

Before the discussion relative to these differences of continuum contribution we can see in figure 17 the determination given by Microtops, which are the lowest values, below 2 cm, and with high scatter values in some cases.

Apart of the differences due to the different instrumentation and methods we must point out the current problems for water vapor determination research in solar spectroradiometry in visible-near infrared region. Recent spectroscopic measurements of water vapor lines in the visible and near infrared show significant differences. Some of them have been recently incorporated into HITRAN96 (*Giver et al.*, 2000) but other are very news and are not incorporated (*Belmiloud et al.*, 2000).

Obviously LOWTRAN7 data are very old compared with the results given by more recent line-by-line models (CKD2 model, see *Ingold et al.*, 2000, *Schmid et al.*, 2000). The new incorporated in recent processing data in sunphotometer do not gives significant differences and less to explain our differences. Perhaps the method used by us to quantify the continuum absorption must be revised. Certainly the differences increases when the water vapor increases but the differences obtained by us in the Intercomparison campaign are very high. Therefore we investigated in more detail the different contributions due to aerosol and continuum involved with our method, in order to observe their influence.

For example we have investigated the influence of aerosol contribution depending on how the Ångström turbidity parameters α and β are obtained. The new water vapor values are depicted in figure 18 (magenta colour squared points) and were obtained using three new windows, (the two earlier windows around the A oxygen band and a new one centered at 860 nm). We have taken an example in figure 19 where the spectrum shown clearly the different behaviour in the visible and infrared. The Ångström parameters determined in the VIS-NIR range do not fit very well in the last part, from 800 to 1 000 nm, therefore we performed a new fit, just in the zone of the 940 nm band with the three mentioned windows.

These new Ångström parameters are not realistic to model the spectrum but are correct to determine the water vapor content in the 940 nm absorption band. The cause of this new choice is due to the same definition of formula and the observation when processing each solar spectrum. The values determined in the visible-infrared region give less good agreement between experimental and modelled data in this far spectral region. We do not take a window around 1 000 nm due to the observed behaviour dependence on temperature of Li-Cor1800 in this spectral region (see figure 19).

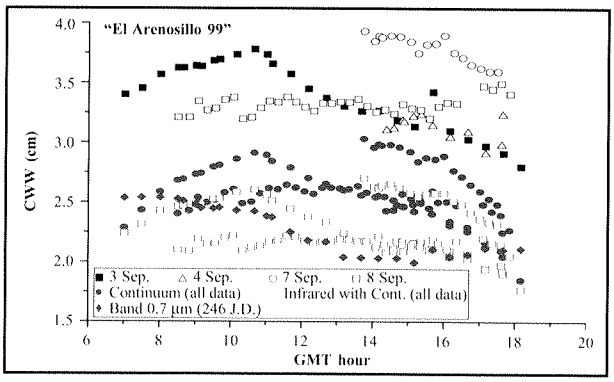

Figure 18. *Temporal evolution of the columnar water vapor without the continuum absorption and considering it with the turbidity parameters determined at the visible-infrared or only in the infrared region (see text). Also added is the determination using band 0.7 µm, for the day 246.*

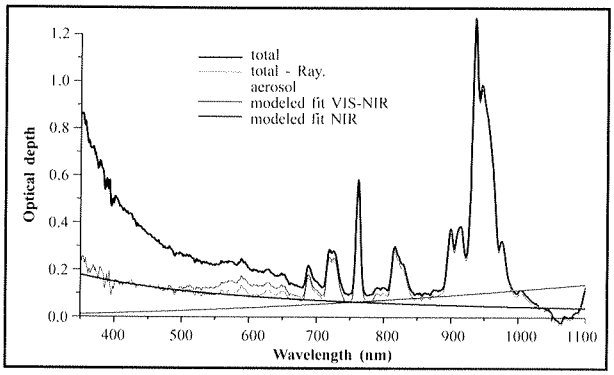

Figure 19. *Optical depths for a processed spectrum showing the two fits using the window method, applied in VIS-NIR spectral range (modelled AOD by blue line) and NIR (modelled AOD by green line).*

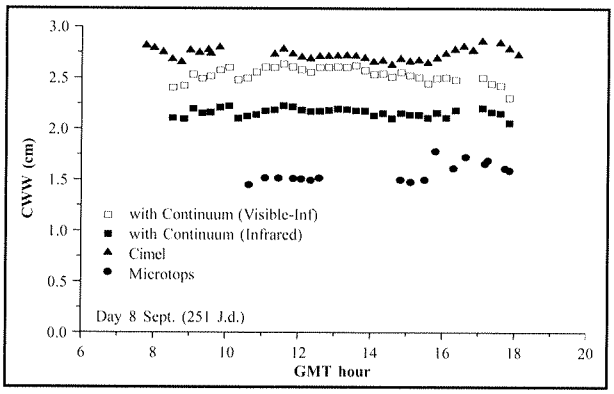

Figure 20. *Temporal evolution of the columnar water vapor with continuum absorption considering the turbidity parameters determined at the visible-infrared (window mwthod) and only in the infrared (see text). Also added is the determination given by microtops and Cimel. The values on shown correspond to Julian day 251.*

The new determined values of the water vapor are also depicted in figure 18 (green circles) where they show the same tendency but are slightly lower (we have considered the continuum absorption).

These results drive us to think in using another absorption band for the determination of water vapor. Using the same method we have taken the 0.7 µm band (0.82 µm band was not chosen because of the observed disagreement between experimental and modelled data) with the Ångström by the window methods. This was applied only to day 3 September and the data can be seen in figure 18 (red rhomboidal points). Also low values were obtained but with a different tendency, compared with their corresponding values using the 940 nm band (back squares). These news results emphasize the problems involved with water vapor determination.

Finally, figure 20 gives the results of day 8 September (251 day) where we have also added the current available data of Cimel. Although the comparison of the CImel data with out Licor data (considering the contiunuum absorption and the window nethod for the turbidity parameters) are very goods, certainly the whole results seem to indicate that this retrieval needs further improvements and assessing. We must note that Li-Cor method is believed to be more accurate than radiosonde and sun-photometer data for integrated vertical water content retrieval. We must note here the similarities and differences of our method respect to the methods applied to sun-photometers (*Schmid et al.*, 2000).

9.8. CONCLUSIONS

The obtained results about the retrievals of the aerosol optical depth and other aerosol properties (turbidity parameter, effective radius, etc.) and water vapor content, during the first Iberian Intercomparison campaign of spectroradiometers in "El Arenosillo" during 1-10 September 1999, show the current research in the determination of these atmospheric parameters in sun-radiometry. The variety of instruments and methods used are a clear exponent of the above sentence.

A very precise and detailed method is used to retrieve the AOD at visible, infrared and UV spectral regions by Li-Cor1800 spectroradiometer. Comparison of AOD at UV with and between Brewers data shows a good agreement, which to our knowledge results in a very original work, furthermore, considering the comparison with Cimel and Microtops in visible and infrared wavelengths. The error associated with the AOD determination drives us to assess the intercomparison at level of irradiance between Li-Cor and Brewer systems.

Other aerosol parameters were also derived from AOD data like the effective radius and the asymmetry parameter and the simple scattering albedo. All of them are necessary for radiative transfer modelling.

The determination of the water vapor by Li-Cor spectroradiometer using band 940 nm points out the problems that exist with this retrieval, which are difficult to detect through photometer determination. The band 0.82 μm is bad modelled by Lowtran7 coefficients and it can not be used for current determination. Bands 0.72 and 0.94 μm give results with very poor agreements. The comparative data with Microtops and Cimel can not help us to assess the detected problems and uncertainties of this spectroradiometric methodology.

ACKNOWLEDGEMENTS

This work was supported by CICYT under project CLI97-0345-CO5-05. The Junta de Castilla y León supported the grant 'FPI' of R. Vergaz. We thanks to L. Sánchez Muniosguren for the coordination of the above project. We also thank to E. Cuevas (INM-Izaña Group), J. A. Martínez-Lozano (Solar Energy Group from University of Valencia), J. Lorente (Dept. of Astronomy and Meteorology from University of Barcelona), B. de la Morena (INTA/El Arenosillo), J. P. Díaz of La Laguna University (Tenerife), D. Henriques (INM-Portugal) as responsible of the Research Groups involved in this Intercomparison campaign. J. P. Díaz and F. J. Expósito for providing calibration files. To M. J. Vilaplana, and J. Gröbner for their specific help in this work and A. Redondas, P. Utrillas and L. Pedrós, for providing data.

REFERENCES

Bais, A. (1997): "Absolute spectral measurements of direct solar ultraviolet irradiance with a Brewer spectrophotometer", *App. Opt.*, **36**, 5199-5204.

Bates, D. R. (1984): "Rayleigh scattering by air", *Planet. Space Sci.*, **32**, 785-790.

Belmiloud, D., R. Schermaul, K. M. Smith, N. F. Zobov, J. W. Brault, R. C. M. Learner, D. A. Newnham and J. Tennyson (2000): "New studies of the visible and near-infrared absorption by water vapour and some problems with the HITRAN Database", *J. Geophys. Letter*, **27**, 3703-3706.

Cachorro, V. E., M. J. González, A. M. de Frutos, and J. L. Casanova (1989): "Fitting Ångström formula to spectrally resolved aerosol optical thickness", *Atmos. Environ.*, **23**, 265-270.

Cachorro, V. E., P. Durán and A. M. de Frutos (1996): "Retrieval of vertical ozone using the Chappuis band with high spectral resolution solar radiation measurements", *Geophys. Res. Lett.*, **23**, 3325-3328.

Cachorro, V. E., P. Utrillas, R. Vergaz, P. Durán, A. M. de Frutos, and J. A. Martínez-Lozano (1998): "A study about the atmospheric water vapor content determination in the 940 nm band using moderate spectral resolution measurements of direct solar irradiance", *Appl. Opt.*, **37**, 4678-4689.

Cachorro, V. E., P. Durán, R. Vergaz and A. M. de Frutos (2000a): "Measurements of the atmospheric turbidity of the north-center continental area in Spain: spectral aerosol optical thickness and Angstrom turbidity parameters", *J. Aerosol Sci.*, **31**, 687-702.

Cachorro, V. E., P. Durán, R. Vergaz and A. M. de Frutos (2000b): "Columnar physical and radiative properties of atmospheric aerosols in north-central Spain". *J. Geophys. Res.*, **105**, 7161-7175.

Cachorro, V. E., P. Durán, R. Vergaz and A. M. de Frutos (2000c): "Measurements and estimation of the aerosol optical depth in the UV spectral region", Actas de la 2.ª Asamblea Hispano-Portuguesa de Geodesia y Geofísica, pág. 441. Lagos, Portugal.

Cachorro, V. E., P. Durán, R. Vergaz and A. M. de Frutos (2000d): "Características del modelo de radiación en el rango visible-cercano infrarrojo y ultravioleta UVA_GOA", Report to INM from GOA-UVA. Versión 1 (Mayo 2000).

Carvalho, F. and D. Henriques (2000): "Use of Brewer ozone spectrophotometer for aerosol optical depth measurements on ultraviolet region", *Adv. Space. Res.*, **25**, 997-1006.

D'Almeida, G. A., P. Koepke and E. P. Shettle (1991): "Atmospheric Aerosol: Global Climatology and Radiative Characteristics", A. Deepak Publishing. Hampton, VA (USA), 1991.

Gardiner, B. G. and P. J. Kirsch (1993): "Second European Intercomparison of Ultraviolet spectrometers", Panorama, Greece. Report to the Commission of EU. Contract STEP CT900076, Brussels, Belgium.

Giver, L. P., C. Chackerian Jr. and P. Varanasi (2000) : "Visible and near infrared $H_2{}^{16}O$ line intensity correction for HITRAN-96", *J. Quant. Spectr. Rad. Transf.*, **66**, 101-105.

Holben, B. N., T. F. Eck, I. Slutsker, D. Tanré, J. P. Buis, A. Setzer, E. Vermote, J. A. Reagan and Y. A. Kaufman (1998): "AERONET – a federated instrument network and data archive for aerosol characterization", *Remote Sensing Environ.*, **66**, 1-16.

Ingold, T., B. Schmid, C. Mätzler, P. Demoulin and N. Kämpfer (2000): "Modelled and empirical approaches for retrieving columnar water vapor from solar transmittance measurements in the 0.72, 0.82 and 0.94-μm absorption bands", (private communication).

JGR: Journal Geophysical Research (1997): "Passive remote Sensing of the Tropospheric Aerosol and Atmospheric Corrections of the Aerosol Effect", (Special Issue). 102 (D14).

Karr, J. B. (1995): "Observed dependencies of atmospheric UV radiation and trends", Proceedings of the NATO advanced Study Institute on Solar Ultraviolet Radiation: Modelling, measurements and effects. NATO ASI Series, Springer, ISBN 3-540-62711-1.

McClatchey, R. A, R. W. Fenn, J. E. A. Selby, F. E. Volz and J. S. Garing (1978): "Optical properties of the atmosphere", sect. 14 from Handbook of Optics, Ed. by W. Driscoll, W. Vaughan. McGraw-Hill, New York.

Mayer, B., G. Seckmeyer and A. Killing (1997): "Systematic long-term comparison of UV measurements and UVSPEC modelling results". *J. Geophys. Res.*, **102(D7)**, 8755-8767.

Marenco, F., V. Santacesaria, A. F. Bais, A. Di Sarra, A. Papayanis and C. Zerefos (1997): "Optical properties of tropospheric aerosol determined by lidar and spectrophotometric measurements (Photochemical Activity and Solar Ultraviolet Radiation Campaign)". *Appl. Opt.*, **36**, 6875-6886.

Martínez-Lozano, J. A., M. P. Utrillas, R. Tena and V. E. Cachorro (1998): "The parameterisation of the atmospheric aerosol optical depth using the Ångström power law", *Solar Energy*, **63**, 303-311.

Morys, M., F. Mims and S. Anderson (1996): "Design, calibration and performance of MICROTOPS II hand-held ozonometer", (provided by Solar Light Company, Inc. (1996).).

National Research Council (1996): "A Plan for a Research Program on Aerosol Radiative Forcing and Climate Change", National Academic Press, Washington DC.

Shettle, E. P. and R. W. Fenn (1979): "Models for the aerosol of the lower atmosphere and the effects of humidity variations on their optical properties", AFGL-TR-79-0214. Environmental Res. Paper n. 676. Hanscom AFL (Mass).

Schmid, B., P. R. Spyak, S. T. Biggar, C. Wehrli, J. Sekler, T. Ingold, C. Maetzler and N. Kaempfer (1998): "Evaluation of the applicability of solar and lamp radiometric calibrations of a precision Sun photometer operating between 300 and 1 025 nm", *Appl. Opt.*, **37**, 3923-3941.

Schmid, B., Michalsky, D. W. Slater, J. C. Barnard, R. N. Halthore, J. C. Liljegren, B. N. Holben, T. F. Eck, J. M. Livingston, P. B. Russell, T. Ingold and I. Slutsker (2000): "Comparison of columnar water vapor measurements during the fall 1997 ARM Intensive Observation Period: solar transmittance methods", (paper sent for publication, private communication).

User's Guide (1996): "Microtops II. Ozone monitor and Sunphotometer", Solar Light Company, Inc.

Vergaz, R. (1996): "Turbiedad atmosférica y caracterización de los aerosoles mediante medidas espectrorradiométricas", MSC Degree. Department of Applied Physics I. University of Valladolid, Spain.

Wang, P. and J. Lenoble (1996): "Comparison between measurements and modelling of UV-B irradiance for clear sky: a case study". *Appl. Opt.*, **33**, 3964-3971.

WCP-112 (1986), World Climate Program: Space Observations of Tropospheric Aerosols and Complementary Measurements, WMO/TD-No. 389. WMO, Geneva.

WMO (1993), Global Atmosphere Watch, Report of the WMO Workshop on the Measurements of Atmospheric Optical Depth and Turbidity, Bruce Hicks, ed., No 101.

CHAPTER 10
MODELING

Xabier de Cabo, Elies Campmany, Miguel Martín and Jerónimo Lorente
Department of Astronomy and Meteorology, University of Barcelona

SUMMARY

Four radiative transfer models of different complexity (two advanced multiple scattering radiative transfer models and two simple radiative transfer models) have been used to compare their simulations with the measurements carried out during *El Arenosillo '99* intercomparison campaign. The average of the global irradiance measurements (spectral irradiance, UV-A and UV-B integrated radiation) carried out with two well-calibrated double monochromator spectroradiometers Bentham 150, (see chapter 5 for details) at the same location and at the same time over a range of different zenith angles, has been taken as a reference for the comparison with the outputs of the models. In addition to meteorological variables like atmospheric pressure, temperature and relative humidity, aerosol optical properties (single scattering albedo, asymmetry parameter, Angström turbidity parameters and aerosol optical depth) at different wavelengths, total ozone and solar zenith angle were known and were provided as input parameters.

The models have a good agreement with measurements for zenith angles lower than 60°. In this last case the differences between models and instrumental measurements of UV index (UVI) are about ±15% depending on the model (corresponding roughly ±0.8 UVI units). These differences are quite good if we consider the usual measuring uncertainty (±10%) and the fact that UVI is meant for distribution to the public.

10.1. INTRODUCTION

The use of radiative transfer models to study the UV solar radiation reaching the earth's surface has a great interest for different reasons. One would be the need of the knowledge of the solar UV doses which population is exposed in different environments as a consequence of the observed decrease of ozone column. However, there are still few places that have the appropriate measurements of this radiation, i. e., there is a lack of a suitable UV network which let us know the distribution of UV solar irradiance, including its variable spectral composition and hence its variable erythema. The main causes of the scarce UV network are the high prices of instrumentation and the need of periodic calibrations and personal dedication for monitoring the measurements of these delicate instruments. Therefore, in order to obtain representative UV data for every place and carry out a daily forecast of such UV doses appears necessary the use of radiative transfer models which would simulate of this radiation for specific places and atmospheric conditions. On the other hand, the use of simulation models is an important tool in atmospheric research and helps us in the understanding of the different processes involved in the solar radiative transfer.

Modeling at UV wavelengths is more complex than longer wavelengths because at shorter wavelengths the influence of ozone column variations becomes very important and because an important proportion of scattered radiation results from shorter wavelengths. This makes Rayleigh scattering more effective as wavelength decreases. One cause of the uncertainty in the output of a certain radiative transfer model is due to model formulation and parameterizations but another factor lies with the uncertainty in the input parameters. *Schwander et al.* (1997) have studied the uncertainties in modelled UV irradiances due to this fact, showing values between 10 and 50% for spectral irradiances depending on wavelength. *Weihs and Webb* (1997) show that this uncertainty could be considerably higher than the uncertainty in measurements for typically available input data. Therefore, to validate models it is necessary to have good measurements of the atmospheric parameters used as input data and, at the same time, also to have good spectral measurements. In the Arenosillo intercomparison campaign we had both.

Different works have been devoted to UV modeling and comparisons with observations. *Mayer and Seckmeyer* (1997) carried out a systematic long-term comparison between UV measurements and model results. The UV measurements were achieved with a Bentham double monochromator spectro-radiometer, and the radiative transfer model was the UVSPEC, a freely available software package based on discrete algorithm DISORT. Their comparisons show systematic differences between measured and modeled spectral irradiances in the range −11 and 2% for 295-400 nm wavelength interval and solar zenith angles up to 80°.

In the frame of COST Action 713 (UVB Forecasting) an interesting model comparison exercise was carried out (*Koepke et al.*, 1998). Eighteen radiative transfer models in use for the UV index (UVI) calculation were compared with respect to their results for more than 100 experimental clod-free atmospheres and different zenith angle combinations, although they made no comparison with instrumental measurements.

Models were classified into three groups: 1) multiple-scattering spectral models, which generally take into account multiple scattering and vertical atmospheric inhomogeneity, considering the atmosphere like a superposition of layers where absorption and scattering of radiation take place; 2) fast spectral models, based generally on the atmospheric transmittance method, where the atmosphere is considered as only one layer and simulations require very short time; 3) empirical models, which include direct parameterizations in the input data for the UV calculations. The main conclusion of this comparison exercise were the good agreement in the UV index simulations between the multiple-scattering models: they agree in ±0.5 UV index values in more than 80% of the atmospheres considered in the study. This is indeed a good result because modeling includes, besides the formulation of the models, a number of constants like extraterrestrial solar irradiance and the absorption properties of atmospheric gases and aerosols. The fast models show a very different agreement and the empirical models show good results but only for the atmospheric conditions for which they were developed.

Comparisons between model outputs with measurements are important tasks in order to validate the models. In the frame of mentioned COST Action 713, *De Backer et al.* (2001)

show an exhaustive comparison using the UVI measures from five different instruments at four locations with different latitude and climate and UVI simulations from 13 models but only location, total ozone and solar zenith angle were provided as input parameters. Due to this situation the modelers had to decide what meteorological parameters, aerosol and albedo they should use. Moreover, most instruments do not measure up to 400 nm and it was necessary to do some interpolation. In these comparisons we have observed a big discrepancy between the outputs when we only slightly changed the aerosol optical properties or the ozone values, always using the same model. This has been confirmed by other authors (*Mayer et al.*, 1997; *Pachart et al.*, 1997; *Weihs and Webb*, 1997; *Lorente et al.*, 1994).

In this chapter, four radiative transfer models of different complexity have been used to compare their simulations with the measurements carried out during the campaign.

10.2. METHOD

During the campaign the following atmospheric variables were available:

- Total ozone column obtained by means of measurements from Brewer spectrophotometers.
- Meteorological variables, like atmospheric pressure, temperature and relative humidity.
- Diverse of optical properties of aerosols like single scattering albedo, asymmetry factor, Angström turbidity parameters and aerosol optical depth (AOD) at different wavelengths. Most of these aerosol parameters were calculated from direct irradiance measurements carried out with two spectro-radiometers Li-Cor 1100 and two different photometers, Microtops II and Cimel (see chapters 7 and 9).

The knowledge of these input parameters has been very important to obtain better fitting between the models and the measurements which only worked with standard input values. The spectral irradiance measurements used for comparisons were the average of those corresponding to two spectro-radiometers Bentham 150 which were operating simultaneously. These instruments, as it is explained in the fifth chapter, presented a good calibration and we also had their slit function.

Taking into account that we only had measurements of two days which did not correspond at the same cloudy situation, we do not show any statistic study. The first day (3.rd of September, day 246) was a cloudless day, whereas the second day (4.th of September, day 247) the cloudiness until noon was between 1/8 and 2/8 of small *cumulus*. During these last measurements the clouds did not cover the sun but they incremented slightly the global irradiance because the appreciable increment of diffuse irradiance which these clouds produced. The few measurements with clouds covering the sun were easily detected by means of the notes taken during the measurements and with the spectral graphics of global irradiance. An example of a measurement with clouds covering the sun, although only for few seconds, can be seen in Figure 9.1 which corresponds at 11:30 UTC of day 247 but it has not been used for the comparison.

From all of the measurements made on 3.rd and 4.th of September we have selected those corresponding, approximately, at 80º, 60º, 45º and 30º zenith angles because these are usually used in model comparisons. Ten daily measurements (five before noon and five after noon) of spectral irradiance in the wavelength interval from 290 nm to 400 nm with spectral resolution of 0.5 nm were considered. The spectral resolution used in the models was 1 nm because it is the maximum resolution of some of the models used.

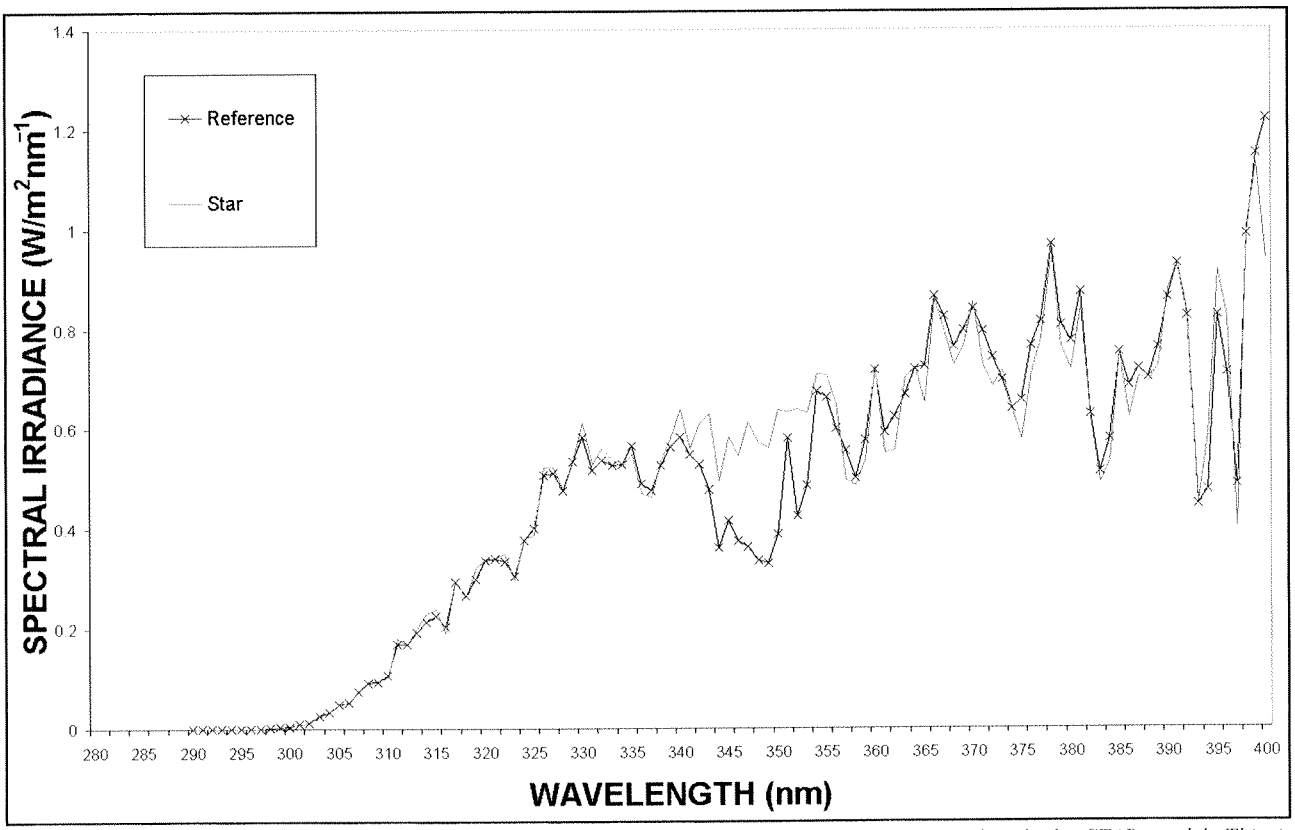

Figure 1. *Global irradiance day 247 at 11:30 GMT compared with the corresponding simulated with the STAR model. This is an example of a measurement with clouds covering the sun during few seconds. While the spectroradiometer is scanning between 340 and 350 nm, the irradiance is lower than it should be.*

The model inputs were: zenith angle; temperature, atmospheric pressure and relative humidity at station level, total ozone column, β and α Ångström parameters, aerosol optical depth (AOD) at 350 nm, 500 nm and 550 nm. Also, when a selected reference atmosphere was necessary, we chose the standard mid latitude atmosphere. For the aerosol atmosphere we considered an oceanic or maritime type. The albedo was of 0.1 for the whole UV spectrum because it is the one that corresponds to forest (pine tree) surface like that which surrounded the whole measurement zone.

To make the comparison we have calculated the absolute and relative differences between models and reference values for ultraviolet index (UVI) and UVA and UVB integrated irradiances. The spectral irradiance from 290 to 400 nm has been considered as well.

The UV index is dimensionless and is defined as:

$$UVI = 40 \int_{290}^{400} I_\lambda \cdot \varepsilon_\lambda \, d\lambda \qquad [9.1]$$

where I_λ is the spectral irradiance at wavelength λ and ε_λ is the CIE action spectrum (*McKinlay and Diffey*, 1987).

10.3. THE MODELS

Four radiative transfer models were used in this work:

a) Two multiple scattering spectral models:

SBDART (***Santa Barbara Disort***) based on a discrete ordinates radiative transfer module (*Stammes et al.*, 1988) and a low atmospheric transmission model with solar data from LOWTRAN7 (*Kneizys et al.*, 1988).

STAR (***System for Transfer of Atmospheric Radiation***) (*Ruggaber et al.*, 1994), developed by the Meteorological Institute of the University of Munich. It is based on matrix operator theory.

b) Two simple spectral models:

SMARTS2: Simple model for the atmospheric radiative transfer of sunshine (*Gueymard*, 1995), is a spectral solar irradiance model based on simple transmittance parameterization of relevant atmospheric parameters.

UVA-GOA, developed by the *Grupo de Óptica Atmosférica* (GOA) (University of Valladolid). The program accounts for the absorption and scattering processes in a single atmospheric layer, but no interaction between both processes has been considered. Single scattering albedo and asymmetry parameter are input parameters and not dependent on wavelength. The aerosol optical depth is given by the Ångström β and α turbidity parameters.

10.4. RESULTS OF THE COMPARISON BETWEEN MODELS AND MEASUREMENTS

10.4.1 UV Index comparison

Multiple scattering models generally show greater UVI values than measured values. This effect has been described in other comparison works (*De Backer et al.*, 2001). We have also observed that the opposite effect happens if we work with simple spectral models and they show lower values than measured ones. Figure 9.2 shows absolute differences between the UVI measured values and the UVI calculated by means of the four models. Around noon, when the UVI reaches its daily maximum values, SMARTS2 and UVA_GOA models always show UVI lower than measurements (between −0.4 and −0.8 UVI units). However, multiple scattering models always produce higher values and with a similar magnitude (between +0.8 y +0.4 units).

It must be noted the opposite behaviour that show these absolute differences in the two days: they are large for multiple

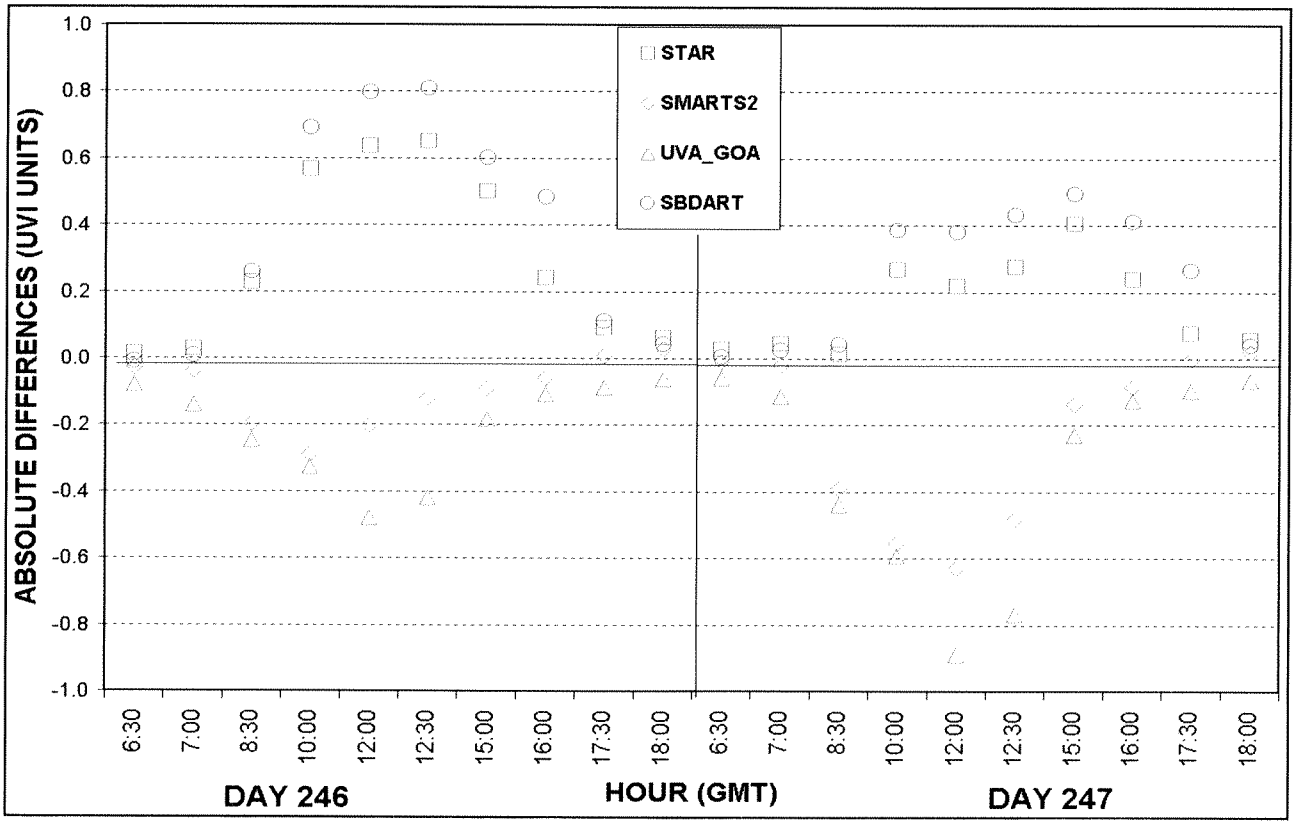

Figure 2. *Diurnal evolution of UVI absolute differences between simulations and experimental values during the campaign. These absolute differences are greater around noon, because the UVI has a higher value. The two multiple scattering models overestimate the reference, while simple models are under it.*

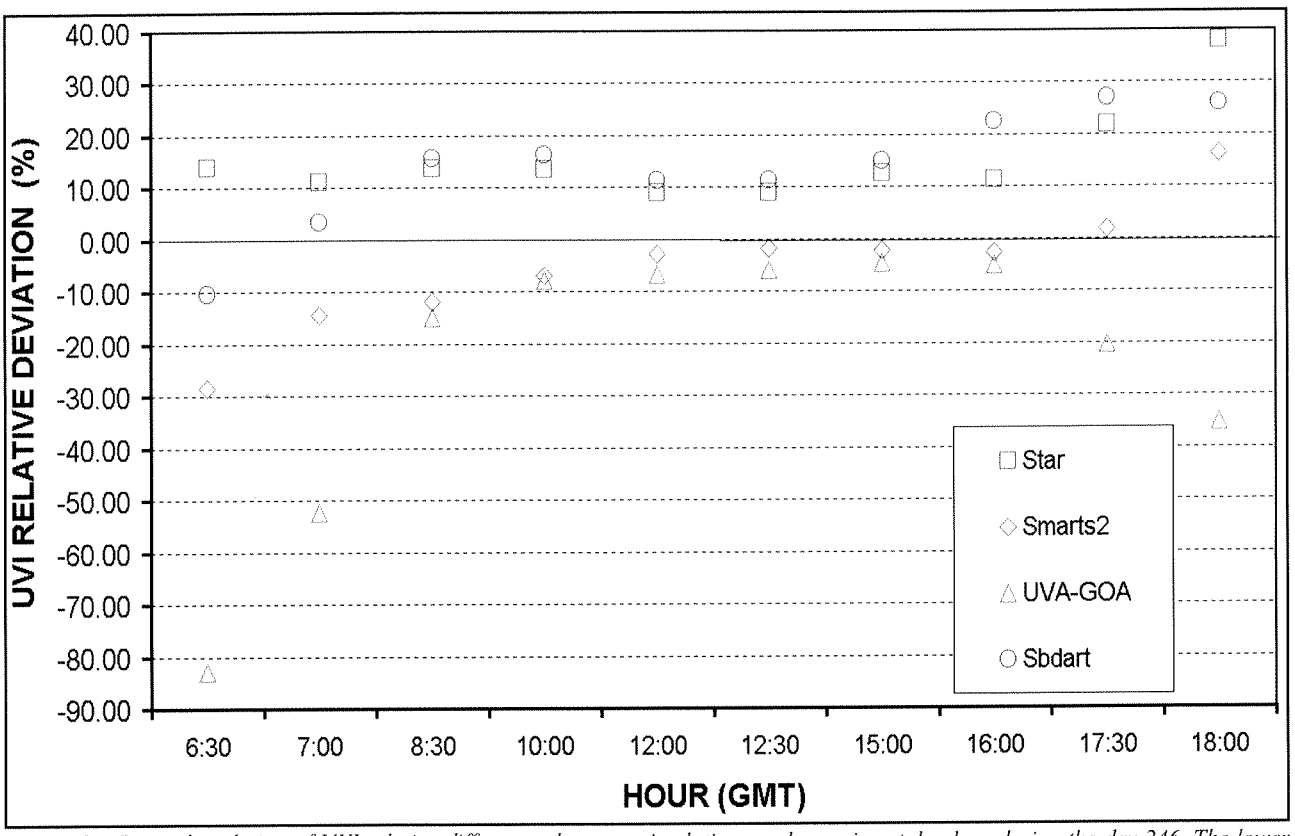

Figure 3a. *Diurnal evolution of UVI relative differences between simulations and experimental values during the day 246. The lower values are observed during noon, just the opposite behaviour than the absolute values. Simple models, specially UVA_GOA, have larger differences with the measurements for great zenith angles.*

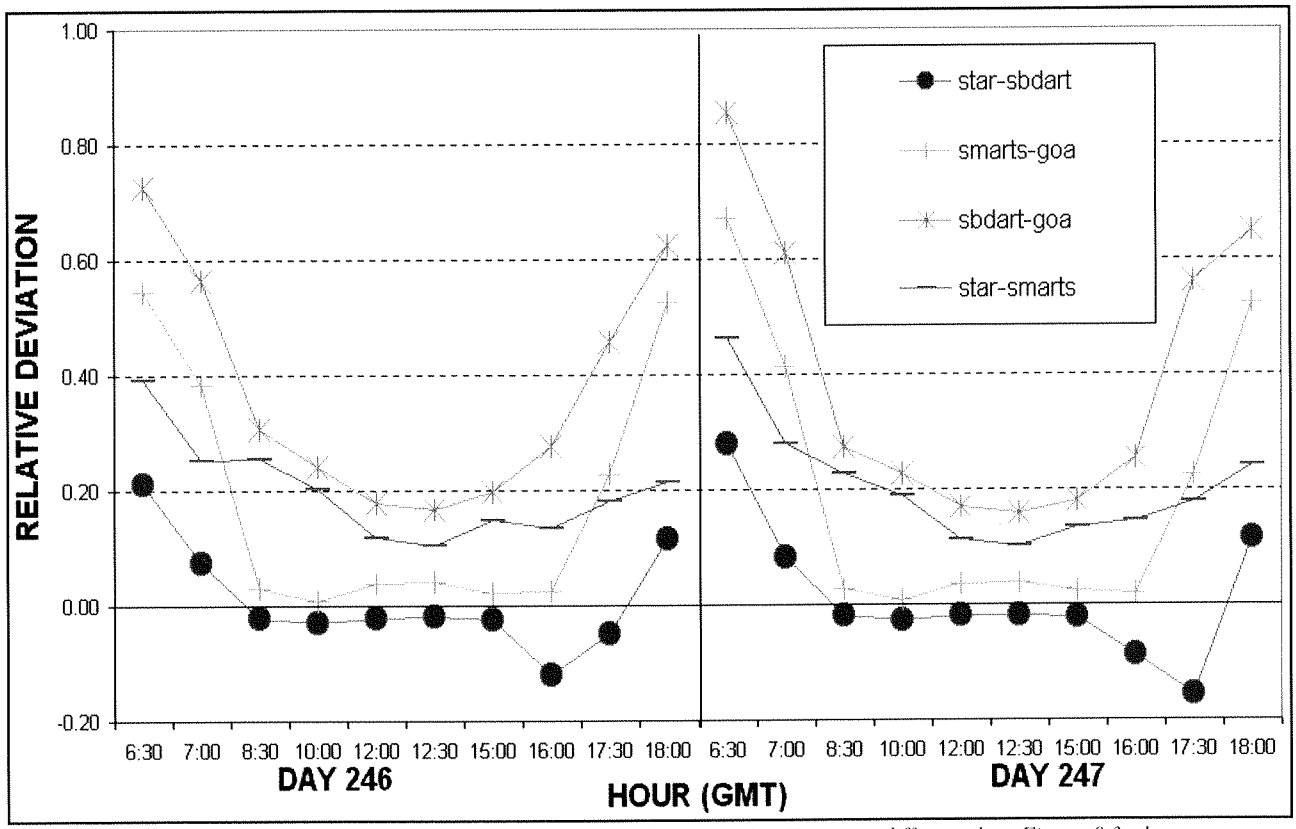

Figure 3b. *Relative differences between models in day 246 and day 247. This Figure is different than Figure 9.3a because we are just comparing the model outputs, but not models with experimental values. As one observes, the lower values correspond to comparison between the two multiple scattering models (SBART and STAR), specially around noon. The higher differences are found between SBDART and UVA_GOA.*

scattering models the first day but the opposite happens for the second day. This is due to the different treatment of scattering for the models when they calculate the diffuse irradiance together with the clouds that were present all the morning which produced an appreciable increment of diffuse irradiance but not a sensible decrease of direct irradiance and, as a result, an increment of global irradiance. For this reason, the UVI values calculated from instrumental measurements are higher for the second day and show a better agreement with the multiple scattering models. Nevertheless, for the cloudless day, they are the simple spectral models which fit better to instrumental measurements (SMARTS2 approximately –0.2 UVI units). Bearing in mind that the UVI is presented to public in entire values, only a maximum difference of ±1 UVI unit could exist between the four models.

Figures 9.3a and 9.3b show the UVI relative differences between modelled and measured values. For the hours near the noon, these differences range between +5% and +15% for multiple scattering models and between –2% and –12% for simple spectral models. Furthermore, we can observe that for zenith angles greater than 60° these differences are very large but as they correspond to little values of UVI they have no influence in the possible biologic effect on people. It must also be kept in mind that the own error of the instrument is about 10%.

In Figure 9.4 we compare the modelled UVI with the observed values and, also, the mean value of all the models.

10.4.2 UVA and UVB global irradiance comparisons

We also have studied the absolute and relative differences between models and observations for the integrated values of global irradiance in UVB and UVA spectral intervals. For the UVA irradiance we can observe that relative deviation is lower than ±10% for zenith angles lower than a 60° (Figure 9.5). For the UVB irradiance and for the same zenith angles, relative deviation has slightly higher values but always lower than ±16%.

Figure 9.6 shows the UVA integrated irradiance. We can see the slightly higher observed values for the second day: about 12% in the two hours before noon, which agrees with the presence of some Cu, and only between 2% and 4% after noon when Cu had disappeared. This effect hardly is present in UVB integrated irradiance (Figure 9.7) where the differences between UVB values of two days is hardly ever between ±2%.

When we only compare model irradiances for two days, UVA and UVB irradiance values are nearly the same because simple spectral models do not consider clouds and furthermore, we did not consider them in multiple scattering models. Only at noon, we can observe for day 247 about 1% lower irradiance values than the first day.

10.4.3 Comparison between models

The UVI differences between multiple scattering models are around 2 or 3% for zenith angles lower than 60°, although they can reach values higher than 12% for low sun elevations. These differences are in agreement with the presented in the Koepke et al. (1998) intercomparison work. For simple spectral models these differences are about 2 and 4% and higher than 20% at the same previous conditions. But when we compare both type of models themselves the differences catch up values between 14-20% for solar zenith angles lower than 60° and greater than 35% for zenith angles higher 60°. It must also be kept in mind that multiple scattering models always give higher irradiance values than simple spectral models.

For UVB integrated irradiances the differences between models are much similar at UVI ones, and for UVA these

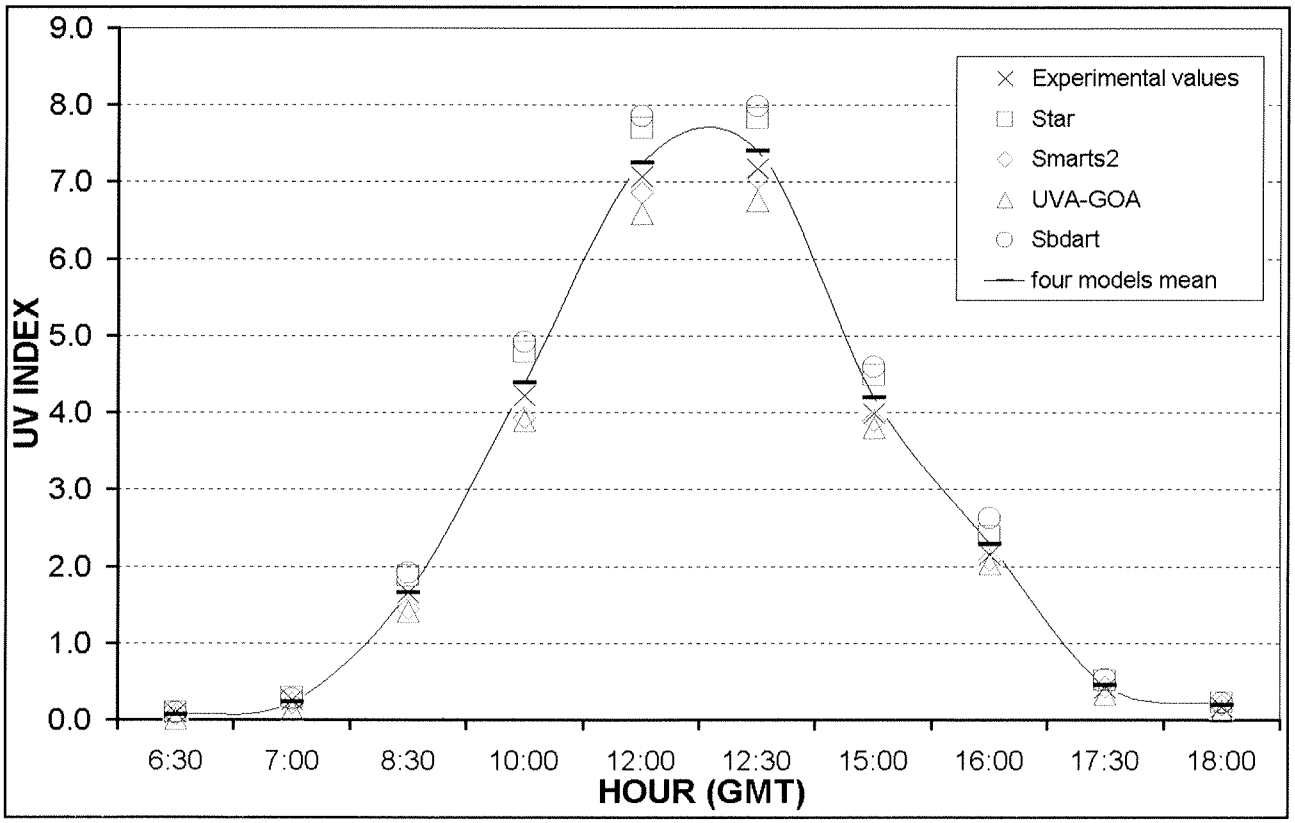

Figure 4. *The UVI evolution during the day 246. In this figure we can apreciate the same effect that it is shown in Figure 9.2, i. e., the multiple scattering models overestimate the UVI and the simple models underestimate it.*

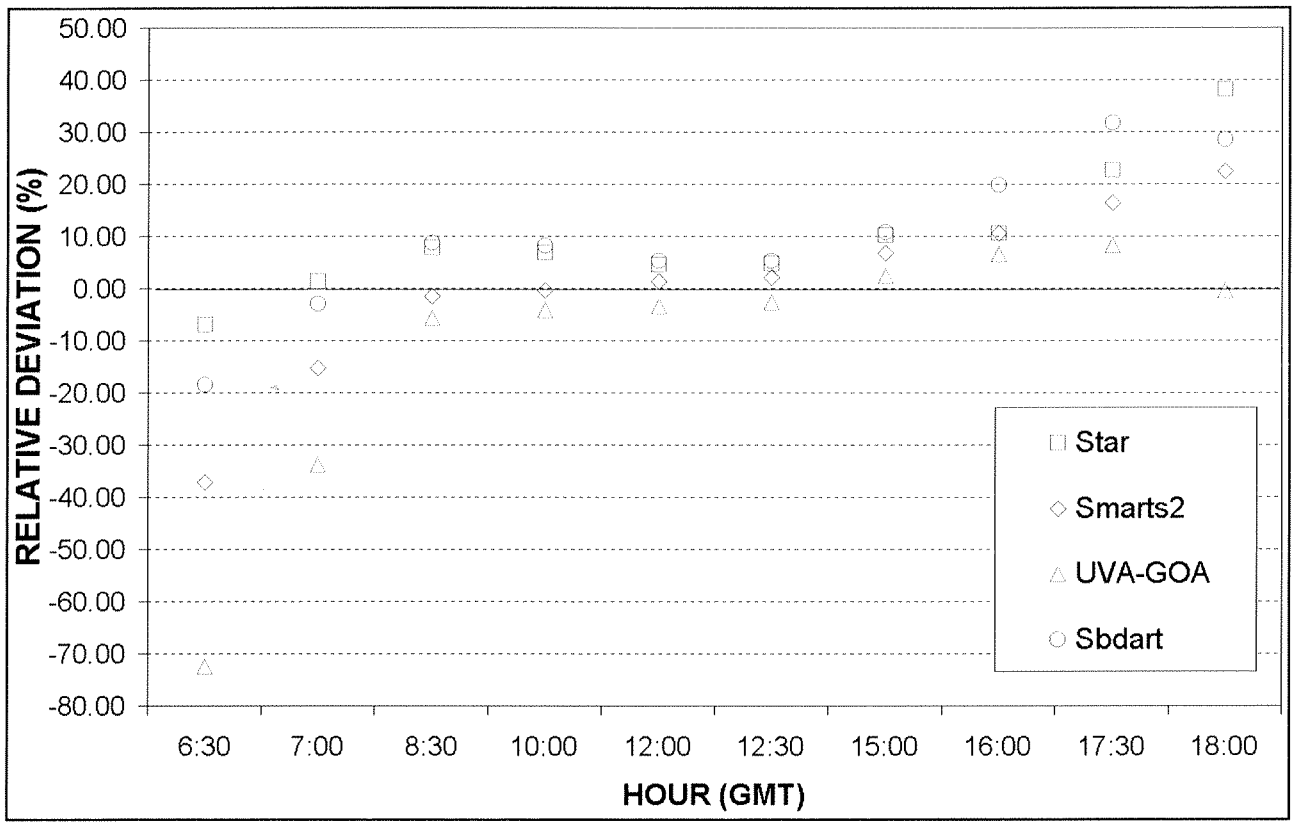

Figure 5. *Relative differences of UVA integrated irradiances between models and experimental values during the day 246. The diurnal evolution has a similar behaviour than the UVI (Figure 9.3) but around noon, the relative desviation of UVA is lower than the UVI relative desviation.*

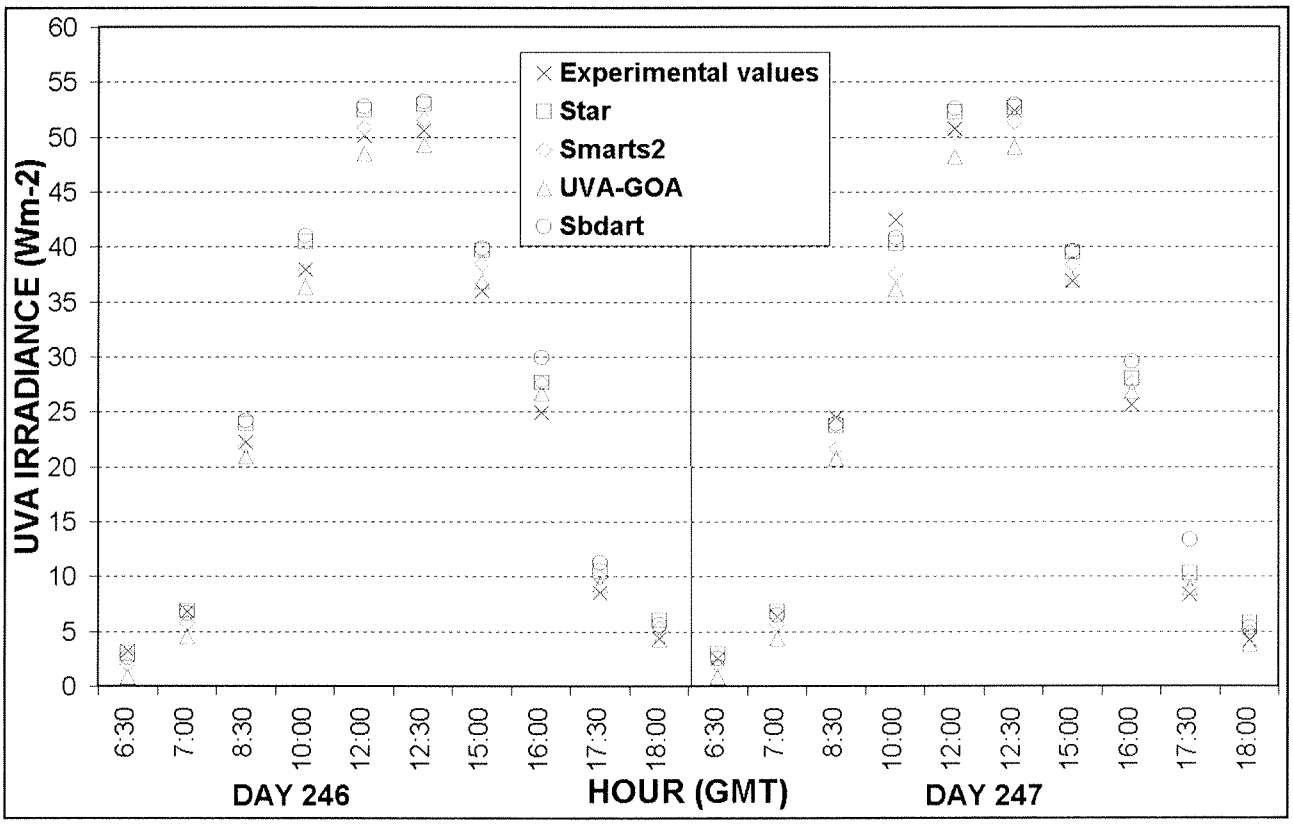

Figure 6. *Evolution of UVA integrated irradiance during the two days.*

differences are lower: only 1% between multiple scattering models and about 3-13% between multiple scattering models and simple spectral models. In Table 1 we can see and average of these deviations. A model sorting (classification) in increasing order of UVA and UVB irradiance values would be the following: UVA-GOA, SMARTS2, STAR and SBDART.

Table 1. *Relative Average Deviation between multiple scattering models (MSM), simple spectral models (STM) and between both (MSM and STM).*

	Relative Average Deviation for θ<60°		
	Between MSM	Between STM	Between Both
UV Index	2%	3%	14%
UVB irradiance	5%	3%	18%
UVA irradiance	1%	4%	6%

If we study the spectral output of the models we can observe they are close together for solar zenith angles 60º. We do not present these figures because there are not distinguishable differences. Only for low sun elevations it is possible to observe that simple spectral models, specially UVA_GOA model, show lower values than reference and multiple scattering model.

10.5. CONCLUSIONS

In this chapter we have applied different models to simulated spectral irradiance during two days in the Arenosillo campaign. Simulations have been compared with observed values of UV spectral irradiances and with the UVI. Although the short period of measurements and the different clear sky conditions observed during the two days, can restrict the validity of the conclusions, some of them appear clearly, like the high uncertainty of all the models for low solar zenith angles. But, for these two days and for zenith angles lower than 60º, the results show a good agreement between models and measurements and between models too. Simple spectral models always underestimated spectral irradiance whereas multiple scattering models overestimated it. As a consequence of this a UV index underestimating will result if we work with simple spectral models. A more exhaustive comparison of modelled results with measurements in different places and environments is essential and would be planned in other future campaigns.

REFERENCES

De Backer, H., P. Koepke, A. Bais, X. de Cabo, T. Frei, D. Gillotay, C. Haite, A. Heikkilä, A. Kazantzidis, T. Koskela, E. Kyrö, B. Lapeta, J. Lorente, B. Mayer, H. Plets, A. Redondas, A. Renaud, A. Schmalwieser and K. Vanicek (2001): "Comparison of measured and modelled UV Indices for the assessment of health risks". *Meteorol. Appl.* **8**, 267-277.

Gueymard, C. (1995): "SMARTS2, A Simple model of the atmospheric radiative transfer of sunshine: algorithms and performance assessment". Florida Solar Energy Center, Rep. FSEC-PF-270-95, 83 pp. Florida.

Koepke, P., A. Bais, D. Balis, M. Buchwitz, H. De Backer, X. de Cabo, P. Eckert, P. Eriksen, D. Gillotay, T. Koskela, B. Lapeta, Z. Litynska, J. Lorente, B. Mayer, A. Renaud, A. Ruggaber, G. Schauberger, G. Seckmeyer, P. Seifert, A. Schmalweiser, H. Schwander, K. Vanicek and M. Weber (1998): "Comparison of models used for UV index-calculations". *Photochem. Photobiol.*, **67**, 6, 657-662.

Lorente, J., A. Redaño and X. de Cabo (1994): "Influence of urban aerosol on spectral solar irradiance". *J. Appl. Meteor.*, **33**, 406-415.

Mayer, B. and G. Seckmeyer (1997): "Systematic long-term comparison of spectral UV measurements and UVSPEC modelling results". *J. Atmos. Res.*, **102**, D7, 8755-67.

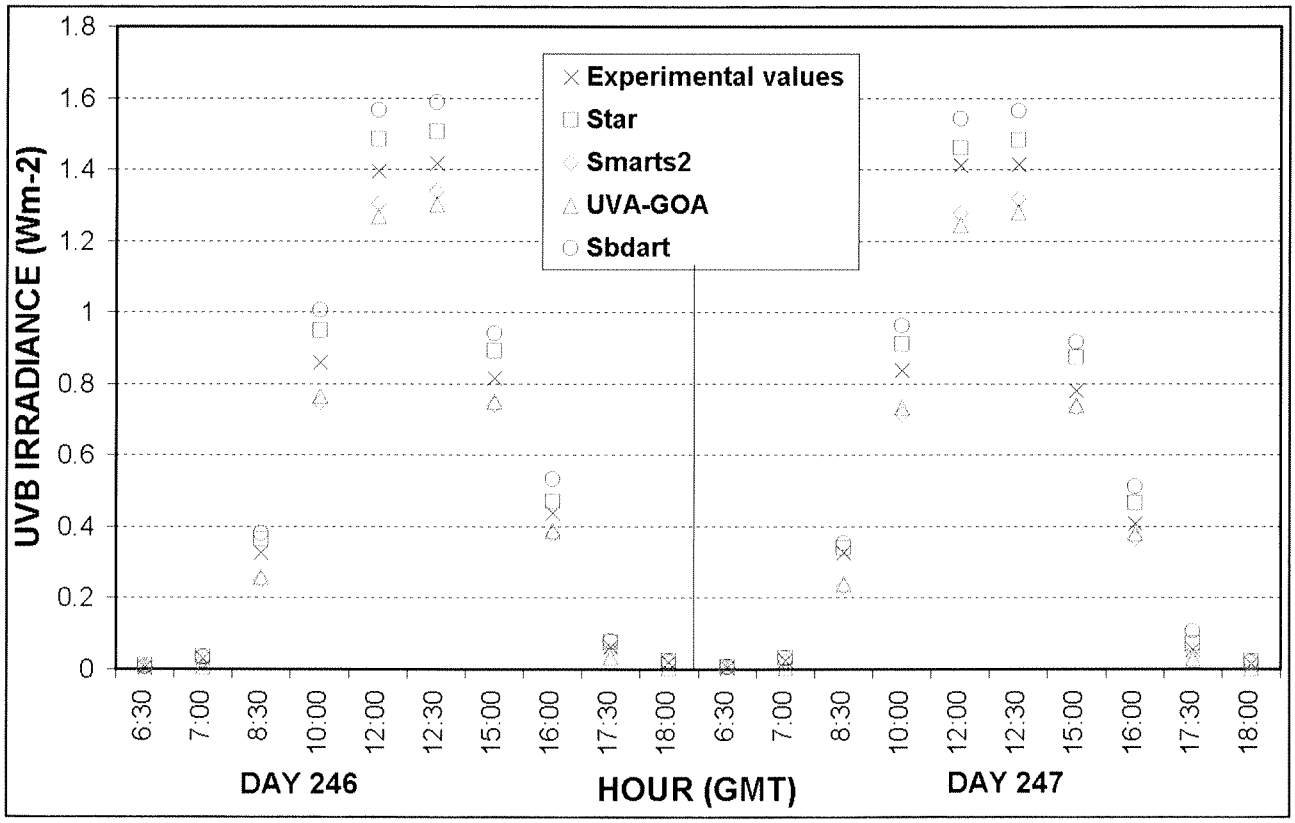

Figure 7. *Evolution of UVB integrated irradiance during the two days. One observes a good fit between experimental and modeled values. Here we observe a greater desviation near noon.*

McKinley, A. F. and B. L. Diffey (1987): "A reference action spectrum for ultraviolet induced erythema in human skin". *CIE J.* **6**, 17-22.

Ruggaber, A., R. Dlugi, and T. Nakajima (1994): "Modeling of radiation quantities and photolysis frequencies in the troposphere". *J. Atmosph. Chem.*, **18**, 171-210.

Schwander, H., P. Koepke and A. Ruggaber (1997): "Uncertainties in modelled UV irradiances due to limited accuracy and availability of input data". *J. Geophys. Res.*, **102**, D8, 9419-9429.

Webbs, P. and A. R. Webb (1997): "Accuracy of spectral UV model calculations". Part I: Consideration of the uncertainties in the input parameters. *J. Geophys. Res.* **102**, 1551-1560.

Conclusions and suggestions

The UV instrument Intercomparison

The methodology followed in this UV Intercomparison is the same that those used in other international intercomparison exercises. The reference is obtained from the Bentham DM-150 from La Laguna University and the two double Brewers from Izaña (INM) and INTA, respectively.

A half of the instruments with one monochromator, ignoring the 290-300 nm range, lay within ±3% of the reference spectra, and the three double monochromators fall in ±1% agreement.

A 80% of the instruments provided UV index (UVI) that agreed the UVI obtained from the reference, and 100% of the instruments agreed within ±1%. These results are outstanding concerning the validation of the UVI forecasting national model.

The overall outcome of the campaign was very encouraging, as it was proven that the majority of the instruments were in very good agreement with each other. It is also worth mentioning that obtained results were consistent with other intercomparison campaigns (NOGIC-93, NOGIC-96 and SUSPEN), held some years ago. It appears, therefore, that there presently exists in Spain a core group of UV spectro-radiometers that is capable of providing quality spectral solar UV measurements.

In this intercomparison, and as first time, lamp calibrations linked the references of each group to the same reference on a national scale, what is extremely important to intercompare data form different sites and instruments.

The total ozone Intercomparison

The scatter in ozone values for all the Brewers that participated in this intercomparison was quite low, and similar to that of the ozone intercomparisons performed in NOGIC-93 and NOGIC-96. After corrections all the Brewer instruments showed an agreement of ±1% with the reference Brewer#017.

The Dobson#120 shows the same agreement and scattering as the Brewers compared to the Brewer#017.

Ozone calculation using global UV measurements with the Brewers is excellent. This alternative method is non-sensitive to cloudiness, although it fails for high airmass.

The Bentham DM-150 shows quite good results when compared with Brewer#017. However, it presents some problems of time synchronization, meaning that total ozone is only acceptable for airmasses lower than 1.4.

The NILU-UV6 shows promising behavior for total ozone determination if a periodical (every one or two weeks) and long term external lamp test procedure is performed.

The Microtops-II is a reliable instrument for intensive campaigns and for detecting, in a first stage, malfunctions in a spectrophotometer network if regular ETC determination is made through Langley Plots performed in high mountain stations.

The infrared and visible instrument Intercomparison

The results obtained for the measurements of global irradiance show that the Licor 1800s presented very significant differences at the beginning and at the end of the day due to the influence of the cosine effect. This fact obliged to limit the analysis of these measurements to solar altitude angles greater than 30°.

The measurements of direct irradiance showed that, even when considering the non-corrected data, the deviations are of the order of the precision of the instruments in the visible range (5%). If correction factors are considered these deviations are reduced to 3%, and when the Licors are compared with the Optronic, the deviations are less than 2%.

The aerosol optical depth and water vapor content Intercomparison

Comparison of AOD at UV with and between Brewers data shows a good agreement considering the comparison with Cimel and Microtops in visible and infrared wavelengths. The error associated with the AOD determination drives us to assess the intercomparison at level of irradiance between Li-Cor and Brewer systems.

The determination of the water vapor content by Li-Cor spectroradiometer points out the problems that exist with this retrieval. The band 0.82 μm is bad modelled by Lowtran7 coefficients and it can not be used for current determination. Bands 0.72 and 0.94 μm give results with very poor agreements. The comparative data with Microtops and Cimel cannot help to assess the detected problems and uncertainties of this spectroradiometric methodology.

General

This UV Intercomparison will help more accurately measure ground-level changes in damaging ultraviolet radiation from the sun in Spain. Such measurements are crucial in assessing effects of ozone depletion in the upper atmosphere on human health, agriculture, fisheries and materials such as concrete, plastics and paints. As ozone levels in the upper atmosphere fall, increased levels of harmful ultraviolet radiation, or UV, will reach ground level.

UV monitoring networks are being established in Spain, however, it will take several years to develop a record from which meaningful trends can be extracted. This is due to variability in stratospheric ozone as well as clouds and air pollution, which also affect the transmission of UV. Furthermore, UV trends are not likely to be large, so it is extremely important that the measurements be done with high accuracy. So, periodical intercomparisons like that carried out at El Arenosillo are extremely important.

Intercomparison of UV, visible and infrared instruments, together, reveal to be quite convenient since some environmentally interesting derived products, as aerosol optical depth, water vapor content, and total column ozone, can be obtained with different instruments and techniques.

The Intercomparison has proved its value by improving our knowledge in methodologies for obtaining better agreement among the instruments and letting us to identify sources of errors in individual instruments.

Training, discussion and exchange of experiences among participants were also very valuable activities in the intercomparison.

The continuity of the intercomparison programs and the technical development related to them should therefore be promoted and supported in the future.

The Editors

APPENDIX
BASIC CONCEPTS AND DEFINITIONS IN SPECTRORADIOMETRY

A. M. de Frutos, R. Vergaz, V. E. Cachorro
Grupo de Óptica Atmosférica (GOA-UVA), Dpto. de Óptica y Física Aplicada, Facultad de Ciencias, 47071, Valladolid, *chiqui@baraja.opt.cie.uva.es*

SUMMARY
In this section we are going to describe the basic concepts and definitions of the systems involved in the instruments used in these experiments (spectrographs and spectrometers), as classical optics explains to us.

1. ROLE OF A DISPERSION SYSTEM

A light source can be characterised by a function named $L(\nu)$, which represents its radiance L as a function of its frequency ν. This function is no more, but not less, than the Fourier transform in time of the expression of the electromagnetic field coming from the source.

The role of any dispersion system is to get for us as much information as possible over this function (also called "spectrum").

It is completely impossible for us to measure the frequency of any visible (and UV and IR) light due to its very high value (typically 10^{15} Hz). So, it is more frequent to characterise the light by the wavelength rather than the frequency. The relation between both magnitudes is well known.

2. RADIANCE: SPECTRAL DENSITY OF RADIANCE

If we can consider our radiation to be monochromatic, its radiance is well defined. It is not possible however to find in the nature any strictly monochromatic source. At the beginning of the sixties, a new light source was developed: the laser. This source is not really a monochromatic source, but taking into account that its spectral width is 5 orders narrower than the narrowest source in the nature one can consider it to be monochromatic.

This means that the characteristic of the "monochromaticity" of a source is related with the "power" of the instrument that we use to measure its spectrum. This light that can be considered as monochromatic for a given instrument, can show some spectral structure with another one and it can no more be considered as monochromatic but polychromatic.

Then if we can not considered a light source as monochromatic we must have into account that its radiance presents dependence with its frequency or its wavelength (or also with its inverse, the wavenumber σ). In this case we can characterise our light with a new magnitude called radiance by unit of wavenumber:

$$L_\sigma = \frac{\partial L}{\partial \sigma}$$

This magnitude is much often called "spectral density of radiance". In this case we can write the total radiance concentrated into a narrow piece of wavenumber as:

$$dL = \frac{\partial L}{\partial \sigma} d\sigma = L_\sigma d\sigma$$

Our dispersion system must get for us this function L_σ as the only way to characterise the temporal Fourier Spectrum of the source.

3. RESOLVING POWER OR *"RESOLVANCE"* OF A DISPERSION SYSTEM

Our system must show a signal proportional to the radiance L for each finite element in which we need to cut the spectral interval under study. We can say that the narrower is each spectral element is the spectrum is *more accurately or more fine resolved*. We can remark this characteristic of our instrument by the magnitude:

$$\Re = \frac{\sigma}{\Delta\sigma} = \frac{\lambda}{\Delta\lambda}$$

This magnitude is the so-called *resolving power*, or in French terminology "*resolvance*". In Spanish terminology we can find the term *"resolvancia"*.

4. LUMINOSITY

The resolving power is not sufficient to characterise completely our instrument. It is necessary that the amount of the signal shown by it was enough to get information about the source and to distinguish it from the always-present noise. In other words the signal to noise ratio must be high enough. This characteristic is called "Luminosity" of the instrument.

It is important to remark that both magnitudes: resolving power and luminosity are not in general independent. It is very clear that the wider is the spectral interval resolved by the instrument (the lower its resolving power) the more light enter the instrument and of course the higher is the luminosity. But, being this apparently obvious, this is not in general true. This is only true for spectrometers, not for spectrographs, as we will try to show in following pages.

5. LINEAR DISPERSION

This magnitude can be defined on the basis of "how much" an increment in the wavelength is physically separated in the exit plane of the instrument. Mathematically we can write it in terms of wavelength and linear units on this plane by:

$$D = \frac{\Delta\lambda}{\Delta l}$$

where l is linear dimension in the exit plane.

In the case of the most useful system, that is the one based on diffraction gratings, it is obvious that (based on the grating law and on the concept of a complete dispersion system) depends only on two parameters: the spatial frequency of the grating and the focal distance of the collecting optical system (usually called "chamber lens").

6. CLASSIFICATION OF THE DISPERSION INSTRUMENTS

In order to get dispersion effects we must identify in the nature any effect, which show different behaviour depending on the wavelength of the light.

The most ancient known is of course the optical prism. Due to the fact that the refraction index depends on frequency, the Snell law will not be equally applied for any incident angle over the separation surface of two different media. This is a dispersion effect and can be used simply taking a prism of optical materials and doing that the light coming from the source under analysis enter it in incidence out of vertical. Sir Isaac Newton described this effect.

Another dispersion effect is of course the so-called "grating law". If we illuminate a grating with polychromatic light, diffraction will force the different spectral components to take different paths.

Finally we can identify another optical phenomenon which presents dispersion effect: the interference of light. It is well known that the intensity produced by two light beams under interference conditions (coherence) depends explicitly on the difference of their optical path. This magnitude depends also explicitly on the wavelength. We have again dispersion effects and we can take profit on it to build interferometers (Michelson or Fabry-Perot, for example) that, under some conditions, can be used as dispersion systems. In the case that we use a Michelson, this originates the Fourier transform spectroscopy.

Another completely different classification can be established depending on the way we receive the disperse light. We can use receptors that respond only to the flux coming on it or receptors with capability to get and show images (spatial resolution).

In the first case it is very obvious that we need any sort of system that presents to the receptor just the part of the spectrum in which we are interested. We can call this instrument "mono-chromator" for obvious reasons. The natural way to get this is to place in plane P (see fig. 1) a slit, which selects a precise spectral interval. We usually call it exit-slit.

If we are interested in a wider spectral range, we need to present onto our detector successively different spectral intervals and record the signal varying with the time. We can call this instrument "spectrometer". One usual way to get this is to use a monochromator and move mechanically its dispersion system (prism, grating or even a mirror system in the case of interferometers), in an adequate way, in order to present, depending on time, different spectral intervals and getting, that's really, the whole spectrum. We can call this kind of instruments as "scanning monochromators".

Finally, if we use a detector with spatial resolution (this means that it must be capable to respond to the flux coming onto different images elements), then we can get perhaps the whole spectrum under study at a time avoiding the need for mechanical systems. We can call this kind of instruments "spectrographs".

The oldest way to get this kind of detector was of course the photographic plate. Fortunately, this ancient detector, which presents several problems (it involves chemical processed, the signal: the optical density provided is not in general proportional to the received flux, etc.) is going to the past and a new generation of detectors with spatial resolution (from now on spectral resolution), such as CCD's, etc., is conquering our instruments.

It is perhaps important to note here that one must not identify the modern concept of spectrometer, which is capable to provide us of a very correct description of the intensity of a spectral interval with a most ancient word "spectrometer", used to describe instruments that were only capable to get properly the wavelength of a spectral line rather that its intensity. This kind of instruments was really in general spectrographs with photographic plates as detectors and was incapable to provide us the intensity of lines with a high lever of accuracy due to the problems described. Unfortunately a very recent instrument that this group (GOA-UVA) have bought are described as "spectrometer", being actually a spectrograph.

It is important to note that the very recent advances on spectral resolution detectors (CCD, etc.) are drawing again into fashion this later instruments, due to the fact that the are stronger (there is no need to use mechanical devices) and can be relatively easily automated.

7. GENERAL PROPERTIES OF PRISM AND GRATING SPECTROGRAPHS

In a very general form any of such spectrographs may be represented following figure 1:

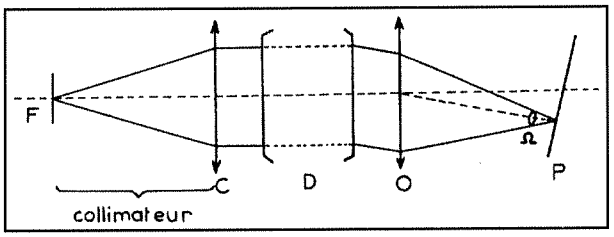

Figure 1. *Schematic view of the functioning principle of any prism or grating spectrograph.*

In this figure one can see:

- *The collimator system* C, which provides a plane wave for any point of the source F. This source must be a slit perhaps with variable width.
- *The dispersion system* D (prism or diffraction grating) gives a different direction for each plane waves depending on wavelength.
- *The chamber system* O (also called collector system) forms monochromatic images of the slit in a plane P where a detector with spatial resolution is placed.

It is important to note here that after the revolution of holography and one of its basic results: the holographic grating, we can build one of such grating in a concave and appropriate surface, simply by making a photography of the interference on the surface of two beams coming from point sources at the correct positions. This is the way in which most of the actual instruments really work. In this way we can substitute the three elements by a unique concave holographic grating which simultaneously collimates, disperses and collects.

Now we will try to understand better the way in which a spectrum can be recorded.

Let us suppose a slit extremely fine (theoretically of width 0). This slit is illuminated by a strictly monochromatic light. In this case the illumination on the reception plane P is done by the Fourier transform of the entrance aperture of the system. If the instrument is working properly this aperture must be the border of the dispersion system (prism or grating) which usually is a rectangle. This figure can be seen in figure 2:

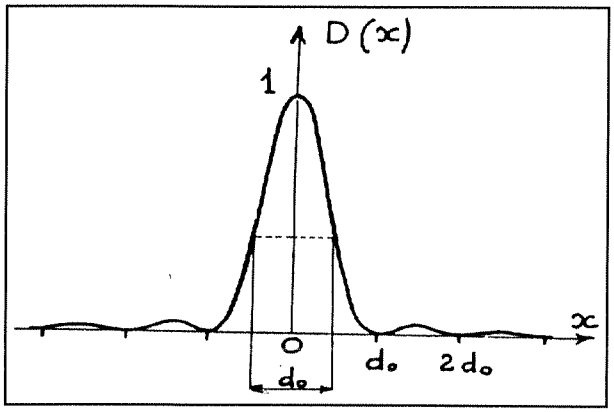

Figure 2. *Distribution of radiance onto plane P (see fig. 1) when the slit is infinitely narrow and the incident radiation is monochromatic.*

This figure (Sinc function in this case) can be characterised by the magnitude d_0, usually called Full Width at Half Maximum (FWHM). It can be in a very approximate (not exactly) way expressed as:

$$d_0 = f\frac{\lambda}{a}$$

where f is just the focal distance of the collector system, λ the wavelength, and a, the size of the border of the dispersion system.

And now, what happens if our extremely fine slit is illuminated by two different wavelengths? Obviously, the collector system must form a figure like fig. 2 for each wavelength, centred, of course, in different points of plane P. Let us suppose now that our two wavelengths, λ and $\lambda+\Delta\lambda$, are such that their respective diffraction figures are placed like figure 3 shows:

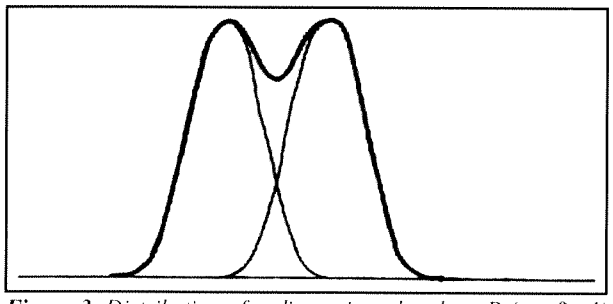

Figure 3. *Distribution of radiance into the plane P (see fig. 1) when two wavelenghts are such that the figures are separated d_0 (Lord Rayleigh's criterion).*

In this figure we have eliminated the secondary maxima (of very poor intensity compared with the central one) and placed both in the following way: the minimum of one of our figures lies directly down the maximum of the other. In figure 3 the result of the addition is also shown. It is very evident that if our two wavelengths are closer than the situation shown by fig. 3 we can not distinguish it as being different. We say now that we have reached the limit of the resolving power of the instrument following the well-known criterion due to Lord Rayleigh.

We have not enough space here to show that this resolving power can be expressed by:

$$\Re_0 = \frac{\lambda}{\Delta\lambda} = a\frac{d\theta}{\Delta\lambda}$$

8. INFLUENCE OF THE WIDTH OF THE ENTRANCE SLIT ON THE RESOLVING POWER AND THE LUMINOSITY OF THE SPECTROGRAPH

The things are apparently very clear: the wider the slits the more light enter the instrument. But this is a very poor analysis. And, if one is interested in resolving power it is directly a catastrophe. What happens if we not more considered our slit to be of width "0"? The obvious response after the Fourier theory of image formation is that the illumination over the plane P of reception is just the convolution of the "image" due to a single point (fig. 2) and the expression of an extended source. One more, we can not have the space for explaining more properly this effect.

We can resume it writing that, for very narrow slits, the diffraction figure is the only important thing. By the contrary, for a more extended slit, the systems can form image of it. The only problem is that the border of any monochromatic image of the slit is not exactly a rectangle, but due to this effect it will show a curvature. Perhaps this is the moment to show figure 4:

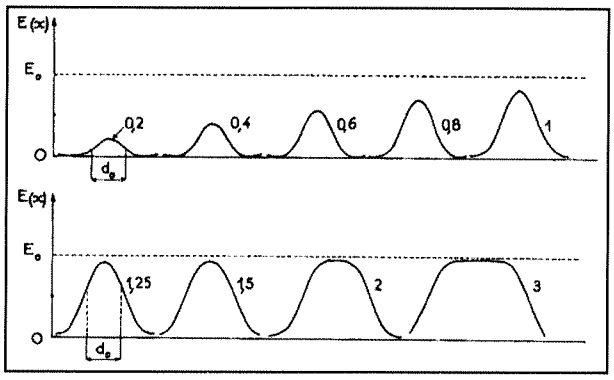

Figure 4. *Evolution of the distribution E(x) of the radiance of the image with the width of the source.*

What is shown in this figure? It is very clear. For very narrow width of the slit the only important magnitude is the diffraction by the border. This means that closing the slit we get two things: we, obviously, eliminate light entering the system, and this is not, of course a good idea. But, in addition we do not win resolving power (this only controlled by the border of the dispersion system, not for the width of our slit).

If we increase the size of our slit, of course we get more light, and this is good for us. Over all because we do not damage our resolving power. But, what happens if we again increase the size of our slit? Well, then any monochromatic image of our slit will be "optically and spatial resolved".

This means that for any monochromatic image of the slit the size of the image of the slit increases. This means that our resolving power decreases for obvious reasons. And, what happens with our luminosity? The answer is very clear after fig. 4: nothing. The image of the slit is optically resolved: then, the signal per pixel will not be increase. Then our SNR will equally not be increase, and this is not good news.

In other words: It is necessary a compromise between the size of the slit and the size of the spatial resolution in our detector. This study could show that, avoiding some effects as diffusion between neighbourhood pixel, etc., the correct size of the slit is almost the size of the maximum resolving power of the detector. This is one of the great limitations of a spectrographic system: there is no choice. An ideal condition exists. Of course, with this limitation, there is some advantage.

9. THE SPECTROMETERS

We have just said that a spectrometer has no spatial resolution and, by consequence, nor "natural" spectral resolution. We also just had said that selecting in the plane P only a narrow amount of spectral interval could get this by a so-called exit-slit. What is the instrument we have build?: of course a monochromator. This is an instrument, which selects a more or less large range of wavelengths.

But, as we had just explained, we could mechanically move the dispersion system, we can "present" just onto the exit-slit a piece of the spectrum that we try to measure. After this, any type of integrating detector will collect the light crossing the exit slit, and we can record the spectrum as a function of time.

But there is a very special difference between both behaviours (spectrographs and spectrometers). Perhaps it will be more clear seeing figure 5:

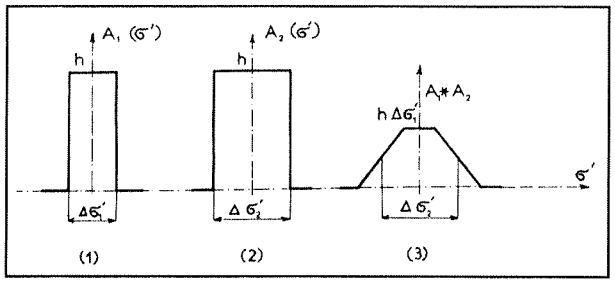

Figure 5. *Defining the instrumental (or "slit") function of a spectrometer.*

Let us suppose that our illumination is monochromatic. Let us represent in the left the entrance slit (1), and also represent the exit slit in the middle of the figure (2). If our radiation is monochromatic our optical system forms the image of entrance slit (see fig. 2) onto the plane in which we our exit slit is located. Now we move our dispersion system. The image of the entrance slit will cross over the exit slit and the detector will collect the total flux traversing the system. What will be the response of our detector? Obviously, the convolution between both figures, that is a trapezium. This is shown in the write part of the figure 5 (3). This controls the resolving power of our instrument. Of course if the two slit are equal the final response of the instrument (its resolving power, as we had just note), is just a triangle: the "slit function" (after some authors); more properly the instrumental function. The more the slits are open, the greater is the width of the instrumental function, and the lower is the resolving power of our instrument. But, the more flux goes into our detector.

Perhaps it is important to note here that the instrumental function is never (nor for a strictly monochromatic radiation) a triangle or a trapezium. The diffraction and aberrations effects make it smoother.

And now, finally, we will try to explain the final difference between both types of systems: spectrographs versus spectrometers.

A spectrograph can record a complete spectrum in a time 0 (of course in reasonable units). This is perfect for a very great variety of physical problems in which the time of the experience is important. But the proper way to work is prefixed. Both in resolving power and luminosity. In order to get a correct measurement we depends only on two parameters: The total amount of light that the source under study can deliver in a transient experiment and, of course, also on our capability to conduct the maximum of this flux into our entrance slit. That's all.

With a spectrometer, by the contrary, we can control the diverse parameters that we have explained here. If we need more flux, we need only to open both slits. Of course our resolving power will decrease. This is the price we must to pay for.

If we need more resolving power, we only close both slits (of course taking into account the diffraction limit). Of course the flux (our signal) coming into our detector will decrease. This is once more a price to pay for.

Finally, if our experiment must have done in a transient situation we must take into account that a spectrometer has obvious limitations in this field.

10. BIBLIOGRAPHY

All the contents presented in this appendix are well-know items in the fields of Optics and Spectroscopy. This is the reason for not to reference any particular text along the sections. Every subject contained here can be found in four references with, perhaps, particular interest in the latest one. For Spanish-speaking readers, we recommend the first reference. English-speaking people have the chance of reading the beautiful Born & Wolf book. The master text in the latest generations about the diffraction theory of image formation is the one of J. Goodman.

In any case, almost all the basic concepts included in this review are completely included in the very classic manual of Spectroscopy due to Prof. Bousquet.

Casas, J. (1994): "Óptica" (7.ª ed.). Coop. de Artes Gráficas LIBRERÍA GENERAL. Zaragoza, Spain.

Born, M. & E. Wolf (1999): "Principles of Optics" (7th expanded edition). Cambridge University Press.

Goodman, Joseph W. (1996): "Introduction to Fourier Optics" (2nd edition). Mc Graw-Hill Int. Ed.

Bousquet, P. (1969): "Spectroscopie Instrumentale", Dunod, Paris.